

# DNA-driven assembly of micron-sized colloids



# DNA-driven assembly of micron-sized colloids

## ACADEMISCH PROEFSCHRIFT

ter verkrijging van de graad van Doctor  
aan de Universiteit van Amsterdam,  
op gezag van de rector magnificus  
prof. dr. D.C. van den Boom  
ten overstaan van een door het college voor promoties ingestelde  
commissie, in het openbaar te verdedigen in de Agnietenkapel

op vrijdag 27 november 2009, te 12.00 uur

door

NIENKE GEERTS

geboren te Den Helder

## Promotiecommissie:

Promotores: Prof. dr. D. Frenkel  
Prof. dr. M. Dogterom  
Copromotor: Dr. E. Eiser  
Overige leden: Prof. dr. G. Rothenberg  
Prof. dr. C.J. Elsevier  
Prof. dr. H.N.W. Lekkerkerker  
Prof. dr. F. Sciortino  
Dr. J.H. van Maarseveen  
Dr. J. Huppert

Faculteit der Natuurwetenschappen, Wiskunde en Informatica



© 2009 by Nienke Geerts. All rights reserved.

Cover: Assembly of colloids into a double helix.

Nederlandse titel: DNA-gestuurde zelforganisatie van micron-grote colloïden.

The work described in this thesis was performed at the FOM-Institute for Atomic- and Molecular Physics, Science Park 104, 1098 XG, Amsterdam, The Netherlands. The work was supported by the Nederlandse Organisatie voor Wetenschappelijk Onderzoek (NWO). The work of the FOM-institute is part of the research program of the Stichting Fundamenteel Onderzoek der Materie (FOM) and is supported by NWO.

ISBN: 978-90-6464-359-0

A digital version of this thesis can be obtained from <http://www.amolf.nl>. Printed copies can be obtained by request via email to [library@amolf.nl](mailto:library@amolf.nl) or by addressing the library at the FOM Institute for Atomic and Molecular Physics (AMOLF), Science Park 104, 1098 XG, Amsterdam, The Netherlands.

*It Sil Heve*  
Ir. Jan Sipkema, 1985

**The work within this thesis is partly based on the following articles:**

**Chapter 2:**

Nienke Geerts and Erika Eiser.

*DNA-driven assembly of colloids*

In preparation: invited contribution to Soft Matter

**Chapter 3:**

Tatiana Schmatko, Behnaz Bozorgui, Nienke Geerts, Daan Frenkel, Erika Eiser and Wilson C.K. Poon.

*A finite-cluster phase in  $\lambda$ -DNA coated colloids*

Soft Matter **3**, 703-706, 2007

**Chapter 4:**

Nienke Geerts, Tatiana Schmatko and Erika Eiser

*Clustering versus percolation in the assembly of colloids coated with long DNA*

Langmuir **24**, 5118-5123, 2008

**Chapter 5:**

Nienke Geerts and Erika Eiser.

*Flying colloidal carpets*

Submitted

Nienke Geerts, Sabrina Jahn and Erika Eiser.

*Direct observation of size-fractionation during colloidal crystallization*

Submitted

Other article by the same author not part of this thesis:

Erika Eiser, Caroline S. Miles, Nienke Geerts, Peter Verschuren and Cait E. MacPhee

*Molecular cooking: physical transformations in Chinese century eggs*

Soft Matter **5**, 2725-2730, 2009 (cover story)

# CONTENTS

<b>1</b>	<b>Introduction</b>	<b>11</b>
1.1	DNA as smart glue . . . . .	11
1.2	Colloids . . . . .	12
1.3	The experimental system . . . . .	13
1.4	Outline of the thesis . . . . .	15
<b>2</b>	<b>DNA-driven assembly of colloids</b>	<b>17</b>
2.1	Introduction . . . . .	17
2.2	DNA-coated colloids . . . . .	20
2.2.1	Synthesis of DNA functionalized nanoparticles . . . . .	21
2.2.2	Synthesis of DNA functionalized micron-sized colloids . . . . .	22
2.3	Phase behavior of DNA-coated colloids . . . . .	24
2.3.1	The number of base-pair matches and spacer length . . . . .	25
2.3.2	Probe-DNA density on the colloidal surface . . . . .	25
2.3.3	Ionic strength in surrounding medium . . . . .	26
2.4	Assemblies of DNA-coated colloids . . . . .	27
2.4.1	One-dimensional assemblies . . . . .	27
2.4.2	Two-dimensional assemblies . . . . .	29
2.4.3	Three-dimensional assemblies . . . . .	31
2.5	Applications of DNA-coated colloids . . . . .	34
2.6	Outlook . . . . .	36
<b>3</b>	<b>A finite-cluster phase in <math>\lambda</math>-DNA coated colloids</b>	<b>37</b>
3.1	Introduction . . . . .	37
3.2	Results and Discussion . . . . .	38
3.2.1	$\lambda$ -DNA driven assembly leads to finite cluster sizes. . . . .	38
3.2.2	$\lambda$ -DNA is responsible for the formation of finite clusters. . . . .	39
3.2.3	Expulsion of DNA from the gap between two bridged colloids can explain the finite sizes. . . . .	40
3.2.4	Monte Carlo simulations agree well with experimental results. . . . .	42
3.2.5	Increasing temperature has no effect on clusters stability . . . . .	43
3.3	Conclusion . . . . .	43
3.4	Materials and Methods . . . . .	43
3.4.1	Preparation of biotin-DNA solutions . . . . .	43
3.4.2	Preparation of DNA-coated colloids . . . . .	44
3.4.3	Preparation and coating imaging chambers . . . . .	45
3.4.4	Confocal imaging . . . . .	45
3.5	Acknowledgements . . . . .	45

<b>4</b>	<b>Clustering versus percolation in the assembly of colloids with long DNA</b>	<b>47</b>
4.1	Introduction . . . . .	47
4.2	Results and Discussion . . . . .	49
4.2.1	Colloidal assembly depends on the length of the DNA bridge. . .	49
4.2.2	Temperature has no effect on clusters stability . . . . .	51
4.2.3	In the absence of specific forces colloidal assembly is negligible. . .	53
4.2.4	Shielding colloidal proteins leads to cluster reversibility . . . . .	54
4.3	Conclusions . . . . .	56
4.4	Materials and Methods . . . . .	56
4.4.1	Preparation of biotin-DNA solutions . . . . .	56
4.4.2	Preparation of DNA-coated colloids . . . . .	57
4.4.3	Preparation and coating imaging chambers . . . . .	58
4.4.4	Confocal imaging . . . . .	58
4.5	Acknowledgements . . . . .	58
<b>5</b>	<b>Colloidal Flying Carpets</b>	<b>59</b>
5.1	Introduction . . . . .	59
5.2	Results and Discussion . . . . .	61
5.2.1	Grafting surfaces with DNA . . . . .	61
5.2.2	DNA-coated colloid assembly above a (complementary) surface . .	62
5.2.3	Depletion forces are not responsible for the assembly . . . . .	63
5.2.4	Colloidal flying carpets are temperature stable . . . . .	64
5.2.5	Examining different control parameters of the system . . . . .	66
5.2.6	Specific binding through ssDNA overhangs is redundant to form flying colloidal carpets . . . . .	68
5.2.7	Two factors are essential for the formation of crystalline colloidal membranes . . . . .	69
5.2.8	Carpet formation precedes (binary) cluster formation for long DNA	71
5.2.9	DNA is not evenly distributed around the colloidal flying carpets	72
5.2.10	Testing a different sample holder . . . . .	74
5.2.11	Conclusion . . . . .	76
5.3	Materials and Methods . . . . .	77
5.3.1	Coating glass-surfaces with DNA . . . . .	77
5.3.2	Preparation of DNA-coated colloids . . . . .	79
5.3.3	YOYO-staining of DNA . . . . .	79
5.3.4	Confocal imaging . . . . .	79
5.4	Acknowledgements . . . . .	80
<b>6</b>	<b>A DNA-string quartet</b>	<b>83</b>
6.1	Introduction . . . . .	83
6.2	Results and Discussion . . . . .	85
6.2.1	Ionic stability of four-way junctions . . . . .	85
6.2.2	Stability of the four-way junction and its intermediates tested by gel electrophoresis . . . . .	87

6.2.3	Optimizing buffer conditions for our colloids . . . . .	89
6.2.4	Designing a construct to string four colloids together with DNA . . . . .	91
6.2.5	Testing the individual DNA-coated colloids . . . . .	91
6.2.6	First experiments on binding four colloids simultaneously by a Holliday junction . . . . .	92
6.3	Conclusions . . . . .	92
6.4	Materials and Methods . . . . .	94
6.4.1	Thermal transition profiles of the quaternary complex . . . . .	94
6.4.2	Gel-electrophoresis of the quaternary complex . . . . .	95
6.4.3	Preparation of junction-DNA-constructs . . . . .	95
6.4.4	Preparation of junction-DNA coated colloids . . . . .	96
6.4.5	Preparation and coating imaging chambers . . . . .	97
6.4.6	Confocal imaging . . . . .	97
6.5	Acknowledgements . . . . .	97
<b>A</b>	<b>Obtaining temperature reversible colloidal systems</b>	<b>99</b>
A.1	Introduction . . . . .	99
A.2	Results and Discussion . . . . .	102
A.2.1	Reducing DNA length may lead to cluster reversibility. . . . .	102
A.2.2	Shielding more neutravidin sites on the colloids is not sufficient for cluster reversibility. . . . .	104
A.2.3	Coating colloids with DNA and a short repulsive brush . . . . .	105
A.2.4	Switching from protein to covalent binding of DNA. . . . .	107
A.2.5	Additional stabilization of cos-coated colloids to reduce the melting temperature. . . . .	109
A.2.6	Smaller colloids have lower Van der Waals forces. . . . .	110
A.3	Discussion and Outlook . . . . .	113
A.4	Future directions . . . . .	116
A.5	Materials and Methods . . . . .	119
A.5.1	Preparation of biotin-DNA . . . . .	119
A.5.2	Preparation of thiol-DNA . . . . .	121
A.5.3	Preparation of DNA-coated colloids . . . . .	121
A.5.4	Preparation and coating imaging chambers . . . . .	122
A.5.5	Confocal imaging . . . . .	123
A.6	Acknowledgements . . . . .	123
	<b>Bibliography</b>	<b>125</b>
	<b>Summary</b>	<b>139</b>
	<b>Samenvatting</b>	<b>143</b>
	<b>Dankwoord</b>	<b>147</b>
	<b>Curriculum Vitae</b>	<b>151</b>



# 1 Introduction

*In biology, DNA is mainly an informational material, while in colloid science, DNA is an excellent structural material due to its natural ability to self-assemble according to well-specified programmable rules. In this thesis, DNA - the molecule that carries life's genetic code - is used to link micron sized colloids in various arrangements, ranging from finite clusters to percolating structures, including two dimensional crystal structures. The assembly method relies on the attractive forces between complementary bases of two single DNA strands.*

## 1.1 DNA as smart glue

Deoxyribonucleic acid (DNA) contains the genetic instructions used in the development and functioning of all known living organisms and some viruses. The main role of DNA molecules is the long-term storage of information. DNA is often compared to a set of blueprints, a recipe, or a code, since it contains the instructions needed to construct other components of cells, such as proteins and ribonucleic acid (RNA) molecules.

Chemically, DNA consists of two long polymers, with backbones made of sugar-molecules and phosphate groups joined by ester bonds. These two strands run in opposite directions to each other. The double-stranded structure arises as the four types of molecules attached to the sugar-molecules, called bases (Adenine (A), Cytosine (C), Guanine (G) and Thymine (T)) form hydrogen bonds between the two separate chains (Figure 1.1). This type of binding, also called hybridization, is highly selective: a sequence of bases will bind strongly to the complementary sequence (A with T and C with G), but not (or to a lesser extent) to any other sequence.

The ability of single-stranded DNA (ssDNA) strands to form (hybridize into) a double-stranded DNA (dsDNA) structure can be used for the design of (nano)structures. By decorating building-blocks with pieces of ssDNA, one can direct building-block 1 to bind to building-block 2, but not to building-block 3. In this manner, one can link different building-blocks in a directed fashion by utilizing ssDNA strands as glue.

A hydrogen bond is a non-covalent bond. Two ssDNA strands held together with hydrogen bonds can be separated by increasing the temperature. At elevated temperatures, the hydrogen bonds are not strong enough to keep the two ssDNA strands together and the double helix will dissociate. At what temperature this transition takes place depends on the amount of hydrogen bonds between the two strands. As a measure of

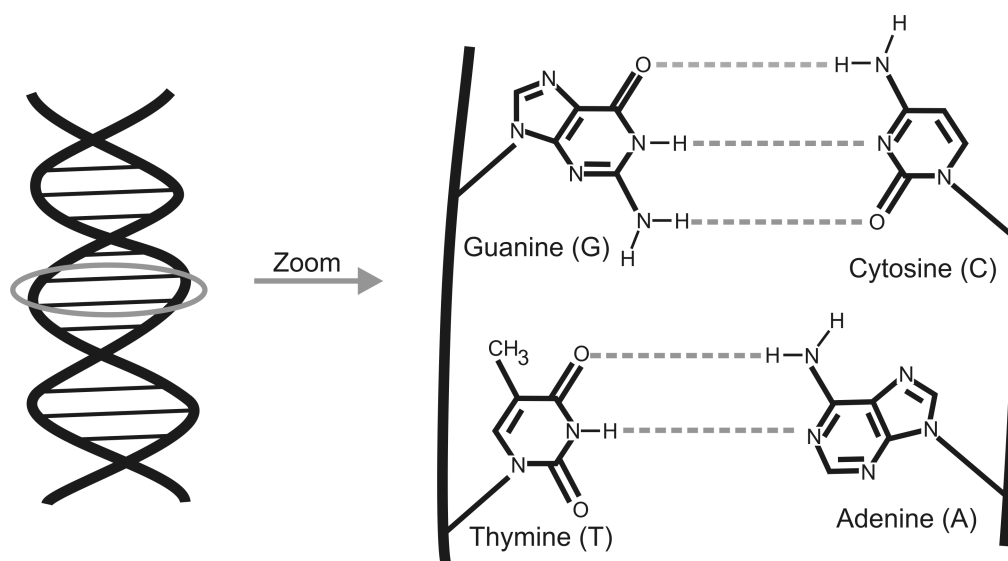


Figure 1.1: Schematic representation of double-stranded DNA. The zoomed in image shows the base pairing between the two single stranded (ss)DNA strands. Inter-strand bonds are non-covalent hydrogen bonds. Only complementary bases can pair: adenine with thymine and guanine with cytosine.

the binding-strength between two ssDNA strands, one can use the melting temperature ( $T_m$ ). The melting temperature is defined as the temperature at which half of the DNA strands are in the double-helical state and half are in the “random-coil” single-stranded states. Sometimes, it is also referred to as dissociation temperature. The fact that the binding process is highly specific and reversible makes DNA not only usable as glue, it also makes it a very smart one.

## 1.2 Colloids

To test if ssDNA strands can be used as a special glue for the design of (nano)structures we are in need of building-blocks. While DNA is advertised above as glue that can bind anything together, there are of course limitations to size and weight. Naturally, a single DNA helix cannot be used to glue a macroscopic object to a wall; the gravitational forces will be too strong. This means that in our search for building-blocks we are limited in size. To use DNA as glue we are looking for objects larger than atoms or small molecules, so we can handle them in the lab, but they have to be smaller than a grain of sand to meet the size-weight restrictions.

Luckily, there is a whole range of sizes in between that are covered by one class of materials: colloids. Colloids are very important in everyday life. There are numerous examples of colloidal suspensions that everyone knows of. One biological example is for instance milk. Milk consists of a watery suspension, with small fat droplets and protein clusters floating around (“dispersed”). Colloids are also abundant in many man-made substances, like paints, inks, and cosmetic products such as toothpaste and hand

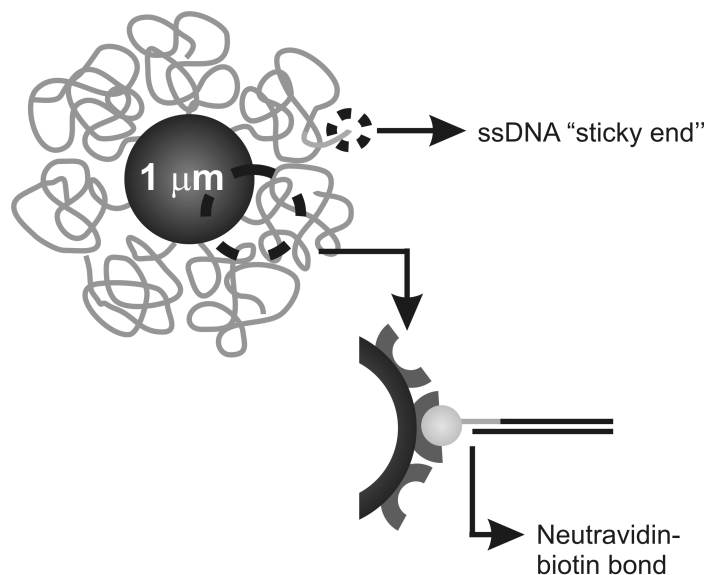


Figure 1.2: Schematic representation of a DNA coated colloid. DNA to colloid binding is realized by a biotin-neutravidin bond. Here an example is given of a colloid coated with a long dsDNA spacer and a 12 base ssDNA “sticky end”.

cream. All these products contain dispersed small objects inside another continuous phase. The typical size of a colloidal particle lies in the range of a few nanometers to several micrometers, perfect for our DNA-gluе.

Besides the size of colloids there is another main characteristic that is very useful for our study and that sets colloidal systems apart from other states of matter: Brownian motion [1]. Brownian motion refers to the random, continuous motion of microscopic particles, when they are suspended in a liquid. The movement is due to continuous collisions with the much smaller solvent molecules. Their perpetual motion gives colloidal particles the ability to explore many different configurations and therefore the ability to spontaneously organize, or “self-assemble”, into larger-scale structures when attractive forces are present.

### 1.3 The experimental system

For all our studies, we used micron-sized polystyrene (PS) spheres, fluorescently labeled and suspended in an aqueous buffer. As colloidal particles are sufficiently large and slow to be observed by straightforward optical techniques such as microscopy we can follow our particles in action. As we use confocal microscopy and our colloids are fluorescently labeled, it is even possible to resolve the three-dimensional structure and dynamics on a single-particle level [2].

The micron-sized polystyrene (PS) spheres are coated with a protein called neutravidin. Neutravidin is a truncated form of streptavidin. Streptavidin is known for its strong binding to biotin. By the removal of carbohydrates and lowering the isoelectric point, neutravidin results in a near-neutral protein that has significantly lower non-

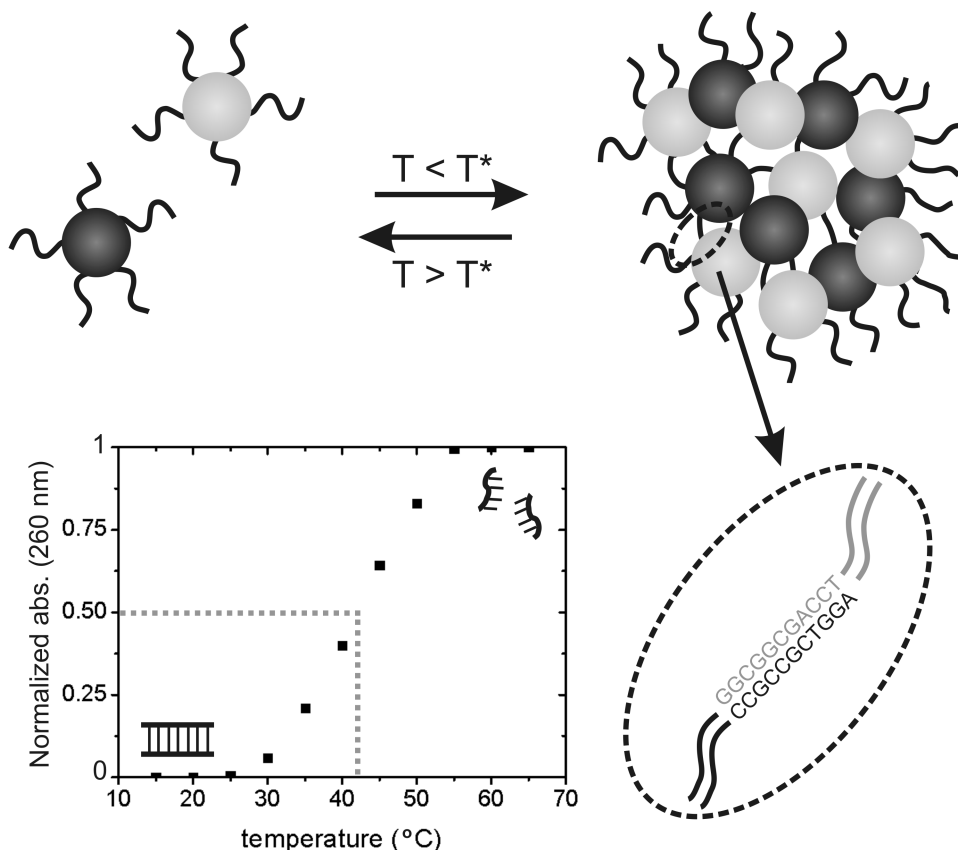


Figure 1.3: Schematic representation of DNA-driven assembly. The complementary 12-base ssDNA “sticky ends” hybridize below their melting temperature. Above this value, hydrogen bonds break and the system should (in principle) redisperse. The inserted graph shows the melting behavior of the 12-base dsDNA strand (without being grafted to a colloid) in solution. The gray dotted lines are a guide to the eye for determining the melting temperature of these ssDNA “sticky ends” ( $\sim 42^\circ\text{C}$ ).

specific binding than conventional streptavidin. We use the strong neutravidin-biotin bonding for grafting DNA to our colloids (Figure 1.2), to reduce interference of nonspecific interactions as much as possible. In this way, the main driving forces in the system are the hydrogen bonds formed between complementary ssDNA strands.

Colloids can be coated with DNA strands of any size. To be able to use DNA as glue, all or at least part of it has to be single stranded (“sticky”). Using very long sequences of ssDNA is not recommended as these strands are very flexible (the persistence length of ssDNA is 1 nm as opposed to 50 nm for dsDNA). The DNA strand can bend backward and attach to the colloid’s surface instead of binding with surrounding colloids. Therefore a double-stranded DNA spacer is used, which forces interacting linker segments of DNA away from the colloid, allowing for more efficient assembly (Figure 1.2). Many of the experiments described in this thesis use similar DNA. We mainly chose to work with a system of colloids displaying the same 12 base ssDNA strands as glue or “sticky end”, but with different lengths of spacer between the colloid and the “sticky end”.

For most experiments a “binary” system of colloids labeled with complementary DNA is used. Upon mixing below the melting temperature, complementary ssDNA ends will bind and hybridize forming larger aggregates of colloids (Figure 1.3). As the assembly is caused by non-covalent hydrogen bonds, heating the system above the DNAs melting temperature will (or should) redisperse the system to a monomeric state. The experimental melting temperature of the “sticky ends” used (in a TRIS-buffer) is measured and depicted in the inserted graph of Figure 1.3.

## 1.4 Outline of the thesis

The work presented in this thesis focuses on DNA-driven assembly of micron-sized colloids. Around the time this project started, the conceptually simple yet powerful idea that functionalized nanoparticles or micron sized colloids might serve as basic building-blocks that can be rationally assembled through programmable base-pairing interactions into highly ordered macroscopic materials already existed for almost ten years [3]. However, the theory of producing ordered DNA structures was well ahead of experimental confirmation. The approach had mainly resulted in polymerization, with modest control over the placement of and the distance between particles within the assembled material. Despite all the elegant pioneering work put in, most of the materials obtained thus far are best classified as amorphous [4–8]. So in the beginning, by using biological materials such as DNA, approaches were still developed to control the assembly of nano- or micron sized objects. However, in order to really turn this attractive approach into a technology, we have to understand the complexity of interaction in such hybrid systems.

Chapter 2 gives a brief overview of all the pioneering work done starting from the early days until mid 2009. A description is given of steps taken in one-, two-, and three-dimensional DNA-driven assembly and few applications are mentioned. Although the description is inevitably incomplete, it does put the work on DNA coated colloids in perspective and shows that there are still many hurdles to be taken in order to obtain all the theoretically predicted structures experimentally.

Chapter 3 describes the first experimental steps that we took to gain more insight into the behavior of DNA coated colloids. We noticed that most experiments directed their effort to short DNA strands, thus not exploiting its polymeric properties. In ref. [9] it is reported that long and flexible DNA strands can act as a spacer as well as a linker. This double function is believed to be a key ingredient in obtaining crystal structures (such as a diamond structure). Therefore, we started our experiments with a long DNA strand:  $\lambda$ -DNA. However, working with this polymer resulted in the formation of finite-sized clusters that do not redisperse, even well above the melting temperature of the DNA used. This suggests that the strong, short-ranged Van der Waals attractions in these systems are not fully shielded by steric and electrostatic repulsions.

In chapter 4 the study on long and flexible DNA strands is continued, in addition steps are taken to increase the obtained cluster sizes. Also some effort is put in obtaining a system that is able to redisperse well above the melting temperature of the DNA used. Considerably bigger colloidal aggregates can be obtained by reducing the length of the dsDNA spacer. To have a temperature reversible system all proteins on the surface of

the colloids have to be shielded. This is realized by using only short nucleotide overhangs instead of dsDNA spacers.

Chapter 5 takes a different approach on DNA-driven assemblies. Instead of a binary system of colloids in solution, here we report on the unique crystallization process of micron sized colloids above a DNA coated surface. Later tests indicate that although the surface does not need to be coated with DNA, the polymeric potential of the DNA is a crucial aspect for this type of crystallization.

In chapter 6 we take some first steps towards the realization of finite clusters with a fixed amount of colloids. By using a more exotic structure of DNA, a four-way or Holliday junction, preliminary experiments are performed towards stringing four colloids together with DNA.

Finally, as the first two experimental chapters mainly resulted in non-ordered gel-like structures unable to redisperse well above the melting temperature of the DNA used, the work of appendix A was directed towards stabilizing colloids. Stabilizing the colloids should result in more systems that are reversible with temperature, i.e. which can redisperse to a monomeric state above the melting temperature of the DNA used. Once formed, micron-sized systems with a dsDNA spacer in between the colloid and the “sticky end” remain clustered at all temperatures. In contrast, systems with the same DNA, but with smaller colloids (390 nm) are often redispersable. This indicates that Van der Waals attractions are an important factor to consider.

# 2

## DNA-driven assembly of colloids

*DNA-coated colloids constitute a completely new class of materials. Due to extraordinary control over the interactions between these colloids, in theory, completely new thermodynamically stable phases can be obtained, that cannot be realized with normal colloidal spheres that have a less specific interaction. In this chapter I describe the route taken towards the first experimental realizations of one-, two- and three-dimensional crystals and clusters. I also briefly discuss potential applications of these new materials.*

### 2.1 Introduction

DNA is the basic building block of life. As soon as the double-helix structure of DNA was discovered, the specific pairing of bases was suggested to be at the root of a possible mechanism to copy genetic information [10]. Indeed, hereditary information is encoded in the chemical language of DNA and reproduced in all cells of living organisms. The double helical structure is built up by two linear chains of four bases (adenine, cytosine, guanine and thymine) that are held together by a backbone of sugar-phosphate molecules. One sugar-phosphate group together with one base is called a nucleotide. Specific pairing of the Watson-Crick bases stack the nucleotides into a helical structure. The pairing of two single strands of DNA (ssDNA) into a double strand (dsDNA) via hydrogen bonds is called hybridization.

The simplicity of the ssDNA combined with the endless possible strand compositions, inspired the synthesis of artificial DNA strands. The ability to synthesize virtually any DNA sequence by automated methods [11] was realized in the mid eighties. As soon as DNA became readily available, its utility for the preparation of new biomaterials and nano-fabrication methods was soon recognized. The power of DNA as a molecular tool was enhanced even more when the ability to amplify any DNA sequence from nanomolar concentrations to macroscopic quantities by polymerase chain reaction (PCR) was discovered [12].

In the early nineties the first reports on using DNA as a building block, to create new materials emerged. Among the pioneers in this field of research were Seeman and coworkers [13–16]. They started by using branched DNA molecules to form specific motifs (small building units with specific sticky ends) that can assemble further [14]. Later more elaborate structures were realized, like cubes [15] or octahedra [16]. As DNA hybridization is a reversible process, solutions were found to lock structures once they were

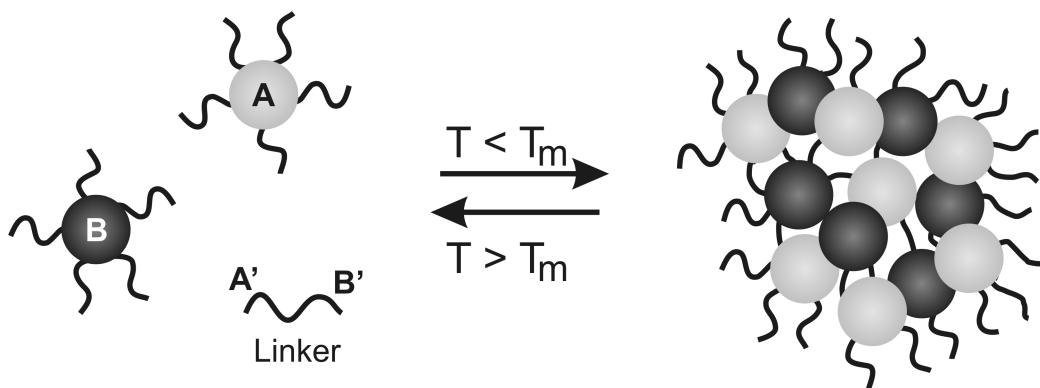


Figure 2.1: DNA-Driven assembly of colloids. Two types of ssDNA coated colloids with non-complementary ssDNA A or B are mixed together with the complementary A'B'-DNA linker. Assemblies arise below the dissociation or melting temperature ( $T_m$ ) of the DNA. As only hydrogen bonds are responsible for the binding, the process can be reversed. Above  $T_m$ , the colloids redisperse to their monomeric state.

synthesized [17]. At that time the theory of producing DNA structures was well ahead of experimental confirmation. It was much easier to design a structure on the computer screen, than it was to synthesize it. Fortunately, through the years experiments caught up with theory, with the experimental realization of more and more exotic structures [18–25]. To go into detail for all structures realized (ranging from geometrical objects to smileys) goes beyond the scope of this thesis. Instead we would like to focus on research in another direction, directly inspired by the realization of synthesizing basic shapes utilizing DNA hybridization.

Even before the time that the use of DNA as a building material emerged, the study of nanoparticle-based systems had evolved into a large (and growing) field of research [26]. These particles exhibit properties that are between those of a macroscopic solid or bulk material and those of a single molecule. The development of high-resolution imaging tools (e.g. transmission electron microscopy (TEM) and atomic force microscopy (AFM)) paved the way to the design of new states of matter from nano-scaled particle assemblies. To realize this, nanoparticles need to be organized in one, two or three dimensions, so that the electronic and optical coupling between the particles can be studied.

Initially, assemblies were mainly formed through covalent linkage of linear dithiols [27]. The disadvantages of this method are that the assemblies are formed irreversibly and the binding-process is difficult to control. Other attempts to assemble metal nanoparticles in well-defined structures include Langmuir-Blodgett techniques [28], molecular self-assembly by ligands [29] and electrostatic coupling to the deposition at pre-structured surfaces [30]. However, these methods suffer from a lack of binding specificity.

In contrast, biomolecules such as proteins and nucleic acids have almost perfect binding properties and biochemical functionality that have been optimized over billions of years of evolution. Self-assembly was already realized with systems of pure DNA.

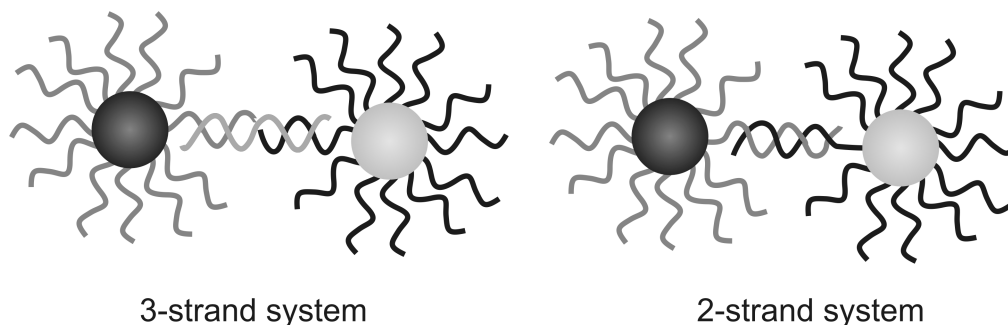


Figure 2.2: DNA-driven assembly can either be initiated by the addition of a linker DNA (3-strand system) or colloids can be coated with fully or partially complementary ssDNA directly (2-strand system).

In 1996 two important articles addressed the strength of DNA as specific glue between nanocolloids. In one of them it was first shown by Mirkin and coworkers that DNA oligonucleotides could be attached to nanoparticles to direct the formation of larger assemblies [3]. For this, the authors made use of a three strand system in which particles coated with ssDNA could only bind after introduction of a linker ssDNA complementary to the two particles types in solution (Figure 2.1). As hydrogen bonds between the complementary base pairs are responsible for the aggregation, increasing the temperature can reverse the process. The work of Mirkin and coworkers focused on the use of ssDNA coated colloids to detect specific linker sequences [3]. However, if the objective is to make specific colloidal assemblies, the use of a linker is not essential. By designing sequences on both species of colloids, that are partially or fully complementary a DNA linker is no longer needed, making it a two-strand system. Figure 2.2 shows both options. The prospect of designing three-dimensional (3D) structures that would self-assemble in a controlled and reversible manner marked DNA as a potential tool in designed self-assembly. Since then, the double-stranded helical structure of the DNA is key to its use in self-assembly applications, through exploiting its storage capacity to program self-assembly on a molecular scale.

Another article on DNA and nanoparticles appeared in the same issue of *Nature*. There, Alivisatos et al. [31] showed that the distance between particles can be manipulated by the sequence of DNA used. This is due to the long persistence length ( $\sim 50$  nm) of DNA, that allows the molecule to behave as a rigid rod at short distances. As nature provided us with a wide variety of specific enzymes that allow the processing of the DNA material with atomic precision and accuracy, an endless variety of strands can be produced that specifically recognize their complementary counterparts. No other (polymeric) material offers these advantages, which are ideal for molecular construction in the range from about 5 nm up to the micrometer scale [19]. Hence, DNA holds the promise of allowing a controlled bottom-up self-assembly of complex nano-devices. Because DNA is widely available at low costs, this molecule promises to be the material of choice in future nano-fabrication.

Since theoretical work indicated that crystal structure formation is possible by the use of a binary mixture of DNA-coated colloids [9], several research groups set their

goal towards obtaining these structures experimentally. Unfortunately, most (if not all) pioneering research of DNA-driven assembly of nanoparticles, mainly resulted in random aggregation, with modest control over the placement of the particles within the assembled material and the distance between them. That is, much of the materials obtained were best classified as amorphous clusters. One disadvantage of working with nanoparticles is that detailed structural characterization of all these systems is limited to TEM of dried samples. This is a significant issue, as drying effects may be responsible for the observed particle consolidation or aggregation [32, 33]. To circumvent this, a few groups shifted their focus to assemblies of micron-sized colloids, which can be characterized through optical and confocal microscopy [5, 6]. Micron-sized colloids were also used more and more, as lattice-spacings comparable to the wavelength of light are required to achieve photonic crystals in the visible range. Even though the possibility of forming crystal structures was theoretically predicted in the beginning of this century, it took some time to realize the first experimental crystal structures. In 2005 Crocker and coworkers [8] were able to obtain the first micron-sized (hexagonal) crystal structures. While the formed structures were crystalline, it only proved possible to grow relatively small crystallites. In the beginning of 2008 the first experimental nano-crystals with body-centered cubic (bcc) and face-centered cubic (fcc) symmetry were made [34, 35]. However, many of the other structures still remain illusive [9]. Apparently, DNA driven assembly is dependent on and controlled by many factors. To obtain a crystal, optimal conditions have to be realized.

Here we give an overview of the journey taken from the early work of Mirkin and coworkers on DNA-coated colloids as “detectors” of specific DNA sequences towards the first realizations of three dimensional crystal structures. A popular saying reminds us of the fact that sometimes the journey is more important than the (preset) goal. This could not have been truer in the case of DNA-coated colloids. As we take you along our journey, assemblies with various dimensionalities will be discussed, as will be the parameters that affect DNA assembly of colloids, to convince you of the enormous potential of this topic.

## 2.2 DNA-coated colloids

In the available literature, numerous ways to functionalize colloids with nucleic acids are described. In general, the connection between the colloid and the probe DNA consists of a binding group, a spacer and a piece of single-stranded probe-DNA. The spacer is needed to give the probe some freedom to explore its surroundings. Usually the spacer is just an additional stretch of DNA, either single or double stranded. The binding group depends on the type of colloid used. In principle any molecule can be used to bind the DNA to the colloid as long as the strength of this bond is much larger than the subsequent probe target binding. Below we will describe some of the most commonly used techniques to graft nucleic acids to colloids.

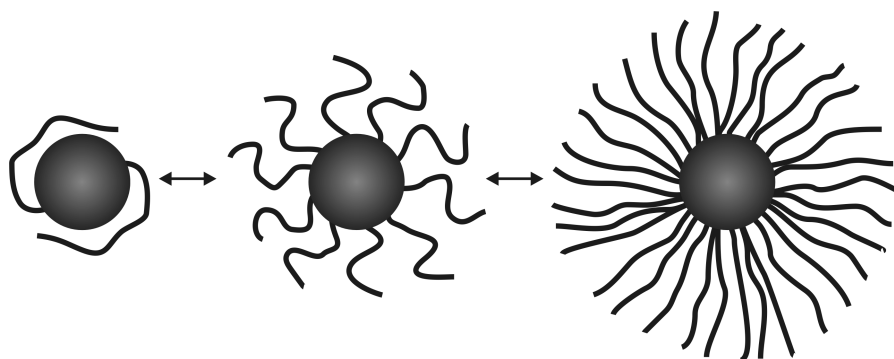


Figure 2.3: Cartoon of DNA-coated colloids with increasing grafting density. As non-specifically anchored DNA chains occupy a bigger volume, this type of binding is less frequent when a higher DNA surface density is used.

### 2.2.1 Synthesis of DNA functionalized nanoparticles

The solid-phase synthesis of DNA oligomers is nowadays routine technology, and DNA sequences up to 140 nucleotides in length, modified with a wide variety of chemical labels (such as amino or thiol groups) attached to the 5'- or the 3'-end, are readily (and commercially) available. These relatively short synthesized DNA strands are typically used in combination with nanoparticles, ranging in size from 3 to 30 nm (diameter). Most protocols nowadays use the same method as described in the early work by Mirkin and coworkers [3]. Briefly, metallic (mainly gold, but silver is also used [36]) nanoparticles are mixed with oligonucleotides functionalized with an alkylthiol group on one end. During incubation the thiol group will bind to the gold surface (Au-S binding). Unbound DNA is removed by centrifugation and subsequent removal of the supernatant. The resulting DNA-coated particles are water soluble and stable for months. With the use of magnetic microparticles (for magnetic separation) as templates, gold-Janus nanoparticles can also be obtained with two different lengths of DNA [37] with the longest length mainly present on one side of the particle (the longer strand is present (after ligation) on the side that was docked to the template microparticle with a linker molecule).

Although this preparation method can be used every time, some factors have to be taken into account. The ssDNA probe has some affinity to the metallic (mainly gold) surface of the nanoparticles. Besides binding specifically by means of the thiol binding group also non-specific binding is possible. Both experimental and theoretical researchers [38–40] attribute this type of binding to the amines in the purine or pyrimidine rings of the nucleotides. As non-specific adsorption complicates the control and interpretation of experimental studies (fraction of active probe unknown), this type of binding needs to be prevented as much as possible. One way to reduce the amount of non-specific bound ssDNA is to treat the samples with mercaptohexanol after the adsorption step. Herne and Tarlov [41] came to this conclusion after comparing the adsorption of thiol functionalized ssDNA versus untreated ssDNA by X-ray photo-electroscopy. Choosing the sequence of the ssDNA spacer wisely also reduces the chance of high amounts of non-specific bound ssDNA strands. The Mirkin research group [42] tested the binding

affinity of the four deoxynucleotides (dA, dT, dC and dG) to gold surfaces. Using a colorimetric assay they found that deoxynucleotide dT has by far the lowest non-specific binding affinity. As the free amines of the nucleotides are held responsible for the non-specific attraction, this finding can easily be understood as dT contains only one free amine, whereas the other nucleotides contain more. Thus, DNA spacers high in dT minimize non-specific adsorption. Another simple technique to reduce the fraction of non-specifically bound ssDNA is to increase the grafting density (Figure 2.3), as non-specifically anchored chains occupy a larger surface area. Adsorption of an excess of thiol-functionalized ssDNA at high salt concentrations facilitates an increase in grafting density [43], as the salt screens the negative charge along the DNA backbone, allowing them to come closer to each other.

For many applications it is essential to be able to quantify the coverage of the DNA on the particles surface. To achieve this, a fluorescence based assay [43] or a PCR method [44] can be used. DNA coated nanoparticles with low surface density can even be purified by gel electrophoresis, separating particles with one to six DNA strands from each other [45–47]. The ability to isolate nanoparticles, with low and well-defined grafting densities is important, because in the low grafting-density regime the number of DNA strands per particle, significantly affects how the particles interact. Instead of binding in every direction, as particles with a high grafting density, at low grafting densities only specific angles are open for binding. The effective “chemical valence” of a DNA-coated colloid (i.e. the number of ssDNA’s available for linking to other colloids) is very important, as the valence controls the width of the gas-liquid coexistence region [48–51].

Niemeyer and coworkers reported the synthesis of “oligofunctional” DNA particles [52]. These particles had a number of different strands ranging from two up to seven. With these particles the specificity of DNA can be optimally used, as multiple binding possibilities are present.

## 2.2.2 Synthesis of DNA functionalized micron-sized colloids

To obtain DNA-functionalized micron-sized colloids with short pieces of DNA, the same commercial strands can be used as described above. To obtain colloids grafted to longer DNA strands, plasmid DNA (obtained from bacteria) provides a good alternative [53, 54]. In general three different grafting methods are used to attach the DNA to the colloids: avidin-biotin linking, water-soluble carbodiimide linking or a polymer swelling/deswelling method.

### Avidin-biotin chemistry

The biotin-avidin system is the strongest non-covalent biological interaction known, having a dissociation constant,  $K_d$ , in the order of  $4.10^{-14}\text{M}$  [55]. The bond forms very rapidly and is stable over a wide range of pHs and temperatures [56, 57]. The strength and the specificity of this interaction led it to be a favorite choice to graft DNA to colloidal particles especially since polystyrene colloids, coated with neutravidin (a special form of avidin) are commercially available. The neutravidin protein differs from avidin and streptavidin in that it has been specially processed to remove carbohydrates

and to lower the isoelectric point, resulting in a near-neutral protein that has significantly lower nonspecific binding than conventional avidin. The grafting method is very similar to the one used for coating nanoparticles. Neutravidin coated colloids are mixed with a solution of biotin-labeled DNA. During incubation, biotin will bind to the avidin of the colloids. Unbound DNA is removed by centrifugation and subsequent removal of the supernatant. Additionally, the DNA-colloid solution is heated to 50 °C to remove non-specifically bound biotin.

### **Water-soluble carbodiimide chemistry**

As stable as the biotin-avidin link is, it remains a non-covalent bond. At high temperatures in non-ionic aqueous solutions, the biotin-avidin interaction can be reversibly broken [58]. Although experiments with DNA-coated colloids are never performed in nonionic solutions, some researchers nevertheless prefer a covalent link to a non-covalent one.

A convenient way to covalently link DNA to colloids is by use of water-soluble carbodiimide chemistry. This involves a two-step mechanism. First, carboxyl-functionalized colloids are activated by adding 1-ethyl-3-(3-dimethylaminopropyl) carbodiimide (EDC). The EDC facilitates the formation of amide linkage between the carboxylate group and the amine group without leaving a spacer molecule, by transforming the carboxyl-group to a nucleophile reactive intermediate [7]. Second, amino-labeled DNA is added to the reaction medium. This molecule attaches to the spheres by an amide bond. As an amide linkage has a much smaller molecular footprint than bulky proteins like neutravidin, a higher surface density of DNA can be achieved.

Despite the apparent simplicity of this method, covalent linkage is technically more difficult and time-consuming than protein binding. More reaction steps are required and often colloids aggregate into small clusters before DNA strands are added.

### **Swelling/deswelling-based chemistry with PEG modification.**

As the covalent coupling method described above can be pre-empted by colloid instability in commonly used buffers and as the use of protein-free systems can be advantageous, a third method of obtaining DNA-grafted colloids was introduced [59]. This method was directly inspired by polymer-protein modifications to improve protein stability [60]. To obtain colloids grafted with DNA, but stable over a wide variety of conditions, triblock-polymers are used to attach the DNA to the colloids. Briefly, triblock copolymers are adsorbed onto the surface of the colloids. Then a small amount of organic solvent is added to swell the colloids. By “liquefying” the colloid, allowing the hydrophobic block of the polymer to penetrate the surface [61], anchoring is possible after deswelling (remove organic solvent by heating). The exposed hydrophilic blocks of the triblock copolymer can readily be labeled with DNA.

The main advantage of this preparation method is that subsequent stabilization by surfactants or polymers is not needed. An assembly of DNA-grafted micron-sized colloids cannot as simply be redispersed by thermal denaturation as an equivalent system of nanoparticles. Obviously, size is a parameter that affects the interactions between

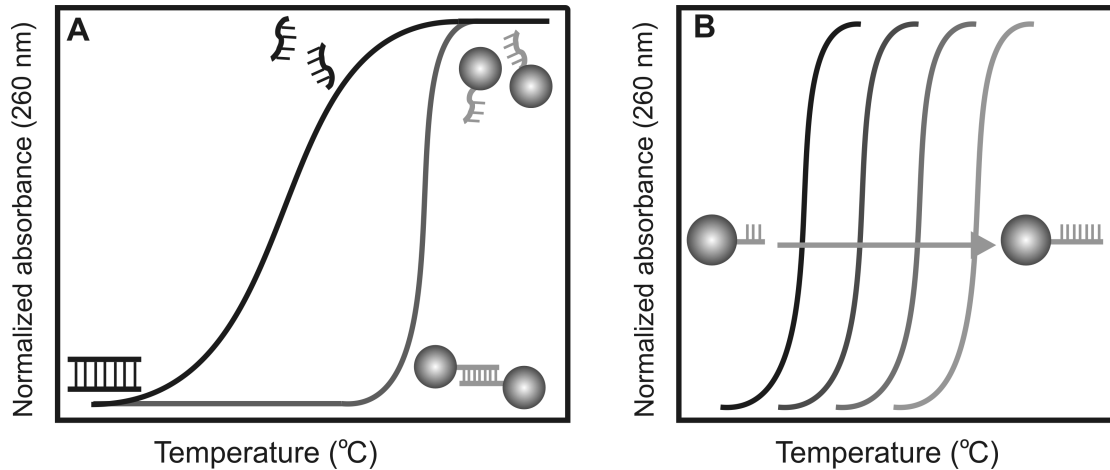


Figure 2.4: Cartoons of dissociation curves of DNA-coated colloids. A: The dissociation of DNA grafted to colloids follows a much more narrow curve than DNA free in solution [4]. B: The number of bases used for the “sticky ends” determines the melting temperature. The more bases the higher the dissociation temperature will be [62].

colloids. In particular, strong Van der Waals interactions can lead to irreversible, non-specific binding. Crocker and coworkers [6] gave an overview of interactions that are important in micron-sized systems. Between DNA coated colloids there is an attractive part,  $U_{dna}$ , due to inter-particle DNA hybridization, a steric and/or electrostatic repulsive part,  $U_{rep}$ , and a strong Van der Waals interaction,  $U_{vdw}$ , at short distances. Control over aggregation and temperature reversibility requires a subtle balance between  $U_{dna}$  and  $U_{rep}$ . For micron-sized colloids, two strategies may be adopted to obtain aggregation reversibility: decreasing  $U_{dna}$  by decreasing the surface density of probe-DNA or increasing  $U_{rep}$ . The latter approach can be achieved by adsorbing polymer stabilizers onto the colloids.

## 2.3 Phase behavior of DNA-coated colloids

The properties of materials formed by the self-assembly of DNA-coated colloids are affected by a number of parameters. The ones judged most important are: the number of base-pair matches, which tune the strength of the attraction between colloids; the grafting density of the DNA strands to tune the strength of  $U_{dna}$ ; the ionic strength of the surrounding medium, which shields the repulsion between negatively charged ssDNA strands and the length of possible spacers connecting the “reactive” single-stranded DNA (ssDNA) to the colloids. Below we give a brief overview on the effects these parameters have on the phase behavior of DNA-coated colloids.

### 2.3.1 The number of base-pair matches and spacer length

The strength of the attraction between colloids can be tuned by the number and type of base-pair matches between colloids coated with complementary ssDNA strands. The Watson-Crick base pairs are not of equal strength. The three hydrogen bonds between a G-C base pair impart greater stability than the two of an A-T base pair. Thus, increasing the G-C content raises the melting temperature at which complementary strands dissociate. The strength of the bond between a pair of nucleotides is also influenced by the chemical nature of the neighboring base pairs. For instance an A-T surrounded by G-C pairs has an enhanced stability. Predicting the DNA duplex stability from the base sequence is possible [63].

Increasing the number of base matches also raises the melting temperature. Crocker et al. [5] found in 2003 that lowering the number of matching base pairs leads to a decrease in melting temperature (Figure 2.4b). Later, other researchers came to the same conclusion [62, 64]. Thorough research on the effect of the number of base pairs on the melting temperature, showed two interesting results. First, linker sequences (3-strand system) with an uneven number of base-pair matches have a slightly lower melting temperature than a linker with one base less would have. DNA free in solution does not display this behavior [64]. It is believed that in DNA-linked nanoparticle assemblies, duplexes with different lengths introduce binding energy disorder and, therefore, slightly lower the stability of the system.

Second, the length of spacer in between the colloid and the probe also influences the melting temperature. Increasing the spacing between adjacent colloids (by increasing the spacer length), leads to higher melting temperatures of the assemblies [65].

Above, one difference between DNA free in solution or grafted to colloids is mentioned. There is another, very important one: the melting curve associated with aggregation of colloids is narrower than the melting curves of DNA without nanoparticles (Figure 2.4a) [65, 66]. While all research groups report comparable melting behavior, different physical mechanisms are held responsible for it. Mirkin and coworkers [4] claim that inter-particle bridges influence each other. The breaking of bridges lowers the local salt concentration, which leads to destabilization of neighboring bridges. This cooperativity is translated into a narrowing of the melting curves. Lukatsky and Frenkel [67] consider the influence of local salt concentrations as less important. Instead their theory stresses the importance of entropic effects on the sharpness of the melting curve in DNA-coated colloid systems with multiple bonds.

### 2.3.2 Probe-DNA density on the colloidal surface

Specific interactions are obtained through DNA hybridization. With most types of binding, the strength of binding increases with the number of bonds made. The same is true for DNA-coated colloids. With an optical tweezers set-up the force of interaction between two DNA coated colloids can be measured directly [68]. Different DNA densities give different strengths of interaction. So by playing with the DNA density a preferred interaction can be found. As a high DNA surface density on the colloid is advantageous in terms of particle stabilization, especially for (gold) nanoparticles at elevated salt con-

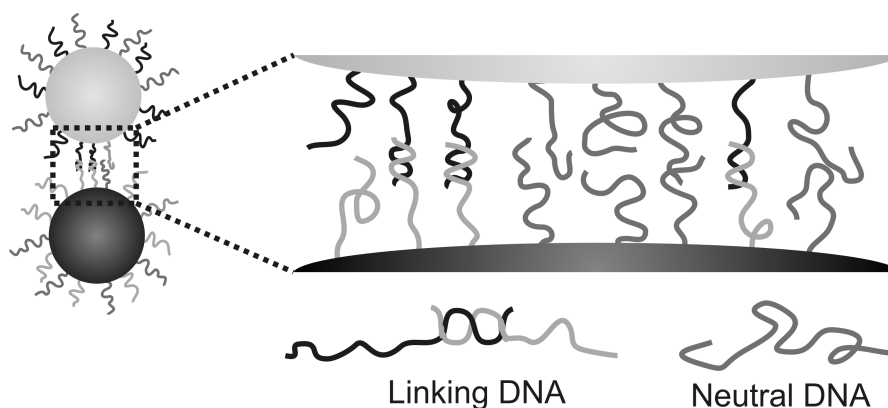


Figure 2.5: Cartoon of zooming in on two colloids coated with both complementary (linking) DNA and non-complementary (neutral) DNA. Using this approach, the “effective” valency of the colloids can be varied, while keeping the grafting density constant

centrations [3]), colloids are usually coated with a combination of binding (probe/linker) and non-binding DNA strands (neutral; Figure 2.5). Biancaniello et al. [69] examined the aggregation behavior of micron-sized colloids for different percentages of hybridizing strands. They found that the affinity between complementary DNA strands in a single duplex is too weak to promote adhesion between colloids of this size. Increasing the probe-DNA concentration 10-fold led to an onset of aggregation, but in their system at least 33% of all DNA on a colloid must be probe-DNA to obtain a system in which all colloids are hybridized. Besides controlling the sizes of obtained aggregates by varying the percentage of probe-DNA [70], also the melting temperature is directionally proportional to the probe-DNA surface density (for short DNA tethers) when the colloid and target concentrations are kept constant. Lowering the density leads to a decrease in melting temperature and a slight broadening of the melting transition [4, 62]. Valignat et al. [6] used a different approach to reduce the number of hybridizing events between two neighboring colloids. They coated their colloids with DNA and an inert polymer. By increasing the length of the stabilizing polymers, colloids were held further apart, thereby reducing the number of possible links. Besides polymers, also dsDNA can be used as stabilizing polymers. With the help of restriction enzymes, appropriate lengths can be created [71]. Again the same relation was found: the existence of fewer links reduces the melting temperature significantly. Only recently it was found that strands neighboring the hybridized bridge in between two colloids, can additionally stabilize the aggregate by non-perfect base pair matching, known as “slipping” [72]. As this type of binding is difficult to interpret, one may choose to prevent them from happening. Diluting strands can help to prevent this type of binding.

### 2.3.3 Ionic strength in surrounding medium

As the backbone of DNA consists of negatively charged sugar-phosphate groups, ssDNA has a net negative charge. To allow close proximity necessary for duplex formation, counter-ions are needed. Adding some salt to the medium is a simple method to increase

the affinity between complementary strands and to prevent later helix dissociation. Already in one of the first studies on micron-sized DNA-coated colloids [5] it was discovered that colloids aggregate faster if the salt concentration was increased. In principle one can speak of two distinct regimes of aggregation kinetics. At low salt concentrations aggregation is shown to be dependent on the rate of duplex formation between colloids, i.e. reaction limited. At higher salt concentrations, aggregation behaves diffusion-limited as it depends on the rate of diffusion of the colloids [73]. Biancaniello et al. [69] were the first to obtain a phase diagram for DNA-functionalized microspheres as a function of salt concentration. They found that to obtain a fully aggregated system a minimum of 100 mM NaCl was necessary. Intermediate concentrations (25-75 mM) led to a system containing small aggregates and monomers, while a homogeneous fluid phase, consisting of dispersed microspheres, was seen for salt concentrations below 20 mM. The absence of or incomplete DNA-mediated colloidal aggregation at low salt concentrations is attributed to dominant electrostatic repulsions. The appearance of larger aggregates at higher salt concentrations was also reported by Jin et al. [4], who studied (gold) nanoparticles.

Besides controlling the speed and size of aggregation, the melting temperature is also affected by an increase in salt. As the double helix is more stable in the presence of counter ions, the melting temperature increases with increasing salt concentration [4].

## 2.4 Assemblies of DNA-coated colloids

DNA-driven assembly of colloids can be classified into three main categories: One-dimensional (1D), two-dimensional (2D) and three-dimensional (3D) assembly. 1D assemblies include long chains, which lead to the formation of nanowires. With a future as nano-electronics, wires are most useful when made from metal or magnetic material. That is why this type of assembly is only performed with nanoparticles. 2D assembly of DNA coated colloids leads to sheets of particles above a surface. Last, 3D assembly leads to a range of structures, from finite to percolating and from ordered to amorphous. The latter categories are used for both nano- as micron-sized colloids.

### 2.4.1 One-dimensional assemblies

In the same issue in which Mirkin introduced the concept of DNA assembly, Alivisatos and coworkers [31] showed that a discrete number of nanoparticles can be assembled along the backbone of DNA. They were able to align the particles with distances of 2 or 6 nm apart, depending on the direction of assembly (head-to-head or head-to-tail). These nanoparticle-DNA conjugates have a high flexibility when the backbone is nicked, while an un-nicked (backbone without a discontinuity) in the double helix significantly lowers the flexibility [74]. Though an elegant approach, it has thus far proven to be a difficult task to assemble the particles in direct contact to each other over extended domains with an inter-particle spacing that is identical and small enough to allow direct dipolar coupling or even electronic transport along the array. Noyong et al. [75] have reported the synthesis of a string-of-beads alignment of 4 nm gold nanoparticles along DNA strands. To achieve identical inter-particle spacings they make use of cisplatin, a

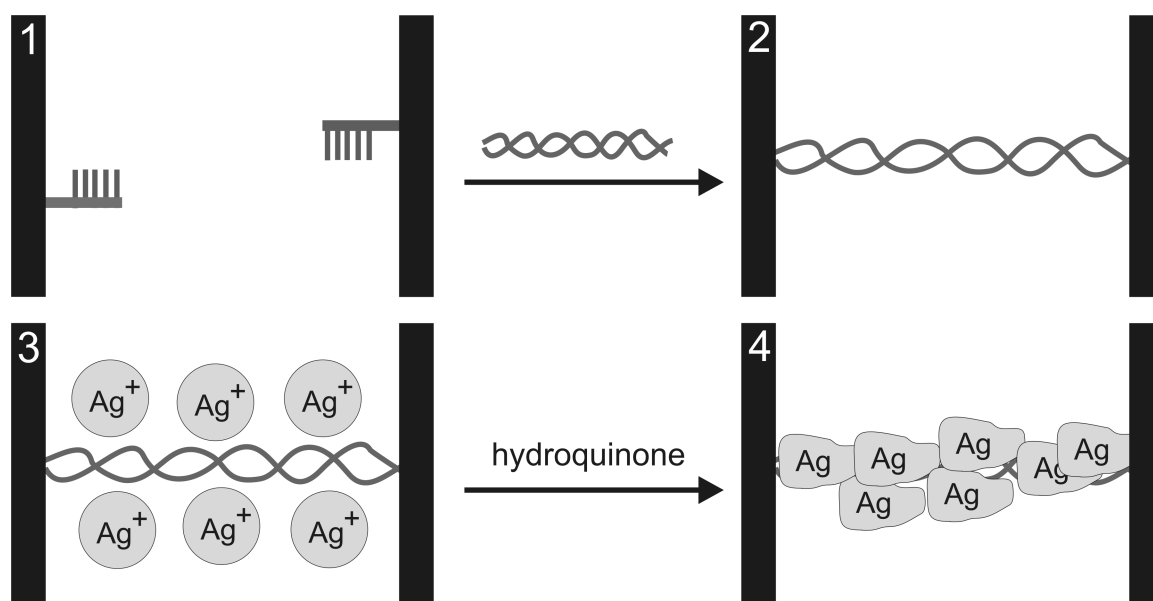


Figure 2.6: A schematic representation depicting the construction of a nanowire via direct metallization. The walls of a 12-16 micrometer wide gap are coated with ssDNA (1). Addition of a dsDNA solution bridges the gap (2). After adding a solution containing silver-ions, these positively charged ions will bind to the negative DNA (3). Hydroquinone induced reduction of the added silver salt, leaves nanoclusters associated with the DNA wire template (4). Images are not to scale.

platinum complex with high affinity for neighboring guanine-guanine nucleotides. Cysteamine stabilized nanoparticles can then selectively bind to the platinum center by exchange of the  $NH_3$ -ligands with  $NH_2$ -groups of the ligand shell. While small particles have a greater potential to serve as building blocks in future nano-electronic devices due to their enhanced charging energy, Hutchinson and co-workers have elaborated a method to organize 1.5 nm gold nanoparticles into linear chains with precisely controlled inter-particle spacings [76]. In this configuration, the spacing between two neighboring nanoparticles is determined by the thickness of the ligand-shell and can thus be varied.

Another method to obtain one dimensional assemblies is the direct metallization of DNA. This method (the metallization by metal-ion reduction) has successfully led to the formation of highly conductive nanowires, which could be applied as metallic interconnections. The use of DNA as a template for the generation of silver nanowires [77] is depicted in Figure 2.6. The 12-16  $\mu m$  gap between two microelectrodes was bridged by a nucleic acid attached with its two ends to complementary thiolated nucleic acids associated with the microelectrodes. Ion exchange of the phosphate counter ions, followed by the hydroquinone induced reduction of the ions resulted in silver nanoclusters associated with the DNA wire template. The subsequent catalytic enlargement of the  $Ag^0$  nanoclusters using an acidic  $Ag^+$  hydroquinone solution resulted in the formation of continuous  $Ag^+$  nanowires that were ca. 100 nm wide. Related methods were applied to synthesize other metal nanowires such as platinum [78], palladium [79] or copper [80]. However, all nanoparticles formed during such processes suffer from an extraordinarily

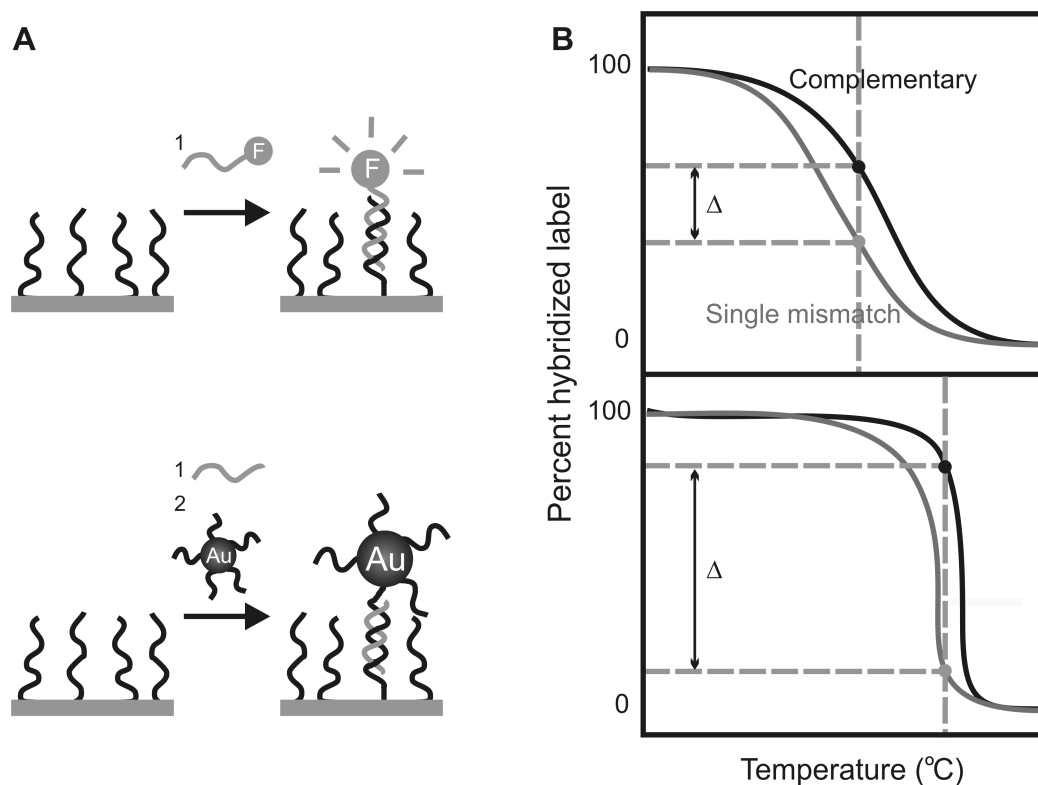


Figure 2.7: DNA mismatch detection with DNA coated colloids compared to detection with conventional fluorophores. A: Cartoon both of the fluorophore-labeled and the colloid-labeled ssDNA binding to the complementary strands on a flat support (e.g. DNA-array). B: Adsorption intensity of dsDNA at 260 nm as function of temperature. At a given temperature the difference between the number of complementary strands hybridized to perfect ssDNA and that to one with a single mismatch is far bigger for a system with DNA coated colloids.

broad size distribution. Thus the metal structures along the DNA wires are highly disordered and none of the size-specific electronic transport properties, which are based on single-electron tunneling, could be observed or even utilized in nanodevices so far.

### 2.4.2 Two-dimensional assemblies

Besides arranging nanoparticles in a 1D-fashion on a DNA strand, attaching oligonucleotides to a solid support to obtain two dimensional assemblies also attracted much attention. Surface-bound ssDNA was initially used to detect specific DNA sequences or to detect single-nucleotide mutations within a DNA sequence [81, 82]. Later, DNA-coated colloids were also attached to a surface for a more material-oriented goal.

Many groups have reported the DNA-directed immobilization of gold nanoparticles to form supramolecular surface architectures. This way of assembly led to the first application of DNA coated colloids. The specific nucleic-acid mediated immobilization of gold nanoparticles can be utilized for the topographic labeling of surface bound DNA targets

[83]. This readily allows the highly sensitive scanometric detection of nucleic acids in DNA-chip analysis. Oligonucleotide array technology depends on the quantitative detection of target DNA hybridized to complementary array elements. Mirkin and coworkers [82] reported a “scanometric” method for detecting DNA targets via hybridization of 13 nm gold nanoparticles to an array functionalized with various oligonucleotides (Figure 2.7a,b). Because of the unusually sharp temperature-induced “dissociation” or melting profiles of the nanoparticles from the surface of the array, the selectivity of the scanometric DNA detection system is intrinsically higher (by a factor of 4) than that of a conventional array system based upon fluorophore probes (Figure 2.7a,b). In addition, enlarging the array bound nanoparticles by gold-promoted reduction of silver permitted the arrays to be imaged, in black and white by a flatbed optical scanner, with 100 times the sensitivity typically observed by confocal fluorescent imaging. Later, the same group found that different sizes of nanoparticles can be used to identify two target sequences in solution, due to their size-selective light scattering [84]. Besides using silver, the use of colloidal gold nanoparticles also allows a signal enhancement in the DNA hybridization detection by means of a quartz crystal microbalance [85, 86], dendritic amplification [87], angle dependent light scattering [88] and surface plasmon resonance [89]. A very sensitive method to detect target DNA is the combination of localizing nanoparticles in an electrode gap and silver deposition. This leads to readily measurable conductivity changes and is able to measure concentrations as low as 500 femtomolar with a point mutation selectivity factor of  $\sim 100.000:1$  [90, 91]. Recently, a detection limit of 1 femtomolar was claimed by using thiolated detection-probe-conjugated nanoparticles that exhibit a high level of unblocked active sites. These sites are easily accessed by p-nitrophenol and  $\text{NaBH}_4$ . Electroactive p-aminophenol is generated at these sites and is then electro-oxidized to p-quinoneimine at the electrode. The p-aminophenol redox cycling by  $\text{NaBH}_4$  offers large signal amplification [92]. DNA mismatch detection depends on (mismatched) DNA strands to dissociate at a lower temperature than the perfectly complementary strand [93].

Immobilizing nanoparticles onto a surface is used for a more material-oriented goal as well. As the “bottom-up” approach in which small molecular building blocks self-assemble to form larger devices, gave irregular shapes in three-dimensional assemblies, the two-dimensional approaches gained more attention [94, 95]. By imprinting surfaces with specific areas (complementary DNA strands) and non-specific areas, site-selective immobilization of gold nanoparticles functionalized with DNA-oligomers was realized [94–97]. Instead of these surfaces, also a DNA grid can be used to arrange nanoparticles into square periodic lattices, resulting in a uniform layer of distributed nanoparticles organized with precise control on inter-particle distance [98, 99]. By coating nanoparticles with multiple DNA strands [52], a next step towards 2D assembly for novel materials can be made. Now one of the strands can be used to immobilize particles onto a surface, while the other type of DNA strand is still available. This one can be used to establish cross links between the particles [100]. By changing the length of the DNA used, the inter-particle distance should be adjustable. Indeed, bifunctional DNA-modified gold nanoparticles at solid substrates generates particle layers with programmable interparticle spacing [101].

While working with DNA oligonucleotides grafted to a surface it is important to graft them well. Non-specific binding of neutravidin proteins to the surface in combination with biotinylated DNA strands can lead to problems as forces above 2 pN per bond can rip the neutravidin from the substrate [102]. The way of surface coating can also lead to surprising effects. A recent study on immobilizing micron-sized colloids onto a DNA-functionalized surface reported the existence of “floating” crystalline 2D membranes above the surface. In this study it seems the polymer alone was sufficient to obtain these structures [103]. Two-dimensional sheets were also formed with nanoparticles dried within a grid [104]. Also in this case, Watson-Crick base pairing is not responsible for the assembly. But whereas the micron-sized colloids were closely packed, the nanoparticles are further apart, with distances depending on the DNA length used.

### 2.4.3 Three-dimensional assemblies

Following the initial approach of Mirkin’s group, DNA hybridization has been used to generate repetitive, three dimensionally linked nanoparticle assemblies (Figure 2.1). As there are numerous reports on nanoparticles as well as micron-sized colloids, we split the two subjects to avoid confusion.

#### Three-dimensional assemblies of nanosized particles

The assembly scheme of Mirkin and co-workers [3] can also be used for the generation of binary networks comprised of different particle sizes. Due to the specificity of Watson-Crick base-pairing, only heterodimeric “A-B” composites of alternating particles are formed [105]. By playing with the ratio between the two sizes used (8 and 31 nm) different aggregates can be attained, ranging from random to satellite structures (one big colloid coated with smaller ones). Ten years after realizing satellite structures, bigger particles can now also be coated on one side only, creating so called “Janus particles” [106]. While experimental efforts do not go beyond binary networks, simulations already studied the aggregation behavior of four different DNA coated particles [107]. In that case a hexagonal crystal can be formed with two alternating bands containing two of the four possible particles.

Ever since it was found that the optical properties of DNA-linked nanoparticle assemblies are governed by aggregate size, regardless of the oligonucleotide linker-length [108], efforts concentrated on controlling this size. A solution was soon found: the extent of aggregation can be controlled by the addition of ssDNA oligomers to an aggregating colloid of the gold nanocrystals modified with complementary strands of DNA. The ssDNA oligomers rapidly form duplexes with the immobilized DNA and the aggregation process can be instantly terminated. Depending on the time of addition of the ssDNA oligomers, this enables one to limit the size of the aggregates formed [73].

The elaborate research done on the phase behavior of these particles, as described before (section 2.3), led to a broader understanding of the colloids and resulted in the first crystal structures of DNA coated nanoparticles [34, 35]. Later, a phase diagram was presented, showing the relation between the ratio of linker DNA to nanoparticles and the volume fraction of particles [109]. In addition to the reasons addressed in the former

section, also complete temperature control seemed of crucial importance. In 2001 it was already found that the thermodynamically most stable assemblies are formed upon heating of the kinetically controlled adducts [110]. Both research groups that obtained these crystal structures stress this point in their article. DNA self-assembly is always accompanied by a competition between the entropic and enthalpic contributions involved in the assembly process at different temperatures. From an entropic standpoint, a close-packed structure is favored over a non-close-packed structure, because the entropy of the entire system can be maximized if the nanoparticles possess the largest possible local free volume [111, 112]. Therefore, it is vital that particles begin to assemble near the melting temperature of the DNA. Here the binding strength is very weak and the enthalpic contribution is small. The assembly process will be dominated by the entropic contribution and thus a close-packed structure forms. However, if the particles are combined several degrees below the melting temperature, the enthalpic contribution will govern the assembly process and a non-close-packed structure forms that maximizes the number of DNA hybridization events.

Besides the most common type of DNA hybridization (double helix), also more exotic DNA structures are used to obtain DNA-driven assembly. DNA can form numerous structures depending on the strands and/or condition used. Examples include G-quadruplexes, a square arrangement of guanines (a tetrad; Figure 2.8a), stabilized by hydrogen bonding; i-motifs, based on intercalated C-C<sup>+</sup> base pairs (Figure 2.8b) and Holliday junctions (see chapter 6), a cross-structure of four DNA strands. Two different research groups used “G-quadruplexes” rather than the double helix to aggregate particles [113, 114]. This DNA-structure depends on the concentration of a cation like Na<sup>+</sup> or (to a lesser extent) K<sup>+</sup> in solution. The “i-motif” was used to self-assemble DNA coated colloids as well [115, 116]. With this DNA structure the pH is responsible for switching between the bound and unbound state, instead of the temperature. Seeman and co-workers [117] used a Holliday structure in combination with nanoparticles to estimate the structural integrity of a combination of 3 to 4 junctions, realizing the first quartet of particles stringed together. Recently, DNA tubules decorated with gold nanoparticles were obtained by closing up 2D DNA tiles [118].

### Three-Dimensional Assemblies of micron-sized colloids

Seven years after the initial DNA-driven assembly experiment of nanoparticles, assemblies of micron-sized colloids were realized as well. Before the first crystal structure was obtained experimentally, Ratna et al. [119] already looked ahead. As spherical colloids can only make “simple” cubic structures, they asked themselves whether one can build complex super lattices by first building a mesoscale sub cell [120]. By using specific diameter ratios between the colloids used (0.23 and 0.42) they were able to construct either a tetrahedron or an octahedron [119]. Both were found, but with an estimated yield of 20% also larger aggregated assemblies were present. While Ratna et al. [119] needed different sized colloids, simulations suggests that equal-sized colloids can also aggregate into geometrical objects [121]. The second study on micron-sized DNA coated colloids [5] was not based on creating finite sized clusters. By mixing two different sizes of colloids only heterodimeric “A-B” composites of alternating colloids are formed. The

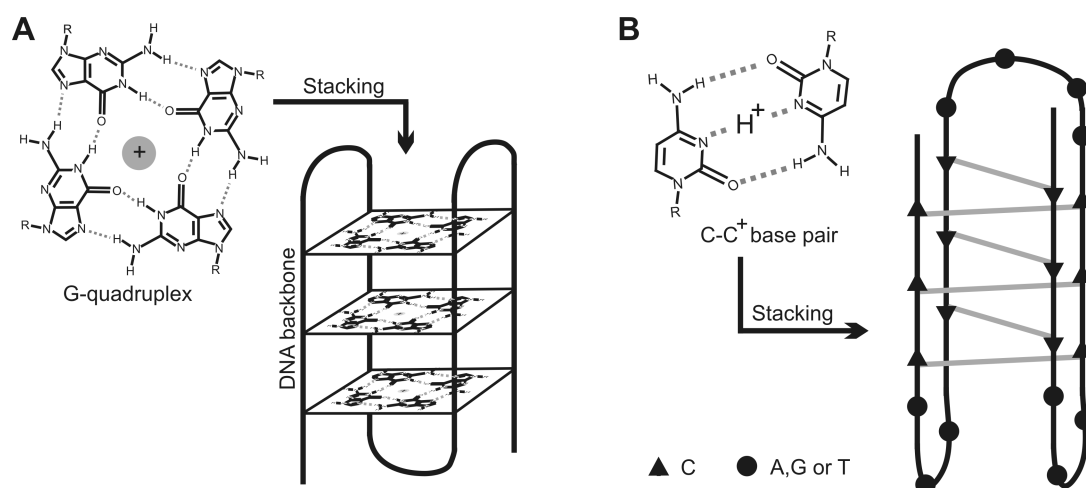


Figure 2.8: Exotic DNA structures. A: G-quadruplex: four guanines bind via hydrogen bonding. The resulting squares are stacked as depicted in the figure. B: I-motif: a strand with a high number of cytosines can make hydrogen bonds between these nucleotides at low pH.

clusters obtained were strand-like aggregates that were temperature stable due to reasons discussed earlier. Two years later, the first temperature reversible systems were reported [6, 7]. As creating a system that is reversible with temperature proved more difficult for micron-sized colloids than for nanoparticles, other techniques were explored to obtain a reversible system. For example, Tison and Milam [122] used competing ssDNA strands to break up assemblies of DNA coated colloids.

Due to the difficulties to obtain appropriate temperature control, it came as a surprise that crystals of micron-sized colloids were experimentally realized before obtaining one made from nanoparticles [8, 123, 124]. Crocker and coworkers were able to grow small hexagonally stacked crystals of micron-sized DNA coated colloids. They proposed that besides temperature response also the surface of the colloids used was of vital importance [123]. The creation of these crystals by Crocker and coworkers was a *tour de force* as most systems of micron-sized DNA-coated colloids get stuck in a non-ordered structures [6, 7, 53, 54, 69]. In fact, most of these disordered structures are not compact but gel-like with a “fractal” structure. Even though order within a gel-like structure is possible [125], gel structures obtained with DNA coated colloids are not ordered. Finite-sized systems have also been realized [53]. It appears that if the length of the polymeric dsDNA spacer is too long (comparable to the size of the colloids), all “sticky ends” of one colloid can bind to those of a neighboring one, forming small clusters. In the experiment the finite clusters were of different size, but simulations suggests that a low density solution containing only dimers can be realized provided that all DNA-coated colloids have the same valency [126].

## 2.5 Applications of DNA-coated colloids

At present, most practical applications of DNA-coated colloids are related to detection of small molecules or DNA sequences. Above we mentioned the ability to detect DNA on a surface (two-dimensional assembly), but DNA detection is also possible in the bulk (three-dimensional). Methods range from detecting clusters obtained with different target DNA, taking the inter-particle distance into account [66] to nanoparticles coated with DNA end-capped by a fluorophore. If single-stranded, the DNA lies on the particle surface, quenching the fluorophore. Upon binding of a target DNA, the molecule stretches, freeing the fluorophore from the surface. This restores the fluorescence [127].

Besides detecting DNA, also some metal ions can be detected. Examples are  $\text{Pb}^{2+}$  [128] and  $\text{Hg}^{2+}$  [129]. The detection methods for both metal ions differ.  $\text{Pb}^{2+}$  detection depends on clustering nanoparticles with DNA containing one RNA nucleotide (Figure 2.9a). The mixture is completed by a DNzyme, whose activity depends on the presence of  $\text{Pb}^{2+}$ . The metal ion is thus detected by the destruction of nanoparticle clusters. Concentrations of  $\mu\text{M}$  could be detected [128]. In contrast,  $\text{Hg}^{2+}$ -ions are detected by assisting in DNA release from nanoparticles. When  $\text{Hg}^{2+}$ -ions interact with the thymidine units of the DNA molecules bound to the nanoparticles, the conformations of these DNA derivatives change from a linear to a hairpin structure. This causes the release of some of the DNA molecules from the surface of the nanoparticles into the bulk solution. There they can be detected with the help of OliGreen, a fluorescent probe that binds to ssDNA but not to dsDNA. The fluorescence of OliGreen-DNA complexes increased with increasing concentration of  $\text{Hg}^{2+}$ , and  $\text{Hg}^{2+}$  could be detected at concentrations as low as 25 nM [129].

The optical monitoring of bio-recognition processes through the separation of DNA-nanoparticle clusters can also be used for the detection of cocaine [130]. One longer strand of DNA is designed not only to link nanoparticles, but also to wrap around cocaine. Due to this wrapping the link between the nanoparticles is destroyed and the assembly falls apart (Figure 2.9b). Again concentrations of  $\mu\text{M}$  could be detected [130]. As a last example of biosensing with DNA-coated particles, we briefly discuss the assay of telomerase. Telomerase is a ribonucleoprotein that elongates the chromosomal telomere units and transforms them into immortal cells. Thus, telomerase is a versatile marker for cancer cells [131]. In a DNA-nanoparticle based assay of telomerase, CdSe/ZnS core shell quantum dots are modified with thiolated nucleic acid 17 that is recognized by telomerase. In the presence of a nucleotide mixture (dNTPs) and the Texas-Red-labeled dUTP together with telomerase extracted from HeLa cancer cells, telomerization of the nucleic acid 17 was initiated in a similar path that proceeds on the ends of the chromosomes [132]. The telomerization results in the incorporation of the Texas-Red units into the telomeres, and the activation of the fluorescence resonance energy transfer (FRET) from the quantum dots to the dye labels (Figure 2.9c). The fluorescence generated by the dye is then used to follow the activity of the telomerase.

Another field of application of DNA-coated (nano) particles is DNA or RNA delivery into cells. It is important to note that in this case the DNA is not permanently grafted to the colloid, rather it is physisorbed so directed delivery is possible. Gold particles are

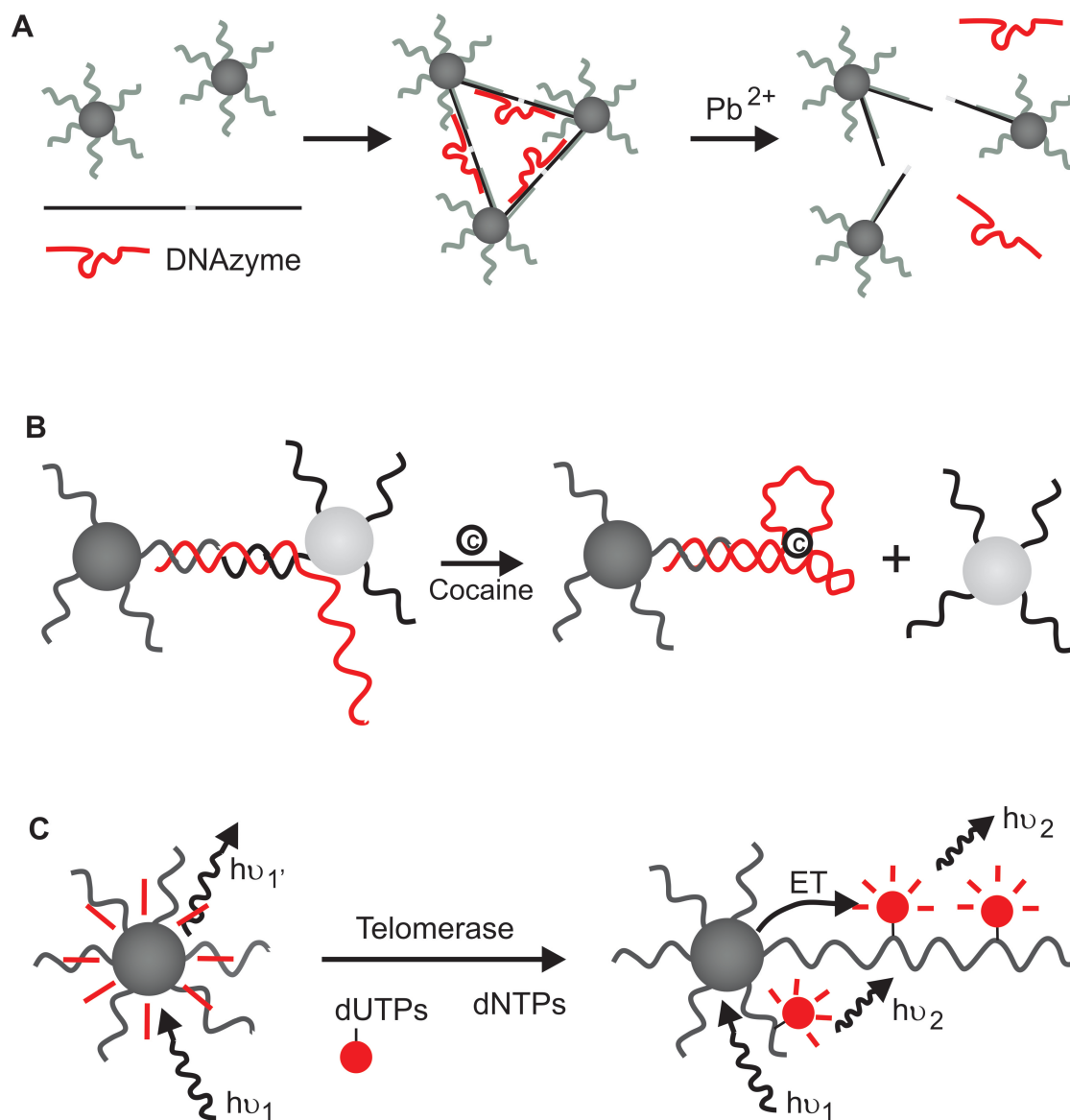


Figure 2.9: Applications of DNA-coated colloids. A: With the use of DNA-coated colloids and a so-called DNAzyme, lead-ions can be detected. B: Also cocaine is a substance that can be detected utilizing DNA-coated colloids. C: Besides detecting substances, DNA-coated colloids can also be used to determine the activity of the enzyme telomerase (All three examples are discussed in more detail in the text).

well-established carriers for the delivery of dsDNA in the so-called gene-gun technology [133]. Gene-gun technology uses DNA (or RNA [134]) that adheres to biologically inert gold nanoparticles. By accelerating this DNA-particle complex in a partial vacuum and placing the target tissue within the acceleration path, DNA is effectively introduced into the cell. An advantage of this technique is that cell removal from the tissue is not necessary. The particles penetrate the cells and release the DNA. Because cells are not removed from the tissue, cell sampling for gene gun bombardment should focus on the superficial cells [135]. As gold is not biodegradable, adverse side effects could arise when particles get accumulated [136]. With that fact in mind, also biodegradable alternatives, like chitosan particles, are examined [137, 138].

## 2.6 Outlook

When Mirkin and co-workers [3] and the group of Alivisatos reported DNA-driven assembly of nanoparticles, many researchers saw the potential of this new class of material. During the past 13 years, progress has been impressive - primarily in the area of detection of biologically relevant bio-molecules. However, there has also been progress in the “materials science” of DNA-coated colloids. Examples are the successful engineering of finite clusters of DNA-coated colloids [119] and the creation of the first crystals of such building blocks [34, 35, 123]. In the present chapter, I presented a brief review of the studies that have been reported that focused on the physics of DNA-based self-assembly. However, realizing the full potential of these new materials certainly still requires much more research. The crystals formed thus far are roughly 90% water, due to the length of spacer used [139]. This makes them too fragile for direct use. Also, as slow annealing appears vital to obtain order within the assemblies, forming DNA-linked crystals is a time consuming business. A solution to speed up the process has been found for nanoparticles [140]. Assemblies can be directed to form on a platform with an electric field. Crystals up to 20 layers can be built this way from a solution of low concentration.

Even though the quest for new materials is still on, DNA-coated colloids already proved useful in other areas as well. Examples include biosensors [81–86, 128–130] or as delivery capsules for therapeutic agents [133]. In time, combining all knowledge comprising theoretical models, simulations and experiments should lead to even more sophisticated self-assembled materials. As with the assembly of pure DNA systems before, the design is ahead of experimental realization, but as experiments with DNA are quickly catching up with more and more elaborate structures [141], it seems safe to speculate that many amazing discoveries lie in front of us.

# 3

## A finite-cluster phase in $\lambda$ -DNA coated colloids

*Inspired by theoretical work indicating that crystal structures can be build with a system of DNA-coated colloids, we studied the aggregation of 1  $\mu\text{m}$  colloids bridged by long flexible DNA with 32  $\mu\text{m}$  contour length. Hereto two species of colloids with grafted double-stranded  $\lambda$ -DNA displaying short, complementary single-stranded “overhangs” as free binding-ends were mixed. Confocal microscopy showed the formation of stable, size limited clusters in which the two species of colloids were at touching contact. The inter-colloidal distance and the size of the DNA used suggests that the DNA is expelled out of the cluster by excluded volume effects. Simulations indicate that the observed close contact and the limitation to grow both result from entropic exclusion of the bridging DNA from the space between nearby colloidal surfaces.*

### 3.1 Introduction

The highly specific nature of complementary-strand binding in double-stranded DNA (dsDNA) offers many possibilities for the use of this biomolecule in micro- and nanotechnology. The specificity of interaction between two complementary DNA strands makes it possible to “tune” the interactions between colloids with different DNA coatings.

Since Mirkin and coworkers [3] showed that the formation of nanoparticles into larger assemblies is possible by the specific recognition of two complementary ssDNA strands, many researchers have focused their attention on building new types of nano-materials based on these assemblies. For example, colloidal particles coated with distinct species of short single-stranded DNA (ssDNA) can bind specifically with each other via suitable DNA “linkers” [4, 6, 7, 123]. Such DNA-coated colloids can be used as sensors for nucleotide polymorphism [4, 93] and may offer a route to novel colloidal crystals [7, 123]. While most research has directed its effort on short ssDNA oligos grafted to gold colloids or nanoparticles, we choose to work with longer, more flexible DNA on micron-sized polystyrene colloids. The bigger colloids have a practical reason. With this size, direct imaging is possible with confocal microscopy. The choice for longer DNA is two fold. First, experiments that use DNA-colloid mixtures with short ss- and dsDNA cannot exploit the molecule’s polymeric potential. Second, the long DNA can function as a spacer as well as a mean of specific linking. Using very long DNA tethers will change the “sticky”-colloid phase diagram qualitatively, as the long tethers allow for rearrangement

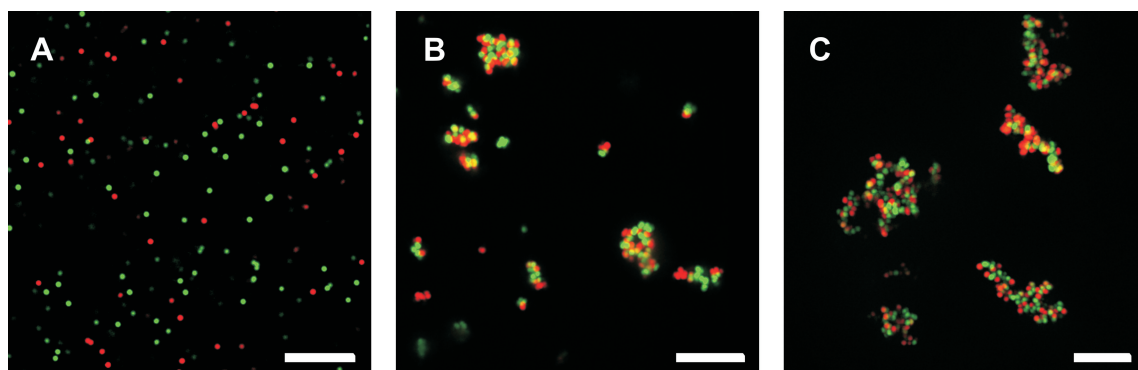


Figure 3.1: Confocal images of the clusters taken at different time points. A: 30 min after mixing - at this stage only monomers, dimers and trimers are present. B: several hours after mixing - multiple colloid clusters start to appear surrounded by dimers and trimers. C: 1 day after mixing - the clusters have reached their final stage and all dimers and trimers have disappeared. All scale bars indicate  $10 \mu m$ .

within the clusters. In particular, theory suggests that the reversible binding between ssDNA overhangs attached to long dsDNA linkers may yield novel crystalline phases [9] forbidden to systems that use only short DNA.

In this chapter we report the first experimental investigation of the aggregation of colloids bridged by long lengths of grafted dsDNA. Hereto we mixed two species of colloids with grafted  $\lambda$ -DNA displaying short, complementary ssDNA “overhangs” as free-ends. Direct imaging and computer simulations suggest that both the polymeric nature of the DNA and the possibility it offers for specific molecular recognition are important in this system.

## 3.2 Results and Discussion

### 3.2.1 $\lambda$ -DNA driven assembly leads to finite cluster sizes.

To examine the aggregation behavior of  $\lambda$ -DNA coated colloids A and B colloids were mixed in equal ratios, a  $20 \mu l$  aliquot of which was displayed in an imaging chamber<sup>1</sup>. This mixture was observed with time by means of confocal microscopy. Some aggregates, mostly of AB doublets, can be seen 30 minutes after mixing (Figure 3.1a). Besides the few small aggregates the sample contains many colloids that remained as singlets. The system is in the induction phase. As the DNA used is long and flexible, the ssDNA ends need time to find each other and hybridize. After several hours, large clusters consisting of  $\sim 10$  colloids from each population have formed (Figure 3.1b), but a significant number of smaller clusters remained. Although cluster growth started, the presence of small

<sup>1</sup>The main experiments described in this chapter are performed by Tatiana Schmatko and Nienke Geerts. The work on YOYO-died clusters is done by Tatiana Schmatko in Edinburgh. Nienke Geerts suggested the control experiment with DNA tethers, where the backbone was not ligated. The Monte Carlo simulations were performed by Behnaz Bozorgui.

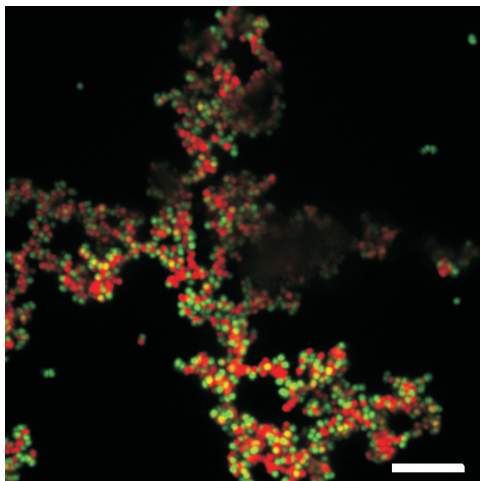


Figure 3.2: Confocal image of the control experiment. Omitting the ligation step in the preparation of DNA-coated colloids and subsequent heating, leads to cos-coated colloids. The colloids have a different aggregation behavior to  $\lambda$ -DNA coated colloids. As they assemble on every contact they form percolating clusters. Scale bar is 10  $\mu m$ .

clusters, indicates that the aggregation process is not completed during this time. Few of the latter were seen after ca one day. At this time the sample shows large clusters that have sedimented (Figure 3.1c). Inverting the sample, however, appeared to separate the sediment into independent clusters. Little change in the samples was observed after ca. one month.

Once two complementary ss-overhangs on two neighboring A and B colloids meet and hybridize, the two colloids are bridged by a continuous piece of dsDNA with 32  $\mu m$  contour length. The radius of gyration of the unbound dsDNA with this contour length can be estimated to be  $2^{0.58} \approx 1.5$  times that of a single  $\lambda$ -DNA, i.e.  $\sim 1.2 \mu m$ , so that the ratio of the radius of the colloid to that of the bridging chain is  $0.5 : 1.2 \approx 0.42$ . We denote this ratio by the symbol  $\alpha$ . Figure 3.1 shows that these bridging chains bring colloids very close together (neighboring A and B colloids are practically touching) to form clusters consisting of multiple colloids of each kind. The observed close approach of bridged colloids is, at first sight, surprising, given the size of the bridging DNA. Another surprise is the apparently self-limiting nature of the cluster growth.

### 3.2.2 $\lambda$ -DNA is responsible for the formation of finite clusters.

Control experiments confirmed that the observed aggregation was caused by the grafted  $\lambda$ -DNA. We repeated our sample preparation protocol without ligation of the DNA backbone after the cos1-biotin and cos2-biotin have been hybridized to the linearised  $\lambda$ -DNA, (Figure 3.6). After incubating the unligated biotinylated  $\lambda$ -DNA with the neutravidin-coated colloids overnight, each batch of colloids was heated to 65  $^{\circ}C$  for 30 minutes. Hereafter the colloids were washed to remove free DNA. Mixing the resulting colloids and following the aggregation in time, showed a huge difference. Fast aggregation was observed to commence immediately and was completed within 1 hour, resulting in large

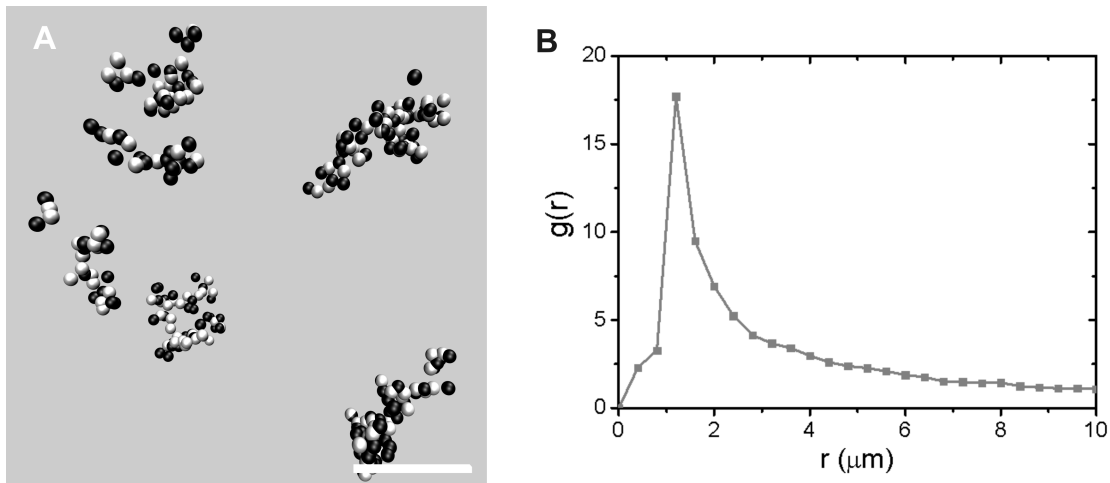


Figure 3.3: Reconstructed 3D image of DNA-driven assembled micron sized colloids and its pair correlation function. A: colloids grafted with  $\lambda$ -DNA. The aggregation time was one month. Long DNA tethers lead to finite sized clusters. Scale bar is  $10 \mu m$ . B: pair correlation function of A-B colloids.

percolating clusters (Figure 3.2).

The lack of ligation means that heating was able to remove the  $\lambda$ -DNA, leaving colloids coated with *cos1* and *cos2*. Such colloids can aggregate on contact. In contrast, colloids with covalently ligated  $\lambda$ -DNA aggregate much more slowly. It takes time for complementary ssDNA-overhangs on the ends of tethered DNAs to find each other and hybridize. In the meantime, before complementary ssDNA-overhangs meet, the grafted DNA acts as an effective steric stabilizer for these colloids.

### 3.2.3 Expulsion of DNA from the gap between two bridged colloids can explain the finite sizes.

During the experiments two unexpected results appeared constantly. The distance between the colloids within a cluster is close to zero and all aggregates are finite in size. To begin to understand these observations, we first inquired the behavior of two colloids with large bridging polymers. Bhatia and Russel [142] made self-consistent field theoretic calculations for a system of two spherical colloids and linear polymers with strongly adhering chain ends. These show that ideal chains of such “telechelic associative polymers” induce an attraction between the colloids. For  $\alpha$ , they predict an attraction with a minimum practically at touching (figure 10 of ref. [142]), with a well-depth of  $2k_B T$  at  $\alpha \approx 0.4$  (figure 11 of ref. [142]). These results include chain configurations in which both adsorbing ends of a telechelic chain are adsorbed onto the same colloid. Such loops contribute a repulsive component to the inter-particle interaction. We certainly do not have such “loops” in our experiments. Their removal from the calculation should deepen the attraction and move the minimum further towards touching. The results of Bhatia and Russel therefore give us reason to expect that a bridging polymer at  $\alpha \approx 0.4$  should

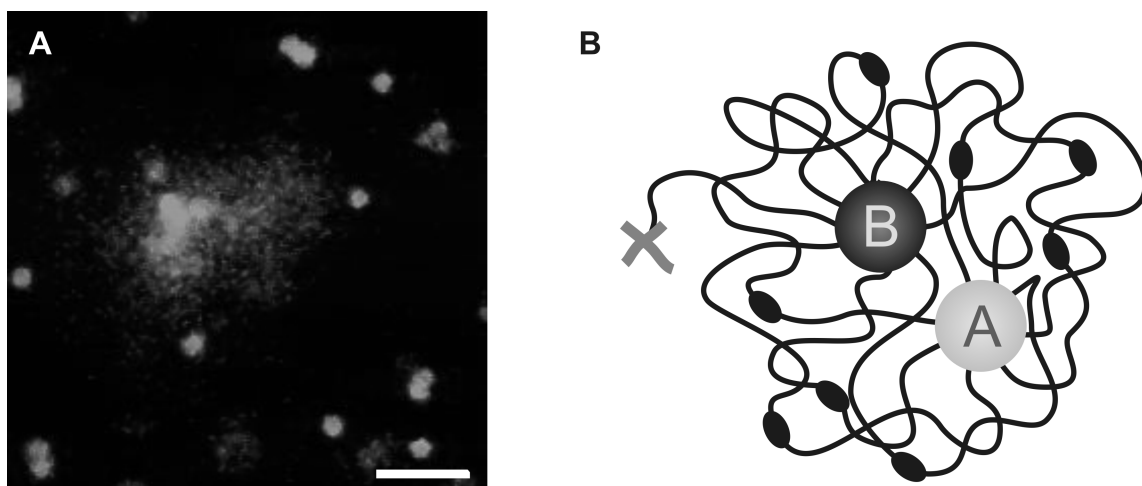


Figure 3.4: DNA gets expelled from the gap between two neighboring colloids. A: Non fluorescent colloids grafted with YOYO stained  $\lambda$ -DNA. Scale bar is  $10 \mu m$ . B: Cartoon of  $\lambda$ -DNA coated colloids. DNA is long enough to stretch over neighboring colloids. No free ends have to be present for dimers or bigger assemblies.

effectively be “expelled” by the two colloids (for entropic reasons), thereby causing them to approach to practically touching.

Experimentally, such expulsion of the bridging DNA can be inferred from the close approach of AB colloids, (Figure 3.1b,c). Confocal microscopy allows us to obtain colloid coordinates [2] although finite pixel size and colloid movement between frames limit the accuracy. With these we can reconstruct 3D images of our finite sized clusters (Figure 3.3a) and construct a pair-correlation function of A-B colloids, which confirms the close contact between colloids (Figure 3.3b). The small shift from  $r = 1 \mu m$  of the first peak, is related to experimental errors, rather than a fixed distance between our colloids.

It can also be explicitly demonstrated by adding the fluorescent dye YOYO, which labels the DNA. Now we can see, (Figure 3.4a), that the DNA forms a “halo” surrounding the colloids in a cluster. Note that Tkachenko’s theory of long-DNA bridged colloids predicts an attractive minimum significantly away from touching [9]. His work, however, relied on the Derjaguin approximation to move from flat plates to curved surfaces; in Bhatia and Russel’s model, this procedure only gives acceptable results in the limit of  $\alpha \gg 1$  [142]. The expulsion of the bridging DNA from the gap between two bridged colloids also suggests an explanation for the observation of size-limited clusters. After a certain degree of aggregation, the cluster is surrounded by DNA expelled from the space between closely-approaching colloids, (Figure 3.4a). The long length of the DNA not only forms this “cloud” of DNA that hinders further aggregation, it also leads to a situation where there are no free “sticky ends” available anymore. The DNA linkers are long enough to find a partner within the cluster (Figure 3.4b).

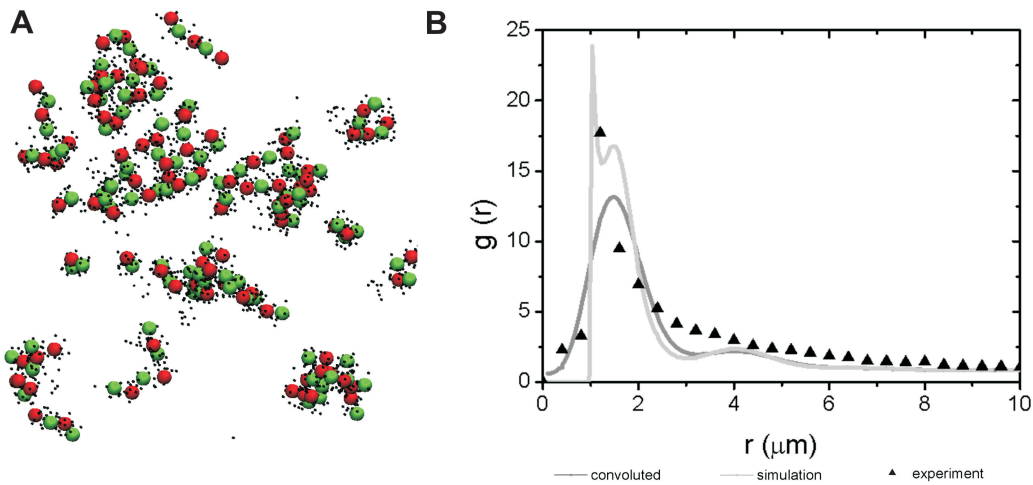


Figure 3.5: Monte Carlo simulations agree well with experiments. A: 2D snapshot in a well-equilibrated simulation with 200 colloids and polymer centers of mass shown as black dots. B: Pair-correlation functions between green fluorescent and red fluorescent colloids, obtained from simulations (lines) and experiment (black triangles). The dark gray line represents the simulation data, convoluted with a Gaussian spread reflecting the experimental smear.

### 3.2.4 Monte Carlo simulations agree well with experimental results.

To test the intuitive picture described above, Bozorgui et al. [53] performed Monte Carlo simulations of our system using a simple model. In her model, polymer coils, modeled as soft spheres [143] are permanently tethered onto purely repulsive spheres by harmonic springs. Two soft spheres on neighboring colloids can form a single reversible bond, again modeled as a harmonic spring. Typical configurations after  $10^6$  Monte Carlo cycles for 10 “polymers” per colloid are shown in Figure 3.5a. These bear striking resemblance to the experimental observations: size-limited clusters displaying many close-to-touching A-B contacts (Figure 3.1c and Figure 3.3a). Also the simulations clearly show that the polymers (represented as the small black dots) surround the clusters.

The calculated A-B pair correlation function is shown in Figure 3.5b (light gray line). The peak at contact illustrates that touching can indeed be induced by the purely repulsive interactions in this system. To compare this pair correlation function with the one from experiments, the latter is displayed in the same figure (black triangles). The simulations agree especially well with the experimental data when they are rebinned to simulate limited distance resolution (1 pixel  $\approx$  400 nm; dark gray line).

Note that in the work by Bhatia and Russel quoted earlier, the polymer bridge between two colloids is irreversible. The simulations show that touching interaction remains with a degree of reversibility in the bridges, which we believe can also be present in our experiments. Finally, in the simulations, polymers link some clusters. We do not have direct evidence for such DNA links from our experiments.

### 3.2.5 Increasing temperature has no effect on clusters stability

The clusters obtained experimentally are surprisingly stable. Heating to 80 °C (and leaving the sample for 6 to 12 hours at that temperature) did not redisperse the colloids. Since we linearise cyclic  $\lambda$ -DNA at 65 °C, we may expect the cos1-cos2 binding holding each piece of bridging DNA together at its mid-point to have dissociated by 80 °C, thereby destroying the clusters. We believe that the observed irreversibility is due to the close-to-touching inter-particle contact engendered by the initial bridging mechanism—an effect predicted both by Bhatia and Russel’s calculations[142] and Bozorgui’s simulations [53]. Close inter-particle contact will bring strong Van der Waals forces into play, causing irreversible binding. Such effects were observed by Valignat et al. when they used neutravidin-grafted short (61 bases) ssDNA with complementary free ends (11 bases) to aggregate colloids [6]. These authors found that aggregation was irreversible unless the colloids were additionally (sterically) stabilized by adsorbed block copolymers.

## 3.3 Conclusion

We have demonstrated by experiments and simulations a novel route for the growth of finite colloidal clusters in a system with only repulsive interactions using long bridging polymer molecules with weak reversibility. Much of the literature on colloidal self assembly to date focuses on generating structures that are potentially unlimited in spatial extent, especially photonic crystals. In contrast, generating nano-devices requires the assembly of building blocks into finite size units. The protocol we have reported represents a novel route towards such assembly.

The mechanism we investigated is an example of micro-phase separation. In our case, a mixture of non-adsorbing  $\lambda$ -DNA and similar-sized colloids will macro-phase separate due to depletion [144]. But the tethering of DNA to colloids leads to the arrest of this macro-phase separation, giving rise to finite-size clusters. These clusters are similar to those observed in mixtures of charged colloids and partially-charged block copolymers [145]. The formation of micelles, with tethered hydrophilic head groups and hydrophobic tails, and the finite-size clusters formed by charged attractive colloids [146] are other instances of such frustration-driven self assembly. Understanding such routes to finite-size self assembly is a key step towards implementing functional nano-devices.

## 3.4 Materials and Methods

### 3.4.1 Preparation of biotin-DNA solutions

A schematic summary of our colloid-preparation protocol is given in (Figure 3.6). We used  $\lambda$ -phage DNA (New England Biolabs), which has a contour length of 16  $\mu m$  (48 500 base pairs (bps)). Special care was taken to handle long  $\lambda$ -phage DNA (New England Biolabs) to avoid any damage due to shear. This DNA was pipetted with tips that were blunted and sterilized before use. The  $\lambda$ -phage DNA, predominately circular at room temperature, was linearised by heating in a 25  $\mu g/ml$  solution to 65 °C.

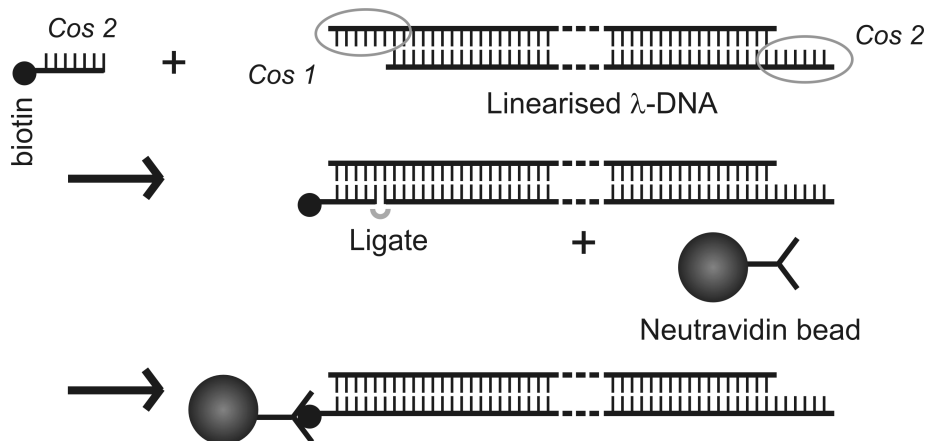


Figure 3.6: Schematic protocol to obtain DNA-coated colloids. In control experiments the ligation step is omitted.

Each linear dsDNA is terminated by two complementary 12 base single strands (ssDNA; “sticky ends”), which we call cos1 and cos2 (cos1 = 5'-GGGCGGCGACCT-3'; cos2 = 5'-AGGTCGCCGCC-3').

We prepared two populations of linear DNA. In each population, one “sticky end” was hybridized and ligated to cos1-biotin or cos2-biotin ( $5 \mu\text{l}$ ;  $20 \mu\text{M}$ ; Eurogentec) using T4 DNA ligase (New England Biolabs). To remove the excess of oligonucleotides and enzyme the samples were centrifuged and washed three times on a Microcon YM100 membrane (Milipore) with Tris-HCl buffer (250 mM, pH = 8). The biotin-DNA solution was then recovered in a clean tube.

### 3.4.2 Preparation of DNA-coated colloids

To obtain DNA-coated colloids the two populations of DNA were then separately mixed with neutravidin-coated green-fluorescent (“A” hereafter; depicted in green or white) and red-fluorescent (“B” hereafter; depicted in red or black) polystyrene colloids (diameter  $1 \mu\text{m}$ , Molecular Probes) dispersed in a Tris-HCl buffer (250 mM, pH = 8). In each case the DNA and colloids were reacted overnight during which they were continuously tumbled.

The next day the samples were pelleted and washed five times to remove excess of non-conjugated DNA. In between these washing steps, samples were heated once for 10 min. at  $50 \text{ }^\circ\text{C}$  and washed once in a NaOH solution ( $0.15 \mu\text{M}$ ) to remove poorly bound DNA. The supernatant was retained to quantify (by UV-spectrometry at 260 nm) the amount of DNA that had effectively bound to the colloids. For  $\lambda$ -DNA this leads to an estimate of some 10 DNA chains per colloid. Given the relative sizes of the DNA and colloids, we expect each colloid to be completely surrounded by grafted DNA. The DNA-coated colloids were diluted in a fresh TRIS-HCl buffer (250 mM final concentration, pH = 8) with  $\text{D}_2\text{O}$  to minimize sedimentation. This yielded two batches of colloids with ds- $\lambda$ -DNA grafted onto their surfaces by strong biotin-neutravidin bonds, displaying complementary single stranded cos1 and cos2 free ends respectively.

Under these conditions, we estimate (by dynamic light scattering, data not shown) the coil size of the linear  $\lambda$ -DNA to be  $\sim 800$  nm (radius).

### 3.4.3 Preparation and coating imaging chambers

To avoid any nonspecific interactions between DNA-coated colloids and glass surfaces of the imaging chambers, coverslips were coated with polyethylene glycol (PEG). The coating of glass slides with PEG is a two-step procedure. First the glass slides were silanized with 3-mercaptoptriethoxysilane (97%, Fluka), then a 5-kDa maleimide modified PEG (Laysan Bio Inc) was tethered to the terminal thiol group of the silane.

Prior to the silanization, the glass slides were cleaned in an UV/ozone box. The cleaned slides were placed in contact with silane vapor overnight. Subsequently, the slides were rinsed with Ethanol, dried with Nitrogen and left in an oven (100 °C) for 30 minutes. Next a drop of concentrated maleimide modified PEG (250 mg/ml in TRIS-HCl buffer) is trapped between two silanized slides and left overnight at room temperature. The excess of PEG is removed by rinsing with ddH<sub>2</sub>O.

A sample chamber is made from two glass coverslips of different size separated by a parafilm spacer (100  $\mu$ m). The parafilm sealed the chamber on three sides. After loading the chamber with 10  $\mu$ l of each population of DNA-coated colloids, reaching a final particle volume fraction of  $\phi \approx 0.004$ , the chamber is completely sealed with glue.

### 3.4.4 Confocal imaging

A and B colloids were mixed in equal ratios, a 20  $\mu$ l aliquot of which was displayed in an imaging chamber (colloids are suspended in a TRIS-HCl buffer (250 mM final concentration, pH = 8) with D<sub>2</sub>O to minimize sedimentation). The mixtures were observed at room temperature using either a Nikon TE 300 microscope and a Biorad Radiance 2100 MP confocal scan head or a Zeiss axiovert microscope with a Perkin Elmer ultraview RS spinning-disc scan head. Fluorescence of the two populations of colloids was excited at 488 nm and 512 nm, and emission observed at 505 nm and above 600 nm respectively. The use of two types of fluorescent colloids and confocal microscopy allowed us to extract colloids coordinates and to reconstruct 3D images [2].

## 3.5 Acknowledgements

I would like to thank C. Tischer for imaging a sample at the EMBL (Heidelberg) and P. Nassoy for advising us on the pegylation of glass surfaces.



# 4

## Clustering versus percolation in the assembly of colloids with long DNA

*We report an experimental study in which we compare the self-assembly of 1  $\mu\text{m}$  colloids bridged through hybridization of complementary single stranded DNA (ssDNA) strands (12bp) attached to variable-length double stranded DNA spacers that are grafted to the colloids. We considered three different spacer lengths: long spacers (48500 bp), intermediate length spacers (7500 bp), and no spacers (in which case the ssDNA strands were directly grafted to the colloids). In all three cases the same ssDNA pairs were used. However, confocal microscopy revealed that the aggregation behavior is very different. Upon cooling, the colloids coated with short and intermediate length DNA's undergo a phase transition to a dense amorphous phase that undergoes structural arrest shortly after percolation. In contrast, the colloids coated with the longest DNA systematically form finite-sized clusters. We speculate that the difference is due to the fact that very long DNA can easily be stretched by the amount needed to make only intra-cluster bonds, and in contrast, colloids coated with shorter DNA always contain free binding sites on the outside of a cluster. The grafting density of the DNA decreases strongly with increasing spacer length. This is reflected in a difference of the temperature dependence of the aggregates: for the two systems coated with long DNA, the resulting aggregates were stable against heating, whereas the colloids coated with ssDNA alone would dissociate upon heating.*

### 4.1 Introduction

The double helix of DNA consists of two negatively charged phosphate-sugar polymer chains held together by hydrogen bonds between complementary bases on each chain. This specific feature makes this biomolecule of great interest to materials science, since it allows for specific and reversible binding. This property of DNA is of particular relevance for the self-assembly of constructs that contain different sequences of single-stranded DNA (ssDNA). This property of ssDNA was initially used to detect specific DNA sequences or to determine mismatches within a genetic code [81, 82]. The selectivity of DNA hybridization has been exploited to build nano- and microstructures in solution [19, 20] and to guide the self assembly of DNA-derivatized structures [147, 148].

In this chapter, we focus on the properties of colloidal particles functionalized with ssDNA. Colloids coated with complementary ssDNA will exhibit a sharp aggregation transition upon cooling. This property was exploited by Mirkin and co-workers [3, 82]

who used the induced aggregation of gold nano-colloids to detect specific gene fragments. From a “materials” perspective, the selectivity of DNA hybridization offers the opportunity to design novel colloidal structures and materials [149]. The number of base-pair matches tunes the strength of the attraction between colloids functionalized with complementary oligonucleotides, but there are many other parameters that control the resulting interaction between the colloids: e.g., ionic strength, grafting density of hybridizing DNA strands and length of possible spacers connecting the “reactive” ss-DNA to the colloids. A number of experimental [4, 150] and modeling [49, 51, 93, 151] studies have focused on the effect of temperature on DNA-driven phase transitions in nanoparticle systems. A recent paper [69] reports a study of the effect of ionic strength and hybridizing strand concentration at constant temperature. However, relatively little is known about the influence of the length of connecting spacers on the phase behavior of DNA-coated colloids. Theoretical work of Tkachenko and co-workers [9] indicated that possible crystal structures of binary colloids coated with DNA should depend strongly on the length of the spacer. We note that it has turned out to be particularly difficult to make crystals of DNA-coated colloids [123]; most of the self-assembled structures observed thus far correspond to large, amorphous aggregates [5–7]. A possible factor might be that the effective range of attraction between colloids coated with short DNA strands is much shorter than the diameter of the colloids. From experiments on polymer-colloid mixtures [152], it is known that gelation often preempts crystallization when the range of attraction between the colloidal particles becomes short. If something similar would hold for DNA-coated colloids, one might expect that varying the length of the DNA spacers might influence the kinetics of crystallization. However, things are not that simple. In earlier work we used colloids coated with extremely long double-stranded DNA linkers that carry a short single-stranded DNA sequence at the free end [53]. We showed that this type of colloids aggregated to form finite-sized clusters, surrounded by a DNA “halo”. Interestingly, the colloids inside these clusters were found to be rather close, an effect that is presumably closely linked with the expulsion of DNA from the inside of the cluster. In fact, a theoretical study of Bhatia and Russel [142], showed that a pair of colloidal particles, linked by long, strongly bound telechelic polymers would attract at short distances under conditions where flat surfaces coated with the same polymers would repel. This therefore shows that the Derjaguin approximation that was employed in the theoretical work of Ref. [9], breaks down for spacers with a radius of gyration that is not small compared to the size of the colloids, and this fact may be relevant for both the stability and the kinetics of formation of possible crystal structures. In addition, the absence of DNA-mediated repulsion at short distances implies that colloids coated with long DNA may get into close contact, so much so that strong, short-ranged attractive forces may cause the aggregation to become irreversible upon heating the system above the DNA melting temperature  $T_m$ .

As was shown in Ref. [123], other stabilizing agents (for instance, the grafting of a dense, inert polymer brush) may be needed to make aggregation fully reversible in such cases.

In this chapter, we study the effect of varying the DNA spacer length on the aggregation behavior of DNA-coated colloids. The work of Bhatia and Russel’s suggests

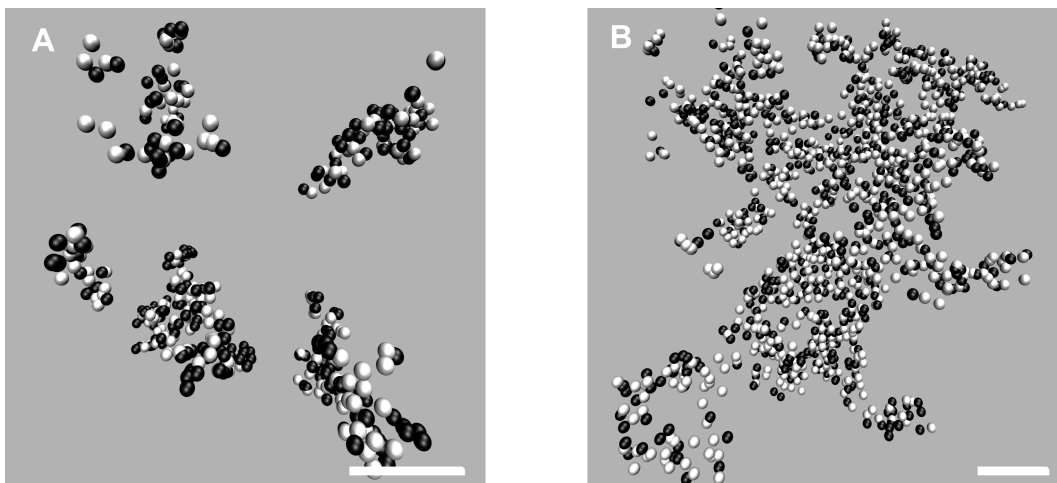


Figure 4.1: Reconstructed 3D image of DNA-driven assembled micron sized colloids, showing the aggregation state after one month. Long DNA tethers lead to finite sized clusters, while shorter dsDNA spacer lead to system-spanning (percolating) clusters. A: Colloids grafted with  $\lambda$ -DNA. B: Colloids grafted with pBelo-DNA. Both scale bars indicate  $10\mu m$ .

that, as the size ratio of colloid to polymer exceeds one, the repulsion at short distances is recovered; the strength of the repulsion depends both on the size of the polymers and their grafting density. In addition to examining the behavior of  $\lambda$ -phage DNA, which has a radius of gyration ( $R_g$ ) of about 800 nm, we studied colloids coated with a pBeloBac11 plasmid ( $R_g \approx 200$  nm), leading to a colloid to polymer ratio of 1.6. The interesting feature of this plasmid is its cos-restriction site. With the use of an enzyme ( $\lambda$ -terminase) we can regenerate the same sticky-ends as with  $\lambda$ -phage DNA, making the length of double stranded DNA (dsDNA) the only difference between the two systems. Finally, we compare the behavior of colloids coated with relatively long dsDNA and short “sticky” ssDNA end with a system coated only with the short ssDNA, and with a system coated with DNA that has no “reactive” ssDNA end groups.

## 4.2 Results and Discussion

### 4.2.1 Colloidal assembly depends on the length of the DNA bridge.

To compare the effect of the length of the dsDNA polymer spacer, two batches of DNA-coated colloids were prepared. One batch contained the longer  $\lambda$ -DNA the other the shorter pBelo-DNA. For both batches, A and B colloids were mixed in equal ratios, a  $20\mu l$  aliquot of which was displayed in an imaging chamber. Cluster formation was followed with time beginning  $\sim 30$  minutes after mixing the colloids. At room temperature both DNA-coated colloid batches follow the same aggregation speed in the beginning. Small differences begin to show after one day and become most apparent after one month

clustering time.

We find that DNA-driven aggregation progresses in different ways for the two DNA bridges used. The longer  $\lambda$ -DNA yields finite-size clusters that appear stable after more than a day (Figure 4.1a). In contrast, we observe a system-spanning cluster containing most colloids in the system, of colloids coated with the shorter pBelo-DNA with 25 sticky arms per colloid (Figure 4.1b). Using the colloid coordinates measured in the confocal images, we employed a cluster analysis program (using a freely available script that can run on IDL-software) to generate a histogram of cluster sizes. In the cluster analysis, we start by determining the nearest neighbors of all colloids. Two colloids are deemed to belong to the same cluster if their distance is less than a preset threshold. The threshold distance depends on the size of the linking DNA: for  $\lambda$ -DNA we chose  $r_c = 4 \mu m$  and for pBelo-DNA,  $r_c = 2 \mu m$ . We verified that the cluster size distribution was insensitive to the precise values of the cutoff. The resulting cumulative cluster-size distributions for  $\lambda$ -DNA are shown in Figure 4.2a. The ones for pBelo DNA are shown in Figure 4.2b. Cluster sizes were determined at five different time points, starting from  $\sim 30$  minutes after mixing until one month of aggregation time. Cluster sizes first increase in time, but the cluster growth comes to a halt after one week when colloids are coated with  $\lambda$ -DNA. Small differences in the graph, compared to the curve of one month old clusters, are only due to statistics rather than a change in the sample. The cluster analysis shows that when colloids are coated with  $\lambda$ -DNA, only finite-sized clusters form. However, the cluster-size distribution is relatively wide: they range from a few colloids up to a hundred colloids. We note that both clusters with an equal number of red and green colloids and with an unequal number of red and green colloids are present. The assumption that all tethers are hybridized after more than a day indicates that the number of tethers per colloid is not fixed but, as expected, fluctuates around its average value of 10 DNA arms. In contrast to  $\lambda$ -DNA, pBelo-DNA coated colloids don't aggregate to a finite sized structure. Figure 4.2b shows only a fraction of all clusters present in the sample after leaving it to aggregate for longer than a day. In fact, after a few days the size of a pBelo-cluster becomes system spanning. The presence of smaller clusters is a bit misleading in this case, as most of them are part of the same system spanning cluster, but connected to the rest by a branch that is outside the field of view of the confocal microscope. This becomes clearer when we image the same sample with an objective with a smaller magnification, (Figure 4.3).

The finite cluster sizes observed in the  $\lambda$ -DNA system is unexpected, in particular, because simulation studies by Starr and Sciortino [49, 51] show that percolating networks of ssDNA/nanocolloids are formed, even when the number of arms per colloid is on an average only 2.1, where 2 is the limiting value. However, in contrast to the short ssDNA used in those studies, we have additional long dsDNA spacers. Hence, a possible explanation for the shift from finite sized cluster to a system spanning aggregate is the length difference of  $\lambda$ -DNA and pBelo-DNA.  $\lambda$ -DNA is long enough for hybridization of all tethers between a pair of colloids; besides the hybridization of tethers on adjacent sides of the colloids, the  $\lambda$ -DNA can easily stretch to link the far side of one colloid to any complementary DNA on its partner. The energy penalty for this stretching should be only in the order of  $k_B T$ , because the force it takes to stretch a polymer coil in good

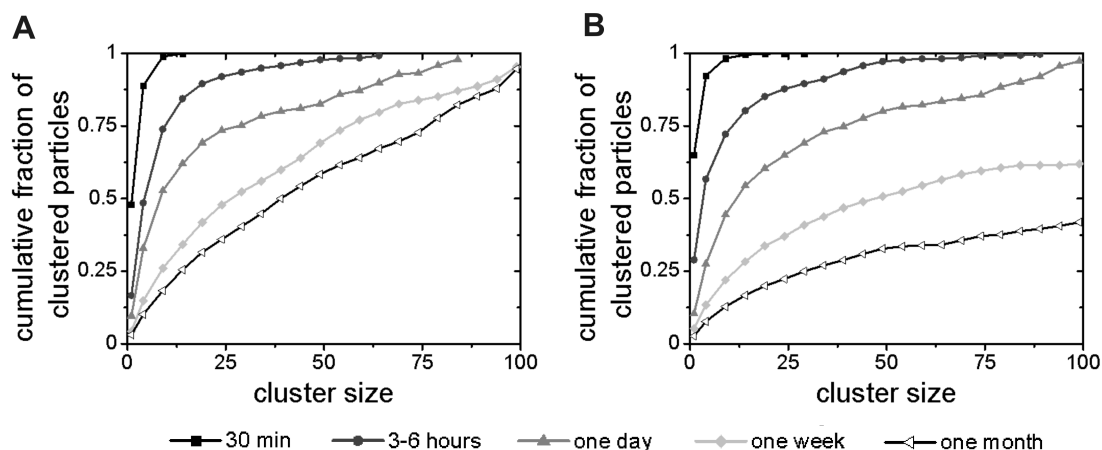


Figure 4.2: Accumulative graph of cluster sizes of DNA-driven assembled micron-sized colloids. Aggregation is followed in time from 30 minutes until a month. Graphs are taken over at least four samples using a minimum of 5000 colloids. Data points shown are averages of 5 data points. A: Colloids grafted with  $\lambda$ -DNA. B: Colloids grafted with pBelo-DNA.

solvent is inverse proportional to its radius of gyration:  $F \sim k_B T / R_g^2$ . This means that clusters of  $\lambda$ -DNA coated colloids are relatively “unreactive”. In order for two clusters to connect, the pre-existing DNA bridges on both colloids should open and then reconnect in such a way that the clusters are linked. This is not impossible, but quite unlikely at room temperature, as the  $\cos 1 / \cos 2$  bond unbinds only at about 42 °C. At the same time, free sticky DNA ends can still diffuse fast enough to find all unbound counterparts within a cluster, thereby saturating all bonds. This would also be true, if the “valency” (number of binding DNA arms per colloid) of individual colloids differ from the average valency. This seems to be confirmed in the longer time measurements that show no further growth of the  $\lambda$ -DNA system after two weeks. In contrast, pBelo-DNA is too short of length to do the same. DNA on the outside of a cluster is less likely to link to a complementary DNA on the same cluster. As a result, the pBelo colloids have “dangling bonds” and are quite reactive when they meet another cluster. As a result, the aggregation process in the pBelo case only stops when effectively all colloids are attached to a single, large cluster. In order to strengthen our hypothesis that it is the length of the spacer dsDNA that drives the two different aggregation mechanisms, we also prepared pBelo samples with only about eight sticky DNA arms per colloid, while the remaining 17 pBelo arms were blunt (no sticky cos end). Long time measurements revealed the same percolation (Figure 4.4a) and cluster growth (Figure 4.4b) as with the ones with only sticky ends.

#### 4.2.2 Temperature has no effect on clusters stability

As noted in Ref. [53], the clusters obtained in the  $\lambda$ -DNA system were extremely stable. Heating to 80 °C did not redisperse the colloids. Since the 12 bp “sticky ends” have a melting temperature of  $\sim 45$  °C, we should expect the bridged DNA to dissociate at

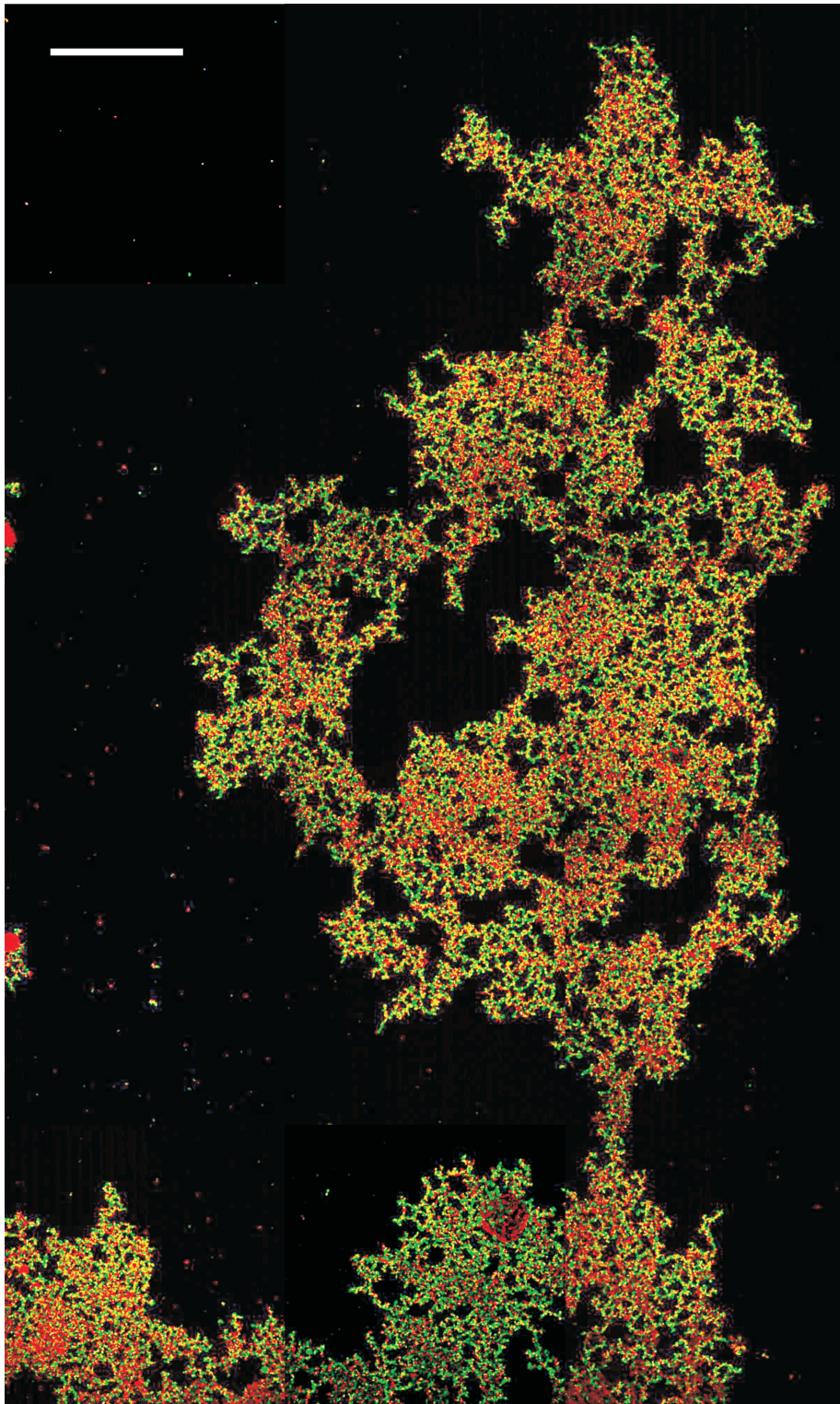


Figure 4.3: Lower resolution confocal image of clustered colloids grafted with pBelo-DNA obtained after letting the sample aggregate for one month. Here several images, taken at the same focal plane, were assembled to get a better in-plane image of the percolating 3D-cluster. Scale bar is  $50 \mu m$ .

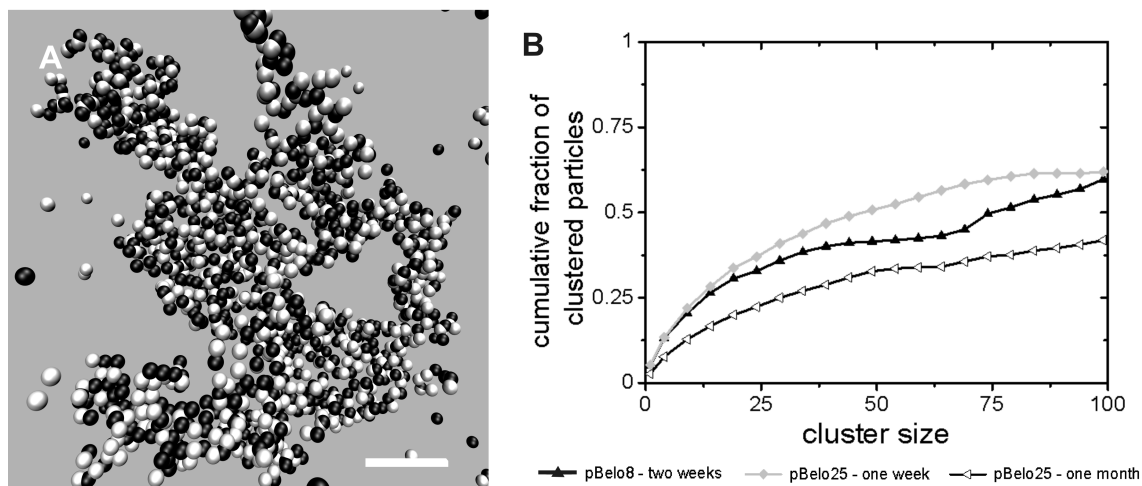


Figure 4.4: The different aggregation mechanisms are driven by the length of the ds-DNA spacer rather than the number of “sticky” arms. A: Typical cluster obtained with pBelo-DNA coated colloids with eight “sticky” arms and 17 blunt dsDNA ends. Scale bar is  $10 \mu m$ . B: Accumulative graph to compare cluster sizes between samples with 8 (black) or 25 (gray/white) “sticky” arms.

$80 \text{ }^\circ\text{C}$ . As argued in Ref. [53], colloids coated with  $\lambda$ -DNA can approach each other close enough for strong Van der Waals forces to come into play, thus causing irreversible binding. Based on the calculations of Bhatia and Russel [142], we should expect some repulsion between colloids coated with pBelo-DNA. Indeed, we find that the A-B pair correlation shows a first peak that is about 200 nanometers away from close contact (data not shown). However, the repulsion is comparable to the thermal energy and therefore does not prevent irreversible binding. Hence, also for pBelo-DNA we find that the aggregates are remarkably stable and do not redisperse upon heating to  $80 \text{ }^\circ\text{C}$ .

This inability to redisperse above  $T_m$  was already described previously [5, 6, 123]. We note that Ref. [123] also points to another possible cause of irreversible binding, namely interactions due to the proteins that are used to graft DNA onto colloids. Since the limited amount of DNA tethers per colloid leaves plenty of unbounded neutravidin on our surface, this can be a good explanation for the samples resistance to melting. This problem will be discussed in more detail in appendix A.

### 4.2.3 In the absence of specific forces colloidal assembly is negligible.

To test whether the aggregation process that we observe is the result of DNA hybridization between complementary “sticky ends”, we also studied the behavior of colloids coated by DNA that lacked a “sticky” ssDNA end. These colloids are covered by a polymer layer of the same length as pBelo-DNA. In the absence of any ssDNA, the DNA “mushrooms” should act as a repulsive barrier. Indeed, when mixed these colloids remain in monomeric form over a period of at least a month (Figure 4.5a). The absence of

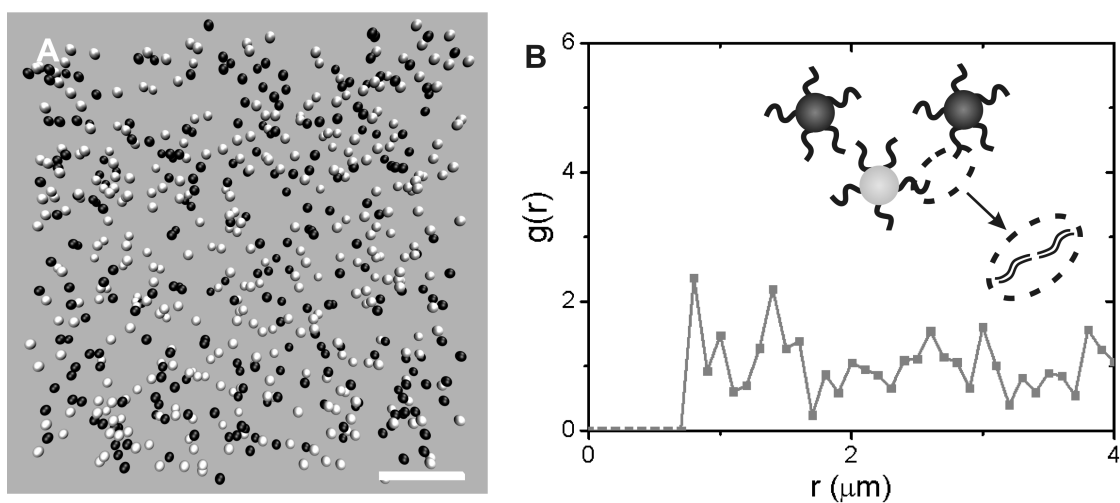


Figure 4.5: Reconstructed 3D image of micron-sized colloids coated with DNA of similar length to pBelo-DNA displaying no complementary single stranded cos1 or cos2 at the ends (blunt DNA). A: Monomers are stable in time. Scale bar is 10  $\mu\text{m}$ . B: Pair correlation function of figure A.

any significant peak in the pair-correlation function belonging to this sample suggests a homogeneous stable solution (Figure 4.5b). This indicates that the non-specific protein binding and strong Van der Waals forces are depending on the DNA bridging to bring the colloids to a close enough distance.

#### 4.2.4 Shielding colloidal proteins leads to cluster reversibility

Bare proteins can lead to non-specific binding. As our DNA-coated colloids are made from dilute solutions of DNA, the grafted DNA must be in mushroom conformation (i.e. swollen but non-interpenetrating coils) at the surface of the colloids. The DNA coverage is thus not limited by the neutravidin grafting density, but by the amount of DNA added and the space occupied by a “mushroom” of DNA. On the surface of the colloid numerous neutravidins are present with no biotin attached (there can be as many as  $10^4$  neutravidin per colloid (Invitrogen)). A polymer grafted on a surface at one point is free to move around. The energy costs for small movements are not high. As already described previously [53], during the aggregation process DNA gets expelled from the gap between two approaching colloids, leaving the protein surface “unprotected”. This can lead to non-specific binding and a strong Van der Waals attraction, resulting in a non-reversible system. To test if the “unprotected” proteins on our colloid surfaces are responsible for the lack of cluster reversibility we produced colloids with the single strands cos1 and cos2 directly bound to the surface leaving out the dsDNA spacer. Because these ends are very small compared to both our DNA bridges, they cover the colloidal surface with a dense brush of short ssDNA overhangs. This system forms large percolating clusters within 30 minutes (Figure 4.6a). The aggregation is very fast and is only “diffusion limited”, in contrast to the colloids with long DNA: there the number

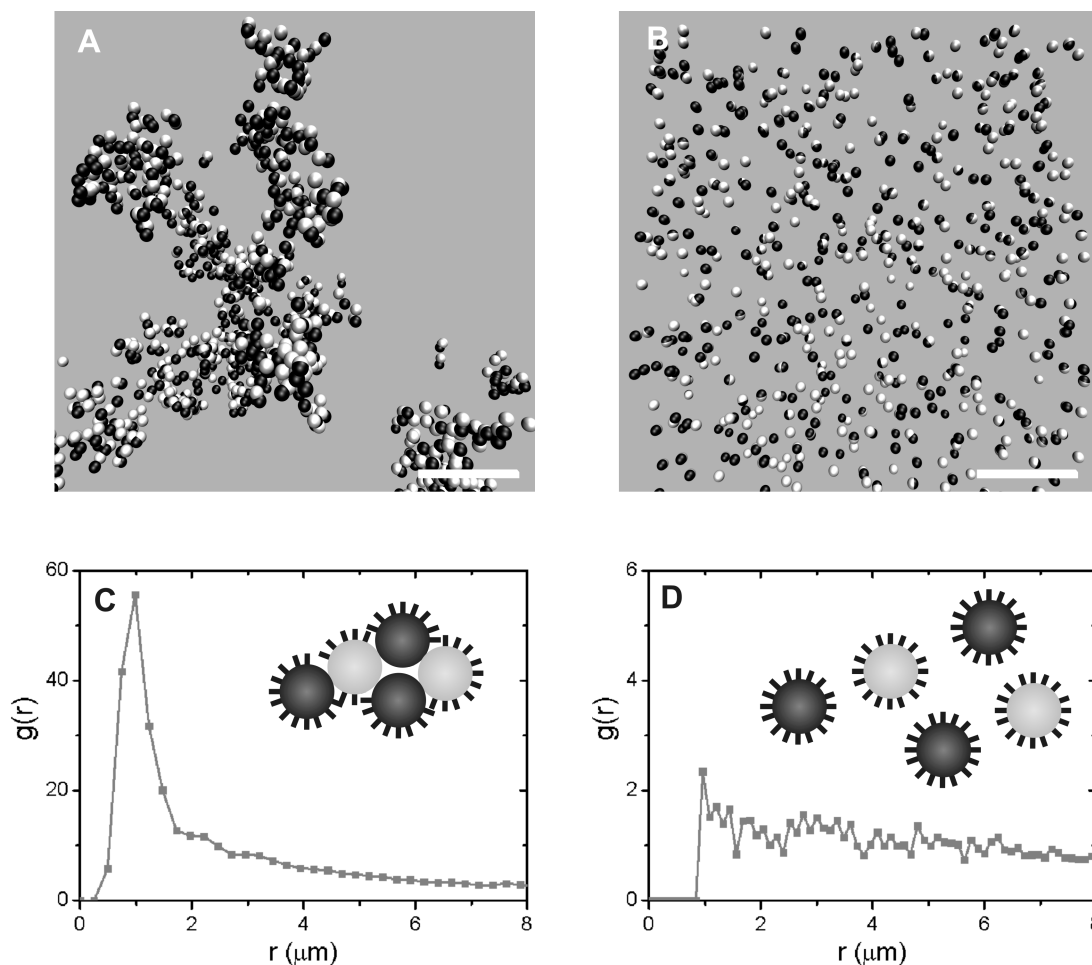


Figure 4.6: Reconstructed 3D image of micron-sized colloids displaying only complementary single stranded cos1 and cos2 ends (no dsDNA spacer present). A: Cluster formation at RT. B: Colloids redisperse at 80 °C. Both scale bars are 10  $\mu m$ . C: Pair correlation function of figure A. D: Pair correlation function of figure B.

of possible contacts per colloid pair is small and hence it is likely that aggregation is “reaction” limited. Leaving a sample of cos1/cos2-coated colloids at 80 °C for 1 hour redispersed all colloids to their beginning state (Figure 4.6b). Computing the pair-correlation functions for both temperatures shows a clear difference. The big cluster at room temperature has a distinct peak at 1  $\mu m$ , indicating close contact (Figure 4.6c). The close contact is expected since the colloids (1  $\mu m$ ) are much larger than the short piece of ssDNA used (12 bps; 40 Å). The pair correlation function of the same sample at 80 °C is absent of any significant peak consistent with the redispersed colloids in the sample (Figure 4.6d).

Shielding all proteins on the colloids surfaces leads to a system that is reversible with temperature. This suggests that the stability observed with the longer dsDNA spacers is indeed due to non-specific interactions among proteins.

## 4.3 Conclusions

In this chapter, we report the aggregation in suspensions of three different kinds of DNA-coated colloids. All systems share the same single stranded 12 base-pair oligonucleotides as sticky ends but differ in the length of dsDNA spacer between the cos-ends and the grafting points on the colloids. The longest DNA spacer ( $\lambda$ -DNA) leads to stable finite-sized clusters, never exceeding 100 colloids. Reducing the length of the DNA bridge (pBelo-DNA) results in an increase of the number of DNAs per colloid and thus a change in valency (i.e., in the number of reactive ssDNA strands per colloid), leading to the formation of macroscopic aggregates. Moreover, by reducing the valency of the pBelo-DNA system such that it is comparable to the  $\lambda$ -DNA system, while not changing the overall pBelo-DNA density per colloid, we observe percolation. This supports our assumption that the finite-size aggregation of the  $\lambda$ -DNA system is due to the saturation of all bonds within a cluster because of the large extension of the dsDNA spacers. Both systems of colloids coated by long DNA aggregate irreversibly, which is something that is not observed if the reactive ssDNA ends are passivated. This implies that the DNA bridging helps the subsequent irreversible binding. The aggregates thus formed remain stable well above the  $T_m$  of the DNA.

In contrast, colloids coated with a dense brush of 12 bp ssDNA oligonucleotides aggregate readily but redissolve upon heating, indicating that the dense DNA-brush prevents irreversible binding due to short-range forces. In order to get a high surface density with long and flexible DNAs, a third component must be used. The DNA we used is too long to self-assemble in a dense brush on a surface in good solvent conditions; it will always go to a mushroom conformation. Stability can be obtained by covering the surface with a mixture of the long DNA tethers and shorter blunt dsDNA stabilizers (without “sticky ends”). Another option is to shift from protein binding to covalent binding of DNA to the colloids, although it seems likely that even then a third stabilizing component may be needed. The clear sensitivity of the kinetics of aggregation to the valency of the colloids indicates that for the controlled assembly of complex structures using ssDNA-coated building blocks experimental control of both the phase diagram and the aggregation kinetics will be of crucial importance and this in turn will necessitate the development of techniques to control the number of ssDNAs per colloid [49, 51].

## 4.4 Materials and Methods

### 4.4.1 Preparation of biotin-DNA solutions

Special care was taken to handle long  $\lambda$ -phage DNA (New England Biolabs) to avoid any damage due to shear. This DNA was pipetted with tips that were blunted and sterilized before use. The  $\lambda$ -phage DNA, predominately circular at room temperature, was linearized by heating in 25  $\mu\text{g}/\text{ml}$  solution to 65 °C. Each linear dsDNA is terminated by two complementary 12 base single strands (ssDNA; “sticky ends”), which we call cos1 and cos2 (cos1 = 5'-GGGCGGCGACCT-3'; cos2 = 5'-AGGTCGCCGCC-3').

The linearized DNA was separated into two batches. One batch was mixed with a

solution ( $5 \mu\text{l}$ ;  $20 \mu\text{M}$ ) of cos1-biotin oligonucleotides (Eurogentec), the other with cos2-biotin oligonucleotides (Eurogentec). To hybridize the oligonucleotides to the DNA, the solution was heated to  $65 \text{ }^\circ\text{C}$  for  $\sim 30$  minutes and then cooled overnight to room temperature. Subsequently, T4 DNA ligase (New England Biolabs) was added to ligate the DNA backbone. To remove the excess of oligonucleotides and enzyme the samples were centrifuged and washed three times on a Microcon YM100 membrane (Milipore) with Tris-HCl buffer ( $250 \text{ mM}$ ,  $\text{pH} = 8$ ). The biotin-DNA solution was then recovered in a clean tube.

The pBeloBac11 plasmid was purchased as a strain (New England Biolabs, ER2420S). To obtain sufficient DNA for coating  $50 \mu\text{l}$  colloids ( $1\%$  solids), the strain was grown overnight at  $37 \text{ }^\circ\text{C}$  in  $60 \text{ ml}$  LB medium (for  $100 \text{ ml}$ : Bacto-Tryptone  $1 \text{ g}$ ; Bacto-Yeast extract  $0.5 \text{ g}$ ; NaCl  $1 \text{ g}$  and  $\text{ddH}_2\text{O}$  to  $100\text{ml}$ ; autoclave to sterilize) in presence of chloramphenicol ( $20 \mu\text{g/ml}$ ). With a spin miniprep-Kit (Qiagen) the plasmid DNA was then isolated. The purity of the DNA was checked by gel electrophoresis on a  $1\%$  agarose gel. The plasmid contains the same cos-site that can be opened by restriction with  $\lambda$ -terminase (BIOzymTC), leaving the same  $12$  base single strands (“sticky ends”). As with the  $\lambda$ -phage DNA, the pBeloBac11 DNA was separated into two batches and modified with biotin according to the same protocol described above.

#### 4.4.2 Preparation of DNA-coated colloids

As in Ref. [53] we used a binary system in which DNA mediated attractions are favorable only between heterogeneous colloids. Green and red fluorescent neutravidin-coated polystyrene micro-spheres (diameter  $1 \mu\text{m}$ , Molecular Probes) were functionalized with DNA carrying complementary “sticky ends”.

Our conjugation protocol is based on the neutravidin-biotin coupling procedure described in Ref. [53]: the two batches of  $\lambda$ -DNA or pBelo-DNA were separately mixed with either green (“A” hereafter) or red (“B” hereafter) fluorescently labeled colloids, coated with neutravidin, that were dispersed in TRIS-HCl ( $250 \text{ mM}$ ,  $\text{pH} = 8$ ). In each case the DNA and colloids were reacted overnight during which they were continuously tumbled. The next day the samples were pelleted and washed five times to remove excess of non-conjugated DNA. In between these washing steps, samples were heated once for  $10 \text{ min.}$  at  $50 \text{ }^\circ\text{C}$ , to remove poorly bound DNA. The supernatant was retained to quantify (by UV-spectrometry at  $260 \text{ nm}$ ) the amount of DNA that had effectively bound to the colloids. For  $\lambda$ -DNA this leads to an estimate of some  $10$  DNA chains per colloid. We prepared two types of pBelo-coated colloids, both with around  $25$  DNA grafted chains per colloid. However, in one sample, all  $25$  pBelo-DNA chains carried sticky cos ends, while in the other, only  $8$ - $10$  sticky arms were present, with the remaining pBelo-DNA being blunted. Latter samples were prepared with a ratio of  $1/3$  of sticky end DNA and  $2/3$  of blunt DNA. Given the relative size of the polymer and the colloids, we expect each colloid to be completely surrounded by grafted DNA. For thermo-reversibility tests, we also prepared colloids, where the complementary ssDNA was directly attached. The polystyrene colloids have a binding capacity of  $4.5 \text{ nmol biotin/mg colloids}$ , providing  $20000$ - $30000$  binding sites for biotin-cos1 or biotin-cos2 nucleotides and thus a much

higher DNA coverage.

The DNA-coated colloids were diluted in a fresh TRIS-HCl buffer (250 mM final concentration, pH = 8) with D<sub>2</sub>O to minimize sedimentation. This yielded two batches of colloids with either ds- $\lambda$ -DNA (10 sticky arms per colloid) or ds-pBelo-DNA (either 8 or 25 sticky arms per colloid) grafted onto their surfaces by strong biotin-neutravidin bonds, displaying complementary single stranded cos1 and cos2 free ends respectively and one batch of colloids directly displaying the cos1 and cos2 free ends (no dsDNA spacer).

### 4.4.3 Preparation and coating imaging chambers

To avoid any nonspecific interactions between DNA-coated colloids and glass surfaces of the imaging chambers, coverslips were coated with polyethylene glycol (PEG). The coating of glass slides with PEG is a two-step procedure. First the glass slides were silanized with 3-mercaptoptriethoxysilane (97%, Fluka), then a 5-kDa maleimide modified PEG (Laysan Bio Inc) was tethered to the terminal thiol group of the silane.

Prior to the silanization, the glass slides were cleaned in an UV/ozone box. The cleaned slides were placed in contact with silane vapor overnight. Subsequently, the slides were rinsed with Ethanol, dried with Nitrogen and left in an oven (100 °C) for 30 minutes. Next a drop of concentrated maleimide modified PEG (250 mg/ml in TRIS-HCl buffer) is trapped between two silanized slides and left overnight at room temperature. The excess of PEG is removed by rinsing with ddH<sub>2</sub>O.

A sample chamber is made from two glass coverslips of different size separated by a parafilm spacer (100  $\mu$ m). The parafilm sealed the chamber on three sides. After loading the chamber with 10  $\mu$ l of each population of DNA-coated colloids, reaching a final colloid volume fraction of  $\phi \approx 0.004$ , the chamber is completely sealed with glue.

### 4.4.4 Confocal imaging

A and B colloids were mixed in equal ratios, a 20  $\mu$ l aliquot of which was displayed in an imaging chamber (colloids are suspended in a TRIS-HCl buffer (250 mM final concentration, pH = 8) with D<sub>2</sub>O to minimize sedimentation). All suspensions were imaged at room temperature by means of an inverted microscope (DMIRB, Leica) with a confocal spinning disc scan head (CSU22, Yokogawa Electric Corp.) and a 60x water immersion objective. Fluorescence of the two populations of colloids was excited at 488 nm and 512 nm. Emission was observed at 505 nm and above 600 nm respectively. The use of two types of fluorescent colloids and confocal microscopy allowed us to extract colloids coordinates and to reconstruct 3D images [2].

## 4.5 Acknowledgements

I would like to thank David Dryden for suggesting the use of pBeloBac11. M. Leunissen, D. Pine and P. Chaikin were very helpful in determining grafting densities of short DNA oligonucleotides using radioactive labeling.

# 5

## Colloidal Flying Carpets

*DNA plays a special role in polymer science not just because of the highly selective recognition of complementary single DNA strands but also because natural DNA chains can be made very long yet perfectly monodisperse. Solutions of such long DNA chains are widely used as model systems in polymer science. Here, we report the unusual self-assembly that takes place in systems of colloids coated with very long double-stranded DNA. We find that colloids coated with such long DNA can assemble into unique “floating” crystalline monolayers that are suspended at a distance of several colloidal diameters above weakly adsorbing substrate. The formation of these monolayers does not depend on DNA hybridization. Floating colloidal structures have potentially interesting applications as such ordered structures can be assembled in one location and then deposited somewhere else. This would open the way to the assembly of multi-component, layered colloidal crystals.*

### 5.1 Introduction

The preceding experimental chapters focused on the DNA-driven assembly of different types of complementary DNA-coated colloids in solution. In the present chapter we take a different approach. Instead of the assembly of complementary colloids in solution, we now consider colloids that cannot bind to each other as they are all coated with identical DNA strands. This DNA may either be terminated with sticky ssDNA ends that can bind to complementary ssDNA that is grafted to the bottom of the sample cell (Figure 5.1a), or it may only interact weakly (and non-specifically) with the substrate. But even in that case, DNA-mediated colloid-colloid binding is not possible as all colloids display the same DNA sequence (Figure 5.1b).

Immobilization of colloids coated with short DNA fragments on a surface coated with complementary DNA was extensively studied by Niemeyer and coworkers [94, 95]. In these experiments, the immobilization of the colloids on a DNA micro-array indicated that the surface adsorption proceeds with complete site selectivity, as few immobilized colloids were observed when non-complementary DNA was used. By printing small areas with ssDNA, a pattern consisting of areas with or without colloids could thus be obtained. The colloids within these areas exhibited no two-dimensional ordering; rather they formed an amorphous layer because the colloids tended to be immobilized on the spot where they landed. Niemeyer et al. also explored if two-dimensional ordering of colloids could be improved by grafting two different sequences on the colloids and

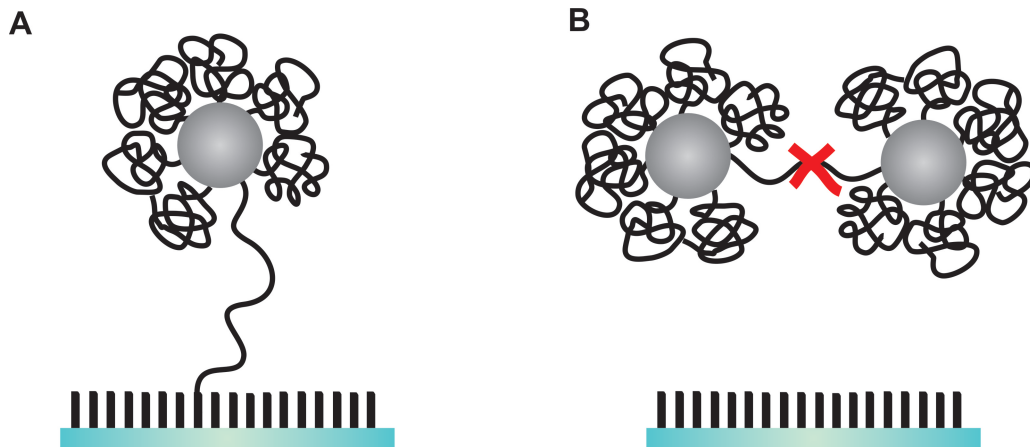


Figure 5.1: DNA-coated colloids above a ssDNA-coated surface. A: Complementary ssDNA ends of the DNA-coated colloids can hybridize to the ssDNA of the surface. B: Colloid-colloid binding is not possible as all colloids display the same ssDNA sequence.

introducing additional “linker” DNA [101]. The first sequence on the colloids was again used to bind (hybridize) to the surface. The second type of colloid-bound oligomers were used to establish cross-links to neighboring colloids by means of the “linker” DNA. While the length of the linker DNA controlled the inter-particle spacings, no additional lateral order was observed in this system. Other authors [96, 97] also observed that DNA-coated colloids bound to a substrate tended to exhibit no lateral ordering. In fact, ordered DNA layers were only observed in cases where the surface had been prepared with an ordered pattern of surface grafted ssDNA strands [96, 97]. In those cases, the order was induced by the “template” rather than by the colloid-colloid interactions.

Seeman and coworkers used a DNA scaffold to align DNA-coated colloids in rows with precisely defined inter-row spacings. The scaffold was prepared before addition of the colloids and contained predetermined hybridization sites. After addition of DNA-coated colloids, rows of aligned colloids appeared. Of course, there exists an extensive literature on colloidal particles that form two-dimensional crystals upon adsorption to a flat and unstructured surface (see e.g. ref. [153, 154]). In these systems, the attraction between colloids and wall leads to a high concentration of mobile adsorbed colloids. At sufficiently high densities, these colloids undergo a (two-dimensional) freezing transition. However, when the attraction between colloids and surface is reduced, these crystals melt again. Density-driven freezing of DNA-coated colloids was observed by Luo et al. [104]. These authors were able to make hexagonally stacked crystal sheets by drying a drop of DNA-coated colloid solution confined in the pores of a super-lattice sheet. By evaporation of the excess solution a free-standing colloidal film appeared. As, in this case, the ordering was density driven, the colloids used in this study did not need complementary ssDNA ends.

In this chapter we show that it is possible to obtain two-dimensional colloidal structures that are floating well above a properly prepared but unstructured surface. While previous studies mainly used short oligonucleotides, we choose to work with longer DNA. As we shall show below, DNA-mediated colloid-surface interactions are not responsible

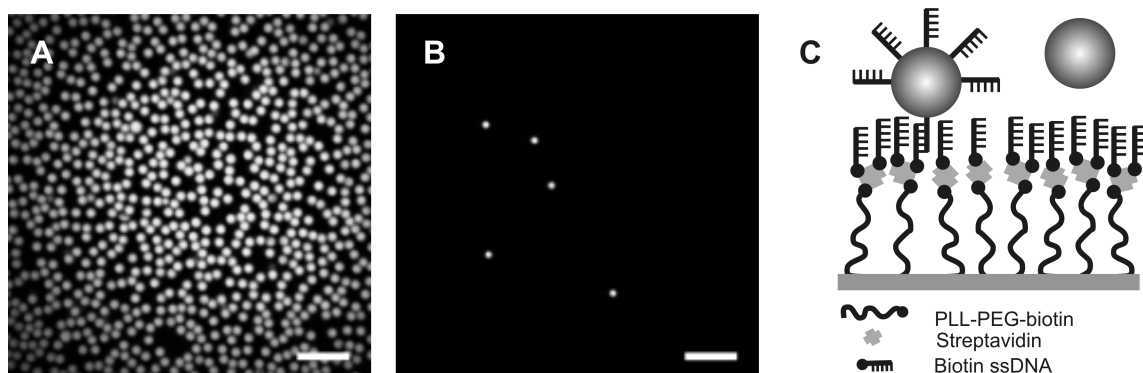


Figure 5.2: A: Coverage of a flat surface coated with single-stranded DNA by colloids carrying complementary short (12bp) ssDNA. B: If the same colloids are used, but now without attached ssDNA, no adsorption is observed. This indicates that in this system, non-specific binding is unimportant. Both scale bars are  $10 \mu m$ . C: Schematic representation of the experiments shown in A and B. The glass is coated with a polylysine-PEG-biotin layer to which streptavidin is connected. Biotinylated-ssDNA is bound to the streptavidin. Colloids coated with complementary DNA can hybridize to this surface. “Bare” PS-colloids remain in solution (Density matching prevents the colloids to sediment in time). Images are not to scale.

for the formation of ordered two-dimensional structures. In fact, in all cases where DNA-mediated colloid-surface interactions are significant, we find that an amorphous layer of adsorbed colloids forms. The formation of floating crystalline monolayers is related to the fact that the DNA grafted on the colloids behaves as a very long, yet monodisperse polymer [155].

## 5.2 Results and Discussion

### 5.2.1 Grafting surfaces with DNA

As a sample chamber we used a 96-well plate (Sensoplate; Greiner bio-one), allowing us to run many experiments under identical conditions. Onto the bottom glass surfaces of these wells we grafted a polymer monolayer holding ssDNA “sticky ends” (Figure 5.2c). To obtain such a layer we first coat the glass surfaces with a polylysine-poly(ethylene glycol)-biotin polymer (PLL-PEG-biotin; SurfaceSolutions). Subsequently we added a layer of streptavidin. In the final step biotinylated ssDNA could be easily attached (Figure 5.2c). Once the DNA-coated surface was formed, we tested the surface for DNA coverage, by exposing it to a suspension of colloids coated with the 12 complementary bases. The high number of colloids bound indicates proper surface coating (Figure 5.2a). Besides providing a suitable method of linking DNA to a glass surface, the polymer layer also prevents non-specific binding of colloids without DNA to the surface. Control experiments in which we disperse colloids without a DNA coating show that far fewer colloids are bound (by physisorption) to the surface (Figure 5.2b).

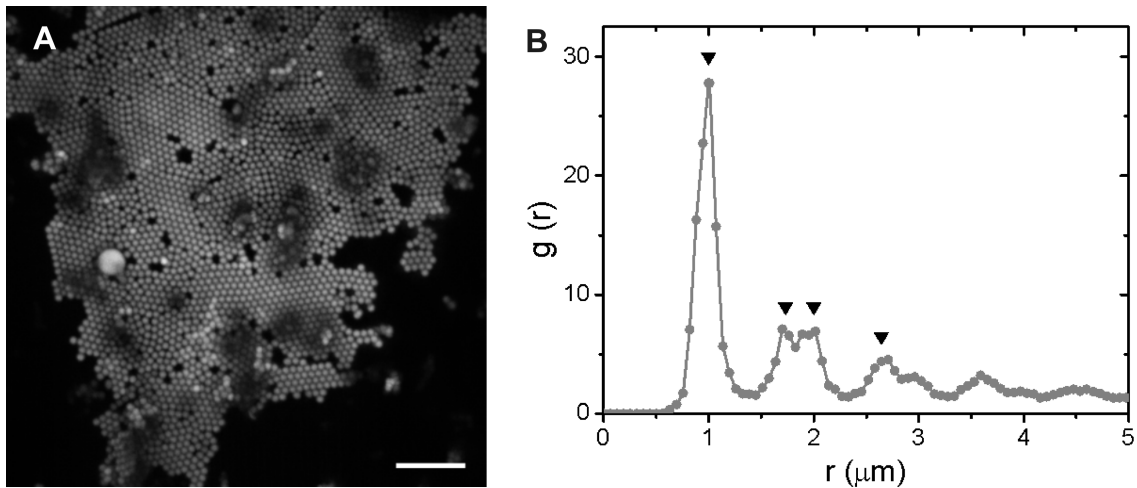


Figure 5.3: Aggregation of  $\lambda$ -DNA coated colloids above a “sticky” surface leads to 2D-flying carpets. A: Image of a flying carpet imaged with a confocal microscope. As the structure is slightly bent in the  $xy$ -plane a  $z$ -projection is shown. Scale bar is  $10 \mu\text{m}$ . B: Pair correlation function of figure A. The first neighbor is at contact, the function also shows peaks for the second, third and fourth neighbor. Black triangles: Guide to the eye; positions of expected peaks for a perfect hexagonal crystal.

### 5.2.2 DNA-coated colloid assembly above a (complementary) surface

The main experiments were performed with  $\lambda$ -coated colloids. This type of DNA is monodisperse and has a  $16 \mu\text{m}$  contour length (485000 bps; radius of gyration  $\sim 800 \text{ nm}$  [53]). The resulting colloids carry long dsDNA spacers with ssDNA “sticky ends” that can bind (hybridize) to the complementary ssDNA on the surface. Hybridization between colloids is not possible as they all display the same ssDNA sequence (5'-AGGTCGCCGCC-3'). As the radius of gyration ( $R_g$ ) of  $\lambda$ -DNA is similar to the colloid-size used, the colloids are coated with no more than 8 to 10 strands [53]. Sedimentation is minimized by density matching the DNA-coated polystyrene colloids with a sucrose-TRIS buffer. In all experiments we work at a low colloidal volume fraction of  $\sim 4.10^{-4}$ .

Two hours after injecting a solution of colloids coated with  $\lambda$ -DNA into the sample cell, we observe the appearance of single layers of close-packed colloids. If left at room temperature for longer times, these structures can grow into large colloidal monolayers that span the entire field of view of the microscope (Figure 5.3a). The structures are clearly crystalline, be it that some crystals contain point defects or even grain boundaries. Indeed, the pair-correlation function of this two dimensional crystal displays distinct peaks corresponding to those of a 2D hexagonal crystal (see black arrowheads, Figure 5.3b). Interestingly, these colloidal sheets float above the bottom of the cell, with colloids surrounding the carpet on either side (Figure 5.4a), at heights ranging from the  $R_g$  of  $\lambda$ -DNA up to  $5 \mu\text{m}$  (Figure 5.4b) with an average around  $2.5 \mu\text{m}$ . Because the colloidal monolayers appear several particle diameters above the substrate, we refer to these two-

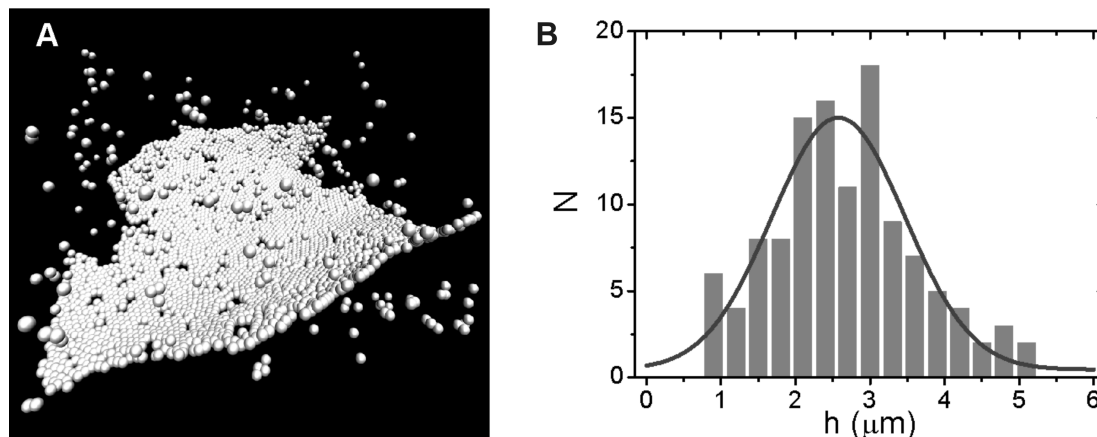


Figure 5.4: The average flying height of colloidal carpets above the surface. A: Reconstructed 3D-image of a carpet surrounded by colloids on either side. B: The 2D colloidal crystals sit not directly on the surface. Instead they are suspended above the surface at heights ranging from  $\lambda$ -DNA  $R_g \sim 0.8$  up to  $5 \mu\text{m}$ . The bars indicate the height a carpet had in respect to the surface from three different experiments (wells). In black a Gaussian fit is drawn to obtain an estimate of the average height:  $2.5 \mu\text{m}$ .

dimensional crystals as “colloidal flying carpets”. We observe this carpet-formation only above the bottom surface of the cell, but not in the bulk of the solution. Besides the two dimensional ordered crystals, also a small number of less ordered shapes is present.

$\lambda$ -DNA coated colloids contain 8 to 10 strands per colloid. If all strands of DNA would anchor to the surface the carpets would be unable to move. By imaging a single carpet at different moments in time, slow movements can be detected. Figure 5.5a shows a carpet with an unusual shape at a given time. After leaving the sample for two hours we imaged the same carpet again. This time there was no sign of growth, but the carpet did rotate (Figure 5.5b). The mobility of the carpet indicates that either not all strands of DNA were hybridized or at the very least, that the hybridization at room temperature is sufficiently weak to make rearrangements possible. As room temperature is well below the melting temperature of our 12 base pair bonds, the first probability is the more likely. Another conclusion that can be drawn from Figure 5.5 is that the crystallites have some time to anneal during growth, as the 2D crystals can even show clear facets.

### 5.2.3 Depletion forces are not responsible for the assembly

As our colloids are designed to have no DNA-mediated interaction with each other, the appearance of close packed colloids must be due to other (non-specific) interactions. The mechanism of self-assembly depends on the effective interaction between colloids mediated by the environment such as solvent, substrate or external fields. The most common non-specific interactions between colloids are: Coulomb interactions, dispersion forces and depletion forces. In the present case, (screened) Coulomb interactions between the colloids are certainly present but, as all colloids are like-charged, the Coulomb interaction

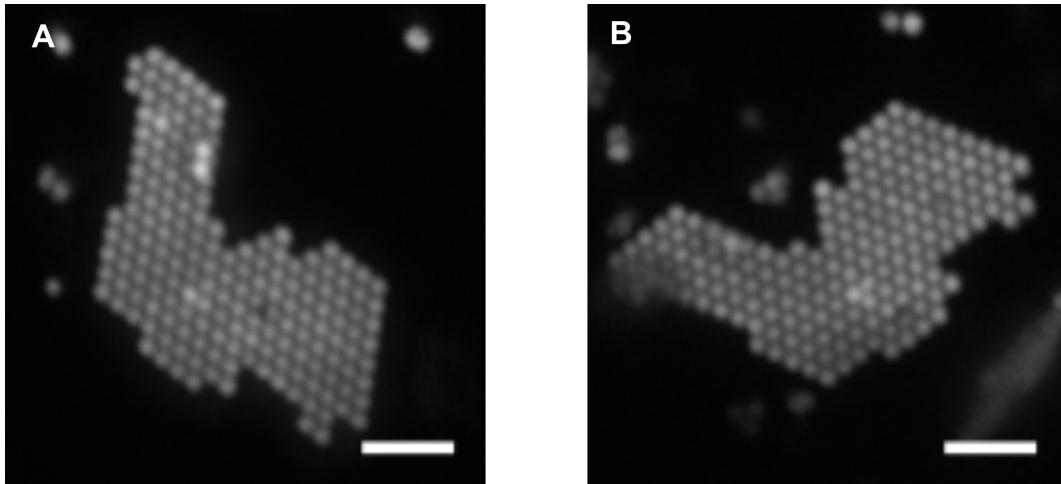


Figure 5.5: Confocal microscope image of a flying colloidal carpet at different moments in time. A: Image taken at  $t = 0$  hr (denoting the time it was observed). B: Image of the same carpet taken at  $t = 2$  hrs. Both scale bars indicate  $5 \mu m$ .

is unlikely to lead to condensation. Depletion forces are entropic, attractive interactions between colloids that can be caused by non-adsorbing polymers [156]. In our system, there is no free DNA and hence one might be tempted to dismiss depletion forces as a possible source of attraction. However, if the colloids move in a semi-dilute mesh of long DNA strands, short-ranged depletion interactions cannot be ruled out a priori - even if the DNA is grafted to the colloids.

To test if depletion forces are responsible for the 2D-aggregation behavior in our system, we repeated the experiment with colloids without DNA coating, but with free  $\lambda$ -DNA in solution. Whereas grafted polymers led to ordered 2D-aggregates (Figure 5.6a), the same concentration of DNA free in solution only yields small 3D aggregates of  $\sim 15$  colloids at most (Figure 5.6b). Even if we increase the  $\lambda$ -DNA concentration a hundred times we still see a clear difference in aggregation behavior. Now the aggregates comprise more colloids, but they consist of 3D branched structures (Figure 5.6c) as opposed to flat 2D crystals (Figure 5.6a). Kim and coworkers [123], who compared depletion forces of colloids of different materials, showed a similar effect for neutravidin-coated colloids. From the obtained pictures it is clear that depletion forces are not responsible for the formation of the “colloidal flying carpets”. These results indicate that the crystallization mechanism is different from previous observations where 2D crystallization from a very dilute colloid/polymer mixture was observed [157].

#### 5.2.4 Colloidal flying carpets are temperature stable

On the basis of the above discussion, it seems most likely that short-range dispersion forces play a key role in the formation of the dense colloidal carpets. As the primary minimum of the dispersion interaction between two colloids is extremely deep, we should expect that colloidal carpets, once formed are very stable. To test this hypothesis, we examined the behavior of the carpets at elevated temperatures. We first prepared

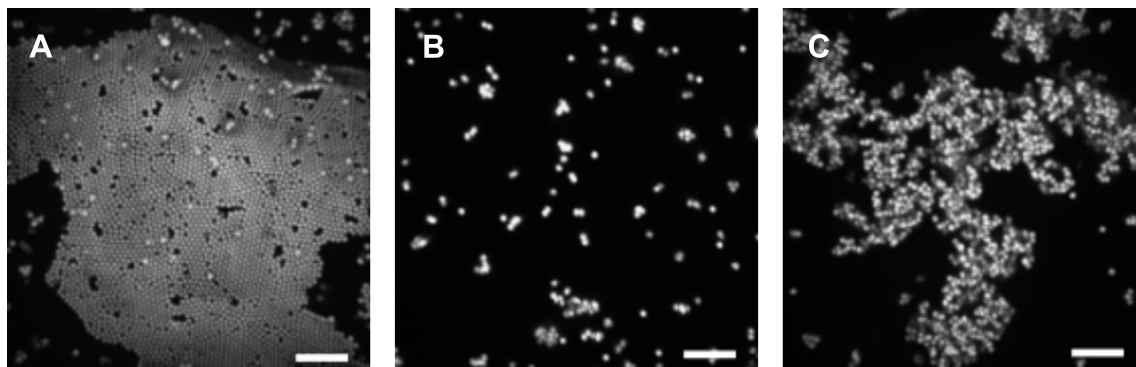


Figure 5.6: Comparison between aggregation of DNA-coated colloids and colloids surrounded by DNA free in solution. A:  $\lambda$ -DNA coated colloids aggregate into a flying colloidal carpet. B: Colloids surrounded by a solution of  $\lambda$ -DNA ( $\lambda$ -DNA is present at the same concentration as used in figure A) hardly aggregate; only small 3D clusters appear. C: If the concentration of  $\lambda$ -DNA is increased 100x, more aggregation is visible. In contrast to figure A this leads to 3D branches rather than 2D carpets. All scale bars are 10  $\mu\text{m}$ .

crystalline colloidal carpets at room temperature (Figure 5.7a). Once these had formed, the sample was heated to 70 °C for several hours (Figure 5.7b). The two-dimensional crystal structures were found to be remarkably stable against heating: even after more than 20 hours at 70 °C only minor changes can be seen (Figure 5.7c). Only at the edges of the carpet some colloids disappeared (compare Figure 5.7a, b and c white arrow heads).

These results strongly suggest that the colloidal carpets are held together by Van der Waals forces. In previous experiments (chapters 3, 4) the 12-base overhang grafted to colloids (with or without spacer) proved difficult to dissociate with elevated temperatures and it seems likely that in that case the DNA linkers “catalyzed” the formation of aggregates but that, once formed, the DNA links were irrelevant for the thermal stability of the aggregates - instead, the colloids stuck together due to dispersion forces. Of course, this short-ranged dispersion attraction can only function if the colloids can get close enough. Hence, if colloids are coated with a dense brush of short ssDNA, we should not expect them to stick to each other, nor to the substrates (provided the temperature is high enough to dissociate the DNA links). We tested whether cos-oligonucleotide functionalized colloids could dissociate from a surface with complementary ssDNA coating upon heating to 70 °C (Figure 5.8a). As this system only showed few colloids bound to the surface at a low volume fraction ( $\sim 4 \cdot 10^{-4}$ ) a significantly higher volume fraction was used ( $\sim 4 \cdot 10^{-3}$ ). First the surface coverage is imaged at room temperature (Figure 5.8b). Then the sample was heated to 70 °C. As can be seen from the figure, after removal of unbound colloids only few colloids remain bound to the surface (Figure 5.8c). This indicates that at 70 °C the 12-base DNA duplex is dissociated. As we showed before, the carpets that form when the colloids are coated with the longer DNA remain near the surface. In section 2.6 we shall argue that this fact is most likely due to gravity rather than to any specific DNA-mediated attraction.

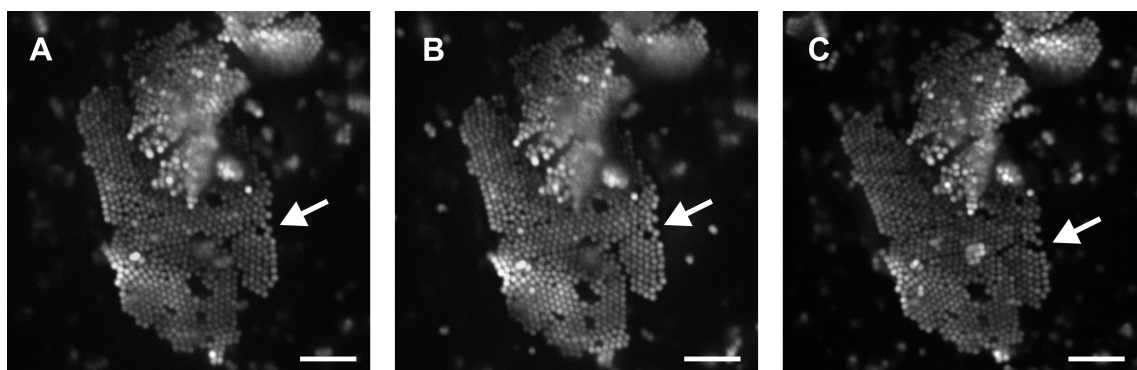


Figure 5.7: Flying colloidal carpets are temperature stable. A: Carpet formation at room temperature. B: After heating at 70 °C for two hours the same carpet is still intact. C: Even after more than 20 hours at 70 °C, the carpet did not melt. Marginal changes appeared in the border of the carpet (white arrowheads, compare to A and B) All scale bars measure 10  $\mu m$ .

### 5.2.5 Examining different control parameters of the system

As the colloids only crystallize near a surface and not in the bulk, other factors than dispersion forces also play a role in the membrane formation. To get more insight into the mechanism by which colloidal carpets form, we performed a series of experiments, where some of the system-parameters that could affect the aggregation process were varied. These are: the method used to attach the ssDNA to the bottom of the sample cell, additives like sucrose present in the buffer and the length of the DNA-coating on the colloids.

#### Method of surface coverage does not control carpet formation

To test the importance of a polymer-based method to graft DNA to the surface, a different approach was chosen to provide a DNA-coated surface. Instead of using a polylysine-PEG coating, we coat the glass surface with a protein-based multilayer. Bovine serum albumin (BSA; Sigma-Aldrich) adsorbs to glass if charge neutral. By using a biotinylated version of BSA and multiple layers of the protein in combination with a streptavidin linker, a DNA-coated surface can easily be built up (Figure 5.9a). Although the surface coverage is lower than before (Figure 5.9b), carpets do form above this surface as well (Figure 5.9c), be it that they are smaller in size and occur less frequently.

#### Carpet formation is not dependent on choice of buffer

In order to test if the sucrose that we used for density matching is responsible for carpet formation, we repeated the experiment in a Tris-HCl buffer in combination with heavy water ( $D_2O$ ; 50-50; 100 mM final concentration) to density match the DNA-coated colloids. The appearance of similar two-dimensional crystalline structures (Figure 5.10a), demonstrates that sucrose is not essential for the aggregation process.

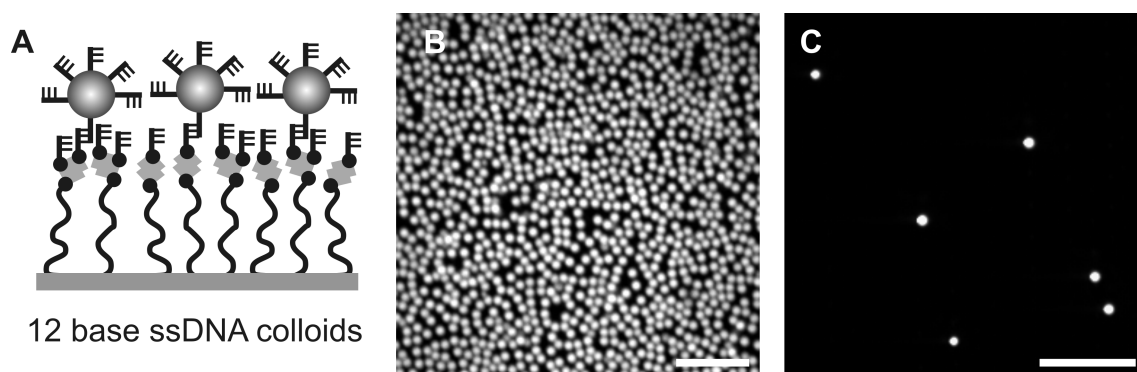


Figure 5.8: Cos-oligonucleotide grafted DNA-coated colloids can be melted off a flat surface functionalized with the complementary ssDNA. A: Schematic representation of cos-oligonucleotide grafted DNA-coated colloids on a surface. B: At RT an amorphous colloidal layer in direct contact with the polymer layer forms. C: When the sample is heated to 70 °C for several hours most colloids dissociate from the surface. Both scale bars indicate 10  $\mu\text{m}$ .

But is density matching a necessary requirement for the 2D crystallization? Repeating the experiment in a pure TRIS buffer (no density matching) indicated that carpets form even without density matching of the DNA-coated colloids (Figure 5.10b), although they appear smaller and closer to the surface. In time, all colloids eventually settle down, so the carpets get buried underneath sedimented colloidal particles (Figure 5.10c).

### Reducing the DNA length inhibits carpet formation

The carpet formation that we described above was observed in systems of colloids coated with very long ( $\lambda$ ) DNA. In order to test the role of the length of the grafted DNA, we repeated the experiments with shorter DNA strands grafted to the colloids. To keep all other interactions similar, DNA with the same 12 base ssDNA overhangs were used: pBelo-DNA (7500 bp;  $R_g \sim 200\text{nm}$  (100 mM Tris-HCl pH 8)) and cos-oligonucleotides (12 bases ssDNA; no spacer). The length of the DNA plays an important role in carpet formation. Whereas  $\lambda$ -DNA (Figure 5.11a) and pBelo-DNA coated colloids (Figure 5.11b) form colloidal carpets, the colloids coated with the cos-oligonucleotides do not (Figure 5.11c). Rather, we observe an amorphous colloidal layer in direct contact with the polymer layer that coats the bottom surface of the sample well. While we did observe the formation of floating 2D crystals with pBelo-colloids, the maximum sizes of the colloidal sheets seemed, on average, smaller than for the  $\lambda$ -DNA coated colloids. Furthermore, the carpets appeared closer to the surface (average  $\sim 1 \mu\text{m}$ ; data not shown), suggesting that the DNA separates the colloids from the surface: the length of the DNA determines the “flying height” of the floating 2D crystal structures.

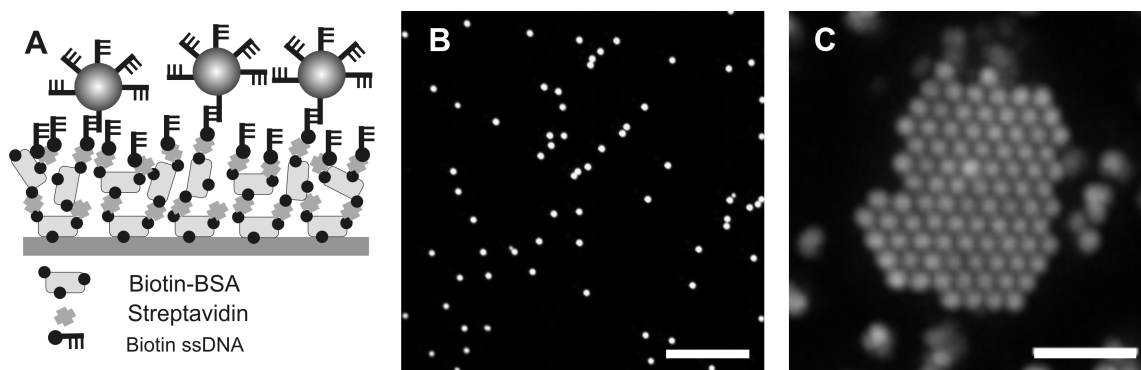


Figure 5.9: The method of adsorbing DNA to the surface is not crucial for carpet formation. A: Schematic representation of a multilayer of biotin-BSA and streptavidin surface, terminated by ssDNA. The surface coverage can be tested with complementary ssDNA-coated colloids. B: The surface coverage of DNA on a protein layered surface is much lower than on a polylysine-PEG-based surface. C: Even though the coverage is lower, carpet formation with  $\lambda$ -DNA coated colloids is still possible. Scale bars indicate  $10 \mu\text{m}$  for B and  $5 \mu\text{m}$  for C.

### 5.2.6 Specific binding through ssDNA overhangs is redundant to form flying colloidal carpets

As increasing the temperature can dissociate the 12-base duplex as shown in figure 5.8c, DNA hybridization cannot be the only factor responsible for keeping the carpets near the surface. Non-specific binding of the dsDNA spacer to the surface may, however, play a role. Whether or not this is the case can be tested by repeating the carpet formation experiments under conditions where DNA-surface hybridization is impossible. Indeed, ref. [158] reports a study on the non-specific DNA interaction with pLL-PEG films. As shown in ref. [158], DNA can adsorb to the polymer layer (Figure 5.12a). The strength of this adsorption depends on the ionic strength of the solution. To test whether non-specific interactions are sufficient to obtain carpets, we prepared polylysine-PEG monolayers on the well-surfaces and grafted colloids with blunt pBelo-DNA. The results (Figure 5.12b) show that DNA hybridization is indeed not necessary to obtain the crystal structures. Note that this is only true for a surface coated with pLL-PEG (or at least a surface coating with a positive charge). The other coating tested, a BSA protein layer (Figure 5.9), is negatively charged [159] at the pH used in the experiments. In this case it seems plausible that ssDNA is necessary to impose an attractive interaction between the surface and the colloids, but we did not test this.

The behavior observed in Figure 5.12a suggested an additional experiment, namely one where the electrostatic attraction between the long (negatively charged) DNA and the (positively charged) polylysine is strongly screened. Indeed, we found that no carpets form when the experiment is performed in the usual buffer but with 100 mM of added salt (data not shown). It would be interesting to test the behavior of the carpets at intermediate ionic strengths. Is there a threshold for carpet formation or does the average size of the carpets decrease continuously to zero?

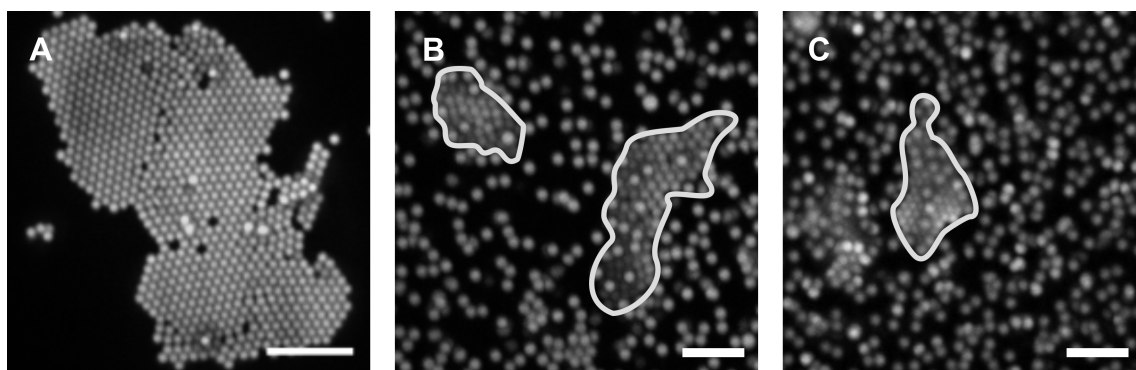


Figure 5.10: Carpet formation is not dependent on choice of buffer. A:  $\lambda$ -DNA-coated colloids also aggregate into flying colloidal carpets when ( $D_2O$ ) is used to match the density of the colloids instead of sucrose. B: Carpets form even without minimizing sedimentation. C: Without any type of density matching carpets get buried under colloids that settle down on the surface. As these carpets are harder to see, a white curve is drawn around one of the buried carpets. Scale bar indicates  $10 \mu m$  for A and  $5 \mu m$  in B and C.

### 5.2.7 Two factors are essential for the formation of crystalline colloidal membranes

The colloids coated with cos-oligonucleotides (no dsDNA spacer; 12 bases ssDNA attached directly to the colloids) were unable to form crystalline sheets. Instead, an amorphous colloidal layer in direct contact with the polymer layer coating the surface of the sample well is formed. This randomness as well as the fact that these colloids can be “melted off” above the hybridization temperature of the 12 bp-bonds ( $T_m \sim 42^\circ C$ ; Figure 5.8c) suggests that two factors are essential for the formation of crystalline colloidal membranes: a. weak binding to the surface that allows colloids to diffuse and b. weak steric stabilization of the colloids against the formation of direct contacts due to

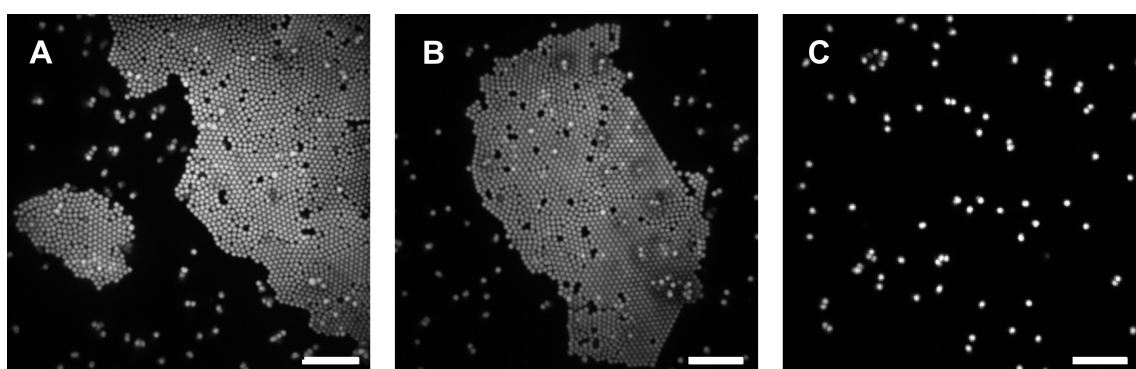


Figure 5.11: The formation of flying colloidal carpets depends on the dsDNA spacer length. A:  $\lambda$ -DNA coated colloids (48500 bps). B: pBelo DNA-coated colloids (7500 bps). C: Colloids coated with 12 bp ssDNA (no spacer). All scale bars measure  $10 \mu m$ .

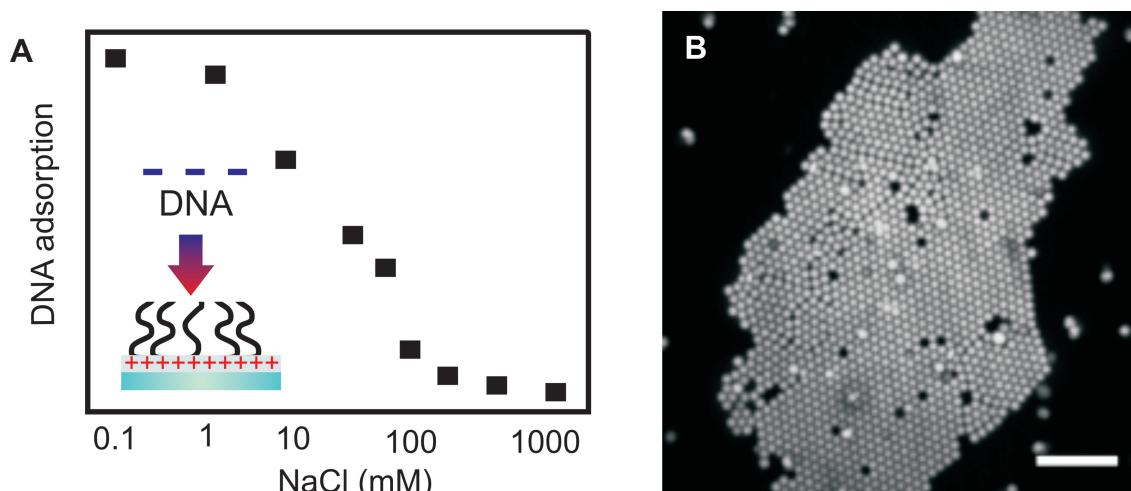


Figure 5.12: As long DNA can adsorb non-specifically to a pLL-PEG layer, “sticky ends” are not needed to form carpets. A: DNA adsorption to pLL-PEG as a function of the ionic strength. This graph is a schematic representation of figure 5 from reference [158]. Insert: schematic representation of the negatively charged DNA interacting with the positive charges of the lysines underneath the PEG monolayer. B: Even colloids coated with blunt ended DNA can form colloidal carpets, indicating that physisorption is enough. Scale bar indicates  $10 \mu\text{m}$ .

strongly attractive dispersion forces. If the colloids are too strongly bound to the surface of the cell, as is the case for the colloids coated with many short ssDNA strands, surface diffusion of the colloids is inhibited and hence amorphous layers can form, since annealing is not possible. In addition, the short DNAs provide steric stabilization against the formation of direct colloid-colloid contacts. Hence, neither condition for the formation of crystalline colloidal carpets is satisfied in the case of colloids coated with short ssDNA.

Colloids grafted with either  $\lambda$ -DNA, or pBelo-DNA with the same ssDNA overhangs do not aggregate in the bulk under the conditions used in the present experiments (chapter 4). This implies that in the bulk of the solution, where the colloidal concentration is low, the DNA cloud that surrounds the colloids is sufficient to prevent aggregation due to non-specific Van der Waals interactions. However, near the bottom cell surface, this situation changes: the charged DNA strands on the colloids are attracted weakly and non-specifically to the (oppositely charged) polylysine layer on the surface. As a consequence of the DNA-surface attraction, the colloidal concentration is significantly enhanced on the surface and colloids come into contact sufficiently frequently to overcome the weak entropic barrier provided by the long dsDNA. Indeed, in the 2D crystals the colloids are effectively touching each other and, as we argued above, the thermal stability in the colloidal membranes is therefore most likely due to the action of short-range dispersion forces. At the same time, the fact that highly ordered 2D crystals form indicates that crystal growth is slow: aggregation is definitely not diffusion limited.

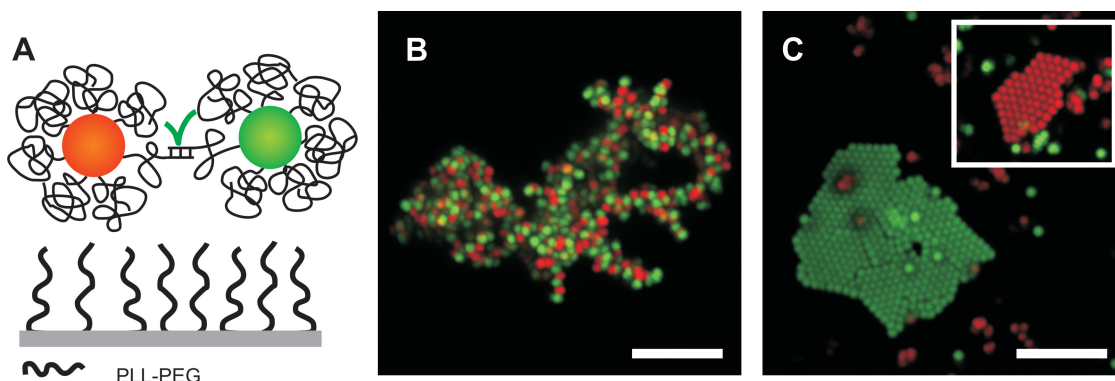


Figure 5.13: Carpet formation precedes (binary) cluster formation for long DNA. A: Schematic representation of the experiment. In the binary colloid mixture, colloid-colloid binding is possible by complementary base pairing. B: Cos-oligonucleotide and pBelo-DNA coated colloids aggregate into 3D-assemblies (cos-cluster depicted) and carpet formation is not observed. C:  $\lambda$ -DNA coated colloids form carpets of single-color. Carpets of green-fluorescent colloids coexist with carpets of red-fluorescent colloids (insert). Note that in the bulk solution red and green colloids are well mixed. Both scale bars are  $10 \mu\text{m}$ .

### 5.2.8 Carpet formation precedes (binary) cluster formation for long DNA

Thus far, we have studied carpet formation in colloids that cannot bind to each other via DNA hybridization. We now consider what happens if such interactions can occur. By allowing colloid-colloid binding we introduce a competition between colloid-colloid binding and colloid-to-surface interactions. We limit ourselves to the case where the colloids cannot hybridize to the surface (Figure 5.13a). All three DNA-coated colloid systems were examined. Both the colloids coated with the cos-oligonucleotides and the colloids grafted to pBelo-DNA formed three-dimensional aggregates comprising both green- and red-fluorescent colloids (Figure 5.13b). The structures that formed were similar to those observed in our previous experiments in bulk (chapter 4). For both systems, colloid-colloid binding is preferred to the interaction with the surface.

In contrast, the samples containing both types of  $\lambda$ -DNA colloids aggregate into two dimensional crystalline structures (flying carpets). Apparently, here the competition turned out in favor of the surface interactions. Surprisingly, all carpets consist of either pure red, or pure green colloids (Figure 5.13c) even though the red and green colloids are well mixed in solution. By comparing the relative aggregation speeds of the different types of DNA-coated colloids, we can arrive at a qualitative explanation for the observed competition between bulk aggregation and surface adsorption. The colloids coated with cos-oligonucleotides bind on contact by DNA hybridization. Aggregation takes place in minutes, i.e. in a time that is much shorter than the time needed to adsorb onto the substrate. Colloids coated with pBelo-DNA can in principle form carpets but they can also aggregate in the bulk. Which of the two scenarios dominates depends on the relative rate of the two processes. In the present experiments, only three dimensional

structures were found. This is not surprising because, under the conditions of these experiments, the formation of carpets with colloids coated with pBelo-DNA takes 5-7 hours. However, as was shown in chapter 4, appreciable bulk clustering of pBelo-coated colloids can take place on this time scale. In fact, the results of chapter 4 suggest that in 5-7 hours pBelo-clusters can form that contain up to  $\sim 90$  colloids (Figure 5.14). The clustering via DNA hybridization is therefore faster than carpet formation. Aggregation of  $\lambda$ -DNA coated colloids is comparable in speed to pBelo-DNA coated colloids, but in contrast to pBelo-DNA coated colloids, carpet formation is faster ( $\sim 1$ -2 hours). On this timescale,  $\lambda$ -DNA clusters are barely present (Figure 5.14). This explains why we see carpet formation in the  $\lambda$ -DNA coated colloids and not with the other two types of DNA coated colloids.

Explaining why the  $\lambda$ -DNA carpets form, does not explain the puzzling observation that individual carpets are made of one type of colloid. One possible explanation could be that the different fluorescent dyes give slightly different physical properties to the red and green colloids. This might affect the range of the DNA “corona” of the colloids or possibly even their density. If this were to be so, the carpets of different colors could appear at different heights above the surface. However, our data shows no difference in the flying height of the red or green carpets (data not shown). There is, however, clear evidence that the dyes do affect the surface charge of the differently labeled colloids. This follows from measurements of the zeta-potential (measured with a Malvern “Zetasizer 2000” - averaged over 5 measurements). For non-fluorescently labeled  $\lambda$ -colloids, the zeta-potential is  $-18.3 \pm 1.6$  mV. In contrast, the red fluorescent  $\lambda$ -colloids have a zeta-potential of  $-13.1 \pm 1.6$  mV and the green fluorescent  $\lambda$ -colloids  $-23.0 \pm 5.6$  mV. These differences in the zeta-potential affect the behavior of the colloids and their DNA corona - clearly, such differences may result in different kinetics of carpet formation. However, at this stage, it is unclear how the differences in electrostatic properties could result in red-green phase separation and further experiments would be needed to sort this out.

### 5.2.9 DNA is not evenly distributed around the colloidal flying carpets

We have now established that grafting long DNA strands is essential for carpet formation. However, we have not yet shown directly where the  $\lambda$ -DNA resides once the carpets have formed. As the colloids within the carpets are closely packed there is little room for the  $\lambda$ -DNA inside the colloidal membrane. To determine the location of the DNA we use YOYO-staining. Because this dye is fluorescent, we use it in combination with non-fluorescent colloids.

The non-fluorescent colloids cannot be imaged with bright field light in the black sample chambers, used in all previous carpet-experiments. Therefore a clear 96-well plate was used instead. These plates are only available with a bottom surface made of plastic rather than of glass. The surface coverage of the polymer-ssDNA is tested in these sample-chambers as well. Figure 5.15a shows that although for some areas the specific binding is similar for both types of surface used (compare to insert), the

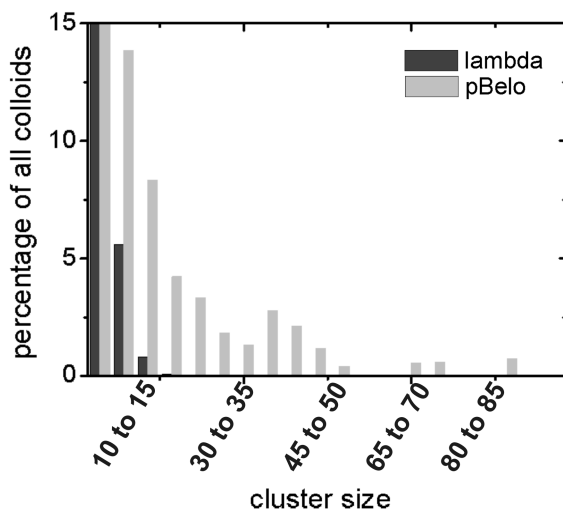


Figure 5.14: Histogram of cluster sizes of  $\lambda$ -DNA and pBelo-DNA coated colloids measured after the typical time the systems need to grow carpets above the surface. Clustering started long before carpet formation for pBelo-DNA coated colloids could take place.  $\lambda$ -DNA coated colloids are only present in small clusters during this time.

surface coating on the plastic plates also shows more and larger “holes” on the surface. Presumably, in these places there is insufficient polymer coating present. Comparing the number of colloids that stick non-specifically to the surfaces (Figure 5.15b) shows the effect of these so-called “holes”. Whereas the number of colloids on the bottom plate made of glass (Figure 5.15b, insert) is very low, this number increases significantly in the case of a plastic bottom plates. The figure indicates that colloids gather in the holes and stick to the unprotected surface.

Samples were loaded and imaged the next day after  $\sim 15$  hours. First the sample was checked with bright field microscopy. Although two-dimensional shapes were found, they contained less order than the colloidal flying carpets depicted earlier in this chapter, but similar to the less ordered shapes mentioned before. After localizing the “carpets”, YOYO is added to the solution. After 20 minutes incubation (in the dark), carpets are imaged (Figure 5.16). The DNA is not evenly distributed. At the surface (Figure 5.16b) non-specifically bound DNA-coated colloids are found. A faint glow is visible from the carpet floating above the surface. Moving up in the sample ( $\sim 3 \mu\text{m}$ ) the edges of the carpet become visible as the carpet is slightly bent ((Figure 5.16c and a,b-insert). Moving further up, we reach the midsection of the carpet, where individual colloids can be seen, due to the DNA staining (Figure 5.16d; note the lack of order). Here the DNA remains mainly around the edges except for a small piece in the middle. Even higher, just above the colloidal carpet (Figure 5.16e) most of the DNA is found, mainly in the midsection. To show the uneven distribution of DNA even clearer a z-projection is made of the entire stack (Figure 5.16f). As there is little DNA below the carpet, the uneven coloring of the DNA on top of the carpet is most likely due to imperfect DNA staining, rather than DNA depleted areas.

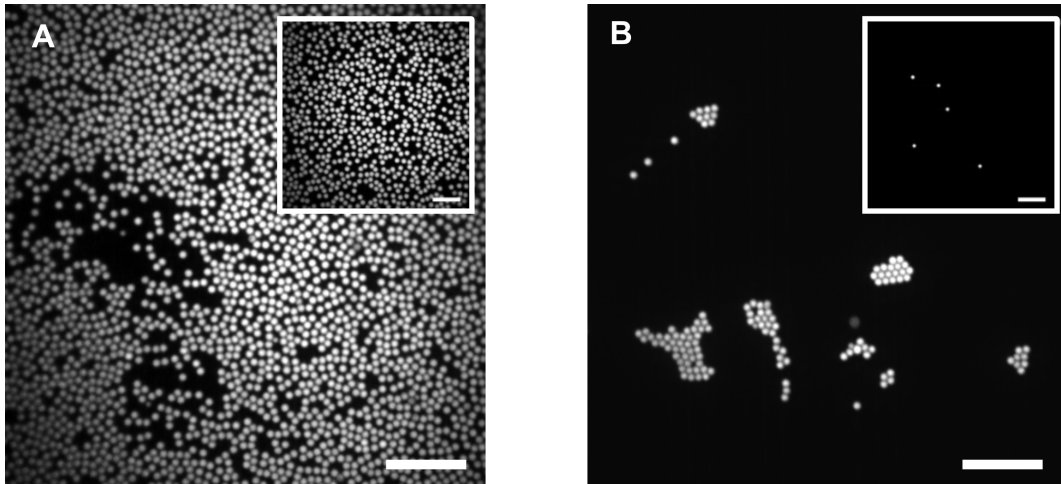


Figure 5.15: Surface coverage of the clear 96-well plate with a bottom made of plastic. The coverage is tested as depicted in Figure 5.2c A: Specific binding; the surface coverage is lower than for the samples with glass bottom plates (insert), some areas seem to be not covered by polymer (holes). B: Non-specific binding; the difference between the two surfaces is most apparent here (compare picture to insert obtained for a glass surface). The holes on the plastic surface now get filled with colloids that stick non-specifically to the plastic bottom plate. Both scale bars indicate  $10 \mu m$

The  $\lambda$ -DNA coated non-fluorescent colloids assemble into less ordered carpets. We point out that the same non-ordered carpets were also found with fluorescent colloids in the 96-well plates with a glass bottom (Figure 5.17b). These structures appeared within the same sample as the ordered ones (Figure 5.17a). For now we do not know what influences the system to create both ordered and non-ordered carpets within one sample.

The results of the DNA staining applies to the disordered carpets. Although it is likely that similar behavior would be observed in the case of ordered carpets, this conclusion is not obvious. Hence, the present experiments provide an ambiguous answer to the question where most of the DNA resides.

### 5.2.10 Testing a different sample holder

It would be interesting to test if we can first assemble a carpet and then transport it elsewhere. One option for this type of transport would be “dragging” a carpet with an optical tweezer, provided that the carpet retains its integrity during such manipulation.

With the 96-well plate such optical-tweezer experiments cannot be done as the bottom plate ( $175 \pm 15 \mu m$ ) is thicker than the focusing distance of the laser. To perform the proposed experiments in the future, new sample holders are needed. Here, we describe a preliminary test of one such sample holder.

To enable experiments with optical tweezers we need to make carpets in a sample containing two thin coverslips as bottom and top surfaces. Not only can we then use optical tweezers to try to move our carpets, but we can also turn the sample to see

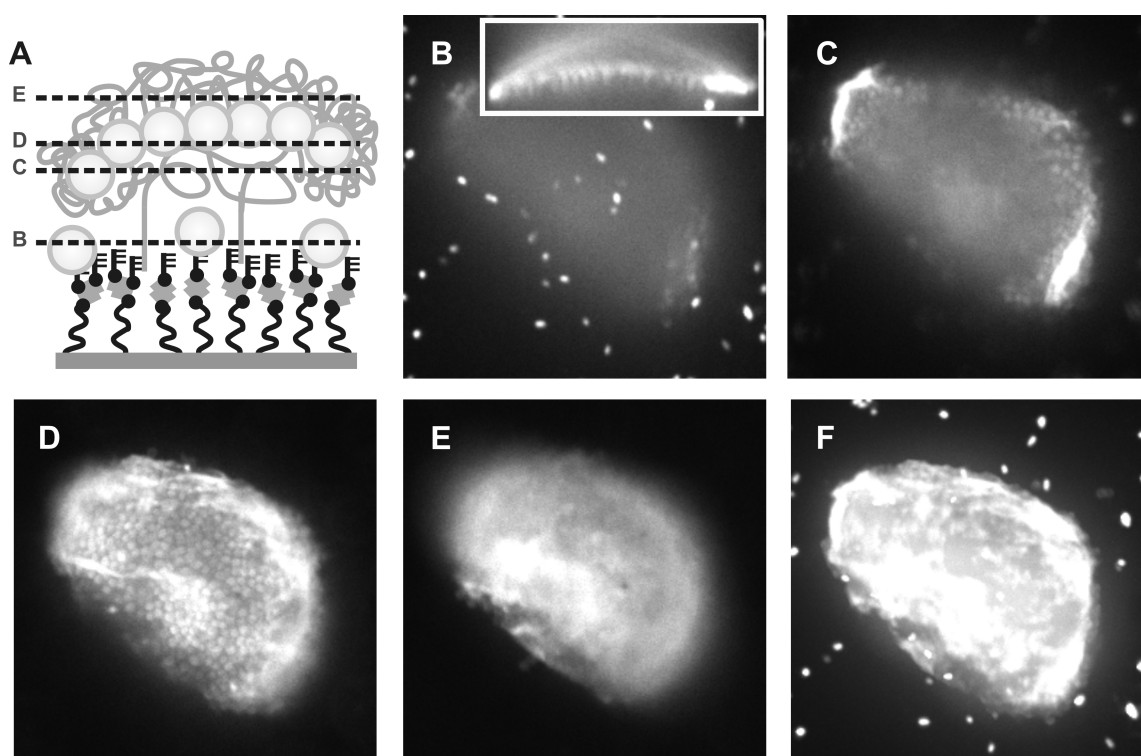


Figure 5.16: DNA is not evenly distributed around the colloidal flying carpets. A: Cartoon of image taken. Non-fluorescent  $\lambda$ -DNA coated colloids form a less ordered carpet above the surface. After YOYO-staining images are taken at different heights from the surface to determine where the DNA is. B: Colloids are stuck to the surface, the glow from the DNA of the carpet above can be seen faintly. Insert: side-view of the stack taken to show the slight bend of the carpet. C: More DNA appears to be present at the borders. D: At this height individual colloids can be seen. The reduced order in this system is clear. The DNA is mainly present at the borders except for a spot in the middle. E: Just above the carpet, a lot of unevenly distributed DNA is present. F: z-Projection of the entire stack showing DNA on top of the assembly and the monomers surrounding the carpet.

whether carpet formation is possible on both bottom and top surface simultaneously.

In the new sample holder (made with two thin coverslips separated with parafilm) surface coverage is tested with neutravidin colloids (Invitrogen;  $1 \mu\text{m}$ ; Figure 5.18a), on both pLL-PEG-biotin (specific; Figure 5.18b) and pLL-PEG (non-specific; Figure 5.18c) coated surfaces. We observe that there are approximately equal amounts of colloids present on both surfaces, indicating that the polymer layer is most likely not uniform or not dense enough. Therefore, we cannot conclude that the colloids in Figure 5.18b are bound specifically.

Despite the poor surface coverage, we tested if we could obtain carpets in these sample holders. The first experiments show that this is possible, but conditions are not yet optimized. In figure 5.19 some results are depicted. For the moment small carpets (Figure 5.19a,b) can be found as well as larger but less ordered ones (Figure

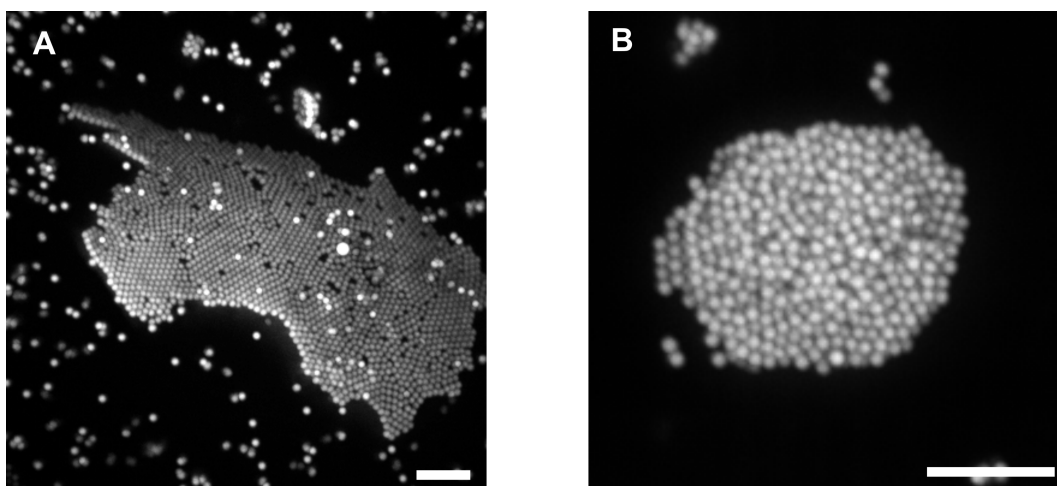


Figure 5.17: In one sample both perfectly ordered and less ordered carpets were found. A: Nicely ordered colloidal flying carpet. B: Two-dimensional shape with less order. Both scale bars indicate  $10 \mu\text{m}$

5.19c). Two shortcomings of these new sample holders are that the number of carpets formed is far lower than in the 96-well plates (from  $\sim 50$  to 4) and that the aggregation time increases to a few days as opposed to a couple of hours needed in the well plates. When the conditions are properly optimized, these sample holders could also be used for YOYO-staining on ordered carpets.

### 5.2.11 Conclusion

We have found that colloids coated with long DNA strands can spontaneously form a crystalline 2D colloidal carpets, hovering several microns above the support surface. Our control experiments suggest that the formation of these colloidal membranes is facilitated by the weak, non-specific adsorption of the DNA-coated colloids (or, more precisely, of the DNA coating of these colloids) to a weakly positively charged lower surface of the sample cell [158]. Under these conditions, the steric stabilization of the colloids by the grafted dsDNA is insufficient to prevent the slow formation of dense 2D colloidal crystals that are subsequently stabilized by short-ranged dispersion forces. Colloids that are coated with very short ssDNA strands bind strongly to the surface via specific interactions between the complementary strands and form an amorphous adsorbate rather than a crystalline floating carpet.

The ability to make floating, yet surface-bound structures, could provide an interesting route to make novel colloidal structures: in particular, by making use of suitable DNA linkers, it should be possible to induce the self-assembly of multiple layers of 2D crystals that can be attached on top of the carpets. Another option would be to use the free “sticky ends” to close the carpets, forming a tube of colloids with DNA on both sides, as possible docking sites to bind other molecules or materials.

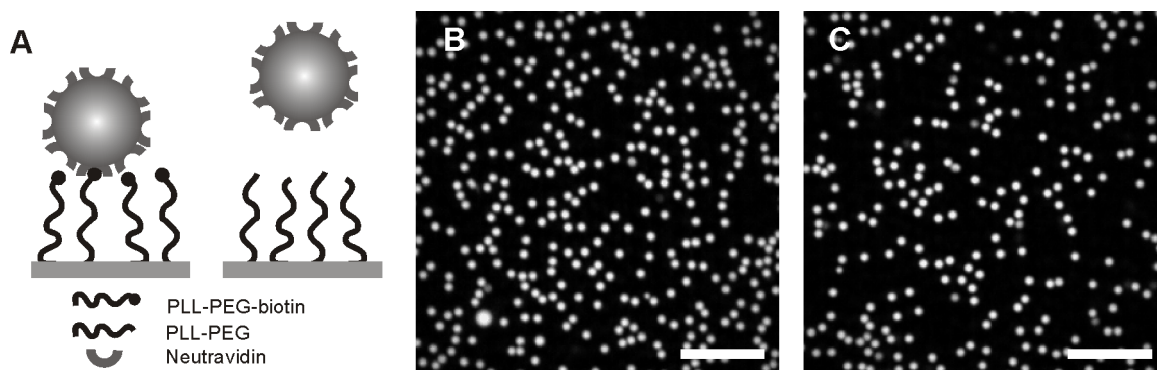


Figure 5.18: The surface coverage on thin glass cover-slips is poor. A: Schematic representation of how specific and non-specific binding is tested. Neutravidin coated colloids can bind to biotin, but not to PEG directly. B: Neutravidin-coated colloid binding to a pLL-PEG-biotin coated surface. C: Neutravidin-coated colloid binding to a pLL-PEG coated surface. Both scale bars indicate  $10 \mu\text{m}$ .

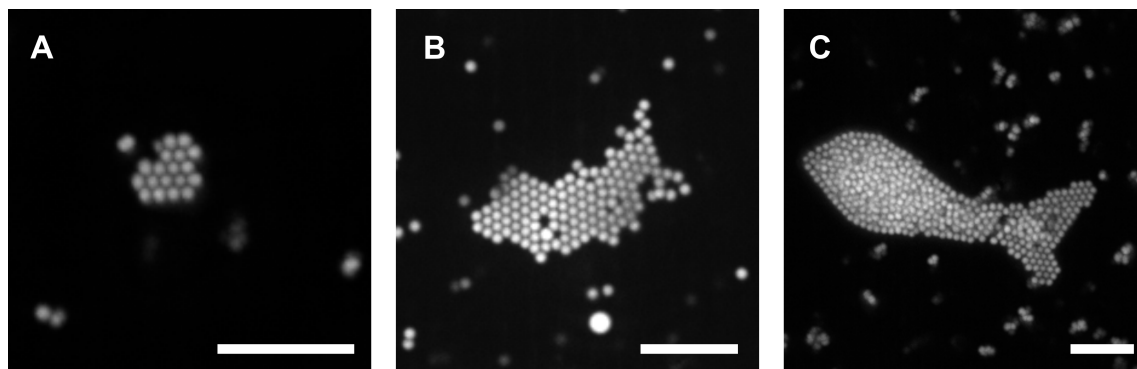


Figure 5.19: Carpets found in the “new” sample holder. A: Small carpet, found after three days. B: Bigger carpet (10 days). C: Big but less ordered carpet (10 days). All scale bars indicate  $10 \mu\text{m}$

## 5.3 Materials and Methods

### 5.3.1 Coating glass-surfaces with DNA

#### Polymer coating

The coating of the glass bottom plates of the 96 well-plates with a polymer is a three step procedure. Firstly, the wells are rinsed with a strong soap solution (Hellmanex; 10% solution) for at least 5 hours. After removing all the soap (rinsing with ddH<sub>2</sub>O) a polylysine-poly(ethylene glycol)-biotin polymer solution (PLL-PEG-biotin (0.5 mg/ml; 50  $\mu\text{l}$ ); SurfaceSolutions) is added. Subsequently we remove the excess of polymer solution. Next, a layer of streptavidin (0.5  $\mu\text{g}/\mu\text{l}$ ; 50  $\mu\text{l}$ ; Invitrogen) is added. We can now easily attach ssDNA in our third step using a biotin-streptavidin bond. A short single strand of 12 bases (5'-GGGCGGCGACCT-3') with a biotin attached to the 3'-

end is added ( $1 \mu\text{M}$ ;  $50 \mu\text{l}$ ; Eurogentec). Surface coverage is tested in a Tris-HCl buffer ( $100 \text{mM}$ ; pH 8) with neutravidin-coated polystyrene colloids (PS-colloids; Invitrogen,  $1 \mu\text{m}$  diameter) coated with the complementary 12 bases. DNA coated surfaces that are not immediately used are kept at room temperature in a sucrose-TRIS buffer ( $150 \text{mg/ml}$  sucrose;  $100 \text{mM}$  TRIS).

### Protein coating

To obtain protein coating we rinse the wells with a strong soap solution (Hellmanex; 10% solution) for at least 5 hours. After removal of all soap residues (rinsing with  $\text{ddH}_2\text{O}$ ) stacked layers of biotin-Bovine serum albumin (biotin-BSA; Sigma-Aldrich) and streptavidin are added. First a layer of biotin-BSA ( $2.5 \mu\text{g}/\mu\text{l}$ ;  $50 \mu\text{l}$ ) is attached in an acetate-buffer ( $20 \text{mM}$  acetic acid/  $80 \text{mM}$  sodium acetate; pH 5.2). Then a layer of streptavidin is added ( $1 \mu\text{g}/\mu\text{l}$ ;  $50 \mu\text{l}$ ; Invitrogen). As the biotin-BSA contains multiple biotins/molecule ( $\sim 3$ ), a branched structure of biotin-BSA can be generated by repeating the two steps once more (Figure 5.9a). Now we can, easily attach ssDNA in our third step using a biotin-streptavidin bond. A short single strand of 12 bases ( $5'$ -GGGCGGCGACCT- $3'$ ) with a biotin attached to the  $3'$ -end is added ( $1 \mu\text{M}$ ;  $50 \mu\text{l}$ ; Eurogentec).

### Stability of the polymer coating at elevated temperatures

A pLL-PEG-biotin surface is coated with neutravidin colloids as shown in Figure 5.18a. After imaging the surface coverage at room temperature (Figure 5.20a) the sample was heated to  $70 \text{ }^\circ\text{C}$ . Before imaging, the sample was rinsed to remove unbound colloids. Images were taken after 2, 7, 12 or  $> 20$  hours. Most of the time there was no evidence of colloids being removed (Figure 5.20b), but sometimes after a sample had been at  $70 \text{ }^\circ\text{C}$  for at least 12 hrs, some colloids disappeared from the surface (Figure 5.20c). After some control experiments we realized this was only the case if an older pLL-PEG-biotin solution was used (over  $\sim$  two/three months old at  $4 \text{ }^\circ\text{C}$ ).

To test if the colloid removal was due to complete removal of the pLL-PEG-biotin polymer or to a breakage in the biotin-neutravidin bond, we repeated the experiment once more. Two samples were placed at  $70 \text{ }^\circ\text{C}$  for  $> 20$  hrs, while being softly shaken to remove as much colloids as possible (Figure 5.20d,g). After imaging, new colloids were added to the samples. One sample received neutravidin colloids (Figure 5.20e), the other sample carboxylated colloids (Figure 5.20h; both of different color to be able to distinguish them). If the whole polymer dissociated, both types of colloids will bind as there is nothing to protect the surface from non-specific binding anymore. If only the biotin-neutravidin bond got broken, the neutravidin colloids will be able to rebind, whereas the carboxylated colloids cannot. The results show (Figure 5.20e,h) that the polymer dissociates from the surface at elevated temperatures. When an overlay is made of the colloids present after heat treatment and of the new colloids bound, we find no difference between neutravidin or carboxylated colloids and complete surface coverage again (Figure 5.20f,i).

### 5.3.2 Preparation of DNA-coated colloids

#### Colloids coated with DNA with a 12 base ssDNA overhang

In this chapter three types of colloids were used with a 12 base ssDNA overhang:  $\lambda$ -DNA, pBelo-DNA and the cos overhang. Colloids are prepared in the same way as described in chapters 3, 4. The only difference is in the final dilution step. Now the DNA-coated colloids were diluted in a fresh TRIS-HCl buffer (100 mM final concentration, pH = 8) to obtain a 0.5% solution and stored at 4 °C until used. For a typical experiment 15  $\mu$ l of the colloidal solution was added in 200  $\mu$ l sucrose-TRIS buffer (150 mg/ml sucrose; 100 mM TRIS).

#### Colloids coated with blunt ended DNA

To obtain blunt-ended DNA the pBelobac11 plasmid was used once more. To obtain an almost full length piece of DNA with one side blunted and the other end biotinylated, the plasmid was restricted with two enzymes: BamHI and HpaI. As these enzymes perform optimally in the same buffer conditions, the restriction can be performed simultaneously. After restriction all DNA is loaded onto a gel and the DNA piece is extracted from it. BamHI leaves a 5'-overhang of 4 bases that can be filled up nucleotide by nucleotide with Klenow exo<sup>-</sup>. (To obtain biotinylated DNA regular dTTP, dCTP, dGTP-nucleotides were used in combination with biotin-dATP; all Invitrogen). The reaction solution was then cleaned from excess nucleotides and enzyme (PCR-purification; Qiagen). The obtained blunt ended DNA was then attached to neutravidin-colloids as described before (see chapters 3, 4).

### 5.3.3 YOYO-staining of DNA

To visualize DNA YOYO-staining can be used. For these experiments non-fluorescent colloids were coated with  $\lambda$ -DNA in the same way as described before. Once aggregates form YOYO is added to the solution (5  $\mu$ M YOYO, final concentration; Invitrogen). After incubating for 20 min in the dark, images can be taken. (YOYO can be excited with the 488 nm laser).

### 5.3.4 Confocal imaging

All suspensions were imaged by means of an inverted microscope (DMIRB, Leica) with a confocal spinning disc scan head (CSU22, Yokogawa Electric Corp.) and a 60x water immersion objective. Fluorescence of the colloids was excited at either 488 nm or 512 nm. Emission was observed at 505 nm or above 600 nm respectively. The use of fluorescent colloids and confocal microscopy allowed us to extract colloid coordinates and to reconstruct 3D images [2].

## 5.4 Acknowledgements

I would like to thank W. Threels for his help with measuring the zeta-potential of the  $\lambda$ -DNA coated colloids (Wageningen University).

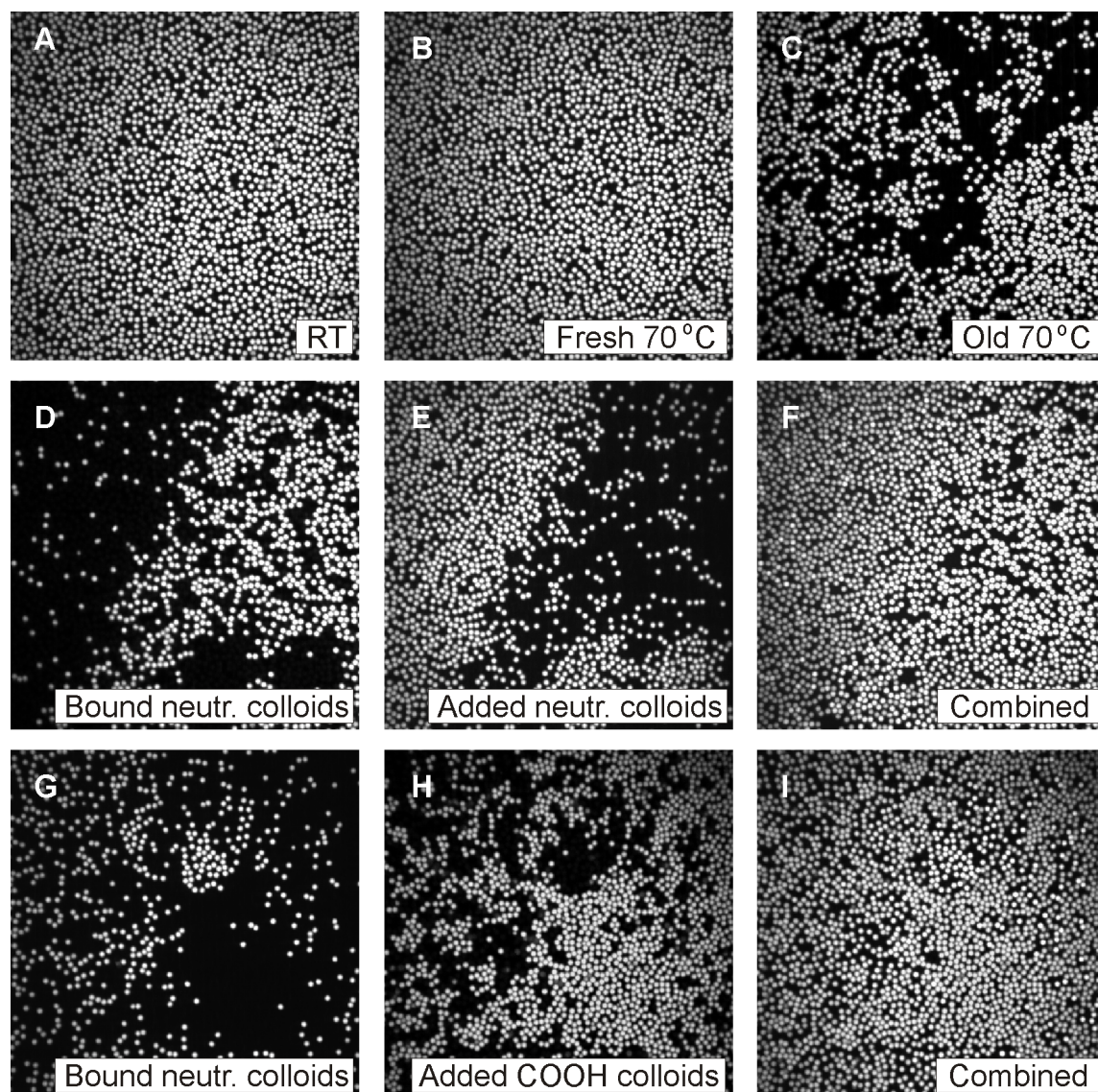


Figure 5.20: Stability of the polymer coating at elevated temperatures. A: Surface coverage of neutravidin colloids above a pLL-PEG-biotin surface at room temperature. B: As long as “fresh” solutions of the polymer are used, elevated temperatures do not disrupt the surface coating. C: With older solutions of the polymer, elevated temperatures can disrupt the surface coverage. D: Image of a sample that has been at 70 °C; 20 hrs. Clearly, almost half of the colloids previously bound are now unbound. E: Addition of a fresh batch of neutravidin colloids fills up the “holes” in the sample. F: figure D and E combined to show complete surface coverage is realized once more. G: same as D, but different sample slot. H: Addition of a fresh batch of carboxylated (COOH) colloids fills up the “holes” in the sample. I: figure G and H combined to show complete surface coverage is realized once more.



# 6

## A DNA-string quartet

*Non-spherical colloidal building blocks can lead to the development of complex colloidal crystals of lower symmetry than is possible with the use of isotropic spherical colloids. In this chapter we describe an exploratory study of a viable strategy to assemble four DNA-coated colloids via a Holliday junction. A Holliday junction consists of four DNA double helices, with a branch point discontinuity at the intersection of the component strands. By the use of this structure we aim to construct tetrahedral colloidal assemblies that are not limited by specific colloid sizes or materials.*

### 6.1 Introduction

Alternate nucleic-acid structures play an important role in biological processes. Multi-branched structures, where three or more duplexes intersect at a single point, serve as possible intermediates in DNA recombination and important permanent structural elements of naturally occurring RNA molecules [162]. Helical junctions may be defined as branchpoints where double-helical segments intersect with axial discontinuities, such that strands are exchanged between the different helical sections. Thus the integrity of junctions is maintained by the covalent continuity of the component strands and the perfect base pairing between the DNA strands.

The four-way DNA junction (see Figure 6.1a for an example) is generally accepted to be the central intermediate in homologous genetic recombination [163–166]. As the structure was first mentioned by R. Holliday [163] it is also commonly referred to as a Holliday junction. Homologous genetic recombination is important in the repair of double-strand breaks in DNA, and in providing the genetic diversity that is necessary for Darwinian evolution. A significant distinction among different four-way junctions lies in their potential ability to undergo branch migration. When a junction is formed by two DNA strands that are homologous (largely identical) it can undergo a sequential exchange of basepairing in which a branchpoint becomes effectively displaced along the DNA sequence. An extreme case is shown in Figure 6.1b. Here a schematic representation of junction formation from an inverted repeat sequence in dsDNA is shown. Further migration is still possible as all bases surrounding the cross-section can also pair. The same could occur in a four-way junction made from four DNA strands. The length of the region of homology will limit the number of steps of branch migration that are possible, from zero (sometimes called an immobile junction; Figure 6.1a) to thousands.

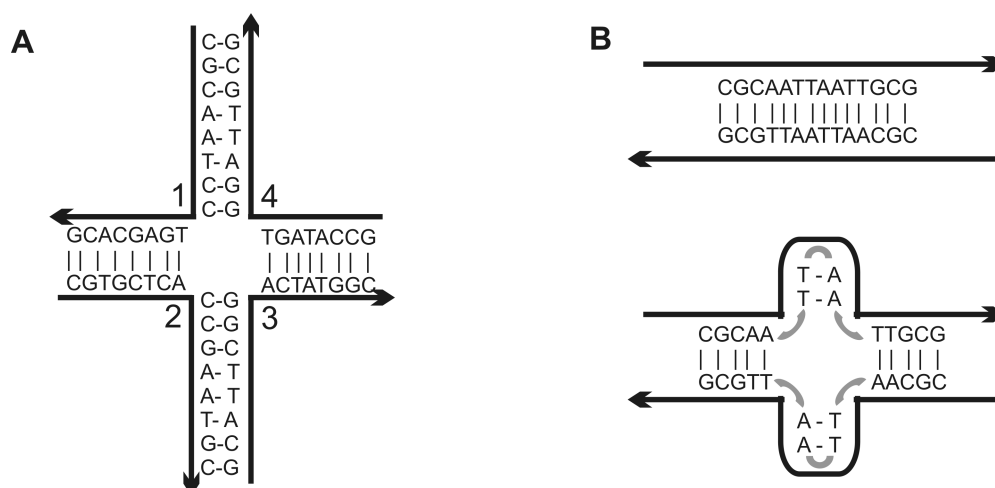


Figure 6.1: Schematic representation of the DNA-junction. A: Sequences of the junction used throughout this chapter [160]. B: One important feature of a DNA-junction is the sequence of its center. Sometimes migration of the center is possible [161]. Note that with the sequence employed in the junction shown above this is not possible.

The structure of the four-way DNA junction is dependent on the presence of divalent metal ions. In the absence of ions or at low salt conditions, the four helices remain unstacked, and the junction is extended [167] (Figure 6.2a). In the presence of divalent metal ions and, to a lesser extent under high-salt conditions, the helices undergo pairwise coaxial stacking into a right-handed anti-parallel structure, termed the stacked X-structure (Figure 6.2b). This structure was first proposed in 1988 [167], on the basis of comparative gel electrophoresis experiments, and confirmed later by fluorescence resonance energy transfer (FRET) analysis [168].

While branched DNA motifs have been used to design objects [20, 21] and periodic arrays [18, 169], they have not been utilized to drive the assembly of colloids. The only literature relevant for this topic that we know of, is a study on the structural integrity of DNA motifs by Seeman and coworkers [117]. In this study, gold nanoparticles are used to test whether multiple-junction-DNA motifs can withstand stresses without changing their geometrical structure.

Assembling a limited number of colloids in a specific geometrical shape has been achieved before. One of the first experimental articles on DNA-driven assembly of micron sized colloids already reported on this very topic [119]. It describes a method to prepare mesoscale polyhedral structures from binary mixtures of microspheres of specific size ratios using DNA as a molecular bridge. The interest in such non-spherical building blocks comes from the fact that their assembly can lead to the development of complex colloidal crystals of lower symmetry than is possible with uniform spherical colloids.

Using a complete different approach, Pine and coworkers [170] were able to assemble four to fifteen colloids together. To this end they mixed particles dissolved in toluene with water, once mixed small numbers of colloidal microspheres are attached to the surfaces of liquid emulsion droplets. After removal of the fluid from the droplets, these

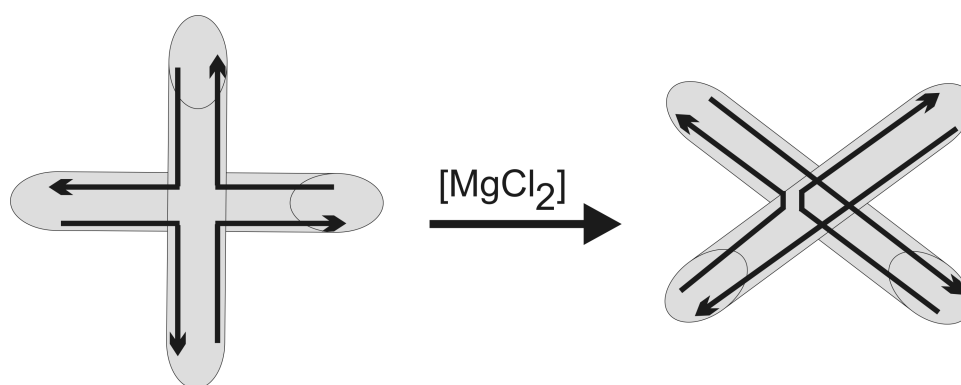


Figure 6.2: Illustration of the ion-dependent folding equilibrium of the four-way DNA junction. At low salt concentrations the junction exists in an extended, unstaked conformation. Upon addition of divalent metal ions, such as magnesium ions, the junction folds into the stacked X-structure [162]

spheres pack in a manner that minimizes the area of the toluene-water interface during drying. The finite-sized clusters that we discussed in chapter 3 were made using  $\lambda$ -DNA coated colloids. Using such building blocks, it is possible to create clusters that contain a limited number of linked colloids. Unfortunately, the resulting clusters display a wide range of sizes and shapes.

By utilizing a Holliday junction we aim to make quartets of colloids. It is expected that, as all constructs use the same DNA-linkage, the aggregates will be very similar in shape as well. In principle, if the system behaves as predicted, we could selectively link colloids of different sizes or compositions. Such selective design is at present not possible with the two systems described above [119, 170].

In order to connect four DNA-coated colloids with a Holliday junction we must first choose an appropriate structure for the junction. As we are interested in assembly, it is important that branch migration is not possible as this would make the aggregates less stable. We therefore used a junction structure (Figure 6.1a) that is known for its high stability [160]. First, we tested the stability of the junction as well as appropriate buffer conditions for both the colloids and the junction. Next, we designed a DNA construct in order to assemble four colloids with one junction (due to spatial constraints a spacer is needed). Then the individual junction-DNA coated colloids were tested on their DNA quality. Finally, we present a first experimental attempt to obtain quartets of colloids connected by a Holliday junction.

## 6.2 Results and Discussion

### 6.2.1 Ionic stability of four-way junctions

The important role of metal ions on the stability of four-way DNA junctions has been established by experimental studies [162]. Under low salt conditions or in the absence of metal ions an extended planar cross-shaped geometry predominates whereas an X-shape

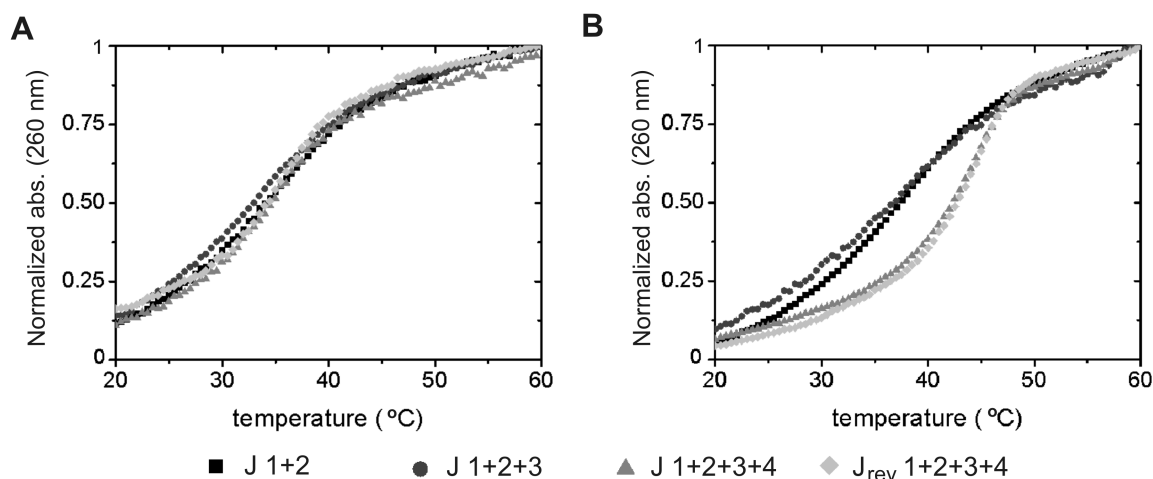


Figure 6.3: Thermal transition profiles of the quaternary complex or two- and three strand compositions. A: With additional sodium (100 mM) the junction is not stable. All strand combinations result in similar curves. Curves were measured from 90 °C to 5 °C and back to 90 °C). For clarity, only one reverse curve is shown (light gray). B: When a divalent salt is used ( $\text{MgCl}_2$ ; 50 mM) the four-armed junction is more stable than the junctions missing one or two arms. This is reflected in the higher melting temperature. As before, only one reverse curve is shown.

with two inter-arm angles of 60° prevails in the presence of metal ions [162]. Higher salt conditions bring about at least a partial folding, but not as effective as with metal ions. Given that a higher stability is attributed to the X-structures, it seemed logical to use either high salt concentrations or to add a metal ion to our buffer. To test the formation of our junction at different salt conditions, UV melting studies were carried out.

First, the junction stability is tested in a buffer containing 100 mM salt (NaCl). The melting curves (Figure 6.3a) show that this buffer does not improve the junction stability. This can be deduced from Figure 6.3a as the pairwise combination, three-way structures and the complete four-way junction all show the same melting profile ( $T_m \sim 34$  °C; this value can be read of from the midpoint of the curve or derived from the first derivative<sup>1</sup>). In contrast to the results for the samples in high salt buffers, the greater stability of a junction formed in the presence of a metal ion ( $\text{Mg}^{2+}$ ) is evident (Figure 6.3b). Whereas the pairwise combination and the three-way structure give the same melting profile, a clear shift is visible for the profile of the complete four-way junction. Here, the melting temperature of the complete junction is significantly higher than that of the incomplete structures ( $T_m \sim 45$  °C (4-way junction) vs  $T_m \sim 36$  °C (2 or 3 strand structure)). Pairwise structures already appear stable. This could later prove useful, as then two sets of dimers can be formed, to later combine into the complete junction.

Initially we chose the  $\text{MgCl}_2$  concentration of 50 mM, to compare similar ionic strengths. However, the available literature suggests that a lower concentration of  $\text{MgCl}_2$

<sup>1</sup>The melting curves are measured by Linda Payet (Figure 6.3) and Sabrina Jahn (Figure 6.4) (Cambridge University), Linda Payet derived the first derivative as well (using Spectro software).

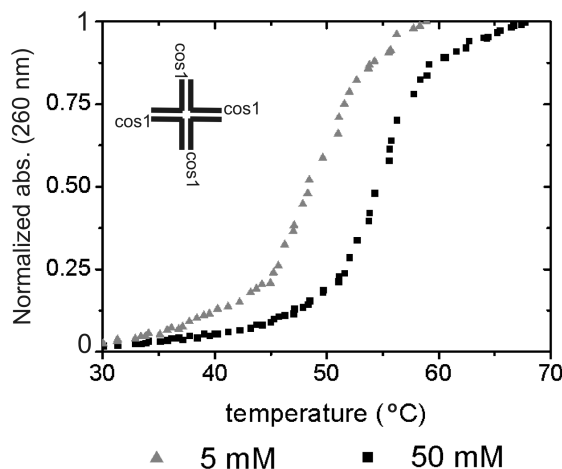


Figure 6.4: Thermal transition profiles of the quaternary complex extended with *cos1*-overhangs. Two concentrations of divalent salt ( $\text{MgCl}_2$ ) are used (5 mM (gray) and 50 mM (black)). The four-armed junction dissociates at a higher melting temperature for higher  $\text{MgCl}_2$  concentrations.

should be possible as well. Therefore, we also measured a melting profile of the complete junction at a far lower  $\text{MgCl}_2$  concentration (5 mM). Comparing the results of the melting profiles of the extended oligonucleotides (the junction sequence attached to a *cos1*-end) at 5 and 50 mM  $\text{MgCl}_2$  (Figure 6.4) indicates that at lower  $\text{MgCl}_2$  the melting temperature of the junction decreases ( $T_m$  55 °C (50 mM) vs  $T_m$  48 °C (5 mM)).

We note that ref. [171] reports on the melting profiles of five-way junctions. Ref. [171] claims that higher melting temperatures are found for strands that did not form a junction, than for those that did: this finding is explained by comparing the experimental results for the “five-way junction” to the profiles of consistent parts of the junction. It turned out that it is possible that a superposition of the melting curves of all possible adjacent two strand combinations leads to the observed melting curve. We believe our results on the four-way junction have a different explanation as the *cos1*-sequences are not complementary and internal looping of this 12 base sequence is not possible. However, the study of ref. [171] makes it clear that UV measurements can sometimes be misleading and need to be interpreted with caution. Therefore, to have a clearer picture of the stability of the four-way junctions and all possible intermediates we also performed gel-electrophoresis.

### 6.2.2 Stability of the four-way junction and its intermediates tested by gel electrophoresis

Gel-electrophoresis experiments were performed<sup>2</sup> on the four-way junction and its intermediates. On a gel, assembled structures migrate slower than single oligonucleotides, junction formation is therefore visible on a gel.

<sup>2</sup>The gel-electrophoresis experiments are performed by Sabrina Jahn (Cambridge University).

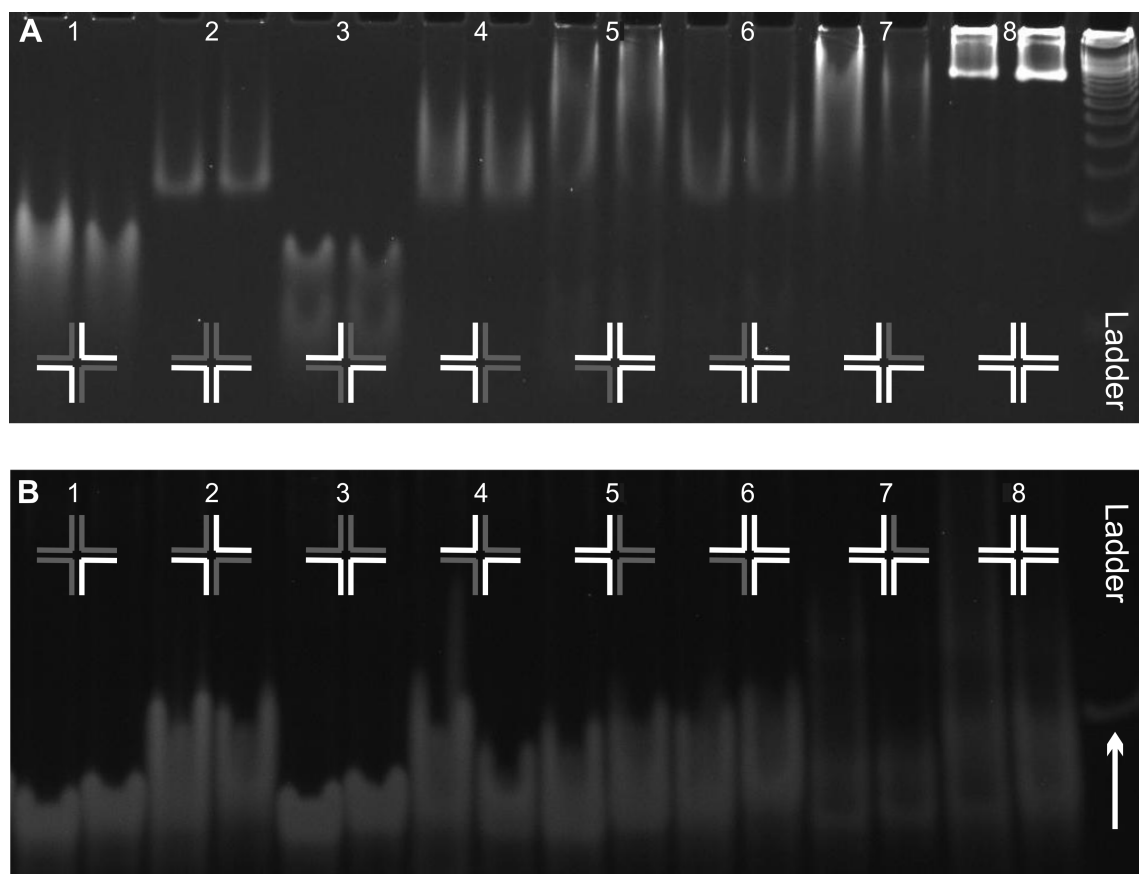


Figure 6.5: Gel electrophoreses of two-, three- and the complete four-stranded junction (samples are loaded in duplicates). A: When  $MgCl_2$  is present, the four-armed junction is more stable than the junctions with one or two arms less (strands loaded on gel are depicted in white in the cartoons). This is reflected in the difference in migration speed on the gel. B: Without  $MgCl_2$  present in the gel or in the running buffer the junctions are all unstable. A 20 base dsDNA is used as a reference (faint band above the arrow-head)

Two experiments are performed. For both experiments, the junctions or intermediate structures were assembled at equimolar concentrations beforehand (4 micromol; Tris 100 mM; pH 8 containing 50 mM  $\text{MgCl}_2$ ). The samples were then loaded and run on a gel with either a buffer containing  $\text{MgCl}_2$  or without  $\text{MgCl}_2$ .

The results shown in Figure 6.5a refer to samples where  $\text{MgCl}_2$  is always present (samples loaded in duplo). Whereas all intermediate structures display a smear of products (lane 1-7), the complete four-way junction results in a sharp band (lane 8). The predominant junction band migrates slower than the dimerized (lane 1-4) or three strands structures (lane 5-7). As observed in the UV-measurement adjacent pairwise combinations or three-strand structures yield comparable results. All bands end at similar heights on the gel. Note the difference in stability between adjacent pairwise combinations (8 base complementary; lane 2 and 4) and opposite pairs (close to zero complementary sequences; lane 1 and 3). The opposite pairs penetrate further into the gel, indicating (mostly) single stranded structures rather than assemblies. Interestingly, the minor difference in complementary base pairs between the two opposite pairs 2+4 and 1+3 is also reflected in the results. Pair 2+4 migrates slightly slower (lane 1) as this pair has more complementary bases (7 vs 3) than pair 1+3 (lane 3).

In Figure 6.5b the junctions were loaded without the presence of  $\text{Mg}^{2+}$ -ions. Instead of showing the pattern of Figure 6.5a, now all samples show a smear rather than sharp bands (lane 1-8). All constructs penetrate as deep as the individual oligonucleotide indicating little construct formation. These results strongly suggest that the ions that keep the junction in its stable form can diffuse away in time, resulting in the subsequent disassembly of the junction.

### 6.2.3 Optimizing buffer conditions for our colloids

To ensure our colloids are stable within the buffer (100 mM Tris, 5 or 50 mM  $\text{MgCl}_2$ , pH 8) control experiments were performed. To this end, neutravidin colloids were added to Tris buffers with a range of  $\text{MgCl}_2$  concentrations (ranging from 0 to 150 mM). Images were taken after a day and after five days. Figure 6.6a shows that after just one day at 50 mM  $\text{Mg}^{2+}$ -ions, small clusters appear, indicating that the colloids are not stable in this solution. The severity of this effect becomes more visible after five days, with all colloids assembled in a gel-like structure (Figure 6.6b). Within the concentration range, colloids in solutions with concentrations below 50 mM (0, 10 and 20 mM) remained stable, whereas at higher concentrations (70, 100 and 150) the colloids gelled within a day (data not shown).

Although it is possible to perform the experiments at 5 mM  $\text{MgCl}_2$ , we prefer to work under conditions where the construct is as stable as possible. Therefore, we add a blocking agent ( $\kappa$ -casein; 0.1 mg/ml) to the tris- $\text{MgCl}_2$  buffer. As  $\kappa$ -casein prevents the neutravidin colloids from aggregating after one day (Figure 6.6c) as well as after five days (Figure 6.6d), a concentration of 50 mM of  $\text{MgCl}_2$  can be used.

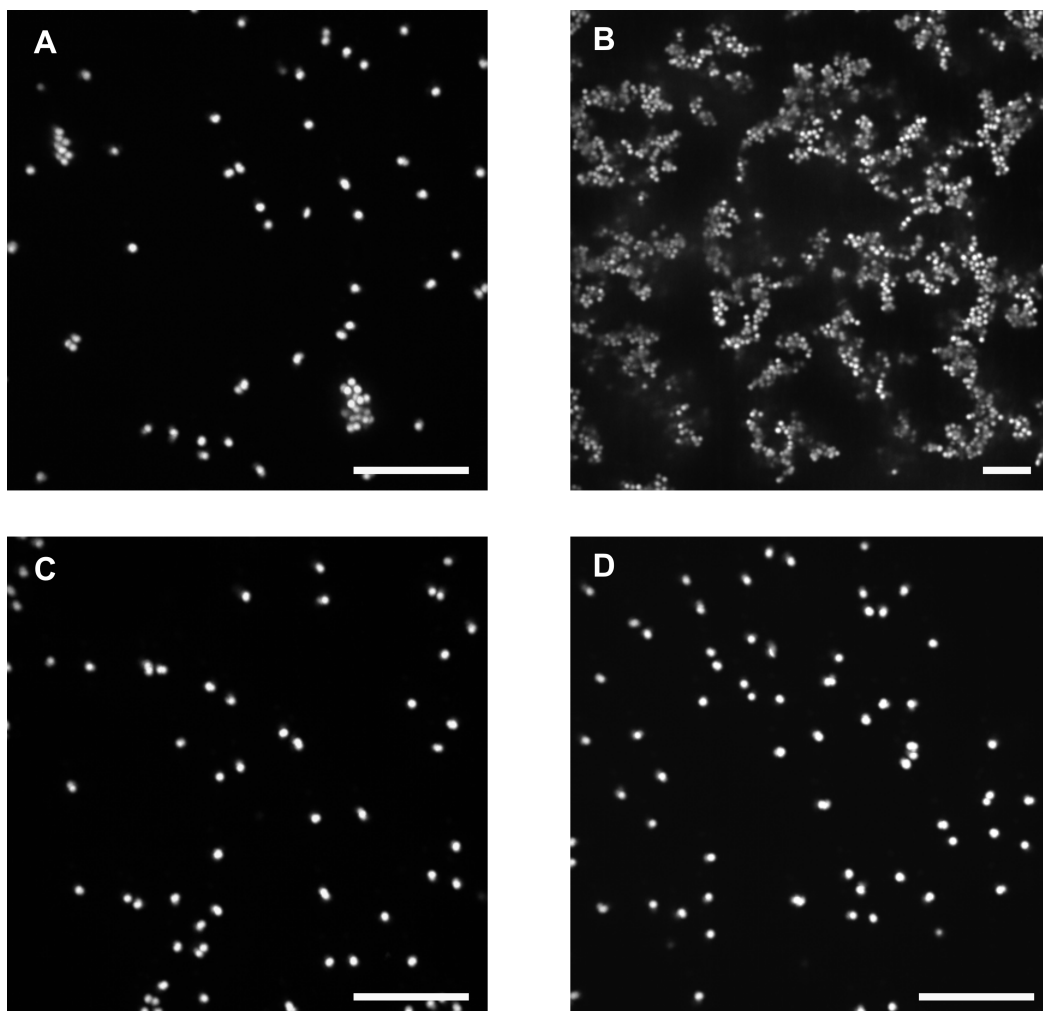


Figure 6.6: Colloid stability tested in buffers containing  $\text{MgCl}_2$ . A: Neutravidin-colloids in TRIS-HCl buffer with 50 mM  $\text{MgCl}_2$ . After one day small clusters appear. B: The same sample as in A, four days later. Neutravidin-colloids are not stable over time in a TRIS-HCl buffer with 50 mM  $\text{MgCl}_2$ . C: Neutravidin-colloids in TRIS-HCl buffer with 50 mM  $\text{MgCl}_2$  and 0.1 mg/ml  $\kappa$ -casein. After one day colloids are now still stable. D: The same sample as in C, four days later. With the addition of  $\kappa$ -casein colloids are now stable over time in a buffer containing  $\text{MgCl}_2$ . All scale bars measure 10  $\mu\text{m}$ .

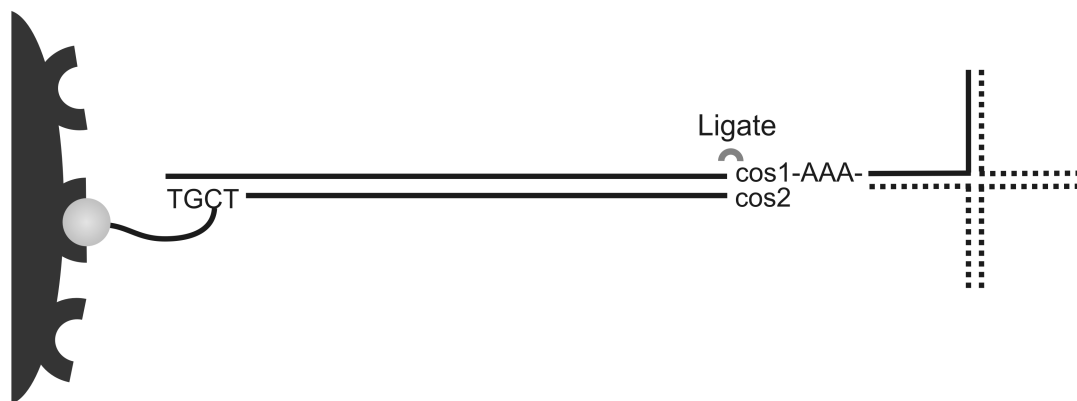


Figure 6.7: DNA construct used to string four colloids together with a DNA-junction. A fragment of the pBelo-DNA is restricted at two sides. One carries a *cos2*-end, which can be used to attach the junction overhang (the AAA nucleotides are added for more flexibility). The opposite end contains a 4-base overhang. This is filled in with 4 nucleotides (TGCT); one labeled with a biotin-tag (dCTP). For clarity the eventual junction is depicted with dotted lines.

#### 6.2.4 Designing a construct to string four colloids together with DNA

A certain minimum length of DNA is required to bind four micron-sized colloids. We estimated this length to be at least  $\sim 450$  bp by drawing a close packed tetrahedral structure and assuming near stretched DNA conformations. As plasmids of this size are not available and ordering a construct of this size is not possible we used the pBeloBac11 plasmid (New England Biolabs). Sufficient amounts of DNA were obtained by amplifying a short fragment of the pBelo DNA (700 bp)<sup>3</sup>. To ensure the calculation is not underestimating the minimum length we decided to use a 540 bp DNA construct as shown in Figure 6.7. One side is used to bind to the colloid by a biotin-neutravidin bond, the other side contains the junction overhang. Note that we added three nucleotides (adenine) to render the overhang more flexible. This idea was inspired by other studies [34, 62], which showed the use of a “flexor” molecule (nucleotide or a short polymer fragment (PEG)) given that greater flexibility can enhance the assembly process. As our construct might be under stress once formed we considered adding a “flexor” could prove useful.

#### 6.2.5 Testing the individual DNA-coated colloids

All junction-DNA coated colloids were tested individually, to ensure that the colloids are coated with the desired DNA construct. The hybridization and ligation of the junction overhangs to the dsDNA is not necessarily a reaction with a 100% yield. To test to what extent the overhang is present, colloids are coated with the complementary 16 base ssDNA strands. Next, the four junction-DNA coated colloids are mixed one-on-one

<sup>3</sup>The amplification of DNA (PCR) was performed by Sabrina Jahn (University of Cambridge).

with these colloids (Figure 6.8a). The cluster in Figure 6.8b shows that the colloids indeed display the junction overhang.

While we now know that the junction-overhang is present this does not imply that all DNA on the colloid contains the overhang. It is possible that a small fraction of DNA did not hybridize to a junction overhang. If this would be the case, our colloids would also display cos2-overhangs (Figure 6.7).

To test whether cos2-overhangs are indeed present on our colloids, we also let our colloids aggregate with cos1-coated colloids (Figure 6.8c). Figure 6.8d shows that the hybridization and ligation of the junction overhangs to the DNA spacer worked well, as practically no small clusters are present.

### 6.2.6 First experiments on binding four colloids simultaneously by a Holliday junction

As the dimer structures with adjacent overhangs are stable, a high concentration of colloids could lead to percolation. Therefore, binding four colloids simultaneously by a Holliday junction requires a lower density than used in the  $\lambda$ , pBelo and cos experiments (volume fraction of  $\phi \approx 0.004$ ). Presently, we work with a six times lower density. The results from the first experiments are promising (Figure 6.9a), but the desired conformation was not yet found. One day after mixing equal amounts of the four types of colloids, dimers and trimers are present (white arrows). The fact that most dimers consist of colloids with both colors, indicates that the binding is most likely specific. However, the existence of one color dimers (black arrows), could indicate unspecific binding. As the non-adjacent junction arms contain some bases that are complementary (7 for 2+4 and 3 for 1+3; see insert), it could be specific as well.

After five days, imaging shows a similar picture (Figure 6.9b). Still, the sample contains mostly monomers, with some dimers and trimers. Although quartets are not visible in the figure, cluster analysis indicates they are present, be it at a very low concentration (0.1%). Compared to the results after one day of aggregation the percentages of monomers (90%) and dimers (3.5%) are similar. The number of trimers shows a small decrease, indicating that some of them found a fourth partner to bind with.

While results look promising, we cannot predict if the system will develop into a system with a higher percentage of quartets present. As bigger clusters are not observed, it may be that a prolonged aggregation time is all the system needs.

## 6.3 Conclusions

In this chapter we described an exploratory study of the possible assembly of four colloids by a Holliday junction. A junction was chosen from literature [160] and tested on its stability in different buffers. Both UV measurements as well as gel-electrophoreses experiments indicate that the junction is stable under experimental conditions.

After testing each type of junction-colloid individually, we concluded that we are indeed capable of constructing the DNA needed. The first experiments look promising, although longer aggregation times are needed. It may also be useful to use longer DNA

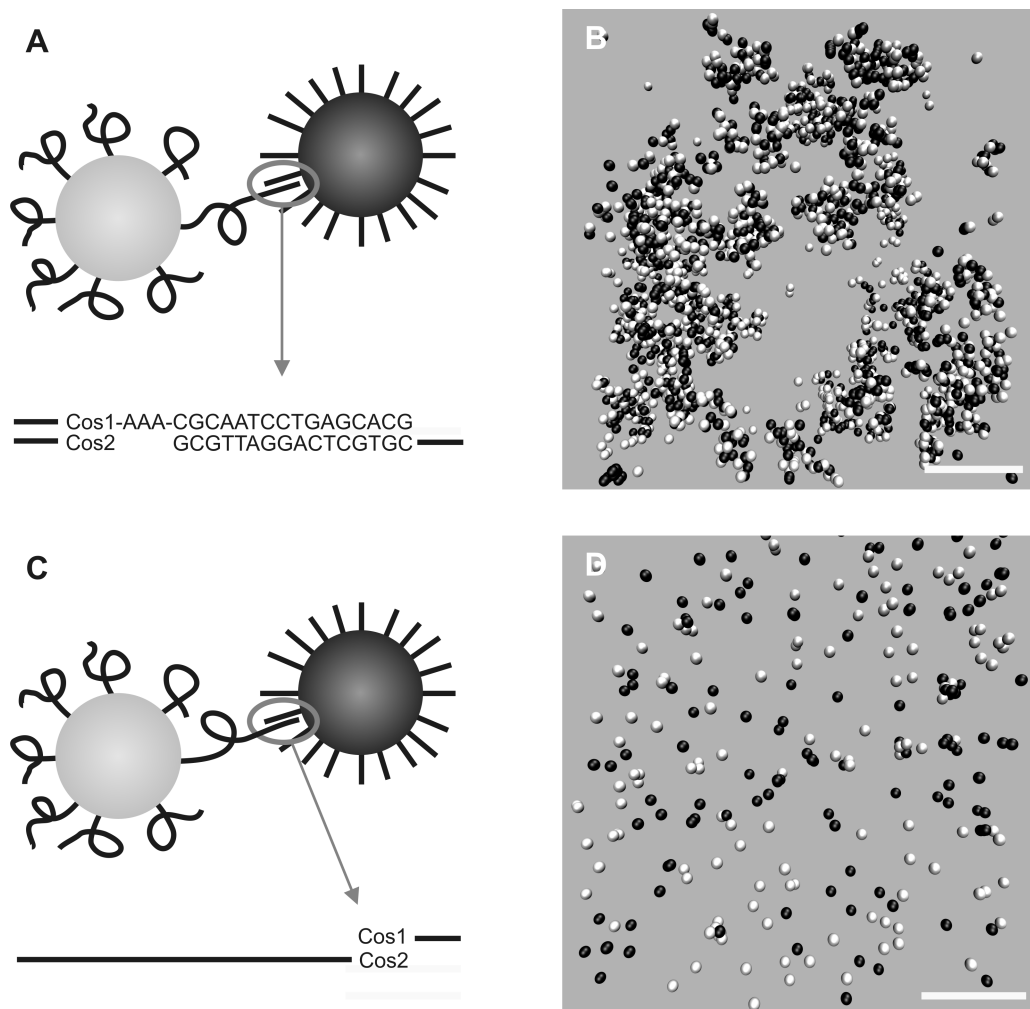


Figure 6.8: Testing the individual DNA constructs on colloids. A: Cartoon of colloids used to test the individual junction overhangs. Instead of combining four colloids by a DNA junction formation, the overhangs are tested individually against their complementary 16 bp sequence directly coated on a colloid. The sequence shown represents junction overhang 1. B: Confocal image of the clustering with colloids as shown in A. C: Cartoon of colloids used to test the individual junction overhangs. If for any reason the hybridization or ligation of the junction overhang to the dsDNA spacer failed, the colloid is left with cos2 overhangs instead. The presence of these (unwanted) overhangs can easily be detected by addition of cos1-coated colloids. D: Confocal image of clustering against cos1-oligonucleotide colloids to test if all DNA on our junction-colloids contain the junction overhang as shown in C. Both scale bars measure 10  $\mu m$ .

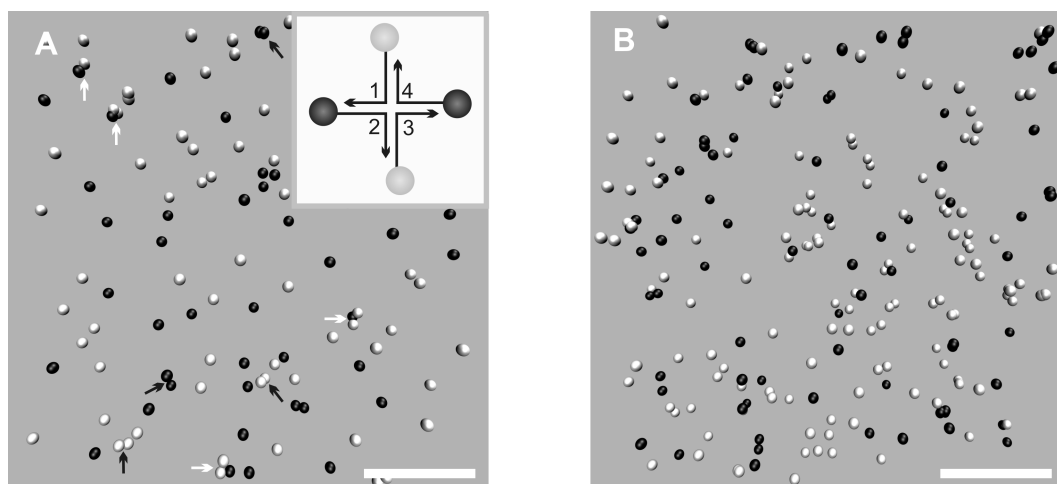


Figure 6.9: First experiment on binding four colloids simultaneously by a Holliday junction. A: Aggregation after one day: both trimers and dimers are present. While some structure appear to be specific binding (white arrow-heads), others are less certain (black arrow-heads). Insert: a cartoon of the structure formed. It is depicted planar to visualize strand binding. B: Aggregation after five days: little change is observed. Cluster-size analysis indicates that 0.1% of all clusters present are tetramers.

“arms” in the Holliday junction as the present constructs are presumably fairly stretched in the tetramer. This is likely to increase the concentration of tetramers. This would be highly desirable as for this type of self-assembly to be useful percentages above  $\sim 25$  are needed. Needless to say that additional experiments are definitely needed.

## 6.4 Materials and Methods

### 6.4.1 Thermal transition profiles of the quaternary complex

The junction sequence was taken from Seeman and coworkers [160] for its high stability. Also, the lack of 2-fold symmetry around the center will prevent migration of the junction.

#### 16 bases junction strands

With UV absorbance measurements (240-260 nm) the melting profile of the junction can be measured. Three- or two-strand combinations were tested to examine the stability of the assemblies formed with these sequences as well. The first set of measurements were performed with the junction sequences themselves (16 base sequences; 1. 5'-CGCA ATCC TGAG CACG-3' 2. 5'-CGTG CTCA CCGA ATGC-3' 3. 5'-GCAT TCGG ACTA TGGC-3' 4. 5'-GCCA TAGT GGAT TGCG-3').

To samples (450  $\mu\text{l}$ ; 2  $\mu\text{M}$ ) 200  $\mu\text{l}$  mineral oil was added (heated to 95  $^{\circ}\text{C}$ ; air-bubble free). The final volume was adjusted to 1 ml (TRIS-HCl buffer 100 mM; pH 8). The

samples were measured in the thermal mode (Cary 300 Bio Visible UV spectrophotometer (Viaran); wavelength 240-260 nm). Two sets of experiments were performed. For the first set, sodium chloride (NaCl; 100 mM) was added to the samples. The second set of experiments used magnesium chloride (MgCl<sub>2</sub>; 50 mM) instead. All samples were measured starting from 90 °C to 5 °C. To test if the junction formation is indeed a reversible process, “reverse” curves were measured (starting from 5 °C to 90 °C) as well.

### 6.4.2 Gel-electrophoresis of the quaternary complex

For gel-electrophoresis assays all samples were prepared at 4  $\mu$ M (TRIS-HCl buffer 100 mM pH 8; 50 mM MgCl<sub>2</sub>) in equimolar concentrations. Two 20% polyacrylamide gels were prepared. One containing 20 mM MgCl<sub>2</sub> and one without additional salt. The same was done with the running-buffer (sigma-powder T7525-4L). For all samples 20  $\mu$ l (including loading dye) was loaded in the gel.

The magnesium containing gel samples were loaded in the following order: in pairwise combinations: 2+4, 2+3, 1+3 and 1+2; as three-way structures: 1+3+4, 2+3+4 and 1+2+3 and as the assembled 4-way junction: 1+2+3+4. As a reference a low range DNA ladder was added (Sigma Aldrich, PCR ladder 1000-20 bp). On the gel without additional salt samples were loaded in the following order: oligonucleotide 3 individually, in pairwise combinations, 2+4, 2+3, 1+3 and 1+2, as three-way structures, 1+3+4 and 1+2+3 and as the assembled 4-way junction, 1+2+3+4. As a reference a 20 base dsDNA piece (Sigma Aldrich) was added as a reference. Both gels were run for 7 hrs at 110 V. The gel was then scanned on a flatbed scanner (UVP, multi doc-it) to capture images.

### 6.4.3 Preparation of junction-DNA-constructs

A fragment around the cos-restriction site of the pBeloBac11 plasmid (New England Biolabs) is amplified by PCR. The pBeloBac11 plasmid was purchased as a strain (New England Biolabs, ER2420S). To obtain DNA to amplify with a PCR-reaction, the strain was grown overnight at 37 °C in 50 ml LB medium (for 100 ml: Bacto-Tryptone 1 g; Bacto-Yeast extract 0.5 g; NaCl 1 g and ddH<sub>2</sub>O to 100ml; autoclave sterilized) in presence of chloramphenicol (20  $\mu$ g/ml). With a spin miniprep-Kit (Qiagen) the plasmid DNA was then isolated. The purity of the DNA was checked by gel electrophoresis on a 1% agarose gel. Next, the pBelo-DNA is diluted 1000x and 1  $\mu$ l of each primer is added (p1: 5'-TAGTCTGGAACCACGGTCCC-3' (placement on plasmid: base 6631); p2: 5'-GCTTTCAGCACCTGTCGTTCC-3' (placement on plasmid: base 7355); both 0.25  $\mu$ M). For a sample, 10  $\mu$ l of the DNA primer mixture is mixed with 10  $\mu$ l of HotStarTaq Plus Master Mix (HotStarTaq Plus DNA Polymerase, PCR Buffer, and dNTPs; Qiagen). The solution provides a final concentration of 15 mM MgCl<sub>2</sub> and 200  $\mu$ M of each dNTP. We used the following cycling protocol for our PCR reaction: 1) initial activation step; 5 min 95 °C. 2) denaturation; 45 sec 94 °C. 3) annealing; 45 sec 67.7 °C. 4) extension; 1 min 72 °C. Step 2 to 4 are repeated 27 times. Finally, the samples are kept at 72 °C for 7 more minutes.

The amplified piece of DNA (724 bp) was restricted at two sides. One side was restricted with BssSI (New England Biolabs), leaving a 4-base ssDNA end. The other

end of the amplified piece of DNA contains the cos-restriction site, that can be opened by restriction with  $\lambda$ -terminase (BIOzymTC), leaving a 12 base single strand (“sticky end”). The 4-base end can be filled up nucleotide by nucleotide with Klenow  $\text{exo}^-$ . (To obtain biotinylated DNA regular dTTP and dGTP-nucleotides were used in combination with biotin-dCTP; all Invitrogen). The cos-end is used to hybridize our piece of junction-DNA to the dsDNA piece. For this end the DNA was divided in four batches and mixed with one of the four cos1-junction-overhang oligonucleotides solutions (5  $\mu\text{l}$ ; 20  $\mu\text{M}$ ; Eurogentec). To hybridize the oligonucleotides to the DNA, the solution was heated to 65 °C for  $\sim$ 30 minutes and then cooled overnight to room temperature. To improve the hybridization this reaction was performed in a special annealing buffer (50 mM TrisHCl pH 8, 1 M NaCl and 0.2 mM EDTA; 10x, diluted with TRIS-buffer pH 8). Subsequently, T4 DNA ligase (New England Biolabs) was added to ligate the DNA backbone. To remove the excess of oligonucleotides and enzyme the samples were centrifuged and washed three times on a Microcon YM100 membrane (Milipore) with Tris-HCl buffer (100 mM, pH = 8). The biotin-DNA-junction solutions were then recovered in a clean tube.

#### 6.4.4 Preparation of junction-DNA coated colloids

In contrast to earlier experiments where a binary system in which DNA-mediated attractions are favorable only between heterogeneous colloids was used, we now have four different pieces of DNA that hybridize to form one construct (DNA-junction). Since we can only excite green and red fluorescent colloids, two batches of both colors were prepared. Green fluorescent colloids (diameter 1  $\mu\text{m}$ , Molecular Probes; depicted in white in figures) were functionalized with junction-1-DNA or junction-3-DNA. Red fluorescent colloids were functionalized with junction-2-DNA or junction-4-DNA (depicted in black in figures).

Our conjugation protocol is based on the neutravidin-biotin coupling procedure described in Ref. [53]: the four batches of junction-DNA were separately mixed with either green or red fluorescently labeled neutravidin-colloids, that were dispersed in TRIS-HCl (100 mM, pH 8). In each case the DNA and colloids were left to react overnight, during which they were continuously tumbled. The next day, samples were pelleted and washed five times to remove excess of non-conjugated DNA. In between these washing steps, samples were heated once for 10 min. at 50 °C to remove poorly bound DNA.

The protocol above results in four batches of colloids coated with 517 bp dsDNA displaying a 16 base ssDNA “sticky end”. Between two colloids only partial hybridization is possible, so to hybridize all ssDNA four colloids have to bind together (two green and two red). To be able to test the constructs individually the four complementary strands of 16 bp were purchased from Eurogentec (complementary 16 base sequences; 1'. 5'-GCGT TAGG ACTC GTGC-3' 2'. 5'-GCAC GAGT GGCT TACG-3' 3'. 5'-CGTA AGCC TGAT ACCG-3' 4'. 5'-CGGT ATCA CCTA ACGC-3'). Colloids coated with this type of DNA were prepared in the same way as cos-oligonucleotide colloids (chapter 4).

### 6.4.5 Preparation and coating imaging chambers

To avoid any nonspecific interactions between DNA-coated colloids and glass surfaces of the imaging chambers, cover slips were coated with polyethylene glycol (PEG). The coating of glass slides with PEG is a two-step procedure. First the glass slides were silanized with 3-mercaptoptriethoxysilane (97%, Fluka), then a 5-kDa maleimide modified PEG (Laysan Bio Inc) was tethered to the terminal thiol group of the silane.

Prior to the silanization, the glass slides were cleaned in an UV/ozone box. The cleaned slides were placed in contact with silane vapor overnight. Subsequently, the slides were rinsed with Ethanol, dried with Nitrogen and left in an oven (100 °C) for 30 minutes. Next a drop of concentrated maleimide modified PEG (250 mg/ml in TRIS-HCl buffer) is trapped between two silanized slides and left overnight at room temperature. The excess of PEG is removed by rinsing with ddH<sub>2</sub>O.

A sample chamber is made from two glass coverslips of different size separated by a parafilm spacer ( $\sim 100 \mu\text{m}$ ). The parafilm sealed the chamber on three sides. After loading the chamber with the four populations of DNA-coated colloids the chamber is completely sealed with glue.

### 6.4.6 Confocal imaging

All suspensions were imaged with an inverted microscope (DMIRB, Leica) with a confocal spinning-disc scan head (CSU22, Yokogawa Electric Corp.) and a 60x water-immersion objective. Fluorescence of the two populations of colloids was excited at 488 nm and 512 nm. Emission was observed at 505 nm and above 600 nm respectively. The use of two types of fluorescent beads and confocal microscopy allowed us to extract particles coordinates and to reconstruct 3D images [2].

## 6.5 Acknowledgements

I would like to thank Julian Huppert for suggesting the use of Holliday-junctions with our colloids. L. Payet and S. Jahn were very helpful in determining the stability of the junction under different conditions (Cambridge University, UK).



# A Obtaining temperature reversible colloidal systems

*In the first two experimental chapters the aggregation behavior of colloids coated with long and flexible DNA strands was discussed. The two different DNA coatings that, for the sake of brevity, we will refer to as “lambda” and “pBelo”, result in different cluster-sizes, but behave similarly with respect to a temperature change. Heating well above the melting temperature of a 12-base ssDNA overhang, did not lead to redispersion of the clustered colloids. To obtain more structured aggregates, preferably crystalline, the ability to redisperse the colloids upon heating is crucial [35]. In this appendix I describe several approaches that were attempted in order to obtain DNA-colloid systems that would exhibit temperature-reversible behavior. We note that, whereas micron-sized colloids with a dsDNA spacer between the colloid and the 12-base ssDNA overhang remain clustered at all temperatures, systems with the same DNA, grafted to smaller colloids (390 nm) are often redispersable. This suggests that Van der Waals attractions are an important factor to consider, while working with micron-sized colloids. Very long DNA linkers provide an additional attraction that allows the colloids to get sufficiently close for the strong dispersion forces to take over: as a consequence, such colloids will remain clustered upon heating.*

## A.1 Introduction

Self-assembly of micron-sized colloids with DNA tethers [5, 119] was reported a few years after the first successful DNA-driven assembly of nanoparticles [3]. Whereas all aggregates formed with nanoparticles redispersed upon heating, the redispersion of micron-sized colloids proved much more problematic. Apparently, increasing the size of the colloids plays an important role. In 2005 Crocker and coworkers [6] proposed an explanation. They computed the strength of the interaction between two (complementary) DNA-coated colloids ( $U_{dna}$ ). The depth of this potential is roughly proportional to the radius of the colloid. This means that in a system containing micron sized colloids the interaction between colloids is two orders of magnitude larger than for a similar system of nanoparticles with a size of 10 nm. Without any protective measures, colloids that are drawn to such small separations will undergo irreversible binding due to the Van der Waals dispersion forces acting between the colloids. On the basis of these observations, ref. [6] suggested two methods to obtain reversibility: decreasing  $U_{dna}$  or increasing the repulsion between colloids ( $U_{rep}$ ), such that colloids do not get trapped in the Van der

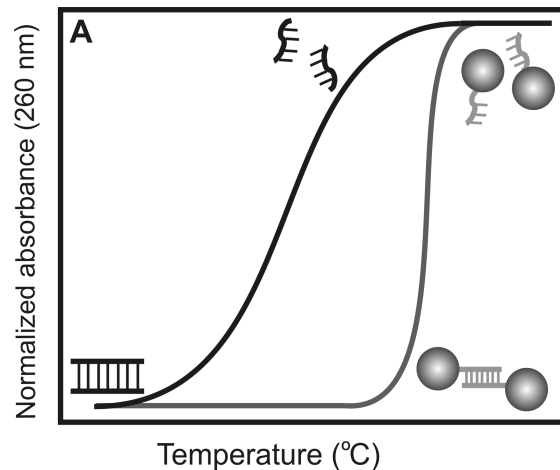


Figure A.1: Schematic representation of the dissociation curve of free DNA in solution compared to the dissociation curve of DNA grafted to colloids. Note that the same DNA has a much narrower melting curve once grafted to colloids. Also the melting temperature shifts toward higher temperatures for colloid bound DNA.

Waals minimum.

Subsequently, several research groups [6, 7] succeeded in making systems of micron-sized DNA-coated colloids that behaved reversibly with regard to temperature. However, the resulting assemblies tended to be amorphous. The temperature at which experiments are performed, is partly responsible for this finding. For DNA in solution it was found that, while the association step has a relatively small activation energy, the activation energy for dissociation is high ( $\sim 6x$  higher) [172]. The kinetics of hybridization in a DNA-linked colloidal system has not been studied in detail, but it seems likely that similar rates will apply individually to each DNA. It should be added that the overall rate of aggregate formation in a colloidal system is also determined by the diffusion of the colloids. As the dissociation rate of DNA duplexes at room temperature is quite small, the aggregation process occurs more rapidly than rearrangements within the structure due to DNA dehybridization. Clustering is therefore irreversible at room temperature. Allowing for rearrangements is a necessary but not a sufficient condition to obtain ordered structures. In fact, there are several examples of systems of micron-sized DNA-coated colloids that behave reversibly under temperature change [6, 7, 54], but thus far only one such system could be made to crystallize [123].

One of the most important reasons why systems of DNA-coated colloids get trapped in a gel-like state, is the very narrow melting curve of DNA grafted to colloids (Figure A.1). To obtain order within a system the DNA bridging has to be a dynamic, reversible process. The only window of temperatures where this happens is on the narrow melting curve. Crocker and coworkers estimated this window for crystal formation to be only  $\sim 0.5$  °C wide [123]. Temperature control is therefore a necessity for crystal formation.

As one of the first research groups to obtain crystal structures with nano-sized particles, Gang and coworkers [34] made an overview of steps necessary to make aggregates with long-ranged order (Figure A.2). After formation of fractal structures, the sample

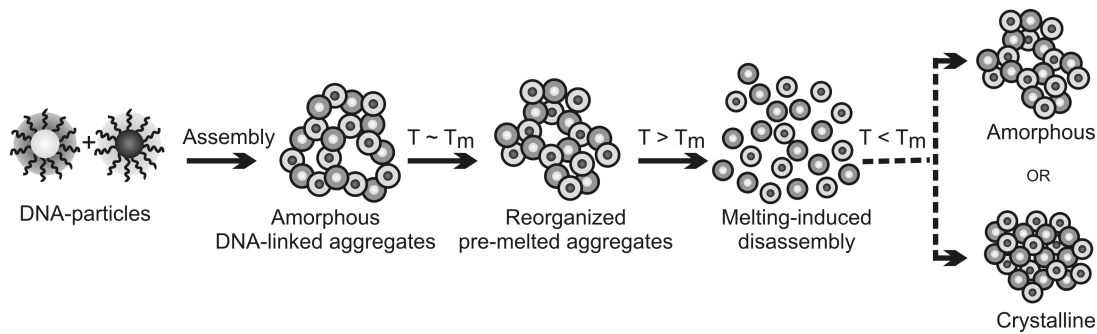


Figure A.2: In order to obtain crystalline structures colloids need to redisperse above their melting temperature. A crucial step is for the system to spend a period of time around the melting temperature of the DNA used, so that DNA rearrangements are possible. Figure courtesy of Dr. O. Gang [35]

needs to spend some time around its melting temperature to allow for reorganization. Then the system might assemble into a long-ranged ordered crystal after being melted and annealed one last time.

In short, to obtain ordered structures it is vital to control the strength of the attractive forces due to the DNA. As described previously, there are two options to manipulate the interactions between colloids. First, we can reduce  $U_{dna}$ . Besides reducing the number of hybridizing strands between two neighboring colloids to lower  $U_{dna}$ , also the number of bases in the “sticky ends” can be adjusted. The second option is increasing (or introducing) the repulsive term  $U_{rep}$ . This will prevent the colloids from coming too close to each other. Keeping colloids at appropriate distances from each other, colloids cannot get trapped in the Van der Waals minimum. Examples of methods to achieve this include adjusting the length of the DNA, adding a third component to the system to increase the repulsion between colloids or using different colloid sizes.

In addition to controlling the attractive forces due to the DNA, we should also try to eliminate unwanted sources of attraction. One such source of attraction can be the neutravidin that is used to graft the ssDNA segments to the colloids. As shielding the neutravidin on the colloid-surface proved successful before (chapter 4, additional test were done to shield the neutravidin in all systems. It turns out that perfect shielding is virtually impossible to achieve. An alternative is to use covalent grafting of DNA to colloids in order to create a protein-free system.

In this appendix we list all our efforts to obtain systems that are temperature reversible. Although the principle is clear, it proved difficult to make DNA-coated colloids that assemble below the melting temperature of the ssDNA used and redisperse above that temperature. Reducing the size of the colloids increased the number of temperature reversible systems. However, when very long DNA was used, it proved impossible to suppress the attractive forces that keep the colloids from redispersing above the melting temperature of the DNA links.

## A.2 Results and Discussion

### A.2.1 Reducing DNA length may lead to cluster reversibility.

Chapter 3 described the aggregation behavior of colloids coated with long and flexible DNA. As described in that chapter, this type of colloids aggregated to form finite-sized clusters, surrounded by a DNA “halo”. The resulting clusters were temperature stable. Even heating to 80 °C, i.e. well above the melting temperature of the overhangs ( $\sim 42$  °C), did not redisperse them. The reason why such colloids tend to aggregate can be understood qualitatively on the basis of a theoretical study of Bhatia and Russel [142]. This study showed that a pair of colloids, linked by long, strongly bound telechelic polymers (with a radius of gyration similar to the size of the colloid itself) would attract at short distances under conditions where flat surfaces coated with the same polymers would repel each other. More precisely: what matters is the ratio of the colloid radius to that of the polymer. If that ratio is not much larger than one, the colloids experience a rather strong attraction at short distances. The strength of the attraction scales (to a first approximation) linearly with the number of polymers. Typically, DNA-coated colloids will also repel due to electrostatics. For free colloids coated with long DNA, the electrostatic repulsion plus the steric repulsion provided by the unlinked DNA’s is enough to keep the colloids stable in solution. However, when the complementary “sticky ssDNA ends” on two colloids hybridize, we have a situation similar to the one described by Bhatia and Russel: now a short-ranged attraction is added to the electrostatic repulsion between the colloids. This change from steric repulsion to “steric attraction” may be just enough to allow the colloids to overcome the free-energy barrier that would otherwise protect them from falling into the deep, primary Van der Waals minimum. Whether or not this happens in practice depends not only on the length of the polymers and the radius of the colloids but also on the nature of the DLVO-interaction between the colloids. In this picture, reducing the length of the DNA spacer sufficiently would protect the system against getting stuck in the primary Van der Waals minimum and would make its phase behavior reversible with respect to temperature.<sup>1</sup>

If the present simple picture is valid, colloids coated with pBelo-DNA should be more resistant to collapse than colloids coated with  $\lambda$ -DNA. While results did show a slight increase in repulsion between neighboring colloids (shift in position of the first peak of the pair correlation function), these colloids, once clustered, did not redisperse at 80 °C (well above the expected  $T_m \sim 42$  °C). The third system (no dsDNA spacers) was able to melt back to its initial state (monomers), suggesting that this length of DNA is below the threshold that marks the transition from an irreversible to a reversible behavior.

To test this hypothesis smaller plasmids are needed. To our knowledge there are no other cos-plasmids available. In order to keep the same “sticky-ends”, the ssDNA cos-ends must be added to dsDNA of desired length. In practice this turned out to be

---

<sup>1</sup>As both pBelo and  $\lambda$ -DNA are very long polymers, one should perhaps also consider the possibility that these chain molecules induce “bridging flocculation” of the colloids (see, e.g. V.K. La Mer, *Discuss. Faraday Soc.* **42** 248 (1966)). We did not explore this possibility because there is no evidence that the DNA is adsorbed (weakly) to the colloids. However, as La Mer already pointed out, bridging flocculation of colloids - by like-charged poly-electrolytes - is possible.

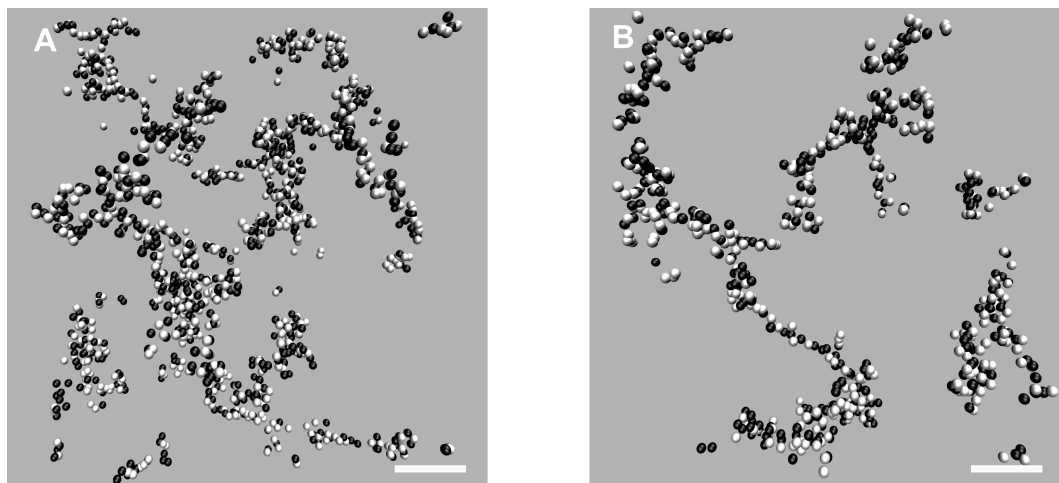


Figure A.3: Reconstructed 3D image of DNA-driven assembly of micron sized colloids with 4-base “sticky-ends”. The aggregation time was one month at 4 °C. A: Colloids grafted with pBR322-DNA (3400 bp). B: Colloids grafted with pUC19-DNA (2000 bp). Both scale bars indicate 10  $\mu\text{m}$ .

impossible: end-ligation of the cos-overhang to the DNA never results in the desired constructs, as available restriction sites resulted into 4-base overhangs. These overhangs are too small for efficient hybridization of a ssDNA strand containing the cos-sequence. To still test the hypothesis, we use reduced lengths of dsDNA with “sticky-ends” of 4 bases, instead of the 12 base overhangs before.

Two plasmids provide smaller dsDNA spacers (pBR322; 4361 bp and pUC19; 2686 bp). A combination of two restriction enzymes shortened the spacers to 3400 and 2000 bp. It is important to choose an overhang that is not a palindrome, so a distinction can be made between the two populations of colloids (only A-B binding is possible as opposed to A-A or B-B binding). The biotin-label is in this case not added by ligation of oligonucleotides, but built in by an enzyme (klenow  $\text{exo}^-$  polymerase; New England Biolabs) that adds nucleotides (one labeled with a biotin) one by one to any 5'-overhang.

Working with ssDNA overhangs of only 4 bases requires some experimental adjustments. The melting temperature of these short overhangs is below room temperature:  $\sim 12$  °C. Indeed, if the colloids are mixed at room temperature and left to aggregate, no sign of cluster formation is seen over a period of two months. In order to study their aggregation behavior we mix them at room temperature, but afterwards place the samples at 4 °C. Reducing the overhang length increases the aggregation time from one day to at least one month. Both sets of DNA-coated colloids aggregated into thin branched percolating clusters (Figure A.3a,b). Despite the further reduced dsDNA length also these systems proved to be temperature stable: increasing the temperature did not redisperse the colloids. Therefore, we decided not to use these DNA linkers.

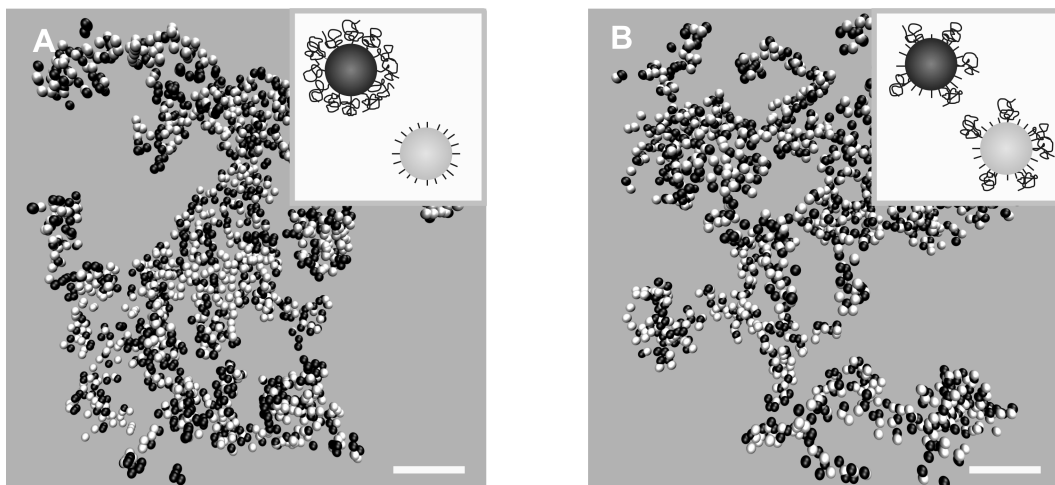


Figure A.4: Shielding colloidal proteins by varying the DNA length. A: Two sets of colloids were used: pBelo-coated colloids and cos-coated colloids. B: Colloids grafted with a combination of two types of DNA: pBelo and cos-oligonucleotides. Both scale bars indicate  $10 \mu\text{m}$ .

### A.2.2 Shielding more neutravidin sites on the colloids is not sufficient for cluster reversibility.

The only DNA-coated colloids that did redisperse upon heating were the cos-coated colloids (no dsDNA spacer). The down side of using these colloids is that we are not able to exploit the polymeric potential of DNA. In chapter 4 we speculate that shielding the neutravidin on the colloids leads to temperature reversible clusters. By using two different sets of DNA-coated colloids (Figure A.4a insert), we shield more neutravidin sites and can still use the polymeric potential of the DNA.

We coat our “A” type colloids with the 12 base oligonucleotide’s (cos 1) and the “B” type colloids with full length pBelo (7500 dsDNA + cos 2). This combination of colloids assembles similar to a system where both colloids are coated with pBelo-DNA (Figure A.4a; chapter 4). Moreover, also these clusters appeared temperature stable.

Another option is to have both sets of colloids coated with a combination of pBelo-DNA (with sticky overhangs) and the same short ssDNA grafted directly to the colloid (Figure A.4b insert). With this method, more neutravidin sites are shielded (compared to pBelo-coated colloids), as the short ssDNA can bind in between alongside pBelo-DNA strands. There is no difference between the clusters obtained with the system of figure A.4a and this system (Figure A.4b). Apparently the extra possibilities to aggregate, due to the cos-oligonucleotides, do not result in different aggregation behavior. Furthermore, this system fails to redisperse as well, when brought to temperatures above the DNAs melting temperature. This could indicate that we did not succeed in shielding all colloidal proteins. Another reason could be that long DNA linkers introduce additional attractive forces [53].

### A.2.3 Coating colloids with DNA and a short repulsive brush

To decide whether the inability to redisperse clusters above the melting temperature of the DNA, is indeed an intrinsic property of colloidal systems coated with long DNA, we examined three more systems. Whereas in the previous sections the focus was on shielding the surface, here we describe systems that are coated with DNA as well as a short repulsive brush and thus introduce a repulsive term  $U_{rep}$  to the system.

#### A polymer-based stabilizer.

Since we use polystyrene beads functionalized with neutravidin, we can graft any third component (to introduce  $U_{rep}$ ) that has a biotin end to the colloids. First, we tried short biotin labeled polyethylene glycol (PEG; Mw 5000;  $\sim 30$  nm). After coating our colloids with pBelo-DNA we dissolved them in a solution of biotin-PEG (10 mg/ml), allowing the polymers to penetrate the thick adsorbed DNA layer around the colloids. After washing away unbound polymers, the aggregation was examined. The pair correlation function of the fractal aggregates, showed no changes with respect to pBelo-DNA coated colloids (data not shown). Moreover, the structures appeared temperature stable above the melting temperature.

#### Short blunt dsDNA stabilizers

Adding short biotin-dsDNA with a blunt end to our pBelo-DNA coated colloids leads to colloids that are similar to the ones in the insert in Figure A.4b, except that the blunt end DNA is longer (75 bp; for sequence see materials and methods). The colloids were prepared in the same two-step approach as described above ( $[dsDNA] 20 \mu M$ ).

Aggregating these colloids leads to the same structures as seen earlier with colloids coated with pBelo-DNA without any third component (chapter 4). Although it appeared that these samples needed more time to cluster (twice as long), too few samples were examined to draw definitive conclusions. Moreover, these structures were also irreversible with respect to temperature.

One possible explanation for the failure of achieving temperature reversibility despite the attempt of grafting a steric brush to the colloids is that we did not succeed in making this brush. Although the monolayer of grafted pBelo-DNA around the colloids is rather dilute, the negatively charged backbone of the DNA itself may present a too large Coulomb repulsion for even short biotin-dsDNA to be able to penetrate.

To test if the DNA-coated colloids are grafted with both the DNA and the additional stabilizer (either the PEG-polymer or the short ds-DNA), we repeated the experiments with cos-coated colloids instead of colloids coated with long DNA. As the length of the stabilizer is in both cases longer than the 12 base sticky end ( $\sim 6$  times for both the PEG polymer and the dsDNA), the latter will get buried. We expect this type of colloid to either aggregate with a longer aggregation time or not to cluster at all, as the sticky ends are not easily accessible anymore. Figure A.5c shows a cluster of these colloids. Clearly the clustering is neither prohibited, nor did the aggregation time increase. Both results indicate that we did not succeed in the formation of a sterically stabilizing brush.

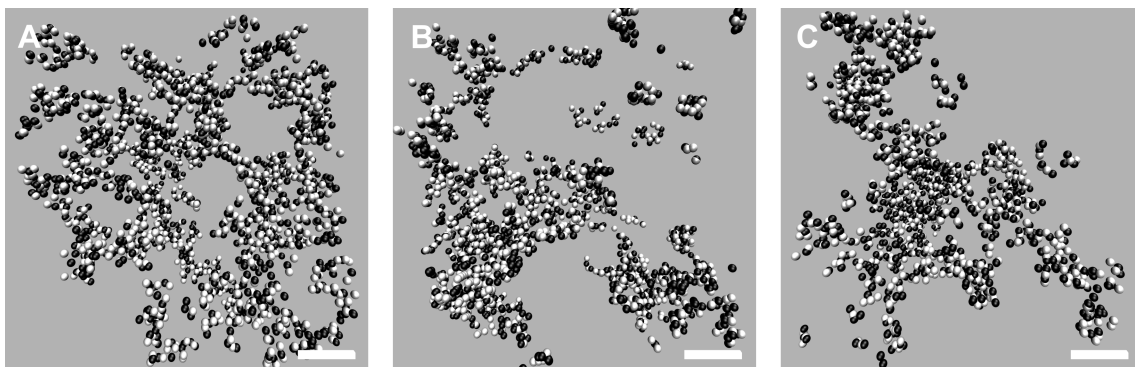


Figure A.5: Addition of a third component to the DNA-coated colloids in an attempt to obtain temperature reversibility. A: pBelo-coated colloids with biotin-PEG (Mw 5000) bound to the surface. B: pBelo-coated colloids with a short dsDNA (75 bp) as a third component. C: Both system aggregated also if cos-oligonucleotides were used instead of pBelo DNA, even though the third component is longer than the “sticky-ends” (the picture depicted is with the dsDNA component). All scale bars correspond to 10  $\mu\text{m}$ .

### Adding Pluronic to enhance stabilization.

Instead of using biotin to attach additional stabilizing molecules to the colloids by a biotin-neutravidin bond, adsorption is also an option. By using adsorption instead of the biotin-neutravidin bond, we can coat our colloids with a stabilizing agent before we add the DNA. While the DNA is not yet present, the negatively charged backbone of the DNA itself cannot present a large Coulomb repulsion for a third component.

A polymer that can adsorb to the colloids is Pluronic. Pluronic are neutral symmetric triblock copolymers of poly-ethylene oxide – poly-propylene oxide – poly-ethylene oxide. The two outer PEO blocks are soluble in water at all temperatures from 0 to 100 °C, whereas the middle block becomes more hydrophobic with increasing temperature. We work with Pluronic of two different lengths. The longest Pluronic is F108 ((PEO)<sub>127</sub>(PPO)<sub>48</sub>(PEO)<sub>127</sub> that forms a sterically repulsive brush of  $\sim 40$  nm (calculated). The shorter block copolymer is F68; (PEO)<sub>76</sub>(PPO)<sub>29</sub>(PEO)<sub>76</sub>; it forms a sterically repulsive brush of  $\sim 20$  nm.

Pluronic adsorb to polystyrene colloids by swelling/deswelling-based chemistry [59]. Briefly, an aqueous suspension of polystyrene colloids is mixed with a soluble triblock copolymer. In toluene, the colloids swell and become porous, allowing the triblock’s hydrophobic middle-block to penetrate into the interior. After replacing toluene by an aqueous buffer, the colloids resolidify, trapping the triblock polymers at the surface of their glassy polymer matrix. All neutravidin proteins are still available for DNA binding as no biotin is present in the system.

The short brush made of Pluronic partially prevents hybridization between cos1- and cos2-coated colloids (F68; Figure A.6a), but the long one prohibits it completely (F108; Figure A.6b). Because the cos-experiments looked very promising, we subsequently prepared F108 and pBelo-coated colloids (Figure A.6c). However, even with a repulsive brush, these colloids failed to redisperse at high temperatures.

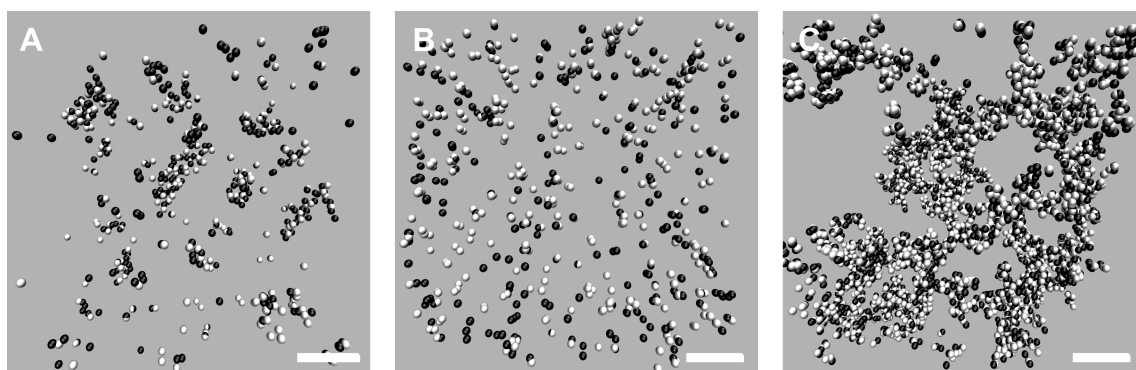


Figure A.6: Adding Pluronics as a third component fully inhibited the aggregation of cos1 and cos2-coated colloids. Colloids coated with long DNA were not affected. A: F68-stabilized colloids; only small clusters were obtained. B: F108-stabilized colloids; aggregation was prohibited C: pBelo-F108 colloids aggregated as before and did not redisperse upon heating. All scale bars indicate  $10 \mu\text{m}$ .

So far, we showed that there are two factors playing a role in the irreversible binding of the colloids. first, the proteins on the surface of the colloids, second the additional attractive forces exerted by the long DNA. To reduce non-specific attractive forces, we next test a protein free system.

#### A.2.4 Switching from protein to covalent binding of DNA.

To avoid protein binding, the DNA could be linked to polystyrene colloids covalently. There are multiple ways to connect DNA to a colloid, but we decided on the protocol drawn in Figure A.7a, with amino-coated polystyrene beads (diameter 810 nm). First, an ester (succinimidyl-[(N-maleimidopropionamido)-dodecaethyleneglycol] ester) is attached to the amino-groups. This ester is not only selected for its maleimide end-group, but also because it has a polymeric midsection that can give additional stabilization. The presence of maleimide groups on our colloids can be tested with help of a Fmoc test [173]. Fmoc-cysteine is a molecule, that can be bound to the maleimide with the thiol-group of the cysteine (Figure A.7b). Adding a base (piperidine) will release the Fmoc, which becomes a fluorophore when in solution, that can be detected quantitatively. Liquid chromatography showed that  $\sim 60\%$  of all amino groups reacted with the added ester. Since the ester is present on the colloids in sufficient amounts, the maleimide colloids are coated with thiol-labeled DNA (prepared similar to biotin-DNA).

The resulting colloids aggregate into a fine stranded network (Figure A.8a). Even though the ester used is specifically selected for its polymeric character, heating up to  $80^\circ\text{C}$  did not redisperse the colloids. In an attempt to stabilize the colloids further, Pluronics is added. This had the reverse effect: colloids with Pluronics aggregated within seconds in the absence of DNA (Figure A.8b). As additional stabilization proved to be impossible and the preparation of these colloids took more time than the protein binding we decided to abandon this route.

The experiments with DNA linked covalently to the colloids show, that by mere

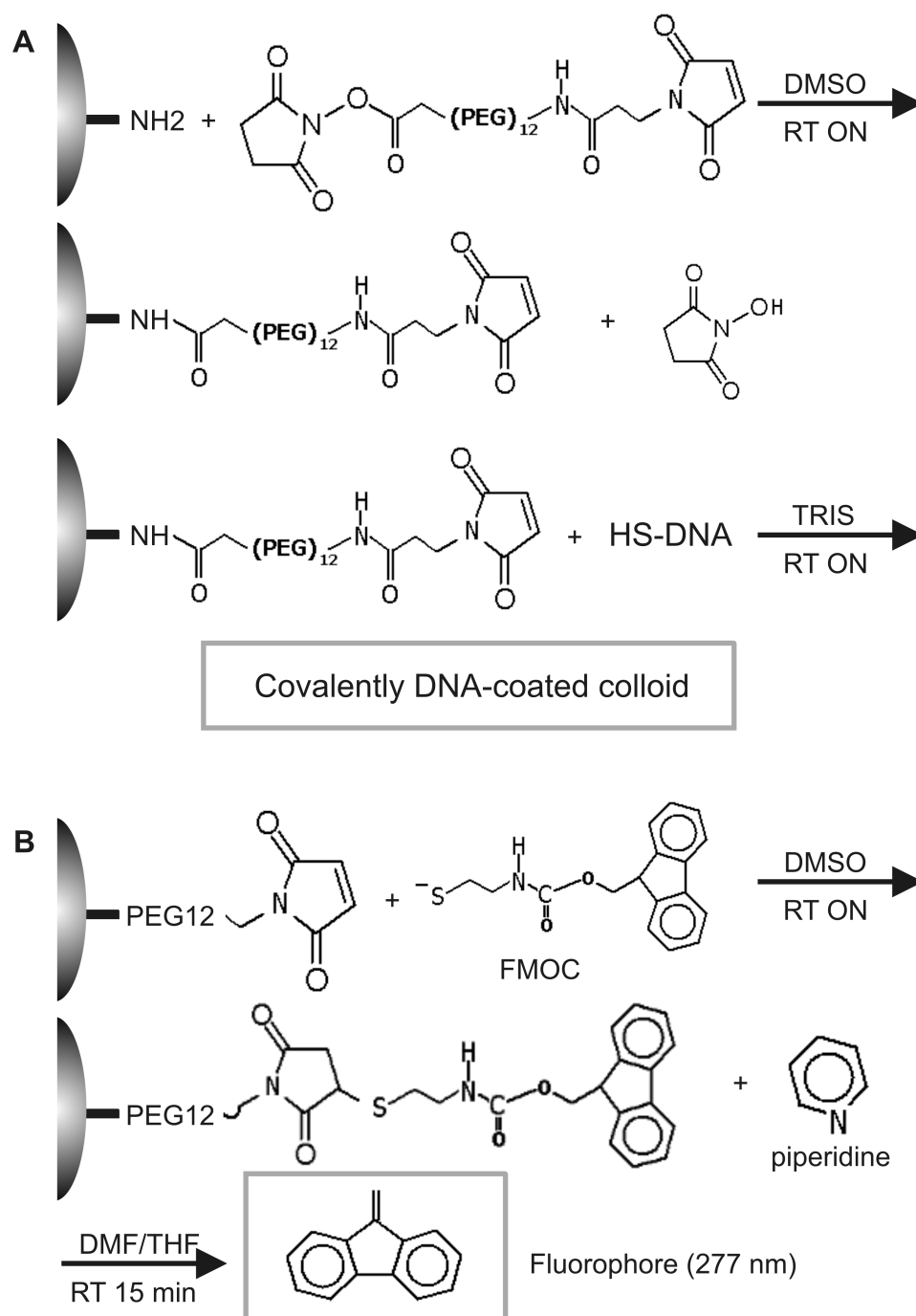


Figure A.7: Overview of molecules and reaction steps used to obtain colloids with covalently bound DNA and of those used to determine the yield. A: Reaction steps used to bind DNA covalently to PS-colloids functionalized with amino-groups. B: To determine the yield of reaction step 2, a Fmoc test was performed (see text).

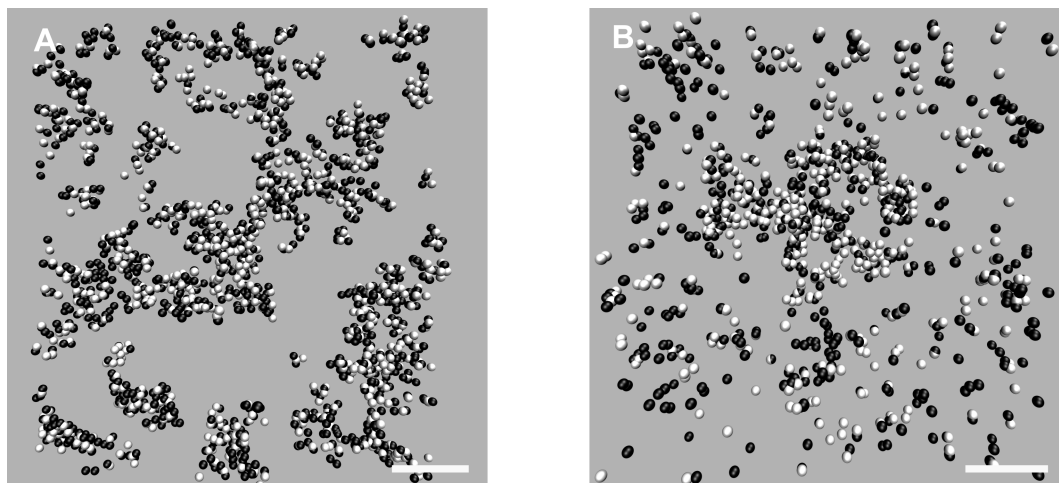


Figure A.8: Colloids with covalently bound DNA. A: Aggregation of colloids with DNA covalently bound to them (the DNA used was pBelo). B: Additional components made these colloids highly unstable; aggregation possible without DNA present. Both scale bars correspond to  $10 \mu m$ .

shielding of the proteins, we will most likely never obtain a micron-sized colloidal system (coated with long DNA) that is temperature reversible.

### A.2.5 Additional stabilization of cos-coated colloids to reduce the melting temperature.

At this point, the only colloids that redispersed are the cos-coated colloids. Even though these colloids can switch between a bound and an unbound state, the temperature at which this takes place ( $80 \text{ }^\circ\text{C}$ ), is higher than the expected melting temperature of DNA of this length ( $42 \text{ }^\circ\text{C}$  for the cos1/cos2 pair). We decided to introduce a short double stranded DNA spacer with 50 bases dsDNA between the biotin and the “sticky ends” (sequence in materials and methods). Addition of the spacer should keep the colloids further apart, thereby lowering attractive surface forces and thus the melting temperature

As expected, these colloids displayed the same aggregation behavior as the cos-coated colloids (Figure A.9a), but instead of lowering the melting temperature, the opposite happened. It was impossible to redisperse these clustered colloids within the accessible temperature window (up to  $80 \text{ }^\circ\text{C}$ ). This shift toward inaccessible melting temperatures may be understood in terms of the possible number of hybridization sites in the contact area. By introducing the double stranded DNA spacer we increase the configurational entropy of the cos-ends and therefore also the number of successful bonds between opposing cos1/cos2 colloids [6].

As the grafting density of “sticky ends” plays a role in temperature reversibility [6], we varied the number of “sticky ends” per colloid. A mixture of biotin-dsDNA of 50 bp with and without the 12 base cos-overhangs is grafted to the colloids. Colloids displayed 10 to 90% “sticky ends”. Still, no reduction in the melting temperature was found.

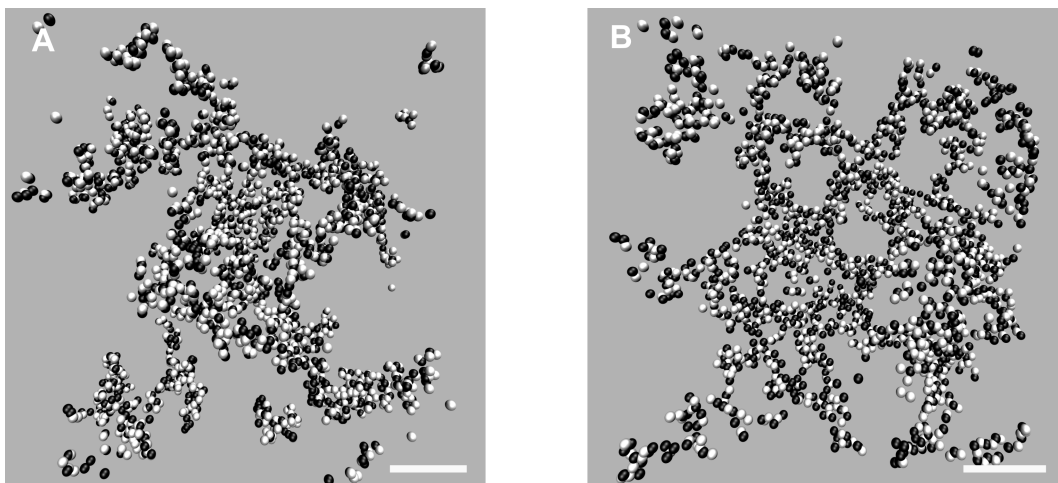


Figure A.9: Adding a short dsDNA piece in front of “sticky-ends” led to clusters that did not redisperse upon heating. A: Colloids with 50 bp dsDNA + “sticky” cos-ends. B: Colloids with 50 bp dsDNA + 8 bases “sticky-ends”. Both scale bars measure 10  $\mu\text{m}$ .

Finally, we repeated the experiments with the colloids also coated with 50 bp dsDNA, but displaying shorter “sticky ends” (8 bases). These eight bases are expected to melt around 30 °C, allowing us to work at room temperature. Again, similar aggregates were found, but once formed no melting could be observed (Figure A.9b).

### A.2.6 Smaller colloids have lower Van der Waals forces.

From the previous paragraphs it appears that non-specific interactions play an important role in our systems. In order to circumvent this problem, we tried smaller colloids, as smaller colloids tend to exert weaker Van der Waals attractions [174]:

$U_{vdw}(r) = -(A/6d)(r/2)$ . Where  $A$  is the Hamaker constant,  $d$  the distance between two colloids and  $r$  the radius of the equal sized colloids. It should be stressed that this expression is only valid in the limit  $d \ll r$  - but that is precisely the region that dominates the “collapse” due to dispersion forces.

#### Unequal colloid sizes.

For practical reasons, we started with colloids of unequal sizes. The smaller colloids we chose to work with (neutravidin-coated polystyrene; diameter 390 nm) were only available in one fluorescent color. The other color had to be custom made (Bangslab).

Most DNA constructs were tested with the smaller green-fluorescent colloids (cos; 50 bp dsDNA + cos ssDNA; 50 bp dsDNA + 8 bases ssDNA and pBelo-DNA). All DNA constructs showed similar aggregation behavior. An example is depicted in Figure A.10a. Reducing the colloid size of the green fluorescent colloids, while keeping the large red fluorescent colloids, resulted in more systems that redisperse upon heating. In contrast to the behavior observed before, now both the systems with the 50 bp dsDNA spacer melted above 80 °C (Figure A.10b). As reducing the size of half the colloids used,

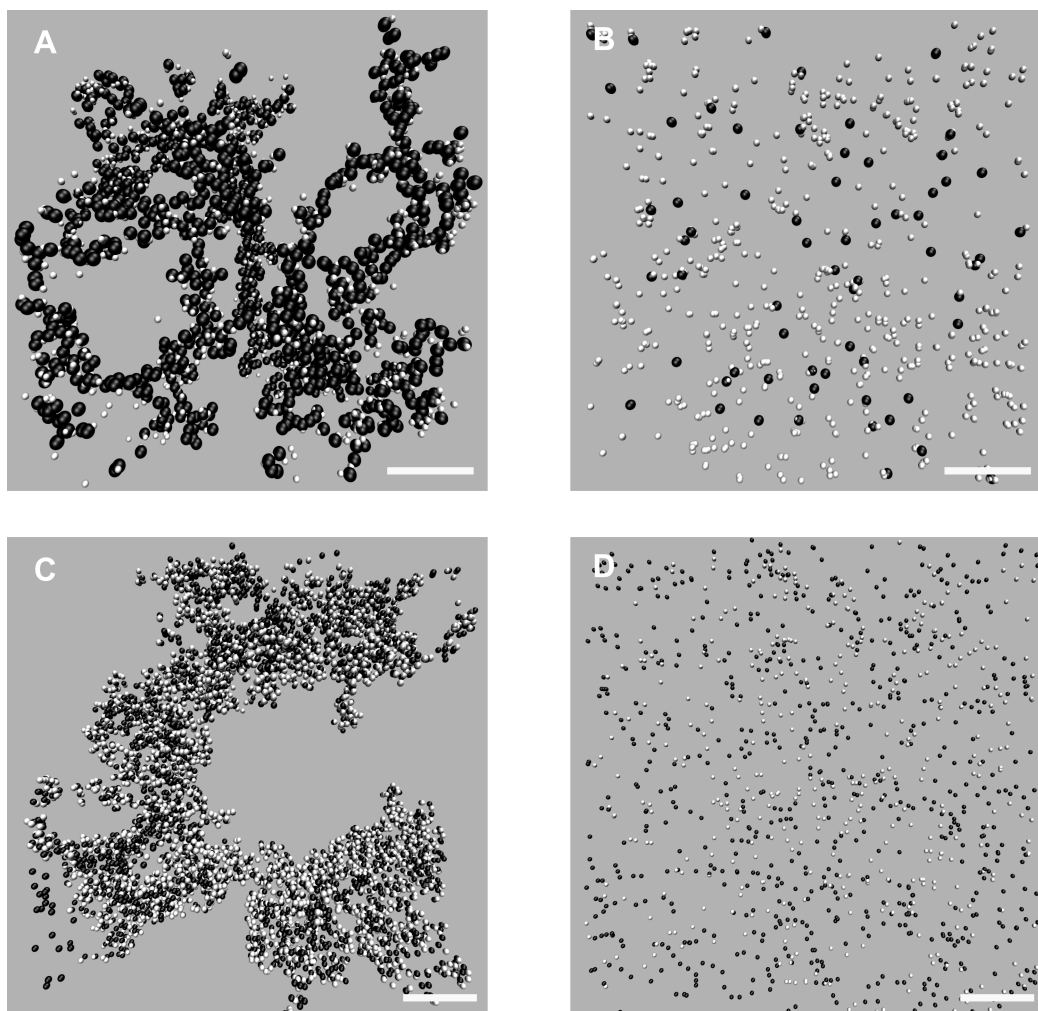


Figure A.10: The Van der Waals attractions between smaller colloids are smaller than for larger ones. A: Unequal bead sizes; combination of  $1\ \mu\text{m}$  colloids and  $390\ \text{nm}$  colloids ( $50\ \text{bp}$  dsDNA +  $12\ \text{ssDNA}$ ). B: By reducing the size of half of all colloids, the samples with  $50\ \text{bp}$  dsDNA redisperse upon heating. C: Aggregate of  $390\ \text{nm}$  DNA-coated colloids ( $50\ \text{bp}$  dsDNA +  $12\ \text{ssDNA}$ ). D: Again, the samples with  $50\ \text{bp}$  dsDNA redisperse upon heating. Scale bars correspond to  $10\ \mu\text{m}$  (A, B) or  $5\ \mu\text{m}$  (C, D).

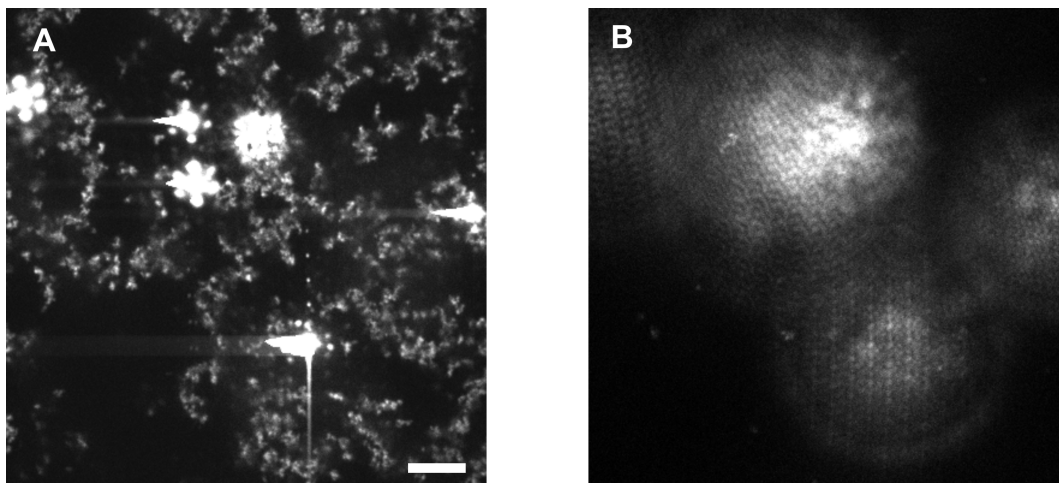


Figure A.11: Smaller colloids are harder to image due to their size, but mainly due to fluorescence interference. A: In time, red-fluorescent unidentified objects start to interfere with imaging (for clarity only the red-fluorescent colloids are shown (in gray)). B: Image with the same unidentified objects out of focus to show the extent of interference. Scale bar measures  $5 \mu\text{m}$ .

resulted in two more DNA-coated systems, it seems that Van der Waals forces indeed prevent bigger colloids from redispersing. But Van der Waals attractions are not the only factor responsible as the colloids coated with pBelo-DNA remained clustered at  $80^\circ\text{C}$ .

### Nano-sized colloids.

Smaller colloids (diameter  $390 \text{ nm}$ ; both colors) were tested with the same set of DNA (Figure A.10c). While all assemblies of the DNA-coated colloids are again similar, differences in melting temperature are detected. Starting at  $50^\circ\text{C}$  and increasing the temperature with steps of  $5^\circ\text{C}/2 \text{ hrs}$ , showed that the 8 bases “sticky ends”-system melted first at  $\sim 60^\circ\text{C}$ . The colloids coated with the same  $50 \text{ bp}$  dsDNA spacer, but with a longer overhang (12 bases) melted at a higher temperature:  $65^\circ\text{C}$  (Figure A.10d). Cos-coated colloids melted at  $\sim 70^\circ\text{C}$  indicating that a short dsDNA spacer indeed keeps colloids further apart. All melted samples are able to reform (cluster again) when brought back to room temperature, indicating that it is indeed due to the melting of the DNA-overhangs (data not shown). The colloids coated with pBelo-DNA remained clustered. With all other samples dispersing, this clustering cannot be due to the size of the colloids alone. Instead, the longer DNA has to play a role in this effect.

Next, we test if we can increase the order within the aggregates by following the work of Gang and coworkers (see Figure A.2, [34]). Briefly, their research stresses the importance of temperature cycles where after formation of fractal structures, the sample needs to spend some time around the melting temperature of the DNA to allow for reorganization. Then the system might assemble into a long-ranged ordered crystal after being melted and annealed one last time.

Colloids coated with 50 bp dsDNA + 8 bases ssDNA are mixed at room temperature and left to aggregate. Then, the sample is placed at the melting temperature of  $\sim 60$  °C (Figure A.12d). (PCR-apparatus; eppendorf mastercycler). The PCR apparatus was used to slowly and controllably cool down the sample (1 °C/min), allowing rearrangements of the DNA. As a control we also added a sample containing “bare” colloids. Unfortunately, the “bare” neutravidin colloids were not stable under the experimental conditions (Figure A.12a), as small aggregates floated in the solution. Although, the sample with DNA-coated colloids (50 bp dsDNA + 8 bases ssDNA) showed different clustering (Figure A.12b) from a sample left at room temperature (Figure A.12c), we did not see an increase in order. The continued lack of order is not a real surprise as Gang and coworkers [34] concluded that DNA needs to be flexible in order for colloids to crystallize and the DNA used in this experiment is rigid.

It would be interesting to test longer DNA constructs (but shorter than pBelo-DNA, see future directions) on this size of colloids. But before these experiments can commence, a minor problem needs to be addressed: the red-fluorescent colloids leak some of their fluorophore in time. After a few days, strongly fluorescent spots prevent proper imaging of the aggregates (Figure A.11a,b). Peculiarly, these fluorescent spots are only detected in samples containing DNA-coated colloids. Colloids without DNA did not leak any fluorophores under identical circumstances. We did try changing the buffer conditions, but did not succeed in preventing the fluorophore from leaking. Additional experiments are needed before the system is optimized to test different spacers lengths on the smaller colloids.

## A.3 Discussion and Outlook

Developing a system of DNA-coated colloids that can assemble or disassemble depending on the temperature of the system, turned out to be very difficult. Theory arguments provided us with a couple of options to try. The results above show that the reality of laboratory experiments can be so complex that simple theoretical arguments may fail.

The few systems that we were able to make temperature-reversible all had short DNA strands (see Table A.1 for an overview). As there are, to my knowledge, at this stage no other experiments on colloids coated with very long, flexible DNA spacers in combination with micron-sized colloids, we cannot compare our results directly to other findings. Our experiments suggest that the long DNA that we use pushes the colloids close together, into a regime where the Van der Waals interactions are too strong to allow subsequent redispersion. Micron-sized colloids coated with short DNA strands have been used by several other groups. However, the systems are slightly different. For instance, the 50 bp dsDNA + 12 bases ssDNA system that we studied did not melt at any temperature. In contrast, Chaikin and coworkers [62] found a melting temperature of 42 °C for a system with 49 bp dsDNA + 11 bases ssDNA. Dreyfus et al. did however use a different type of colloid (Dyna-magnetic colloids) - as Dyna-magnetic colloids are also polystyrene based, the difference must be due to the (unknown) details of the chemical synthesis of the colloids.

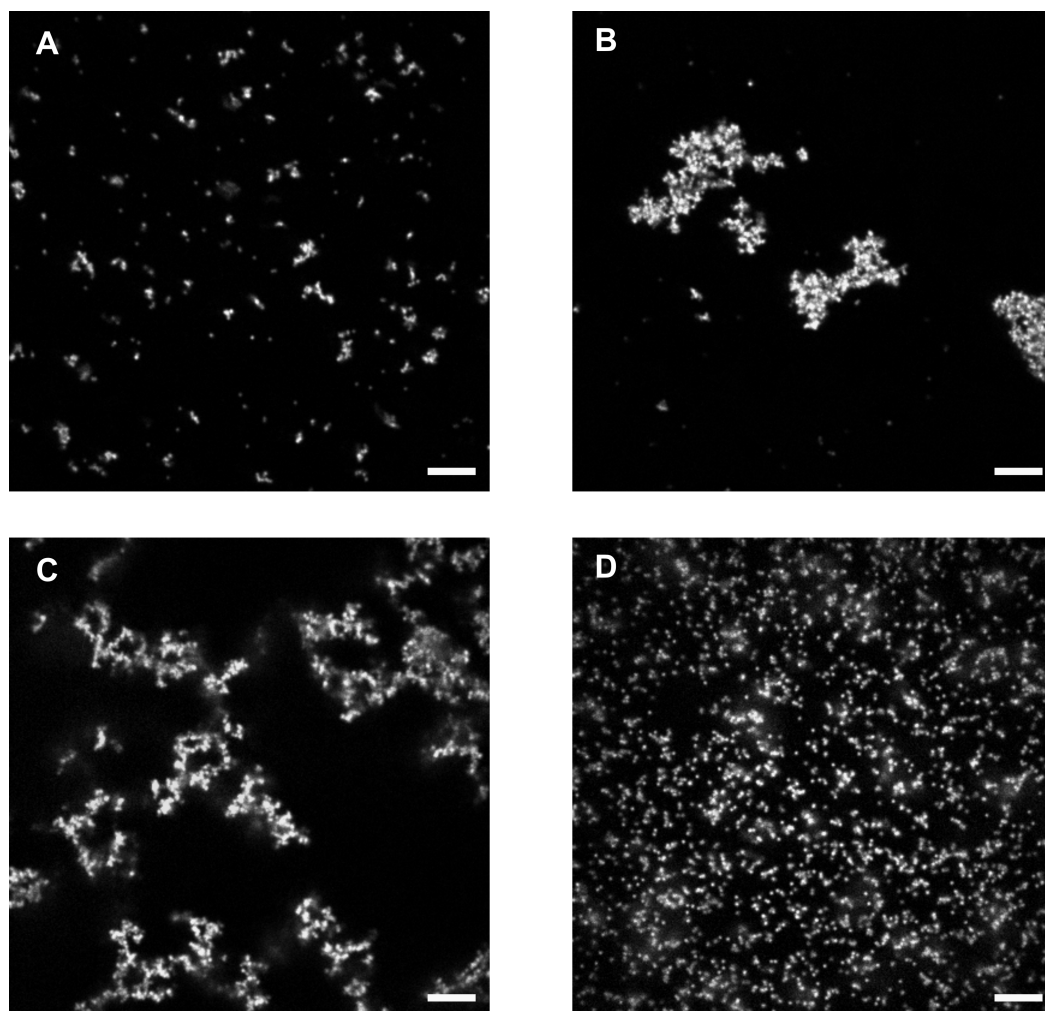


Figure A.12: Starting the assembly process above the melting temperature does not lead to an increase in order. A: “Bare” colloids (no DNA) are not stable under the experimental conditions. B: DNA-coated colloids (50 bp dsDNA + 8 bases ssDNA) that were assembled above the melting temperature. Although the assemblies look different than before, we think this is due to the removal from the PCR apparatus rather than a temperature effect. C: Control sample, mixed and left at room temperature to aggregate. D: Control sample, mixed and left at  $\sim 50$  °C to aggregate. All scale bars indicate  $5 \mu m$ .

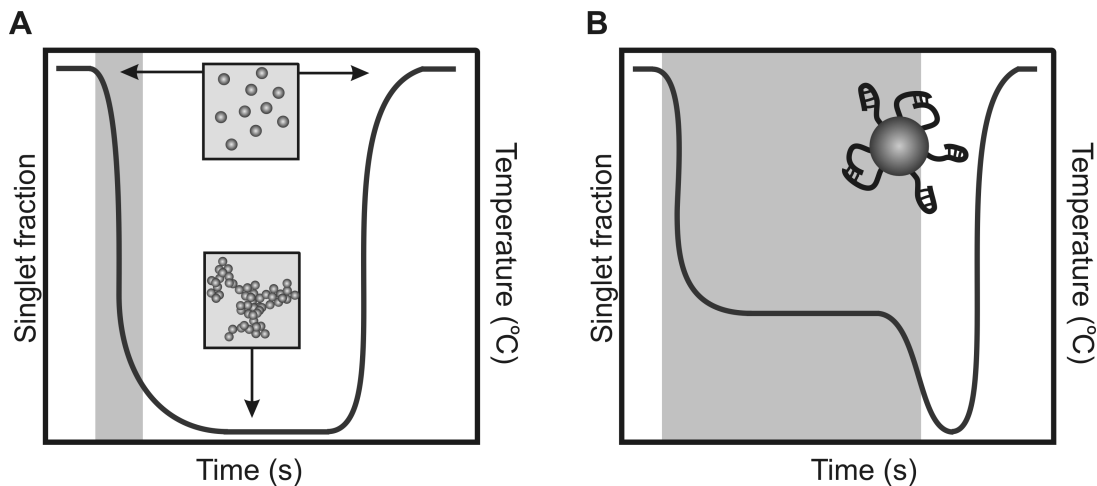


Figure A.13: Schematic representation of the singlet fraction in a colloidal system with respect to time and temperature. A: DNA-coated colloids follow a sharp melting transition. As rearrangements of the DNA are crucial for obtaining order, there is only a small working window with this type of colloids (see gray shaded area). B: The latest system of DNA-coated colloids of Chaikin and coworkers [175], changes the steepness of the curve by using DNA-coated colloids, with DNA that can form hairpin structures and intra-particle DNA bridges. Now the area where DNA rearrangements can occur, is increased significantly (compare shaded areas from A and B).

The steepness of the melting curve for DNA-coated colloids remains a problem. Positioning mistakes that occur during this aggregation process, immediately cause colloids to bind in the wrong place as there is no time for rearrangements (Figure A.13a). A recent paper [175] described a procedure to change the slope (and path) of this temperature curve by using DNA-coated colloids that could not only hybridize to each other, but were also able to form hairpin structures with their “sticky ends”. Hairpin formation leads to self-protected (inert) overhangs. Starting at high temperatures, these colloids first get prepared in a state where most colloids are relatively inert monomers - these monomers are then arranged into the desired pattern and are then made to hybridize with their neighbors by increasing the temperature, such that the hairpins unfold and the inter-colloid DNA-links can form (Figure A.13b).

Crocker and coworkers also pointed out the importance of the type of colloid used. With a depletion study of four different types of colloid against small carboxylated colloids they discovered differences in aggregation behavior. Whereas the big carboxylated colloids and their homemade PEGylated spheres formed close-packed crystal structures under depletion (Figure A.14a), the neutravidin- and glycine modified colloids rather formed large aggregates (Figure A.14b). This supports the suggestion that the failure to crystallize our temperature reversible systems might not be an effect of the DNA alone. Rather, the colloidal surface chemistry may affect the ability of these colloids to anneal into ordered structures being dependent on the colloids surface chemistry. However, as chapter (chapter 5) showed, colloids coated with long DNA can form crystal structures, be it under rather different conditions.

Table A.1: Overview of all DNA-coated colloidal systems studied. If a system is temperature reversible, the melting temperature is listed. A “X” indicates that once aggregates formed with that type of DNA-coated colloids, the system could not be redispersed at any temperature.

colloid sizes	DNA-construct	$T_m$
A: 1 $\mu m$ ; B: 1 $\mu m$	$\lambda$ -DNA	X
	pBelo-DNA	X
	pBR322-DNA	X
	pUC19-DNA	X
	50 bp dsDNA + 12 ssDNA	X
	50 bp dsDNA + 8 ssDNA	X
	cos (12 ssDNA)	80 °C
	pBelo + cos (12 ssDNA)	X
A: 390 nm; B: 1 $\mu m$	pBelo-DNA	X
	50 bp dsDNA + 12 ssDNA	80 °C
	50 bp dsDNA + 8 ssDNA	80 °C
	cos (12 ssDNA)	80 °C
	pBelo + cos (12 ssDNA)	X
A: 390 nm; B: 390 nm	pBelo-DNA	X
	50 bp dsDNA + 12 ssDNA	65 °C
	50 bp dsDNA + 8 ssDNA	60 °C
	cos (12 ssDNA)	70 °C
	pBelo + cos (12 ssDNA)	X

## A.4 Future directions

It would be interesting to test longer DNA constructs (but smaller than pBelo-DNA) on colloids of 390 nm. At the moment, a system of colloids coated with dsDNA of 50 base-pairs and a 12 base “sticky ends” is temperature-reversible, whereas the use of a pBelo spacer (7500 bp) leaves a system irreversible with respect to temperature. As there is more than two orders of magnitude difference in the length of these two types of DNA strands, there is a clear need for a systematic study of the self assembly of colloids coated with DNA of intermediate length. In this appendix two more lengths were already examined, but it seems preferable to clone the cos-overhang into plasmids of different sizes (Figure A.15a). With such an approach the dsDNA spacer can be varied at will as plasmids are available in a broad size range (1000 to 1000.000 bp) and restriction enzymes can shorten plasmids to the exact desired length, while the ssDNA overhang (attractive part) will be the same for all colloids studied (in contrast to the 4-base overhangs used before).

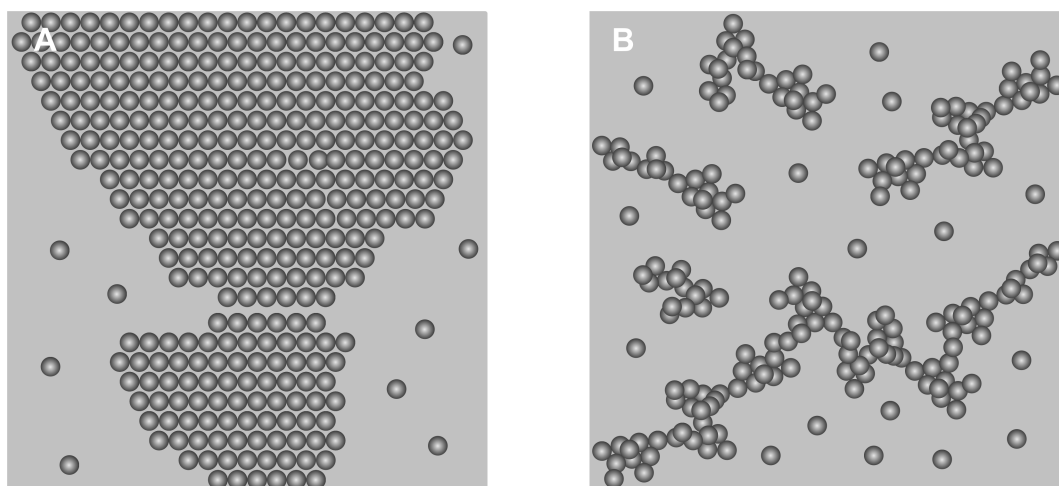


Figure A.14: Schematic representation of depletion study as performed by Crocker and coworkers [123]. A: Carboxylated or home made PEGylated colloids form close packed crystals under depletion. B: Neutravidin- or glycine modified colloids form branched aggregates under the same depletion conditions.

Both experimental papers that reported the observation of three-dimensional crystals [34, 35] stress the importance of flexible spacers, this is another reason why a systematic study of intermediate spacer lengths would be definitely worthwhile.

If the steepness of the melting curve remains to be a problem, it may be worthwhile to consider the use of colloids coated with temperature-switchable DNA hairpins for the formation of ordered structures [175]. In order to be able to clone these in plasmids of different sizes, one would have to order two hairpin sequences extended on one side with a sequence of DNA with a known restriction site within the plasmid of choice (Figure A.15b), together with two complementary DNA strand to the sequence before the hairpin. Before cloning, the two hairpin sequences need to be hybridized together with the two complementary sequences of the restriction sites. This will result in a piece of DNA with two nicks into the backbone, see Figure A.15b. As cloning goes best if two different restriction enzymes are used, the extensions on the hairpin DNA sequences cannot be the same (indicated with two scissors of different color). Two different restriction sites work best, as then the receiving plasmid cannot close without uptake of the donor DNA strand. Note that the resulting hairpin-plasmid is like a  $\lambda$ -DNA vector: it can open upon heating as the backbone is not intact, while the new cosmid has to be cleaved just like the pBelo-plasmid. If this last cloning method would not yield the desired result, one can consider using nicking enzymes instead. Then the extended sequence should contain a nicking recognition site as well as a restriction site.

By varying the length of DNA one can examine if one could also self assemble micron-sized colloids into a three dimensional crystal, opening routes to test if all crystal-structures predicted theoretically can also be realized experimentally.

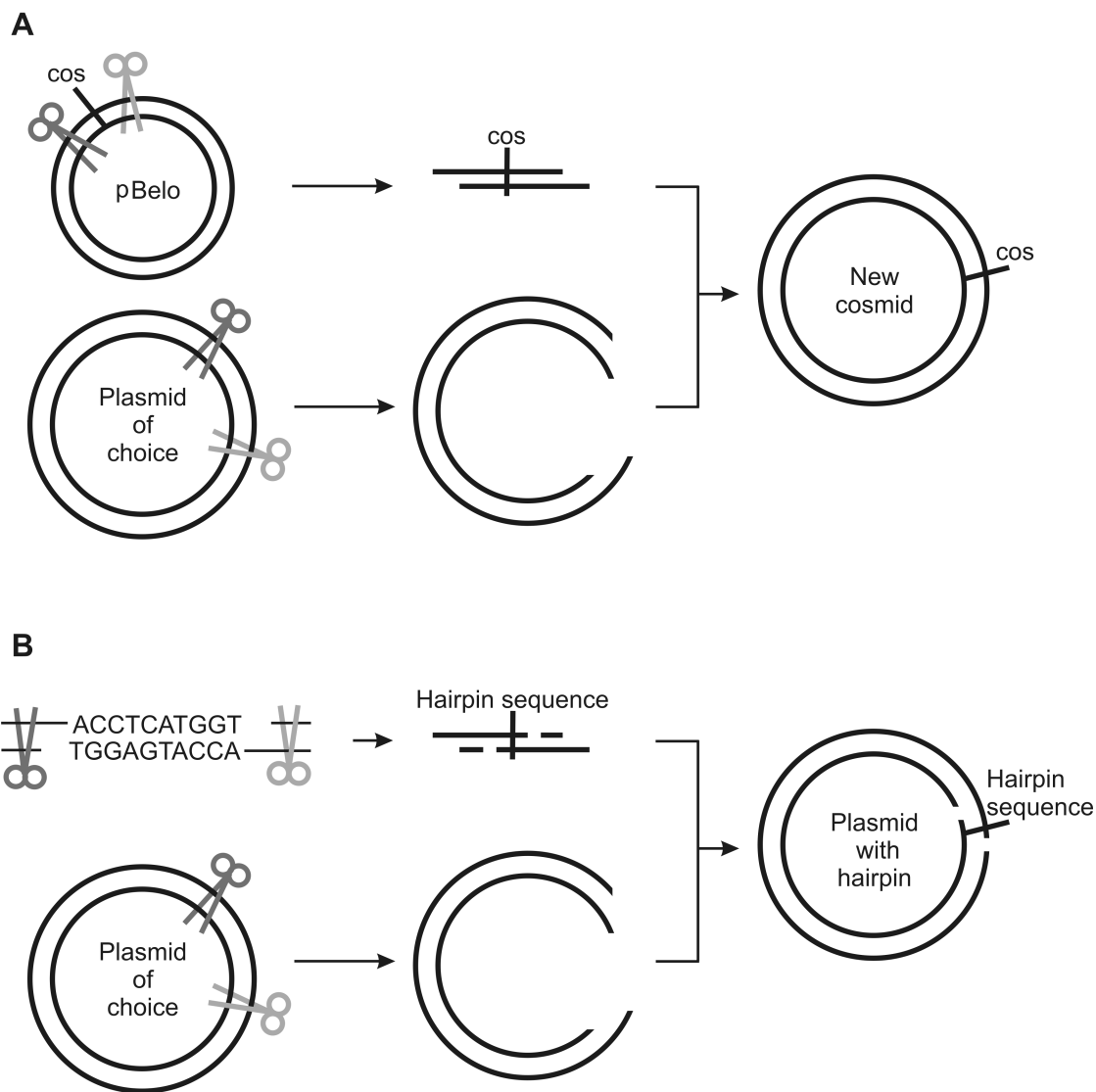


Figure A.15: Cloning strategies to obtain different dsDNA spacer lengths. A: New cosmid-plasmids can be obtained by cloning the cos-site sequence of pBelo into any plasmid of choice. B: Obtaining dsDNA ended by a hairpin ssDNA sequence could in principle also be realized with cloning techniques. This protocol could be more troublesome due to the non-continuous backbone of the plasmid.

## A.5 Materials and Methods

### A.5.1 Preparation of biotin-DNA

#### pBelo-DNA

The pBeloBac11 plasmid was purchased as a strain (New England Biolabs, ER2420S). To obtain sufficient DNA for coating 50  $\mu\text{l}$  colloids (1% solids), the strain was grown overnight at 37 °C in 60 ml LB medium (for 100 ml: Bacto-Tryptone 1 g; Bacto-Yeast extract 0.5 g; NaCl 1 g and ddH<sub>2</sub>O to 100ml; autoclave to sterilize) in the presence of chloramphenicol (20  $\mu\text{g}/\text{ml}$ ). With a spin miniprep-Kit (Qiagen) the plasmid DNA was then isolated. The purity of the DNA was checked by gel electrophoresis on a 1% agarose gel. The plasmid contains a cos-site that can be opened by restriction with  $\lambda$ -terminase (BIOzymTC), leaving two 12 base single strands (“sticky ends”). The linearized DNA was separated into two batches. One batch was mixed with a solution (5  $\mu\text{l}$ ; 20  $\mu\text{M}$ ) of cos1-biotin oligonucleotides (Eurogentec), the other with cos2-biotin oligonucleotides (Eurogentec). To hybridize the oligonucleotides to the DNA, the solution was heated to 65 °C for  $\sim$ 30 minutes and then cooled overnight to room temperature. Subsequently, T4 DNA ligase (New England Biolabs) was added to ligate the DNA backbone. To remove the excess of oligonucleotides and enzyme the samples were centrifuged and washed three times on a Microcon YM100 membrane (Milipore) with Tris-HCl buffer (250 mM, pH = 8). The biotin-DNA solution was then recovered in a clean tube.

#### pBR322-DNA

The pBR322 plasmid was used to obtain shorter length DNA. To obtain dsDNA with complementary ssDNA “sticky ends”, two preparation methods were used. For our “A”-type colloids, the circular plasmid (New England Biolabs) was first restricted with HindIII (New England Biolabs), leaving two 4-base ssDNA ends. Both ends were then filled up nucleotide by nucleotide with Klenow  $\text{exo}^-$ . (To obtain biotinylated DNA regular dTTP, dATP, dGTP-nucleotides were used in combination with biotin-dCTP; all Invitrogen). The reaction solution was then cleaned from excess nucleotides and enzyme (PCR-purification; Qiagen). The obtained DNA was further restricted with BsaI (New England Biolabs) to obtain a 4-base “sticky end” (5'-CGGT-3'). To remove excess enzyme and the shortest end of the restricted DNA, again the DNA was cleaned (PCR-purification-kit; Qiagen) and recovered in a clean tube. For our “B”-type colloids, the circular plasmid (New England Biolabs) was first restricted with AflIII (New England Biolabs), leaving two 4-base ssDNA ends. Both ends were then filled up nucleotide by nucleotide with Klenow  $\text{exo}^-$ . (To obtain biotinylated DNA regular dTTP, dATP, dGTP-nucleotides were used in combination with biotin-dCTP; all Invitrogen). The reaction solution was then cleaned from excess nucleotides and enzymes (PCR-purification; Qiagen). The DNA was then also restricted with BsaI (New England Biolabs) to obtain a 4-base “sticky end” (5'-ACCG-3'). To remove excess enzyme and the short end of the restricted DNA, again the DNA was cleaned (PCR-purification-kit; Qiagen) and recovered in a clean tube. Both sets of enzymes were chosen to obtain dsDNA of almost the same length (3398 bp vs 3407 bp) with complementary ssDNA “sticky ends”.

### pUC19-DNA

Besides pBR322, another plasmid was used to further reduce the dsDNA length. Again two preparation methods were needed to obtain dsDNA with complementary ssDNA “sticky ends”. Here, for our “A”-type colloids, the circular plasmid (New England Biolabs) was first restricted with HindIII (New England Biolabs), leaving two 4-base ssDNA ends. Both ends were then filled up nucleotide by nucleotide with Klenow  $\text{exo}^-$ . (To obtain biotinylated DNA regular dTTP, dATP, dGTP-nucleotides were used in combination with biotin-dCTP; all Invitrogen). The reaction solution was then cleaned from excess nucleotides and enzymes (PCR-purification-kit; Qiagen). The obtained piece of DNA was further restricted with BseYI (New England Biolabs) to obtain a 4-base “sticky end” (5'-CTGG-3'). To remove excess enzyme and the sort piece of restricted DNA, again the DNA was cleaned (PCR-purification-kit; Qiagen) and recovered in a clean tube. For our “B”-type colloids, the circular plasmid (New England Biolabs) was first restricted with BsaI (New England Biolabs), leaving two 4-base ssDNA ends. Both ends were then filled up nucleotide by nucleotide with Klenow  $\text{exo}^-$ . (To obtain biotinylated DNA regular dTTP, dATP, dGTP-nucleotides were used in combination with biotin-dCTP; all Invitrogen). The reaction solution was then cleaned from excess nucleotides and enzymes (PCR-purification; Qiagen). This piece of DNA was then also restricted with BseYI (New England Biolabs) to obtain a 4-base “sticky end” (5'-CCAG-3'). To remove excess enzyme and the sort piece of restricted DNA, again the DNA was cleaned (PCR-purification-kit; Qiagen) and recovered in a clean tube. Both sets of enzymes were chosen to obtain dsDNA pieces of almost the same length (2023 bp vs 2036 bp) with complementary ssDNA “sticky ends”.

### 50 bp dsDNA + 12 base overhang (ssDNA)

This length of DNA does not require the restriction of a plasmid. Instead, needed sequences can be ordered on demand (Eurogentec). To obtain this type of DNA three ssDNA sequences were ordered. First a 50 base ssDNA piece of DNA labeled with a biotin-tag on its 3'-end. (seq1: 5'-GGGTT TTAAG CTTAC CATGG GATAT CCCTA TGATG TGCCA GACTA CGCGG-3'). Then two pieces of 62 bases ssDNA, containing the complementary 50 bases from sequence one plus either cos1 or cos2 (12 bases). (seq2 (cos1): 5'- CCGCG TAGTC TGGCA CATCA TAGGG ATATC CCATG GTAAG CTTAA AACCC GGGCG GCGAC CT-3'; seq3 (cos2): 5'-CCGCG TAGTC TGGCA CATCA TAGGG ATATC CCATG GTAAG CTTAA AACCC AGGTC GCCGC CC-3'). The DNA construct was prepared by mixing equimolar solutions (20  $\mu\text{M}$ ; Tris HCl-buffer, 100mM, pH = 8) of either sequence 1 and 2 or sequence 1 and 3. The mixed solutions were heated to 65 °C for ~30 minutes and then cooled overnight to room temperature, resulting in 50 bp dsDNA with complementary 12 base ssDNA “sticky ends”.

### 50 bp dsDNA + 8 base overhang (ssDNA)

This type of DNA was prepared according to the same protocol as described above. To obtain 8 base overhangs we simply ordered the last 8 bases of the cos-sequences. This

resulted in the following sequences: seq1; 5'-GGGTT TTAAG CTTAC CATGG GATAT CCCTA TGATG TGCCA GACTA CGCGG-3', seq2 (shortened cos1): 5'-CCGCG TAGTC TGGCA CATCA TAGGG ATATC CCATG GTAAG CTTAA AACCC CGCCG CCC-3', seq3 (shortened cos2): 5'-CCGCG TAGTC TGGCA CATCA TAGGG ATATC CCATG GTAAG CTTAA AACCC CGCCG CCC-3'.

### A.5.2 Preparation of thiol-DNA

To obtain thiol-labeled pBelo-DNA the same protocol was used as to obtain biotin-labeled pBelo-DNA. Instead of mixing the two batches with cos-biotin oligonucleotides, cos-thiol oligonucleotides were used (Eurogentec; 5  $\mu$ l; 20  $\mu$ M). As a disulfide group protects the more reactive thiol-group, the oligonucleotides have to be cleaved to be able to react with colloids.

To cleave of the protective group, a solution of tris(2-carboxyethyl)phosphine (TCEP; 10 mM final concentration) was added to thiol-pBelo DNA. This solution was allowed to react overnight at 4 °C. The next day the solution was cleaned with a PCR-purification-kit (Qiagen) to remove excess TCEP and the protective group. The reaction described is sensitive to air, so all solutions added were first degassed ( $N_2$ ). The thiol-DNA was collected in a clean tube, and used directly.

### A.5.3 Preparation of DNA-coated colloids

#### protein binding

As in Ref. [53] we used a binary system in which DNA mediated attractions are favorable only between heterogeneous colloids. Green and red fluorescent neutravidin-coated polystyrene micro-spheres (diameter 1  $\mu$ m, Molecular Probes) were functionalized with DNA carrying complementary “sticky ends”.

Our conjugation protocol is based on the neutravidin-biotin coupling procedure described in Ref. [53]: the batches of DNA were separately mixed with either green (“A” hereafter) or red (“B” hereafter) fluorescently labeled colloids, coated with neutravidin, that were dispersed in TRIS-HCl (250 mM, pH = 8). In each case the DNA and colloids were reacted overnight during which they were continuously tumbled. The next day the samples were pelleted and washed five times to remove excess non-conjugated DNA. In between these washing steps, samples were heated once for 10 min. at 50 °C, to remove poorly bound DNA.

All types of DNA-coated colloids were diluted in a fresh TRIS-HCl buffer (250 mM final concentration, pH = 8) with  $D_2O$  to minimize sedimentation.

#### covalent binding

In order to covalently bind DNA to colloids, we ordered amino-coated polystyrene colloids (diameter 800 nm, Microparticles GmbH). These colloids were first coated with an ester (Pierce; succinimidyl-[(N-maleimidopropionamido)-dodecaethyleneglycol]). This ester binds to the amino groups of the colloids and displays a maleimide end group to

later link thiol-labeled DNA to. An overview of the reaction steps is given in Figure A.7a.

To start coating colloids with the ester, 25  $\mu\text{l}$  (1%) of both types of colloids were washed and redispersed in 50  $\mu\text{l}$  dimethylsulfoxide (DMSO). To this, 20  $\mu\text{l}$  of 250 mM ester-solution (DMSO; Sigma-Aldrich) was added. The reaction was allowed to proceed overnight at room temperature. The next day the excess of ester was removed by pelleting the colloids and five subsequent washing steps with DMSO. Colloids were redispersed in 25  $\mu\text{l}$  DMSO and stored at 4 °C.

The yield of this reaction can be tested by performing a Fmoc test (Figure A.7b). To this end, 10 mg of Fmoc-cysteine (Chem-Impex) in 50  $\mu\text{l}$  DMSO is added to 25  $\mu\text{l}$  ester-coated colloids. The reaction is allowed to proceed overnight at 4 °C. The next day, the excess of Fmoc is removed by pelleting the colloids and washing them five times (DMSO). After removal of the supernatant, the colloids are dried by a Nitrogen air-flow. It is important to weigh the dried colloids to obtain the yield of the reaction. To the dried colloids 100  $\mu\text{l}$  20% piperidine (Sigma-Aldrich) in Dimethylformamide (DMF; Sigma-Aldrich) is added. Immediately afterwards, 900  $\mu\text{l}$  Tetrahydrofuran (THF; Sigma-Aldrich) is added and the sample is mixed. After 15 minutes, the absorbance can be measured at 277 nm. By comparing the obtained value to a calibration curve of reacted Fmoc-cysteine, the yield can be determined. For the above protocol  $\sim 60\%$  of all amino-groups reacted with the added ester. In practice this means the colloids are coated with  $\sim 1.5 \cdot 10^6$  reactive groups. As this is far more than DNA strands can be added, no steps were taken to improve the protocol.

The maleimide modified colloids were mixed with thiol-labeled DNA. The mixture was left overnight (at 37 °C) during which they were continuously tumbled. The next day the samples were pelleted and washed five times (TRIS; 250 mM) to remove the excess of non-reacted DNA. Then DNA-coated colloids were diluted in a fresh TRIS-HCl buffer (250 mM final concentration, pH = 8) with D<sub>2</sub>O to minimize sedimentation.

#### A.5.4 Preparation and coating imaging chambers

To avoid any nonspecific interactions between DNA-coated colloids and glass surfaces of the imaging chambers, coverslips were coated with polyethylene glycol (PEG). The coating of glass slides with PEG is a two-step procedure. First the glass slides were silanized with 3-mercaptoptriethoxysilane (97%, Fluka), then a 5-kDa maleimide modified PEG (Laysan Bio Inc) was tethered to the terminal thiol group of the silane.

Prior to the silanization, the glass slides were cleaned in an UV/ozone box. The cleaned slides were placed in contact with silane vapor overnight. Subsequently, the slides were rinsed with ethanol, dried with nitrogen and left in an oven (100 °C) for 30 minutes. Next a drop of concentrated maleimide modified PEG (250 mg/ml in TRIS-HCl buffer) is trapped between two silanized slides and left overnight at room temperature. The excess of PEG is removed by rinsing with ddH<sub>2</sub>O.

A sample chamber is made from two glass coverslips of different size separated by a parafilm spacer (100  $\mu\text{m}$ ). The parafilm sealed the chamber on three sides. After loading the chamber with 10  $\mu\text{l}$  of each population of DNA-coated colloids, reaching a

final particle volume fraction of  $\phi \approx 0.004$ , the chamber is completely sealed with glue.

### A.5.5 Confocal imaging

All suspensions were imaged by means of an inverted microscope (DMIRB, Leica) with a confocal spinning disc scan head (CSU22, Yokogawa Electric Corp.) and a 60x water immersion objective. Fluorescence of the two populations of colloids was excited at 488 nm and 512 nm. Emission was observed at 505 nm and above 600 nm respectively. The use of two types of fluorescent beads and confocal microscopy allowed us to extract colloids coordinates and to reconstruct 3D images [2].

## A.6 Acknowledgements

I would like to thank Dr. J.H. van Maarseveen and Dr. J.W. Back (University of amsterdam) for their help with creating a protocol to covalently bind DNA to colloids and Dr. W.T. Kok and L. van Buuren (University of amsterdam) for determining the yield of these reactions with liquid chromatography.



## BIBLIOGRAPHY

- [1] W. Russel, D. Saville, and W. Schowalter. *Colloidal Dispersions*. Cambridge University Press., Cambridge (1989).
- [2] J. C. Crocker and D. C. Grier. *Methods of Digital Video Microscopy for Colloidal Studies*. Journal of Colloid and Interface Science, **179**, 298 – 310 (1996).
- [3] C. A. Mirkin, R. L. Letsinger, R. C. Mucic, and J. J. Storhoff. *A DNA based method for assembling nanoparticles*. Nature, **382**, 607–609 (1996).
- [4] R. Jin, G. Wu, Z. Li, C. A. Mirkin, and G. C. Schatz. *What Controls the Melting Properties of DNA-Linked Gold Nanoparticle Assemblies?* Journal of the American Chemical Society, **125**, 1643–1654 (2003).
- [5] V. T. Milam, A. L. Hiddessen, J. C. Crocker, D. J. Graves, and D. A. Hammer. *DNA-Driven Assembly of Bidisperse, Micron-Sized Colloids*. Langmuir, **19**, 10317–10323 (2003).
- [6] M. P. Valignat, J. C. Theodoly, O. Crocker, W. B. Russel, and C. P. M. *Reversible self assembly and directed assembly of DNA linked micrometer sized colloids*. Proc. Natl. Acad. Sci., **21**, 4225–4229 (2005).
- [7] P. H. Rogers, E. Michel, C. A. Bauer, S. Vanderet, D. Hansen, B. K. Roberts, A. Calvez, J. B. Crews, K. O. Lau, A. Wood, D. J. Pine, and P. V. Schwartz. *Selective, Controllable, and Reversible Aggregation of Polystyrene Latex Microspheres via DNA Hybridization*. Langmuir, **21**, 5562–5569 (2005).
- [8] P. L. Biancaniello, A. J. Kim, and J. C. Crocker. *Colloidal Interactions and Self-Assembly Using DNA Hybridization*. Phys. Rev. Lett., **94**, 058302 (2005).
- [9] A. V. Tkachenko. *Morphological Diversity of DNA-Colloidal Self-Assembly*. Phys. Rev. Lett., **89**, 148303 (2002).
- [10] J. D. Watson and F. H. C. Crick. *Molecular Structure of Nucleic Acids*. Nature, **171**, 737 – 738 (1953).
- [11] M. H. Caruthers. *Gene Synthesis Machines: DNA Chemistry and its Uses*. Science, **230**, 281–285 (1985).
- [12] K. B. Mullis. *Polymerase chain reaction*. Angewandte Chemie, **106**, 1271–1276 (1994).
- [13] N. C. Seeman. *The use of branched DNA for nanoscale fabrication*. Nanotechnology, **2**, 149–159 (1991).

- [14] Y. Wang, J. E. Mueller, B. Kemper, and N. C. Seeman. *Assembly and characterization of five-arm and six-arm DNA branched junctions*. *Biochemistry*, **30**, 5667–5674 (1991).
- [15] J. Chen and N. C. Seeman. *The electrophoretic properties of a DNA cube and its substructure catenanes*. *Electrophoresis*, **12**, 607–611 (1991).
- [16] Y. Zhang and N. C. Seeman. *Construction of a DNA-Truncated Octahedron*. *Journal of the American Chemical Society*, **116**, 1661–1669 (1994).
- [17] M. K. Herrlein, J. S. Nelson, and R. L. Letsinger. *A Covalent Lock for Self-Assembled Oligonucleotide Conjugates*. *Journal of the American Chemical Society*, **117**, 10151–10152 (1995).
- [18] E. Winfree, F. Liu, L. A. Wenzler, and N. C. Seeman. *Design and self-assembly of two-dimensional DNA crystals*. *Nature*, **394**, 539 – 544 (1998).
- [19] N. C. Seeman. *DNA in a material world*. *Nature*, **421**, 427–431 (2003).
- [20] W. M. Shih, J. D. Quispe, and G. F. Joyce. *A 1.7-kilobase single-stranded DNA that folds into a nanoscale octahedron*. *Nature*, **427**, 618–621 (2004).
- [21] P. W. K. Rothemund. *Folding DNA to create nanoscale shapes and patterns*. *Nature*, **440**, 297 – 302 (2006).
- [22] C. M. Erben, R. P. Goodman, and A. J. Turberfield. *A Self-Assembled DNA Bipyramid*. *Journal of the American Chemical Society*, **129**, 6992–6993 (2007).
- [23] F. A. Aldaye, A. L. Palmer, and H. F. Sleiman. *Assembling Materials with DNA as the Guide*. *Science*, **321**, 1795–1799 (2008).
- [24] K. Fujibayashi, R. Hariadi, S. H. Park, E. Winfree, and S. Murata. *Toward Reliable Algorithmic Self-Assembly of DNA Tiles: A Fixed-Width Cellular Automaton Pattern*. *Nano Letters*, **8**, 1791–1797 (2008).
- [25] A. Y. Koyfman, S. N. Magonov, and N. O. Reich. *Self-Assembly of DNA Arrays into Multilayer Stacks*. *Langmuir*, **25**, 1091–1096 (2009).
- [26] J. M. Thomas. *Colloidal metals: past, present and future*. *Pure Appl. Chem.*, **60**, 1517–1528 (1988).
- [27] M. Brust, M. Walker, D. Bethell, D. J. Schiffrin, and R. Whyman. *Synthesis of thiol-derivatised gold nanoparticles in a two-phase LiquidLiquid system*. *J. Chem. Soc., Chem. Commun.*, **7**, 795–797 (1994).
- [28] G. Markovich, C. P. Collier, and J. R. Heath. *Reversible Metal-Insulator Transition in Ordered Metal Nanocrystal Monolayers Observed by Impedance Spectroscopy*. *Phys. Rev. Lett.*, **80**, 3807–3810 (1998).

- [29] G. Schmid, M. Bumle, and N. Beyer. *Ordered Two-Dimensional Monolayers of Au Clusters*. *Angewandte Chemie International Edition*, **39**, 181–183 (2000).
- [30] S. Liu, R. Maoz, G. Schmid, and J. Sagiv. *Template Guided Self-Assembly of Au55 Clusters on Nanolithographically Defined Monolayer Patterns*. *Nano Letters*, **2**, 1055–1060 (2002).
- [31] A. P. Alivisatos, K. P. Johnsson, X. Peng, T. E. Wilson, C. Loweth, M. Bruchez, and P. Schultz. *Organization of 'nanocrystal molecules' using DNA*. *Nature*, **382**, 609–611 (1996).
- [32] J. J. Guo and J. A. Lewis. *Aggregation Effects on the Compressive Flow Properties and Drying Behavior of Colloidal Silica Suspensions*. *Journal of the American Ceramic Society*, **82**, 2345 – 2358 (1999).
- [33] R. D. Deegan, O. Bakajin, T. F. Dupont, G. Huber, S. R. Nagel, and T. A. Witten. *Capillary flow as the cause of ring stains from dried liquid drops*. *Nature*, **389**, 827–829 (1997).
- [34] S. Y. Park, A. K. R. Lytton-Jean, B. Lee, S. Weigand, G. C. Schatz, and C. A. Mirkin. *DNA-programmable nanoparticle crystallization*. *Nature*, **451**, 553 – 556 (2008).
- [35] D. Nykypanchuk, N. N. Maye, D. Van der Lelie, and O. Gang. *DNA-guided crystallization of colloidal nanoparticles*. *Nature*, **451**, 549 – 552 (2008).
- [36] J. S. Lee, A. K. R. Lytton-Jean, S. J. Hurst, and C. A. Mirkin. *Silver Nanoparticle-Oligonucleotide Conjugates Based on DNA with Triple Cyclic Disulfide Moieties*. *Nano Letters*, **7**, 2112–2115 (2007).
- [37] X. Xu, N. L. Rosi, Y. Wang, F. Huo, and C. A. Mirkin. *Asymmetric Functionalization of Gold Nanoparticles with Oligonucleotides*. *Journal of the American Chemical Society*, **128**, 9286–9287 (2006).
- [38] P. Sandstrom, M. Boncheva, and B. Akerman. *Nonspecific and Thiol-Specific Binding of DNA to Gold Nanoparticles*. *Langmuir*, **19**, 7537–7543 (2003).
- [39] M. Cardenas, J. Barauskas, K. Schillen, J. L. Brennan, M. Brust, and T. Nylander. *Thiol-Specific and Nonspecific Interactions between DNA and Gold Nanoparticles*. *Langmuir*, **22**, 3294–3299 (2006).
- [40] B. K. Pong, J. Y. Lee, and B. L. Trout. *First Principles Computational Study for Understanding the Interactions between ssDNA and Gold Nanoparticles: Adsorption of Methylamine on Gold Nanoparticulate Surfaces*. *Langmuir*, **21**, 11599–11603 (2005).
- [41] T. M. Herne and M. J. Tarlov. *Characterization of DNA Probes Immobilized on Gold Surfaces*. *Journal of the American Chemical Society*, **119**, 8916–8920 (1997).

- [42] J. J. Storhoff, R. Elghanian, C. Mirkin, and R. L. Letsinger. *Sequence-Dependent Stability of DNA-Modified Gold Nanoparticles*. *Langmuir*, **18**, 6666–6670 (2002).
- [43] L. M. Demers, C. A. Mirkin, R. C. Mucic, R. A. Reynolds, R. L. Letsinger, R. Elghanian, and G. Viswanadham. *A Fluorescence-Based Method for Determining the Surface Coverage and Hybridization Efficiency of Thiol-Capped Oligonucleotides Bound to Gold Thin Films and Nanoparticles*. *Analytical Chemistry*, **72**, 5535–5541 (2000).
- [44] E. Y. Kim, J. Stanton, R. A. Vega, K. J. Kunstman, C. A. Mirkin, and S. M. Wolinsky. *A real-time PCR-based method for determining the surface coverage of thiol-capped oligonucleotides bound onto gold nanoparticles*. *Nucleic Acids Research*, **34**, e54 (2006).
- [45] D. Zanchet, C. M. Micheel, W. J. Parak, D. Gerion, and A. P. Alivisatos. *Electrophoretic Isolation of Discrete Au Nanocrystal/DNA Conjugates*. *Nano Letters*, **1**, 32–35 (2001).
- [46] W. J. Parak, T. Pellegrino, C. M. Micheel, D. Gerion, S. C. Williams, and A. P. Alivisatos. *Conformation of Oligonucleotides Attached to Gold Nanocrystals Probed by Gel Electrophoresis*. *Nano Letters*, **3**, 33–36 (2003).
- [47] W. J. Qin and L. Y. L. Yung. *Nanoparticle-DNA Conjugates Bearing a Specific Number of Short DNA Strands by Enzymatic Manipulation of Nanoparticle-bound DNA*. *Langmuir*, **21**, 11330–11334 (2005).
- [48] E. Bianchi, J. Largo, P. Tartaglia, E. Zaccarelli, and F. Sciortino. *Phase Diagram of Patchy Colloids: Towards Empty Liquids*. *Physical Review Letters*, **97**, 168301 (2006).
- [49] J. Largo, F. W. Starr, and F. Sciortino. *Self-Assembling DNA Dendrimers: A Numerical Study*. *Langmuir*, **23**, 5896–5905 (2007).
- [50] J. Largo, P. Tartaglia, and F. Sciortino. *Effective nonadditive pair potential for lock-and-key interacting particles: The role of the limited valence*. *Physical Review E (Statistical, Nonlinear, and Soft Matter Physics)*, **76**, 011402 (2007).
- [51] F. W. Starr and F. Sciortino. *Model for assembly and gelation of four-armed DNA dendrimers*. *Journal of Physics: Condensed Matter*, **18**, 347–353 (2006).
- [52] C. M. Niemeyer, B. J. Ceyhan, and P. Hazarika. *Oligofunctional DNA-Gold Nanoparticle Conjugates*. *Angew. Chem. Int. Ed.*, **42**, 5766–5770 (2003).
- [53] T. Schmatko, B. Bozorgui, N. Geerts, D. Frenkel, E. Eiser, and W. C. K. Poon. *A finite-cluster phase in  $\lambda$ -DNA-coated colloids*. *Soft Matter*, **3**, 703–706 (2007).
- [54] N. Geerts, T. Schmatko, and E. Eiser. *Clustering versus Percolation in the Assembly of Colloids Coated with Long DNA*. *Langmuir*, **24**, 5118–5123 (2008).

- [55] N. M. Green. *Avidin and streptavidin*. *Methods Enzymol.*, **184**, 51–67 (1990).
- [56] X. Tong and L. Smith. *Solid-phase method for the purification of DNA sequencing reactions*. *Analytical Chemistry*, **64**, 2672–2677 (1992).
- [57] E. P. Diamandis and T. K. Christopoulos. *The biotin-(strept)avidin system: principles and applications in biotechnology*. *Clin Chem*, **37**, 625–636 (1991).
- [58] A. Holmberg, A. Blomstergren, O. Nord, M. Lukacs, and M. Lundeberg, J. Uhlen. *The Biotin-streptavidin interaction can be reversibly broken using water at elevated temperatures*. *Electrophoresis*, **26**, 501–510 (2005).
- [59] A. J. Kim, V. N. Manoharan, and J. C. Crocker. *Swelling-Based Method for Preparing Stable, Functionalized Polymer Colloids*. *Journal of the American Chemical Society*, **127**, 1592–1593 (2005).
- [60] C. Monfardini, O. Schiavon, P. Caliceti, M. Morpurgo, J. M. Harris, and F. M. Veronese. *A Branched Monomethoxypoly(ethylene glycol) for Protein Modification*. *Bioconjugate Chemistry*, **6**, 62–69 (1995).
- [61] L. E. Dewalt, H. D. Ou-Yang, and V. L. Dimonie. *Competition between micellization and adsorption of diblock copolymers in a colloidal system*. *Journal of Applied Polymer Science*, **58**, 265–269 (1995).
- [62] R. Dreyfus, M. E. Leunissen, R. Sha, A. V. Tkachenko, N. C. Seeman, D. J. Pine, and P. M. Chaikin. *Simple Quantitative Model for the Reversible Association of DNA Coated Colloids*. *Physical Review Letters*, **102**, 048301 (2009).
- [63] K. J. Breslauer, R. Frank, H. Blocker, and L. A. Marky. *Predicting DNA duplex stability from the base sequence*. *Nature*, **83**, 3746–3750 (1986).
- [64] N. C. Harris and C. H. Kiang. *Disorder in DNA-Linked Gold Nanoparticle Assemblies*. *Physical Review Letters*, **95**, 046101 (2005).
- [65] Y. Sun, N. C. Harris, and C. Kiang. *Melting transition of directly linked gold nanoparticle DNA assembly*. *Physica A Statistical Mechanics and its Applications*, **350**, 89 – 94 (2005).
- [66] R. Elghanian, J. J. Storhoff, R. C. Mucic, R. L. Letsinger, and C. A. Mirkin. *Selective Colorimetric Detection of Polynucleotides Based on the Distance-Dependent Optical Properties of Gold Nanoparticles*. *Science*, **277**, 1078–1081 (1997).
- [67] D. B. Lukatsky and D. Frenkel. *Surface and bulk dissolution properties, and selectivity of DNA-linked nanoparticle assemblies*. *The Journal of Chemical Physics*, **122**, 214904 (2005).
- [68] K. Kegler, M. Salomo, and F. Kremer. *Forces of Interaction between DNA-Grafted Colloids: An Optical Tweezer Measurement*. *Physical Review Letters*, **98**, 058304 (2007).

- [69] P. L. Biancaniello, J. C. Crocker, D. A. Hammer, and V. T. Milam. *DNA-Mediated Phase Behavior of Microsphere Suspensions*. *Langmuir*, **23**, 2688–2693 (2007).
- [70] D. Nykypanchuk, M. M. Maye, D. Van der Lelie, and O. Gang. *DNA-Based Approach for Interparticle Interaction Control*. *Langmuir*, **23**, 6305–6314 (2007).
- [71] C. K. Tison and V. T. Milam. *Manipulating DNA Probe Presentation via Enzymatic Cleavage of Diluent Strands*. *Biomacromolecules*, **9**, 2468–2476 (2008).
- [72] H. D. Hill, S. J. Hurst, and C. A. Mirkin. *Curvature-Induced Base Pair Slipping Effects in DNA-Nanoparticle Hybridization*. *Nano Letters*, **9**, 317–321 (2009).
- [73] S. Cobbe, S. Connolly, D. Ryan, L. Nagle, R. Eritja, and D. Fitzmaurice. *DNA-Controlled Assembly of Protein-Modified Gold Nanocrystals*. *The Journal of Physical Chemistry B*, **107**, 470–477 (2003).
- [74] C. J. Loweth, W. B. Caldwell, X. Peng, A. P. Alivisatos, and P. G. Schultz. *DNA-Based Assembly of Gold Nanocrystals*. *Angewandte Chemie International Edition*, **38**, 1808–1812 (1999).
- [75] M. Noyong, K. Gloddek, J. Mayer, T. Weirich, and U. Simon. *cis -Pt Mediated Assembly of Gold Nanoparticles on DNA*. *Journal of Cluster Science*, **18**, 193–204 (2007).
- [76] G. H. Woehrle, M. G. Warner, and J. E. Hutchison. *Molecular-Level Control of Feature Separation in One-Dimensional Nanostructure Assemblies Formed by Biomolecular Nanolithography*. *Langmuir*, **20**, 5982–5988 (2004).
- [77] E. Braun, Y. Eichen, U. Sivan, and G. Ben-Yoseph. *DNA-Templated Construction of Copper Nanowires*. *Nature*, **391**, 775–778 (1998).
- [78] J. Richter, M. Mertig, W. Pompe, I. Monch, and H. K. Schackert. *Construction of highly conductive nanowires on a DNA template*. *Applied Physics Letters*, **78**, 536–538 (2001).
- [79] M. Mertig, L. Colombi Ciacchi, R. Seidel, W. Pompe, and A. De Vita. *DNA as a Selective Metallization Template*. *Nano Letters*, **2**, 841–844 (2002).
- [80] C. F. Monson and A. T. Woolley. *DNA-Templated Construction of Copper Nanowires*. *Nano Letters*, **3**, 359–363 (2003).
- [81] M. Chee, R. Yang, E. Hubbell, A. Berno, X. C. Huang, D. Stern, J. Winkler, D. J. Lockhart, M. S. Morris, and S. P. A. Fodor. *Accessing Genetic Information with High-Density DNA Arrays*. *Science*, **274**, 610–614 (1996).
- [82] T. A. Taton, C. A. Mirkin, and R. L. Letsinger. *Scanometric DNA Array Detection with Nanoparticle Probes*. *Science*, **289**, 1757–1760 (2000).

- [83] J. Reichert, A. Csaki, J. M. Kohler, and W. Fritzsche. *Chip-Based Optical Detection of DNA Hybridization by Means of Nanobead Labeling*. *Analytical Chemistry*, **72**, 6025–6029 (2000).
- [84] T. A. Taton, G. Lu, and C. A. Mirkin. *Two-Color Labeling of Oligonucleotide Arrays via Size-Selective Scattering of Nanoparticle Probes*. *Journal of the American Chemical Society*, **123**, 5164–5165 (2001).
- [85] L. Lin, H. Zhao, J. Li, J. Tang, M. Duan, and L. Jiang. *Study on Colloidal Au-Enhanced DNA Sensing by Quartz Crystal Microbalance*. *Biochemical and Biophysical Research Communications*, **274**, 817 – 820 (2000).
- [86] S. Han, J. Lin, M. Satjapipat, A. J. Baca, and F. Zhou. *Oligonucleotide-Capped Gold Nanoparticles for Improved Atomic Force Microscopic Imaging and Enhanced Selectivity in Polynucleotide Detection*. *Biochemical and Biophysical Research Communications*, **279**, 265 – 269 (2000).
- [87] F. Patolsky, K. T. Ranjit, A. Lichtenstein, and I. Willner. *Dendritic amplification of DNA analysis by oligonucleotide-functionalized Au-nanoparticles*. *Chemical Communications*, 1025 – 1026 (2000).
- [88] G. R. Souza and J. H. Miller. *Oligonucleotide Detection Using Angle-Dependent Light Scattering and Fractal Dimension Analysis of Gold-DNA Aggregates*. *Journal of the American Chemical Society*, **123**, 6734–6735 (2001).
- [89] L. He, M. D. Musick, S. R. Nicewarner, F. G. Salinas, S. J. Benkovic, M. J. Natan, and C. D. Keating. *Colloidal Au-Enhanced Surface Plasmon Resonance for Ultrasensitive Detection of DNA Hybridization*. *Journal of the American Chemical Society*, **122**, 9071–9077 (2000).
- [90] R. Moller, A. Csaki, J. M. Kohler, and W. Fritzsche. *Electrical Classification of the Concentration of Bioconjugated Metal Colloids after Surface Adsorption and Silver Enhancement*. *Langmuir*, **17**, 5426–5430 (2001).
- [91] S. Park, T. A. Taton, and C. A. Mirkin. *Array-Based Electrical Detection of DNA with Nanoparticle Probes*. *Science*, **295**, 1503–1506 (2002).
- [92] T. Selvaraju, J. Das, K. Jo, K. Kwon, C. H. Huh, T. K. Kim, and H. Yang. *Nanocatalyst-Based Assay Using DNA-Conjugated Au Nanoparticles for Electrochemical DNA Detection*. *Langmuir*, **24**, 9883–9888 (2008).
- [93] D. B. Lukatsky and D. Frenkel. *Phase Behavior and Selectivity of DNA-Linked Nanoparticle Assemblies*. *Phys. Rev. Lett.*, **92**, 068302 (2004).
- [94] C. M. Niemeyer, B. J. Ceyhan, M. Noyong, , S. Gao, L. Chi, S. Peschel, and U. Simon. *Site-selective immobilization of gold nanoparticles functionalized with DNA oligomers*. *Colloid Polymer Science*, **279**, 68–72 (2001).

- [95] S. Peschel, B. Ceyhan, C. M. Niemeyer, S. Gao, L. Chi, and U. Simon. *Immobilization of gold nanoparticles on solid supports utilizing DNA hybridization*. Materials Science and Engineering: C, **19**, 47 – 50 (2002).
- [96] D. M. Hartmann, M. Heller, S. C. Esener, D. Schwartz, and G. Tu. *Selective DNA attachment of micro-and nanoscale particles to substrates*. Journal of Material Research, **17**, 473–478 (2002).
- [97] E. M. Puchner, S. K. Kufer, M. Strackharn, S. W. Stahl, and H. E. Gaub. *Nanoparticle Self-Assembly on a DNA-Scaffold Written by Single-Molecule Cut-and-Paste*. Nano Letters, **8**, 3692–3695 (2008).
- [98] J. D. Le, Y. Pinto, N. C. Seeman, K. Musier-Forsyth, T. A. Taton, and R. A. Kiehl. *DNA-Templated Self-Assembly of Metallic Nanocomponent Arrays on a Surface*. Nano Letters, **4**, 2343–2347 (2004).
- [99] J. Zhang, Y. Liu, Y. Ke, and H. Yan. *Periodic Square-Like Gold Nanoparticle Arrays Templated by Self-Assembled 2D DNA Nanogrids on a Surface*. Nano Letters, **6**, 248–251 (2006).
- [100] C. M. Niemeyer, B. J. Ceyhan, M. Noyong, and U. Simon. *Bifunctional DNA-gold nanoparticle conjugates as building blocks for the self-assembly of cross-linked particle layers*. Biochemical and Biophysical Research Communications, **311**, 995 – 999 (2003).
- [101] B. Zou, B. Ceyhan, U. Simon, and C. M. Niemeyer. *Self-Assembly of Crosslinked DNA-Gold Nanoparticle Layers Visualized by In-Situ Scanning Force Microscopy*. Advanced materials, **17**, 1643–1647 (2005).
- [102] Y. Zhang, A. O. Eniola, D. J. Graves, and D. A. Hammer. *Specific Adhesion of Micron-Sized Colloids to Surfaces Mediated by Hybridizing DNA Chains*. Langmuir, **19**, 6905–6911 (2003).
- [103] N. Geerts and E. Eiser. *Colloidal Flying Carpets*. Submitted (2009).
- [104] W. Cheng, M. J. Campolongo, S. J. Cha, J. J. and Tan, C. C. Umbach, D. A. Muller, and D. Luo. *Free-standing nanoparticle superlattice sheets controlled by DNA*. Nature Materials, **8**, 519 – 525 (2009).
- [105] R. C. Mucic, J. J. Storhoff, C. A. Mirkin, and R. L. Letsinger. *DNA-Directed Synthesis of Binary Nanoparticle Network Materials*. Journal of the American Chemical Society, **120**, 12674–12675 (1998).
- [106] M. M. Maye, D. Nykypanchuk, M. Cuisinier, D. Van der Lelie, and O. Gang. *Stepwise surface encoding for high-throughput assembly of nanoclusters*. Nature Materials, **8**, 388–391 (2009).

- [107] D. B. Lukatsky, B. M. Mulder, and D. Frenkel. *Designing ordered DNA-linked nanoparticle assemblies*. Journal of Physics: Condensed Matter, **18**, S567–S580 (2006).
- [108] J. J. Storhoff, A. A. Lazarides, R. C. Mucic, C. A. Mirkin, R. L. Letsinger, and G. C. Schatz. *What Controls the Optical Properties of DNA-Linked Gold Nanoparticle Assemblies?* Journal of the American Chemical Society, **122**, 4640–4650 (2000).
- [109] H. Xiong, D. van der Lelie, and O. Gang. *Phase Behavior of Nanoparticles Assembled by DNA Linkers*. Physical Review Letters, **102**, 015504 (2009).
- [110] S. J. Park, A. A. Lazarides, C. A. Mirkin, and R. L. Letsinger. *Directed assembly of periodic materials from protein and oligonucleotide modified nanoparticle building blocks*. Angewandte Chemie Int. Ed., **40**, 2909–2912 (2001).
- [111] E. V. Shevchenko, D. V. Talapin, N. A. Kotov, S. O’Brien, and C. B. Murray. *Nonspecific and Thiol-Specific Binding of DNA to Gold Nanoparticles*. Nature, **493**, 55–59 (2006).
- [112] D. Frenkel. *Colloidal crystals Plenty of room at the top*. Nature materials, **5**, 85–86 (2006).
- [113] Z. Li and C. A. Mirkin. *G-Quartet-Induced Nanoparticle Assembly*. Journal of the American Chemical Society, **127**, 11568–11569 (2005).
- [114] F. Seela, A. M. Jawalekar, L. Chi, D. Zhong, and H. Fuchs. *Gold DNA-Conjugates: Ion Specific Self-Assembly of Gold Nanoparticles via the dG-Quartet*. Nucleosides, Nucleotides and Nucleic Acids, **24**, 843 – 846 (2005).
- [115] W. Wang, H. Liu, D. Liu, Y. Xu, Y. Y., and D. Zhou. *Use of the Interparticle i-Motif for the Controlled Assembly of Gold Nanoparticles*. Langmuir, **23**, 11956–11959 (2007).
- [116] F. Seela and S. Budow. *Ph-Dependent Assembly of DNA-Gold Nanoparticles Based on the i-Motif*. Nucleosides, Nucleotides and Nucleic Acids, **26**, 755 – 759 (2007).
- [117] J. Zheng, P. S. Lukeman, W. B. Sherman, C. Micheel, P. A. Alivisatos, P. E. Constantinou, and N. C. Seeman. *Metallic Nanoparticles Used to Estimate the Structural Integrity of DNA Motifs*. The Journal of Physical Chemistry B, **95**, 3340 – 3348 (2008).
- [118] J. Sharma, R. Chhabra, A. Cheng, J. Brownell, Y. Liu, and H. Yan. *Control of Self-Assembly of DNA Tubules Through Integration of Gold Nanoparticles*. Science, **323**, 112–116 (2009).
- [119] C. M. Soto, A. Srinivasan, and B. R. Ratna. *Controlled Assembly of Mesoscale Structures Using DNA as Molecular Bridges*. Journal of the American Chemical Society, **124**, 8508–8509 (2002).

- [120] Y. Yin, Y. Lu, and Y. Xia. *A Self-Assembly Approach to the Formation of Asymmetric Dimers from Monodispersed Spherical Colloids*. *Journal of the American Chemical Society*, **123**, 771–772 (2001).
- [121] N. A. Licata and A. V. Tkachenko. *Self-assembly of DNA-coded nanoclusters*. *Physical Review E (Statistical, Nonlinear, and Soft Matter Physics)*, **74**, 040401 (2006).
- [122] C. K. Tison and V. T. Milam. *Reversing DNA-Mediated Adhesion at a Fixed Temperature*. *Langmuir*, **23**, 9728–9736 (2007).
- [123] A. J. Kim, P. L. Biancaniello, and J. C. Crocker. *Engineering DNA-Mediated Colloidal Crystallization*. *Langmuir*, **22**, 1991–2001 (2006).
- [124] A. J. Kim, R. Scarlett, P. L. Biancaniello, T. Sinno, and J. C. Crocker. *Probing interfacial equilibration in microsphere crystals formed by DNA-directed assembly*. *Nature Materials*, **8**, 52–55 (2009).
- [125] A. I. Campbell, V. J. Anderson, J. S. van Duijneveldt, and P. Bartlett. *Dynamical Arrest in Attractive Colloids: The Effect of Long-Range Repulsion*. *Phys. Rev. Lett.*, **94**, 208301 (2005).
- [126] B. Bozorgui and D. Frenkel. *Liquid-Vapor Transition Driven by Bond Disorder*. *Physical Review Letters*, **101**, 045701 (2008).
- [127] D. J. Maxwell, J. R. Taylor, and S. Nie. *Self-Assembled Nanoparticle Probes for Recognition and Detection of Biomolecules*. *Journal of the American Chemical Society*, **124**, 9606–9612 (2002).
- [128] J. Liu and Y. Lu. *Accelerated Color Change of Gold Nanoparticles Assembled by DNazymes for Simple and Fast Colorimetric Pb<sup>2+</sup> Detection*. *Journal of the American Chemical Society*, **126**, 12298–12305 (2004).
- [129] C. Liu, C. Huang, and H. Chang. *Control over Surface DNA Density on Gold Nanoparticles Allows Selective and Sensitive Detection of Mercury(II)*. *Langmuir*, **24**, 8346–8350 (2008).
- [130] J. Liu and Y. Lu. *Fast Colorimetric Sensing of Adenosine and Cocaine Based on a General Sensor Design Involving Aptamers and Nanoparticles*. *Angewandte Chemie International Edition*, **45**, 90–94 (2006).
- [131] C. B. Harley, A. B. Futcher, and C. W. Greider. *Telomeres shorten with aging*. *Nature*, **345**, 458–460 (1990).
- [132] F. Patolsky, R. Gill, Y. Weizmann, T. Mokari, U. Banin, and I. Willner. *Lighting-Up the Dynamics of Telomerization and DNA Replication by CdSe-ZnS Quantum Dots*. *Journal of the American Chemical Society*, **125**, 13918–13919 (2003).

- [133] C. Gan. *Gene Gun Accelerates DNA-Coated Particles To Transform Intact Cells*. The Scientist, **3**, 25 (1989).
- [134] A. Elbakry, A. Zaky, R. Liebl, R. Rachel, A. Goepferich, and M. Breunig. *Layer-by-Layer Assembled Gold Nanoparticles for siRNA Delivery*. Nano Letters, **9**, 2059–2064 (2009).
- [135] K. K. Peachman, M. Rao, and C. R. Alving. *Immunization with DNA through the skin*. Methods, **31**, 232 – 242 (2003).
- [136] M. L. Chang, J. C. Chen, C. T. Yeh, M. Y. Chang, C. K. Liang, C. T. Chiu, D. Y. Lin, and Y. F. Liaw. *Gene Gun Bombardment with DNA-Coated Gold Particles Is a Potential Alternative to Hydrodynamics-Based Transfection for Delivering Genes into Superficial Hepatocytes*. Human Gene Therapy, **19**, 391–395 (2008).
- [137] K. A. Janes, P. Calvo, and M. J. Alonso. *Polysaccharide colloidal particles as delivery systems for macromolecules*. Advanced Drug Delivery Reviews, **47**, 83 – 97 (2001).
- [138] P. W. Lee, S. F. Peng, C. J. Su, F. Mi, H. L. Chen, H. J. Wei, M. C. and Lin, and H. W. Sung. *The use of biodegradable polymeric nanoparticles in combination with a low-pressure gene gun for transdermal DNA delivery*. Biomaterials, **29**, 742 – 751 (2008).
- [139] J. C. Crocker. *Golden handshake*. Nature, **451**, 528–529 (2008).
- [140] D. A. Dehlinger, B. D. Sullivan, S. Esener, and M. J. Heller. *Directed Hybridization of DNA Derivatized Nanoparticles into Higher Order Structures*. Nano Letters, **8**, 4053–4060 (2008).
- [141] E. S. Andersen, D. M., M. M. Nielsen, K. Jahn, R. Subramani, W. Mamdouh, M. M. Golas, B. Sander, H. Stark, C. L. P. Oliveira, J. S. Pedersen, V. Birkedal, F. Besenbacher, K. V. Gothelf, and J. Kjems. *Self-assembly of a nanoscale DNA box with a controllable lid*. Nature, **459**, 73–77 (1996).
- [142] S. R. Bhatia and W. B. Russel. *End-Capped Associative Polymer Chains between Nanospheres: Attractions in Ideal Solutions*. Macromolecules, **33**, 5713–5720 (2000).
- [143] A. A. Louis, P. G. Bolhuis, J. P. Hansen, and E. J. Meijer. *Can Polymer Coils Be Modeled as Soft Colloids*. Phys. Rev. Lett., **85**, 2522–2525 (2000).
- [144] R. Verma, J. C. Crocker, T. C. Lubensky, and A. G. Yodh. *Entropic Colloidal Interactions in Concentrated DNA Solutions*. Phys. Rev. Lett., **81**, 4004–4007 (1998).
- [145] J. F. Berret, G. Cristobal, P. Hervé, J. Oberdisse, and I. Grillo. *Structure of colloidal complexes obtained from neutral/poly- electrolyte copolymers and oppositely charged surfactants*. The European Physical Journal E, **9**, 301–311 (2002).

- [146] A. Stradner, H. Sedgwick, F. Cardinaux, W. C. K. Poon, S. U. Egelhaaf, and P. Schurtenberger. *A 1.7-kilobase single-stranded DNA that folds into a nanoscale octahedron*. *Nature*, **432**, 429 – 495 (2004).
- [147] C. M. Niemeyer. *Progress in "engineering up" nanotechnology devices utilizing DNA as a construction material*. *Applied Physics A*, **68**, 119–124 (1999).
- [148] R. Bashir. *DNA-mediated artificial nanobiostructures: state of the art and future directions*. *Superlattices and Microstructures*, **29**, 1–16 (2001).
- [149] G. Subramanian, V. Manoharan, J. Thorne, and D. Pine. *Ordered Macroporous Materials by Colloidal Assembly: A Possible Route to Photonic Bandgap*. *Advanced Materials*, **11**, 1261–1265 (1999).
- [150] L. M. Dillenback, G. P. Goodrich, and C. D. Keating. *Temperature-Programmed Assembly of DNA: Au Nanoparticle Bioconjugates*. *Nano Letters*, **6**, 16–23 (2006).
- [151] F. Pierce, C. M. Sorensen, and A. Chakrabarti. *Aggregation-Fragmentation in a Model of DNA-Mediated Colloidal Assembly*. *Langmuir*, **21**, 8992–8999 (2005).
- [152] W. C. K. Poon, J. S. Selfe, M. B. Robertson, S. M. Ilett, A. D. Pirie, and P. Pusey. *An experimental study of a model colloid-polymer mixture*. *Journal de Physique II*, **3**, 1075–1086 (1993).
- [153] J. J. Cerdà, T. Sintes, C. M. Sorensen, and A. Chakrabarti. *Kinetics of phase transformations in depletion-driven colloids*. *Phys. Rev. E*, **70**, 011405 (2004).
- [154] P. Pusey, A. Pirie, and W. Poon. *Dynamics of Colloid Polymer Mixtures*. *Physica A*, **201**, 322–331 (1993).
- [155] T. T. Perkins, D. E. Smith, and S. Chu. *Single Polymer Dynamics in an Elongational Flow*. *Science*, **276**, 2016–2021 (1997).
- [156] S. Asakura and F. Oosawa. *On Interaction between Two Bodies Immersed in a Solution of Macromolecules*. *Journal of Chemical Physics*, **22**, 1255–1256 (1954).
- [157] U. Gasser. *Crystallization in three- and two-dimensional colloidal suspensions*. *Journal of Physics: Condensed Matter*, **21**, 203101 (2009).
- [158] R. Schlapak, D. Armitage, N. Saucedo-Zeni, W. Chrzanowski, M. Hohage, D. Caruana, and S. Howorka. *Selective protein and DNA adsorption on PLL-PEG films modulated by ionic strength*. *Soft Matter*, **5**, 613–621 (2009).
- [159] E. Edri and O. Regev. *pH Effects On BSA-Dispersed Carbon Nanotubes Studied by Spectroscopy-Enhanced Composition Evaluation Techniques*. *Analytical Chemistry*, **80**, 4049–4054 (2008).
- [160] N. R. Kallenbach, R. I. Ma, and N. C. Seeman. *An immobile nucleic acid junction constructed from oligonucleotides*. *Nature*, **305**, 829 – 831 (1983).

- [161] C. Altona, J. A. Pikkemaat, and F. J. J. Overmars. *Three-way and four-way junctions in DNA: a conformational viewpoint*. *Current Opinion in Structural Biolog*, **6**, 305–316 (1996).
- [162] D. M. J. Lilley. *Structures of helical junctions in nucleic acids*. *Quarterly Reviews of Biophysics*, **33**, 109159 (2000).
- [163] R. Holliday. *A mechanism for gene conversion in fungi*. *Genetics Research*, **5**, 282–304 (1964).
- [164] H. Potter and D. Dressler. *On the mechanism of genetic recombination: electron microscopic observation of recombination intermediates*. *Proc. Natl. Acad. Sci.*, **73**, 3000–3004 (1976).
- [165] H. Potter and D. Dressler. *In vitro system from Escherichia coli that catalyzes generalized genetic recombination*. *Proc. Natl. Acad. Sci.*, **75**, 3698–3702 (1978).
- [166] A. Schwacha and N. Kleckner. *Identification of Double Holliday Junctions as Intermediates in Meiotic Recombination*. *Cell*, **83**, 783–791 (1995).
- [167] D. R. Duckett, A. I. H. Murchie, S. Diekmann, E. Von Kitzing, B. Kemper, and D. M. J. Lilley. *The Structure of the Holliday Junction, and Its Resolution*. *Cell*, **55**, 79–89 (1988).
- [168] A. I. H. Murchie, R. M. Clegg, E. Von Kitzing, D. R. Duckett, S. Diekmann, and D. M. J. Lilley. *Fluorescence energy transfer shows that the four-way DNA junction is a right-handed cross of antiparallel molecules*. *Nature*, **341**, 763 – 766 (1989).
- [169] J. Zheng, P. Constantinou, C. Micheel, P. A. Alivisatos, R. A. Khiel, and N. C. Seeman. *Two-Dimensional Nanoparticle Arrays Show the Organizational Power of Robust DNA Motifs*. *Nanoletters*, **6**, 1502–1504 (2006).
- [170] V. N. Manoharan, M. T. Elsesser, and D. J. Pine. *Dense Packing and Symmetry in Small Clusters of Microspheres*. *Science*, **301**, 483–487 (2003).
- [171] J. L. Kadrmas, A. J. Ravin, and N. B. Leontis. *Relative stabilities of DNA three-way, four-way and five-way junctions (multi-helix junction loops): unpaired nucleotides can be stabilizing or destabilizing*. *Nucleic Acids Research*, **23**, 2212–2222 (1995).
- [172] L. E. Morrison and L. M. Stols. *Sensitive fluorescence-based thermodynamic and kinetic measurements of DNA hybridization in solution*. *Biochemistry*, **32**, 3095–3104 (1993).
- [173] E. Kaiser, R. L. Colescott, C. D. Bossinger, and P. I. Cook. *Color test for detection of free terminal amino groups in the solid-phase synthesis of peptides*. *Analytical Biochemistry*, **34**, 595 – 598 (1970).

- 
- [174] J. N. Israelachvili. *Intermolecular and surface forces*. Academic press inc., San Diego (1985).
- [175] M. E. Leunissen, R. Dreyfus, F. C. Cheong, D. Grier, R. Sha, N. C. Seeman, and P. M. Chaikin. *Switchable self-protected attractions in DNA-functionalized colloids*. *Nature Materials*, **8**, 590–595 (2009).

## SUMMARY

In the natural world, DNA provides a kind of blueprint that directs a complex molecular dance which culminates in the creation of a much larger, more complex object be it a bacterium or an elephant. In the material world however, this molecule proves very useful in constructing larger assemblies. This assembly method relies on the attractive forces between complementary bases of two single DNA strands.

### **Designing new materials**

A monodisperse colloidal system with non-specific interactions will typically crystallize into a closed-packed structure or body-centered cubic (bcc) lattice. Attractive specific forces, on the other hand, could potentially drive colloidal crystallization at much lower volume fractions through recognition-mediated assembly. In addition, specific forces can potentially enable us to construct unique colloidal structures that are otherwise entropically unfavorable. An example of a molecule that can provide a colloidal system with specific attractive forces is DNA. Indeed, theoretical work by Tkachenko predicted numerous crystal structures for a system of equal sized colloids coated with DNA [9]. The predicted structures range from a simple cubic lattice to the more complex diamond structure. The prediction of a self-assembled diamond lattice is especially exciting, because of its potential as a photonic crystal. That is why this system shows great promise in obtaining new materials.

### **The DNA-zipper**

Not only is DNA the carrier of the genetic code - it also turns out to be a beautiful building material due to its intrinsic properties. Chemically, DNA is composed of building-blocks called nucleotides consisting of a sugar molecule, a phosphate group, and one of the four bases - adenine (A), thymine (T), guanine (G), and cytosine (C). The phosphates and the sugars of adjacent nucleotides are linked together through covalent bonds, forming a long linear polymer. Together, two of such polymer chains form a twisted upright ladder due to the formation of hydrogen bonds between the bases. The rungs of the ladder can only be formed by complementary bases (A with T and C with G). This process - also called hybridization - is highly selective: a chain of bases will bind strongly to its complementary partner, but not (or scarcely) to any other DNA chain.

Hydrogen bonds are not a covalent bonds, this makes them much weaker. Therefore the formation of a bond between two single DNA strands can be made undone by increasing the temperature. At elevated temperatures the hydrogen bonds are not strong enough to keep the two chains together. The number of hydrogen bonds between two DNA strands determines at what temperature the double DNA helix dissociates into two single strands.

### **DNA as a building material**

The ability of single DNA strands to hybridize and thus form a double-stranded DNA structure can be used for the design of complex structures. By decorating building-blocks with pieces of single-stranded DNA, one can direct building-block 1 to bind to building-block 2, but not to building-block 3. In this manner, one can link different building-blocks in a directed fashion by utilizing single DNA strands as glue.

Typical examples of building-blocks are colloidal spheres that range in size from a few nanometers up to several micrometers in diameter. By mixing two solutions containing DNA-coated colloids with complementary sequences, aggregates will form due to hybridization between the two complementary DNA strands. As, besides mixing, no further measures are needed to obtain aggregates, this process is called “self-assembly”. If one is not content with the obtained aggregate, the solution can be heated in order to redisperse the colloids. Subsequent cooling leads to a new hybridization process, which could lead to a different (better) cluster.

### **Applications**

This research-area is still in its early stages. Eventually the goal is to obtain artificial material that can repeatedly copy itself. The ability to create new materials in this way could provide new routes to building regular structures like those used in microelectronics. Or it could produce entirely new materials, such as photonic crystals that control the movement of light through them in a way akin to how electricity flows through a semiconductor. An application that is already utilized is the use of DNA-coated colloids as bio-sensors. Several diseases that are caused by DNA mutations can be diagnosed with these sensors. This technique is very sufficient, with sensors sensitive enough to detect concentrations as low as a few molecules.

### **This thesis**

The subject of my dissertation is DNA-driven assembly of micron-sized colloids. As mentioned above colloids are small spheres. I mostly use spheres with a diameter that is one thousands of a millimeter (micron). They are made of plastic (polystyrene). As the spheres are very small, one can not distinguish them individually by eye. Though, with the help of a microscope they can be seen. By coating these colloids with DNA, I was able to assemble monomers into more complex structures. By using colloids with a specific protein-coating (neutravidin), coating them with DNA is simple. By modifying one end of the DNA strands with a molecule (biotin) that strongly binds to the proteins on the colloids, mixing of DNA and colloids is enough. This process together with some properties of the DNA are described in chapter 1.

In chapter 2 a short overview of available literature is given. Here, nano- and micron-sized colloids are discussed. Different coating procedures are mentioned as well as important parameters to control the assembly. Finally, some applications, as the ones briefly mentioned above, are explained in more detail.

Starting from chapter 3, I discuss the experiments I performed during my PhD-research. We started with coating colloids with a very long DNA chain. Of this strand only the very last 12 bases are single strand and thus “sticky”. The reasoning behind this was to introduce a linker as well as a spacer with one molecule. As the spacer was

of similar size as the colloids, some space between adjacent colloids was expected. The results of chapter 3 proof this basic assumption wrong. Aggregates obtained with this type of colloids are finite in size and colloids are closely packed. As colloids are closely packed, the DNA is expelled to the outer sides of the cluster. Because the DNA I used is very bulky and carries a net negative charge, it acts as a repulsive barrier, preventing further growth of the aggregates.

While finite size building-blocks can be useful, we next tried to improve the size of the clusters obtained. In chapter 4 it is shown that reducing the length of the DNA spacer, while keeping the sticky-end the same, leads to percolating clusters. A good example of this is shown in figure 4.3. Both the clusters obtained with the very long DNA as the ones formed with DNA of intermediate length were unable to redisperse at temperatures well above the melting temperature of the DNA (i.e. the temperature where a 12 base double stranded DNA strand will dissociate). Reducing the spacer length drastically, leaving only the sticky overhangs on the colloid surface, resulted in a temperature reversible system. Preliminary conclusions suggested that complete covering of all neutravidin on the colloidal surface might be responsible for this.

More research indicated that this assumption was not completely true (appendix A). It turns out that micron-sized colloids coated with long and flexible DNA strand are so closely packed within aggregates that after assembly, colloids are held together by van der Waals forces instead of DNA bridges. Hence the lack of redispersal of the colloids at elevated temperatures.

In chapter 5 a different approach is chosen. Instead of a binary system of two types of colloids in solution, now only one type of colloid is allowed to assemble above a surface coated with complementary DNA. This type of assembly resulted into two-dimensional structured aggregates. As the DNA keeps these crystals from direct contact with the surface, we named them “flying carpets”.

Besides the most common DNA structure (the double helix), also more exotic structures are possible. One of these structures is a 4-way junction (also called a Holiday junction) made of four DNA strands. With this structure, I would like to link four colloids together, obtaining well defined, finite sized clusters. In chapter 6 I describe the steps already taken to obtain these aggregates. Formation of the Holiday junction is realized as well as increasing the length of the construct to make it suitable for micron-sized colloids. Even though the first trial experiments look promising, the yield of this reaction is still very low.

The work described in this thesis is part of fundamental research, increasing the knowledge of DNA as a building material. Self-assembly becomes more and more important as there is a constant demand for smaller and smaller machinery and building-parts. To be able to utilize DNA in its full extent, the molecule and all its properties need to be understood extremely well.



## NEDERLANDSE SAMENVATTING

Lijm. Iedereen gebruikt het wel, en waarschijnlijk is het je ook al eens overkomen dat het plakken niet geheel vlekkeloos verliep. Dingen plakken aan elkaar die niet aan elkaar horen te zitten of dingen hangen hopeloos scheef. Op zulke momenten zou het handig zijn als het plakproces niet onomkeerbaar zou zijn. Of nog beter, dat de lijm zou weten wat er geplakt dient te worden en wat niet.

Als ik je nu eens vertelde dat die lijm al lang bestaat?

Op veel gebieden ligt de natuur ver voor op onze wetenschap. In tegenstelling tot de keus te beperken tot de synthetische materialen die we nu als lijm gebruiken, kan het antwoord gevonden worden in een van de meest belangrijke moleculen in de natuur. Dit molecuul ligt aan de basis van al het leven op aarde, maar als we het puur alleen als een “plakmiddel” zouden gebruiken, is het de slimste lijm ooit. De naam van dit molecuul: DNA.

### **De DNA-ritssluiting**

DNA is niet alleen de drager van de genetische code - het blijkt ook een prachtig bouw-materiaal te zijn. DNA bestaat uit twee lineaire ketens van suiker-fosfaat groepen, die samen een dubbele helix vormen. Deze structuur ontstaat doordat zich tussen de organische basen (Adenine, Cytosine, Guanine en Thymine) van de twee afzonderlijke ketens waterstofbruggen vormen. Deze bruggen zijn echter alleen tussen de complementaire basen (C met G, A met T) mogelijk. Dit proces - ook wel hybridisatie genoemd - is heel selectief: een keten van basen bindt zich sterk aan een complementair segment, maar niet (of nauwelijks) aan een willekeurig ander segment.

Waterstofbruggen zijn geen covalente bindingen. Dit betekent dat de binding tussen twee DNA ketens ongedaan gemaakt kan worden door de temperatuur te verhogen. Bij een hoge temperatuur zijn de bindingen niet sterk genoeg om bij elkaar te blijven. Het aantal waterstofbruggen tussen de DNA ketens bepaalt bij welke temperatuur de dubbele DNA keten enkelstrengs wordt.

### **DNA als bouw materiaal**

De hybridisatie-eigenschap van DNA kan worden toegepast bij het ontwerpen van complexe nanostructuren. Door verschillende bouwstenen te bekleden met stukjes enkelstrengs DNA kun je ervoor zorgen dat bouwsteen A alleen bindt (hybridiseert) met bouwsteen B, maar niet met C etc. Op deze manier kun je dus heel gericht bouwstenen aan elkaar koppelen door de stukjes DNA als het ware als lijm tussen de bouwstenen te gebruiken.

Als bouwsteen worden vaak colloïde deeltjes gebruikt. Dit zijn zeer kleine bolletjes. Door een oplossing van bolletjes met een bepaald stukje DNA te mixen met een oplossing

van bolletjes met het complementaire stukje DNA eraan, zal DNA hybridisatie voor clustering zorgen. Dit proces wordt ook wel “self-assembly” genoemd. Mocht je niet tevreden zijn met het ontstane resultaat, dan is het mogelijk het hybridisatie proces terug te brengen naar de begin situatie door de clusters te verwarmen. Afkoelen leidt tot een nieuw hybridisatie proces, wat een ander (beter) cluster tot gevolg kan hebben.

### **Toepassingen**

Dit onderzoeksgebied staat nog in de kinderschoenen. Het streven is om met deze techniek eenheden te bouwen, die zichzelf kunnen vermenigvuldigen en zo zelfstandig de gewenste structuren te vormen. Daarbij kun je denken aan mogelijke toepassingen als nano-machines of zelfgenererende computerchips. Ook zijn er computersimulaties die de mogelijkheid tot het maken van (fotonische) kristallen voorspellen. Dit ligt echter nog allemaal in de toekomst. Op dit moment wordt de selectiviteit van DNA binding wel al toegepast in bio-sensoren. Hiermee worden bijvoorbeeld bepaalde ziektes vastgesteld bij patiënten. Deze techniek werkt erg goed, een aantal sensoren is zo gevoelig is dat ze een stof kunnen detecteren bij een concentratie van slechts enkele moleculen.

### **Mijn proefschrift**

Het onderwerp van mijn proefschrift is DNA-gestuurde zelforganisatie van micron-grote colloïden. Hierboven heb ik al aangegeven dat colloïden niets meer en niets minder zijn dan zeer kleine bolletjes. In mijn geval zijn ze doorgaans een duizendste van een millimeter (micron) groot en gemaakt van plastic (polystyreen). Met het oog zijn deze bolletjes niet individueel te onderscheiden, maar met behulp van een microscoop zijn ze prima te zien. Ik gebruik deze deeltjes om mijn DNA-lijm te testen. Door colloïden te gebruiken met een speciale eiwit-coating (neutravidin) kan ik DNA gemakkelijk aan de bolletjes vastzetten. Hiervoor hoef ik alleen één uiteinde van het DNA te bevestigen aan een molecuul (biotin) dat sterk bindt aan de eiwitten op de bolletjes. In mijn geval gebruik ik een neutravidin-biotin binding, die hetzelfde werkt als een drukknoop. Dit is beschreven in hoofdstuk 1.

In hoofdstuk 2 beschrijf ik de literatuur over DNA-gestuurde zelforganisatie van zowel nano- als micron-grote colloïden. Ik leg uit hoe verschillende soorten bolletjes aan DNA gebonden kunnen worden en hoe de plak-kracht van de lijm kan worden gevarieerd. Ook komen enkele toepassingen aan het bod, welke ik hierboven al kort beschreven heb.

Vanaf hoofdstuk 3 beschrijf ik de experimenten die ik heb uitgevoerd. Ik ben mijn onderzoek begonnen met een zeer lange DNA keten, waarbij alleen het allerlaatste stukje enkelstrengs is. De gedachte hierachter was dat een zeer lange keten niet alleen als linker (lijm) kan worden gebruikt, maar ook als afstandhouder om de bolletjes niet te dicht bijeen te krijgen. De resultaten uit hoofdstuk 3 laten zien dat deze aanname niet juist was. Het DNA bleef niet tussen de bolletjes zitten, maar werd als het ware naar buiten geduwd. Hierdoor ontstonden kleine klompjes van bolletjes. Deze waren geheel omringd door DNA, wat verdere groei uitsloot.

Net zoals in het dagelijks leven, kan een teveel aan lijm het eindproces beïnvloeden. In hoofdstuk 4 laat ik zien dat kortere DNA ketens tot grotere structuren leidt. Doordat het overschot aan DNA nu niet meer in de weg zit, kunnen alle colloïden met elkaar binden. Een goed voorbeeld hiervan kan gevonden worden in figuur 4.3.

In hoofdstuk 5 gebruik ik de DNA-lijm op een iets andere manier. In plaats van bolletjes aan elkaar te plakken, is het doel hier om bolletjes aan een oppervlakte te binden. Hiervoor breng ik eerst een laagje DNA-lijm aan op een glasplaatje. Daarna druppel ik de bolletjes vloeistof er boven op. Deze manier van self-assembly levert platte kristal structuren op. Een kristal structuur wil zeggen dat de bolletjes geordend aan elkaar binden in plaats van willekeurig als in een druiventros. Omdat de DNA ervoor zorgt dat deze twee-dimensionale vlakken niet op het oppervlak liggen, maar erboven zweven, heb ik ze vliegende tapijten genoemd.

Naast de meest bekende structuur van DNA (de dubbele helix), kan DNA ook met vier strengen tegelijk binden. Het vormt dan als het ware een kruispunt, waarbij alle vier de strengen rechts afbuigen. Deze speciale manier van binden wil ik graag gaan gebruiken om telkens vier colloïden aan een te binden (tetrameer). In hoofdstuk 6 beschrijf ik welke stappen ik al ondernomen heb om dit voor elkaar te krijgen. Op dit moment ben ik in staat om een DNA-kruispunt te genereren. Hoewel de eerste experimenten met dit type DNA en bolletjes er hoopvol uitziet is de opbrengst van tetrameren op dit moment nog zeer laag.

Tenslotte heb ik nog een appendix toegevoegd. Hierin heb ik de resultaten samengevoegd die niet gepubliceerd zullen worden. In de eerste paragraaf heb ik verteld over een lijm die super slim is, omdat deze zeer selectief plakt en de binding reversibel is. Dit is niet in alle gevallen zo. Het blijkt dat zeer lange DNA ketens het plak-proces dusdanig verstoren dat structuren die eenmaal gevormd zijn, niet meer ongedaan gemaakt kunnen worden. Oplossingen om dit probleem te omzeilen zijn beschreven in de appendix, al blijkt dat in sommige gevallen er geen oplossingen zijn.

Al het werk beschreven in dit proefschrift is deel van fundamenteel onderzoek en draagt bij aan de kennis van DNA als slimme lijm. Self-assembly heeft de toekomst in een wereld waar een constante vraag is naar steeds kleinere machines en onderdelen. Om DNA optimaal te kunnen benutten in dit proces moet het molecuul en al zijn kwaliteiten volledig worden begrepen.



## DANKWOORD

*Dankbaarheid tonen is een prachtig gebaar. Het is ook (in mijn ogen) on-hollands of misschien gewoon niet zo mijn “ding”, wat dit stukje het lastigste onderdeel van mijn proefschrift maakt. Dit wil niet zeggen dat ik doorgaans niet dankbaar ben en zeker niet dat ik graag wil geloven dat ik helemaal alleen tot dit punt in mijn leven ben gekomen.*

*Ik wil dan ook graag beginnen met Erika. Erika, voor mij was je een ideale (co)-promotor. Je natuurlijke nieuwsgierigheid naar alle mogelijke experimenten hebben het voor mij mogelijk gemaakt om veel uit te proberen, ook al wilde sommige experimenten nog wel is falen. Ik was niet geheel zeker hoe jou verhuizing naar Cambridge zou uitpakken, maar het bleek prima te werken. Niet alleen kon ik een aantal maal Cambridge bezoeken, ook hebben je nieuwe collega's mijn onderzoek verrijkt met hun kennis en hun inzet (special thanks to Julien, Linda and last but not least Sabrina). Gelukkig bleef ik niet alleen achter te AMOLF, als tweede wil ik dan ook graag Marileen bedanken. Ik heb het als bijzonder prettig ervaren om onderdeel uit te maken van jouw groep (bedankt voor de adoptie). Ook hebben je adviezen zeker bijgedragen aan de resultaten in dit proefschrift. Omdat je nooit genoeg support kan hebben tijdens je onderzoek, wil ik ook graag Daan bedanken. Daan ik ken echt niemand met meer kennis en ben je zeer dankbaar voor het helpen verklaren van resultaten en het verfijnen en bijschaven van mijn artikelen.*

*Nu we het toch over het verbeteren van tekst hebben wil ik ook graag de onofficiële leescommissie bedanken. Ana, Liedewij, Marina en Marjon bedankt voor jullie suggesties en correcties op de eerste, tweede en soms zelfs derde versie van de hoofdstukken.*

*AMOLF voelt als een tweede thuis, dit komt voornamelijk door de aangename sfeer en de geweldige mensen die er werken. Vanaf de eertse week werd ik opgenomen in het sociale netwerk dat “de overloop” heet. Was het eerst vooral de Spaans/Italiaanse mafia binnen Daan z'n groep die me welkom heette, later kwamen daar velen bij. Met het risico namen te vergeten wil ik toch een paar mensen noemen. Als eerste Koos, ik vond het super om een kantoor met je te delen de afgelopen vier jaar. Ik wil je hartelijk bedanken voor het aanhoren van al mijn verhalen en stel het zeer op prijs dat je alleen ging klagen als ik wel erg hard met de radio aan het meezingen was =]. Sanne en Ana, fijn dat jullie besloten hebben in Amsterdam te blijven. Ik hoop dat de groep-etentjes nog lang door zullen gaan.*

*Door mijn adoptie in de bio-assembly groep van Marileen, ben ik goed bevriend geraakt met “de girlz”. Liedewij, Paige, Laura en Svenja ik heb me prima vermaakt met jullie de afgelopen vier jaar. Naast de werk discussies, wil ik jullie vooral bedanken voor jullie vriendschap buiten het lab. Beloof me dat we nog vele malen samen gaan dansen, eten of gewoon bijeen komen voor de laatste roddels. De groep is niet altijd grilz-only geweest, er waren ook male-members die niet onder deden voor de meiden. Graag wil ik dan ook Christian, Julien en Gert-Jan bedanken.*

*De overloop bestaat uit veel meer mensen: Wiet, Mel, Thorsten, Filipe, Siebe, David,*

*Niels, Laurens, Bertus en Daan julie droge humor ga ik zeker missen. Marina, Iza en Marjon bedankt voor julie gezelschap op het lab. Net nu mijn tijd op AMOLF bijna afgelopen is, komen er een hoop nieuwe mensen binnen: Jose, ik ken je nog maar net, maar ik vind je nu al een aanwinst voor het lab. Milena, top dat je meteen meedeed aan de sportdag, een jaren 80 aerobics outfit staat je goed! Als laatste member van de overloop wil ik graag Kostya noemen. Kostya ik vind het geweldig hoe jij iedereen helpt op de overloop. Voor mij was vooral je oneindige wiskunde en latex kennis ideaal.*

*Naast de mensen van AMOLF wil ik ook nog even de tijd nemen om de mensen die mijn leven in Amsterdam zeer aangenaam hebben gemaakt te bedanken. Als eerste Sanne en Alex, superleuk dat jullie straks als paranimfen naast mij komen staan op de grote dag! Het is meer dan logisch dat mijn beste buddies van de UvA, ook mijn laatste verdediging meemaken. Daarnaast wil ik graag de mensen van de dinner-club bedanken, het was fijn samen te studeren, maar nog fijner dat we elkaar nog steeds zien. Verder wil ik graag nog wat mensen bedanken die me behoeden voor compleet nerdschap. Voor de Den-Helder gang, ik ben blij dat onze vriendschap niet beëindigd is na mijn verhuizing naar A'dam. Ing, Jes, Peet, Roet en Dais ik ga mijn best doen om een topplek uit te zoeken voor mijn volgende baan. Dat jullie maar vaak langs mogen komen. Door in een nieuwe stad te gaan wonen, heb ik veel nieuwe mensen leren kennen. Ik wil vooral alle basketbal-sterren bedanken voor de vele uren sport-plezier, maar bovenal voor hun warme vriendschap buiten het veld.*

*Tenslotte wil ik graag mijn familie bedanken. Helen, Jen en Kris, ik weet dat er geen bloedband tussen ons bestaat, maar we zijn al zo lang bevriend dat ik me geen betere familie kan wensen. Als laatste wil ik graag mijn vader, moeder en broer bedanken. Het is goed te weten dat ik altijd op julie kan bouwen!*

*-xxx-*

*Nienke*

*PS Mocht ik namen zijn vergeten, bij deze mijn excuses. Mocht je niet persoonlijk genoemd zijn, maar vind je dat je best bedankt had mogen worden, bij deze: harstikke bedankt!*

*PS2 I know my whole word of gratitude is in Dutch, though not all people I thank are native Dutch speakers. As my time at AMOLF thought me that all foreigners are perfectly capable of reading and listening in Dutch, I decided to write in Dutch. Of course I'm happy to clarify some or all parts not clear to you.*



*Thanks  
xxx*



## CURRICULUM VITAE

Nienke Geerts was born in Den Helder, The Netherlands, on November 9th, 1981. From 1994 to 2000 she attended 'Voorbereidend wetenschappelijk Onderwijs' (VWO) at O.S.G. Nieuwediep in Den Helder. Next, she started her studies in (Bio-)Chemistry at the University of Amsterdam. Her undergraduate research was done at the Swammerdam Institute for Life Sciences (SILS) under supervision of Dr. D.P.E. Satijn. In her Master's thesis, entitled *Manipulation of EZH2 function in HL 60 cells: Localization of PcG domains and their role in recruiting and silencing of PcG target genes*, she describes the effect of EZH2 on proliferation and differentiation, using mutant proteins.

After graduating in 2005, she started her PhD research at the FOM Institute for Atomic and Molecular Physics (AMOLF) in Amsterdam. Throughout this period she was supervised by Dr. Erika Eiser, Prof. dr. Daan Frenkel and Prof. dr. Marileen Dogterom. Although officially a member of the Biophysics group of Prof. dr. D. Frenkel, she was daily supervised by Dr. Erika Eiser (Complex Fluids group - Van 't Hoff Institute for Molecular Sciences (University of Amsterdam)) as she did experimental Biophysics rather than computer-simulations. The results of this research are described in this thesis.

